2023

# Molecular biology of peripheral nerve regeneration: Expression and role of Netrin-1, DCC and Runx2

Lolita Singh

---

PHD

# Molecular biology of peripheral nerve regeneration: Expression and role of Netrin-1, DCC and Runx2

Singh, Lolita

**Award date:**
2023

*Awarding institution:*
University of Plymouth

## Copyright Statement

**Molecular biology of peripheral nerve regeneration:**

**Expression and role of Netrin-1, DCC and Runx2**

By

**Lolita Singh**

A thesis submitted to the University of Plymouth

in partial fulfilment for the degree of

**DOCTOR OF PHILOSOPHY**

Peninsula Medical School

**July 2023**

**Covid -19 impact statement**

Covid-19 has had several impacts on the work done for the presented thesis. Primarily, access to the laboratory was disrupted for a period of four months in 2020 following which the access was restricted (on a shift basis) for approximately two months. During the period of lab disruption, in collaboration with my research group, I utilised the time to perform analysis of previously published RNA sequencing data.

Additionally, the breeding of all mouse lines and experiments were paused for a period of approximately five months in 2020. Once animal work was resumed, breeding had slowed down for a few months owing to the age of the breeding pairs which also delayed the progress of the experiments.

The closure of the electron microscopy (EM) centre and its restricted access for a period of almost two years meant that the training, sample processing and imaging that I had intended to do before Covid was also impeded. Therefore, both sample processing and imaging was carried out by Mr. Glenn Harper of the EM centre. However, only selected few samples were analysed owing to the huge demand and workload on the small number of staff that were permitted entry at the EM centre.

Although at the start of my PhD I had helped with some preliminary work on the Runx2 project, this project was later handed to my colleague, Rong Hu. However, following Covid-19, she returned to her home country and therefore the remaining work for this

project was carried out by me and is presented in this thesis. I did receive an extension of four months for my third year of PhD that enabled me to complete some but not all intended experiments presented in this thesis.

## Acknowledgements

**Author's Declaration**

At no time during the registration for the degree of Doctor of Philosophy has the author been registered for any other University award without prior agreement of the Doctoral College Quality Sub-Committee.

Work submitted for this research degree at the University of Plymouth has not formed part of any other degree either at the University of Plymouth or at another establishment.

This study was financed by a studentship from the University of Plymouth.

**Publication:**

Chen, B., Banton, M.C., Singh, L., Parkinson, D.B. and Dun, X.P., 2021. Single cell transcriptome data analysis defines the heterogeneity of peripheral nerve cells in homeostasis and regeneration. Frontiers in Cellular Neuroscience, 15, p.624826. doi: 10.3389/fncel.2021.624826.

**Word count of main body of thesis: 50,207**

Signed:

**Date: 21st July, 2023**

**Title: Molecular biology of peripheral nerve regeneration: Expression and role of Netrin-1, DCC and Runx2**

By Lolita Singh

**ABSTRACT**

Damage to the peripheral nerves causes a series of molecular, cellular, and structural changes critical to initiating a successful regenerative process involving degeneration, inflammation, axon re-growth and innervation of the denervated target, and finally functional recovery.

In this thesis I sought to study the expression and role of an axon guidance molecule - Netrin-1 in peripheral nerve repair. Using a Schwann cell-specific Netrin-1 knockout mouse model, I showed an increased disorganisation and misdirection of re-growing axons within the nerve bridge following transection injury. However, this did not affect the number of axons innervating the distal nerve. Moreover, functional recovery was not impacted after a crush injury. Additional studies on axon outgrowth following crush injury, and analysis of Schwann cell proliferation, migration and remyelination of axons following injury, showed that Schwann cell-derived Netrin-1 is expendable for these functions.

Furthermore, on analysing recently compiled single-cell RNA sequencing data for the sciatic nerve following injury, I report the highest expression of Netrin-1 in perineurial cells with low expression of Netrin-1 in Schwann cells both before and after injury.

Therefore, I attempted to generate a global knockout of Netrin-1 in adult mice to study the effect of the overall loss of Netrin-1 on peripheral nerve regeneration, however this attempt unfortunately proved to be unsuccessful.

Netrin-1 has been shown to mediate attraction on growing axons during development by binding to its receptor - deleted in colorectal carcinoma (DCC). To study the role of DCC in peripheral nerve injury and repair, I generated a global knockout of DCC in adult mice using a Tamoxifen inducible Cre recombinase system. A transection injury in DCC global knockout mice revealed aberrant trajectory of axons in the nerve bridge, however innervation of the distal nerve was not affected. Similar to the Schwann cell-specific Netrin-1 mouse model, functional recovery was comparable to the control following a crush injury. My data suggested that DCC might not be important for successful end-target innervation of axons as well as functional recovery following peripheral nerve injury.

The final part of my thesis focused on studying the role of runt related transcription factor-2 (Runx2) in peripheral nerve regeneration. While the published literature and my in-silico analysis showed significant upregulation of Runx2 in Schwann cells following peripheral nerve injury, Runx2 has no previously established role in peripheral nerve repair. Therefore in collaboration with other members of my research group we established a Schwann-cell specific Runx2 knockout mouse model and investigated the

effect of loss of Runx2 on the events of peripheral nerve repair. My work on the Runx2 mouse model showed normal myelination of axons by Schwann cells during development, however remyelination was impaired following a crush injury in the sciatic nerve. I also attempted to validate three predicted injury associated Runx2 targets; however, my results showed that they were not apparently regulated by Runx2. My results for this project, along with that of my research group identified Runx2 as a novel regulator of Schwann cell plasticity with a role in the regulation of peripheral nerve regeneration biology.

**Table of Contents**

## List of Figures

**List of Tables**

**Abbreviations**

| | |
|---|---|
| **CNS** | Central nervous system |
| **BDNF** | Brain derived neurotrophic factor |
| **BNB** | Blood-nerve barrier |
| **BSA** | Bovine serum albumin |
| **cAMP** | Cyclic Adenosine Monophosphate |
| **DCC** | Deleted in colorectal cancer/ carcinoma |
| **DRG** | Dorsal root ganglia |
| **ECM** | Extracellular matrix |
| **FBS** | Fetal Bovine Serum |
| **FGF** | Fibroblast growth factor |
| **GFP** | Green fluorescent protein |
| **IHC** | Immunohistochemistry |
| **Krox20** | Early growth response protein 2 |
| **MBP** | Myelin basic protein |
| **MPZ** | Myelin protein zero |
| **NCC** | Neural crest cells |
| **NF** | Neurofilament heavy chain |
| **NGF** | Nerve growth factor |
| **NGFR** | Nerve growth factor receptor |
| **NgR** | Nogo receptor |
| **NT-3** | Neurotrophin-3 |
| **NT-4/5** | Neurotrophin-4/5 |
| **Ntn1** | Netrin-1 |
| **Oct6** | POU domain class 3 transcription factor 1 |

| OL | Oligodendrocytes |
|---|---|
| Olig1 | Oligodendrocyte transcription factor 1 |
| Pax3 | Paired box gene 3 |
| PBS | Phosphate buffer saline |
| PCR | Polymerase chain reaction |
| PDGF | Platelet-derived growth factor |
| PFA | Paraformaldehyde solution |
| PNI | Peripheral nerve injury |
| PNR | Peripheral nerve regeneration |
| PNS | Peripheral nervous system |
| PTX | Triton X-100 solution in PBS |
| ROBO1 | Roundabout Guidance Receptor 1 |
| Runx2 | Runt-related transcription factor 2 |
| SC | Schwann cells |
| SHH | Sonic hedgehog |
| Sox2 | SRY (sex determining region Y)-box 2 |
| SSI | Static sciatic index |
| TBST | Tris-Buffered Saline with 0.1% Tween® 20 Detergent |
| TEM | Transmission electron microscopy |
| Trks | Tyrosine kinase receptors |
| TSF | Toe spread factor |
| UNC5 | Uncoordinated-5 |
| WD | Wallerian degeneration |
| WM | Whole mount staining |

# CHAPTER 1: INTRODUCTION

## 1.1 PERIPHERAL NERVE STRUCTURE

The nerves and ganglia outside of the central nervous system (CNS) constitute the peripheral nervous system (PNS). The main function of the PNS is to transmit communication between the CNS (comprising of the brain and spinal cord), and the rest of the body. Peripheral nerves contain sensory, motor and autonomic axons. Sensory axons consist of somatic afferent axons that carry nerve impulses from sensory receptors on skin, muscles and other tissues to the CNS and the visceral afferent axons that carry information from the organs to the CNS. Similarly, the motor axons include somatic efferent axons that relay communication from the CNS to the somatic muscles; branchial motor axons to the skeletal muscles originating from the branchial arches, and visceral motor axons to muscles in organs such as the heart. The autonomic axons are responsible for regulating involuntary physiologic processes such as heart rate and blood pressure essential to maintaining homeostasis. Motor axons have their cell bodies in the gray matter of ventral horn of the spinal cord whereas sensory axons have the cell bodies in the dorsal root ganglia (DRG), along cranial nerves and trigeminal ganglia as well as some in the dorsal horn of the spinal cord. Peripheral nerves, such as the sciatic nerve, are made of a mix of both sensory and motor nerve axons.

Several axon populations in the PNS are myelinated while many remain unmyelinated and this property is highly dependent on the size of the axons. The axons have been

classified into class A (with several sub-types), B, and C based on the diameter of the axons, conduction velocities of nerve impulses and state of myelination. Large diameter axons such as the A-alpha fibres that are responsible for muscle contraction, are myelinated in the PNS. Myelinated axons are wrapped around with plasma membrane of Schwann cells (SCs) known as the myelin sheath in a 1:1 ratio. Each SC myelinating an axon is interrupted along the longitudinal length of an axon with periodic 1-2 μm gaps called the Node of Ranvier and the divided segments of myelin are termed as internodes (Figure 1). Small diameter axons, such as the C fibres that respond to thermal, mechanical, and chemical stimuli are responsible for producing the sensation of ache and delayed pain, are non-myelinated. This means that they are not wrapped in a myelin sheath however they are surrounded by SC processes such that they do not allow the axons to physically touch each other and are called Remak bundles. Light and electron microscopy in human tissue has revealed that these unmyelinated axons have a diameter of 0.2-3.0 μm while the myelinated axons have a diameter of 2-14 μm (Ochoa and Mair, 1969). SCs are covered by a thin basal lamina, made up of extracellular matrix (ECM) molecules such as fibronectin, heparan sulphate proteoglycans, laminins and type IV collagen, with a role in regulating several aspects of SC development and peripheral nerve regeneration (PNR) (Gonzalez-Perez et al., 2013; Monk et al., 2015).

Three connective tissues, namely the endoneurium, perineurium and the epineurium serve to support the peripheral nerve and axons within (Figure 1). The innermost

endoneurium located between individual axons comprises of endoneurial fluid and also houses fibroblasts, macrophages and mast cells. The axons, along with myelin (or without), basal lamina and surrounding endoneurium are bundled into fascicles which are enveloped by a dense middle connective tissue called perineurium (Figure 1). Perineurium is made up of circular layers of large and flat perineurial cells. Pockets with extracellular matrix (ECM) are located between the neighbouring perineurial cell layers (Peltonen *et al*., 2013). The ECM made up of collagens and fibronectin allow the perineurium to regulate the effect of external stretching forces. The perineurium creates a metabolically active continuous diffusion barrier with a role in maintaining homeostasis of the endoneurium (Shanthaveerappa and Bourne, 1962).

Finally, the outermost epineurium comprises of dense irregular connective tissues made up of collagen and holds all the fascicles together along with blood vessels and adipocytes (Figure 1). The epineurium also provides mechanical strength and elasticity to the peripheral nerve against forces of injury such as stretching. The epineurium also contains lymphatic vessels and the vasa nervorum, the blood supply of the peripheral nerve (Figure 1). The vasa nervorum can be segregated into intrinsic and extrinsic vessels (Boissaud-Cooke *et al.,* 2015). The extrinsic blood supply are the regional blood vessels from adjacent muscles and organs, located outside of the epineurium and supply the intrinsic vessels. The intrinsic blood supply consists of vessels within the epineurium, perineurium and endoneurium along the length of the nerve. The epineurial vessels are

large and their endothelium has fenestrations with open clefts thereby allowing the movement of serum proteins from the blood across the walls of the vessels, and therefore they are not involved in maintaining the blood-nerve barrier (BNB) (Olsson *et al.,* 1971). The blood-nerve-barrier also known as the blood-nerve-interface (BNI) maintains homeostasis within the endoneurium to create compartment pressures required for blood flow as well as to provide an environment favourable for conduction of action potentials by the axons (Weerasuriya and Mizisin, 2011). The BNB consists of perineurial cell layers and the endothelial microvessels of the endoneurium and their tight junctions that prevents the entry of large molecules into the nerve while permitting entry to small ions (Rechthand *et al.,* 1987). The perineurial vascular network is important for supplying the fascicles with circulation (Boissaud-Cooke *et al.,* 2015). The endoneurial microvasculature consists of capillaries that navigate the perineurium and enter the endoneurium. They are highly anastomotic, with no fenestrations and have tight junctions at endothelial junctions.
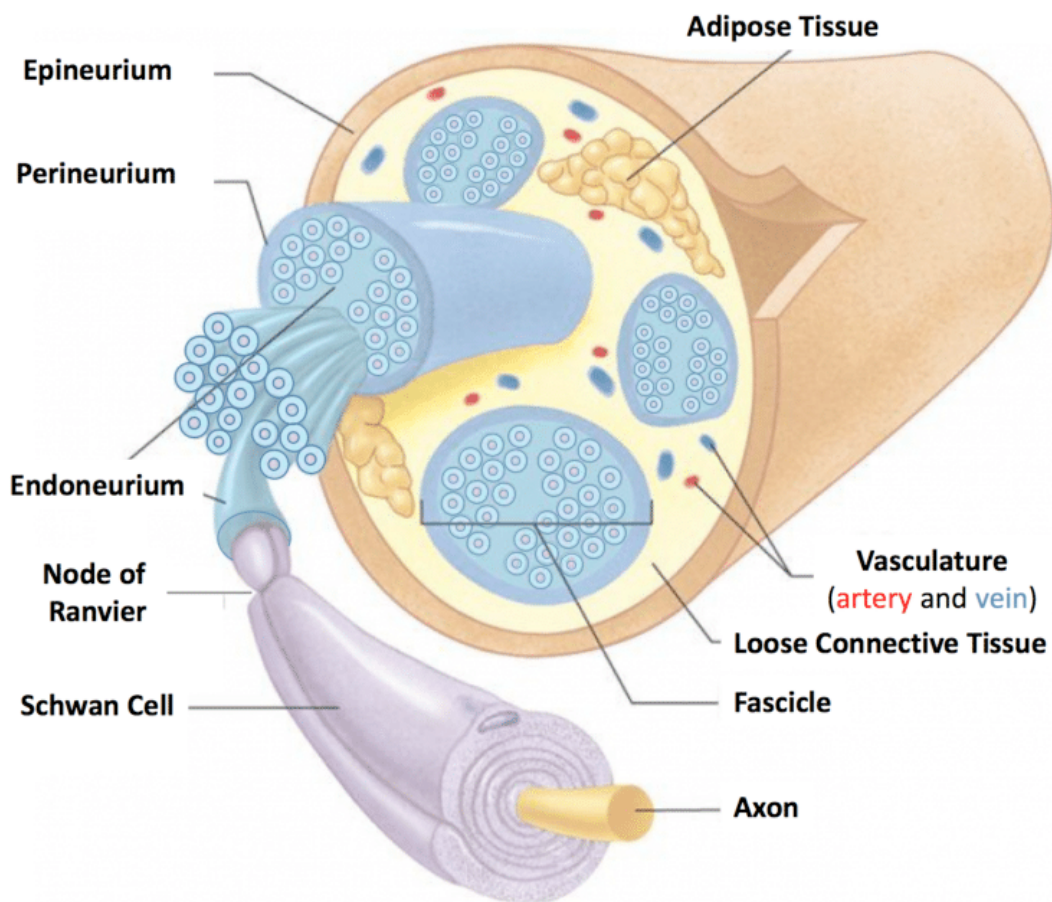
**Figure 1: Structure of the peripheral nerve**

The three outer connective tissue layers of the peripheral nerve – the outermost epineurium, the perineurium in the middle and the innermost endoneurium. Nerve impulses in the peripheral nerve are transmitted via axons that are either enveloped by Schwann cells (myelin sheath) or remain unmyelinated. A nerve fascicle is a collection of axons enclosed by the perineurium. Several blood vessels also run through a peripheral nerve with only the epineurial vasculature shown in the image (Kuliasha *et al.*, 2018).

## 1.2 SCHWANN CELLS AND THEIR ROLE IN DEVELOPMENT

Schwann cells' (SCs) function in a normal adult nerve is to support axons, whether by myelination and/or trophic support. SCs also have a major role in both development and injury of the peripheral nerve. During development neural crest cells (NCCs) differentiate into SC precursors (among several other cell types) which generate immature SCs with the ultimate goal of forming myelinating and non-myelinating mature SCs (Jessen and Mirsky, 2005).

### 1.2.1 From neural crest cells to Schwann cell precursors

Neural crest cells (NCC) are multipotent embryonic progenitors and give rise to several other structures such as craniofacial bone and cartilage, neurons and other glial subtypes of the PNS and the enteric nervous system. NCC induction requires the activation of several signalling pathways and transcription factors. Among them fibroblast growth factor (FGF) and Wnt signalling induce neural crest progenitors at the edge of the neural and non-neural ectoderm (Stuhlmiller and García-Castro, 2012). Expression of transcription factor sex-determining region Y-box 10 (Sox10) and neuregulin-1(NRG1) is required for the generation of Schwann cell precursors (SC precursors) from NCCs which occurs around embryonic day 12.5 (E12.5) in mice (Britsch *et al.,* 2001; Birchmeier and Nave, 2008). The formation of SC precursors signifies the start of gliogenesis, a process defined by the generation of non-neuronal cells, in the developing nerves.

All NCCs express Sox10 which is necessary for the specification of glial cells of the PNS, as observed in Sox10 null mice resulting in absence of peripheral glia, however Sox10 expression is turned off in differentiated neurons (Britsch *et al.,* 2001). Additionally, Sox10 also regulates the response of NCCs to neuregulin-1 (NRG1) by controlling the expression of one of the NRG-1 receptors ErbB3 (Britsch *et al.,* 2001). In vitro NRG1 was shown to be an inhibitor of neurogenesis or neuronal differentiation from NCCs which is crucial for gliogenesis to occur (Shah *et al.,* 1994).

Very akin to the neural crest cells, SC precursors are proliferative and migratory and give rise to several cell types such as immature SCs, enteric neurons, endoneurial fibroblasts and dental mesenchymal stem cells among several others (Furlan and Adameyko, 2018). SC precursors unlike the NCCs begin to associate with the newly formed axons. In this context, axonal contact via NRG1 is important for survival of SC precursors, with NRG1 type 3 specifically implicated for its expression by axons and binding with ErbB2/3 receptors on SC precursors (Meyer and Birchmeier., 1995; Dong *et al.,* 1995; Birchmeier, 2009).

## 1.2.2 From Schwann cell precursors to immature Schwann cells

Next, SC precursors give rise to immature SCs (E15-16 in mice), a process that requires the activation of Notch signalling (Recombination signal binding protein for immunoglobulin kappa J region (RBP-J) (Woodhoo *et al.,* 2009). This period is also

consistent with axons making their first synaptic contact and the downregulation of N-Cadherin (Wanner *et al.,* 2006). It has been suggested that N-Cadherin is involved in compaction of the nerve and its downregulation at the time of immature SC generation causes endoneurial space to appear between the glial cells, along with increased vascularisation and the development of the perineurium (Wanner *et al.,* 2006; Woodhoo and Sommer, 2008). Immature SCs, like SC precursors, are in close proximity to the axons but their survival is no longer dependent on this contact. Instead, their survival is mediated by an 'autocrine survival loop' involving a medley of survival factors including insulin-like growth factor -2 (IGF-2), leukemia inhibitory factor (LIF), neurotrophin 3 (NT3), lysophosphatidic acid and platelet-derived growth factor- β (PDGF-β) (Meier *et al.,* 1999; Weiner and Chun, 1999). Jessen and Mirsky (2005) suggested that SC precursors' dependence on axons for survival might be necessary to match the number of SCs to axons, whereas immature SCs 'autocrine survival loop' is to solely ensure SC survival and allow axon regeneration in a scenario wherein axons are injured.

The formation of immature SCs coincides with increased proliferation. Low level of intracellular cAMP promotes neuregulin-dependent proliferation (Arthur-Farraj *et al.,* 2011). It is worth noting that high levels of cAMP is required for NRG1-dependent myelin differentiation (Arthur-Farraj *et al.,* 2011). Notch signalling is also key in controlling proliferation of immature SCs thus maintaining their population for matching axon/SC numbers (Woodhoo *et al.,* 2009).

## 1.2.3 Radial sorting and formation of mature Schwann cells

Immature SCs develop an extracellular matrix (ECM)-rich basal lamina which persists in normal adult nerves. Endoneurial fibroblasts also secrete vital ECMs and separate mixed caliber axons into bundles with their associated immature SCs into 'families' (Webster *et al.*, 1973). Webster *et al.*'s (1973) work in studying this process in developing nerves, shed some light on the mechanism of radial sorting, a process involving the segregation of single axons from their families to be enveloped by a single SC in preparation for myelination. These surrounding immature SC families, extend cytoplasmic processes among the axon bundle and separates the larger axons at the edge of the bundle. Notch signalling also delays myelination during this stage to prevent premature myelination without interfering in radial sorting (Woodhoo *et al.,* 2009). SCs subdivide the axon bundles and ensheath the large caliber axons in 1:1 ratio, after depositing SC's own basal lamina (termed as defasciculation), a prerequisite for myelination.

G protein-coupled receptor Gpr126 has been shown to be required for axonal sorting in mice, with a delay in axonal sorting observed in Gpr126 knockout mice and SC-specific Gpr126 knockout mice from postnatal day 1 (P1) (Monk *et al*., 2011; Mogha *et al*., 2013; Monk *et al*., 2015). However, in Gpr126 mutant zebrafish radial sorting was not affected (Monk *et al.,* 2009). Importantly, in both zebrafish and mouse Gpr126 mutant models, SCs were arrested at the promyelinating stage and failed to myelinate the axons (Monk

*et al.*, 2009; Monk *et al*., 2011; Mogha *et al*., 2013). The level of cAMP was shown to be regulated by Gpr126, with elevation of cAMP and protein kinase A (PKA) in vitro restoring myelination in DRG cultures derived from Gpr126 knockout mice (Mogha *et al.,* 2013). The extracellular N-terminal fragment of Gpr126 was shown to be important for radial sorting in zebrafish while the seven transmembrane (7TM)-containing C-terminal fragment (CTF) was important for cAMP-dependent activation of myelin gene expression (Petersen *et al.,* 2015). Additionally, these functions of the two fragments of Gpr126 in SC development is regulated by interactions of Gpr126 with Laminin-211 (Peterson *et al.,* 2015). While Laminin-211 activity has been thought to promote myelination, it may also suppress the activity of Neuregulin 1 type III to inhibit PKA activation in myelination, which may be aberrant in hypermyelinating neuropathies (Ghidinelli *et al.,* 2017).

Radial sorting is suggested to be highly ECM dependent, with laminin available in the basal lamina interacting with β1 integrins on SCs. This is required to polarise SCs and regulate their signalling including regulating SC proliferation (around E19/20 in mice), crucial to maintaining the 1:1 ratio (Feltri *et al.,* 2002; Yu *et al.,* 2005). This polarisation of SCs is required to organise the cytoskeleton for the cytoplasmic protrusions and to contact and identify large caliber axons (Feltri *et al.,* 2016). Rac1, a Rho family GTPase was demonstrated as a downstream effector responsible for extension of the SC cytoplasm for radial sorting (Nodari *et al.,* 2007; Benninger *et al.,* 2007).

As mentioned, the larger axons during radial sorting have SCs envelop them and thus begins the creation of the myelin sheath that improves the conduction of nerve impulses. Whereas non-myelinating SCs (Remak SCs) surround multiple small caliber axons, however a 1:1 ratio of axons with non-myelinating SCs is also possible contributing to approximately 15% of unmyelinated axons in several mammals (Jessen and Mirsky., 2008). Myelination is initiated around the time of birth in rodents, with the differentiation of immature SCs to the pro-myelinating SCs requiring several molecular changes and downregulation of genes that are prevalent during immature SC formation and proliferation (Woodhoo and Sommer, 2008). These molecular changes for establishing myelination are suggested to be in part contributed by large caliber axons that require myelination. One such example is axonal NRG1 that has been shown to be essential for regulating myelin thickness and precise SC to axon association (Michailov *et al.,* 2004). As mentioned above Gpr126 has been shown to be important for SC myelination (Monk *et al*., 2009; Monk *et al*., 2011; Mogha *et al*., 2013).Other secreted molecules such as those from the neurotrophic factor family – brain derived neurotrophic factor (BDNF), glial cell line derived neurotrophic factor (GDNF) and Neurotrophin-1 (NT-3) among others, have been shown to promote myelination in vitro (Chan *et al.,* 2001; Höke *et al.,* 2003).

Several transcription factors are also involved in myelination such as Krox-20, a key myelination driver and a suppressor of immature SCs; and POU transcription factor Oct-

6, important for the transition of pro-myelin SCs to myelinating SCs (Topilko *et al.,* 1994; Jaegle *et al.,* 1996). The alignment of the Remak cells around non-myelinating axons suggests that there might be molecular changes that drive this existence, however this has not been widely elucidated (Harty and Monk, 2017).

Finally in a mature peripheral nerve, SCs can be segregated into two types – myelinating SCs that ensheath several axons and non-myelinating or Remak SCs (Griffin *et al.,* 1995). The former is responsible for forming a multi-layered myelin sheath surrounding the motor and sensory axons. They are uniformly located along the length of an axon and surround a single axon. Myelinating SCs insulate the axons thus allowing the axons to transmit action potentials considerably faster than they could without the myelin sheath. Meanwhile, Remak cells, loosely enclose small, 0.5 to 1.5 µm diameter axons. The non-myelinating SCs use their cytoplasmic processes to partition the axons.

Although the developmental differentiation and generation of mature SCs has been studied there are still gaps in key molecular changes during the different transitions. The intricacy of SC generation during development is almost as and, in many ways, more complex in the event of an injury wherein SC plasticity or their ability to acquire a repair phenotype to aid in regeneration and repair of the injury site is highlighted.

## 1.3   PERIPHERAL NERVE INJURY

Traumatic peripheral nerve injuries (PNI) are becoming increasingly common and most severe injuries require surgical repair. These injuries often cause neuropathic pain and, in several cases, permanent loss of motor and sensory function (Siemionov and Brzezicki, 2009). This further affects the quality of life of such patients, resulting in physical disability, and in many cases leads to damaging social and economic consequences.

There are several causes of PNI such as direct trauma, stretching, vibration, compression, and microvascular injury. Seddon (1943) classified nerve injuries into three types – Neuropraxia is a comparatively milder form of nerve injury which commonly occurs when a nerve is compressed or stretched such that there is demyelination at the site of injury whereas axonal continuity remains intact (Figure 2) (Seddon *et al.*, 1943). Axonotmesis, the second type of injury occurs because of compression or more serious trauma to the nerve causing damage to the axons and the myelin sheath (Figure 2) (Seddon *et al.*, 1943). The outer connective tissues of the nerve namely the perineurium and the epineurium are not affected, due to which the structural shape of the nerve is maintained. Neurotmesis is the most critical form of injury characterised by a full transection of the axons and the layers covering the nerve (Figure 2) (Seddon *et al.*, 1943). Surgical intervention is required for this type of injury, however complete recovery is highly unlikely.
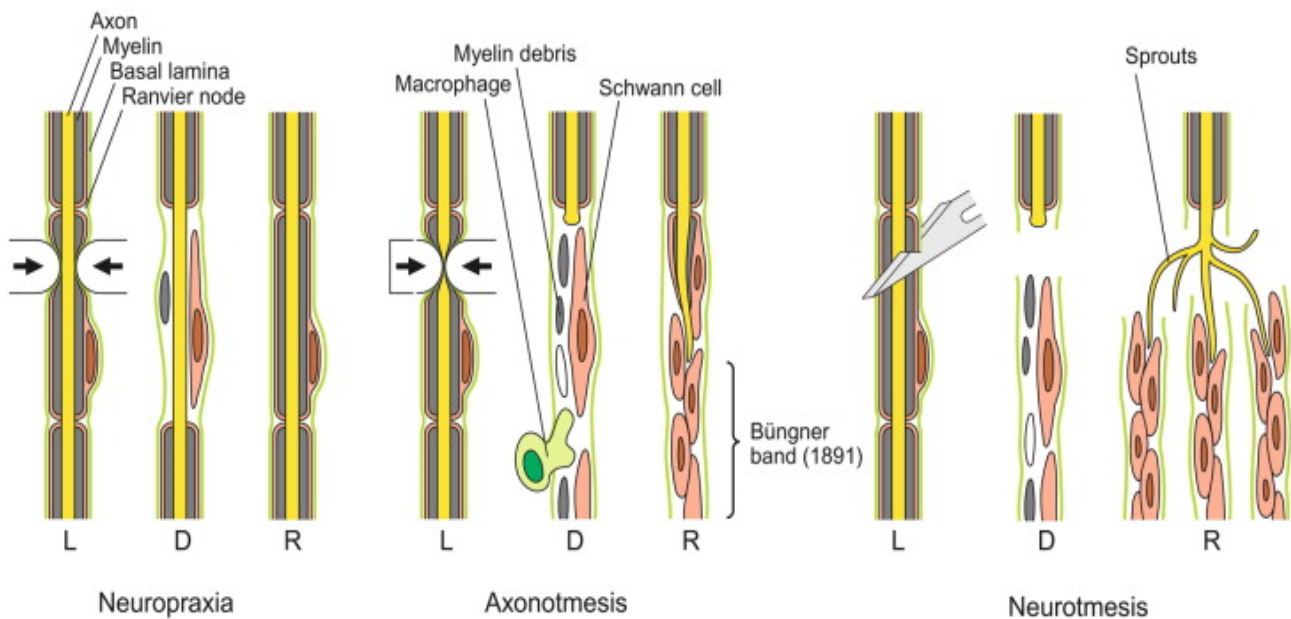
**Figure 2: Illustration of three classes of peripheral nerve injuries**

Three classes of nerve injury – neuropraxia, axonotmesis and neurotmesis have been described by Seddon *et al.* (1943). L, D and R denotes lesion/injury site, demyelination/Wallerian degeneration, and regeneration, respectively for the three types of peripheral nerve injuries. In neuropraxia only the myelin sheath is damaged. In axonotmesis both, the axons and surrounding myelin sheath is damaged however the outer connective tissues remain intact. In neurotmesis, the nerve is completely severed. Wallerian degeneration involving demyelination of myelin and removal of myelin debris is more pronounced in axonotmesis and neurotmesis requiring Schwann cells to aid in the regeneration of axons (Fugleholm, 2013).

## 1.4 CENTRAL VS PERIPHERAL NERVOUS SYSTEM IN REGENERATION

When compared to the central nervous system (CNS), nerves of the PNS are able to regenerate mainly owing to the presence of Schwann cells (SCs) and recruitment of

macrophages. Following a traumatic injury to a peripheral nerve such as the sciatic nerve, axons can regenerate and reinnervate their targets again (Scheib and Höke, 2013). In an injury with damage to the axons, axons degenerate, and SC demyelination of axons occurs which then requires the elimination of the myelin and axonal debris by SCs and macrophages. This is then followed by axonal regeneration and the formation of new myelin for myelinating axons and new Remak bundles for non-myelinating axons (Scheib and Höke, 2013; Lutz and Barres, 2014). Although the regenerated nerve is almost similar in structure and function as that of an uninjured nerve, the new myelin is often thinner and the internodal distance of myelinating axons is reduced (Schröder, 1972; Sherman and Brophy, 2005). This entire process of degeneration and regeneration in the peripheral nervous system (PNS) is covered in detail in the next few sections. In comparison, in the CNS, oligodendrocytes (OLs) (that myelinate axons), microglia and astrocytes are the major cell types involved in injury response (Rotshenker, 2011).

The experiments of David and Aguayo (1981) clearly demonstrated the environment of the PNS and CNS as the reason for their differing capacity to regenerate injured nerve fibres. Using rat sciatic nerve as a bridge graft connecting spinal cord and the lower medulla, with the grafting site acting as injury, axons elongated from both ends and were ensheathed by SCs suggesting that it is the environment within the CNS that does not support axon growth. Another striking difference is the ratio of myelinated to unmyelinated axons in both systems. In the CNS very few axons are unmyelinated thus

in intact CNS, there is faster conduction of nerve impulses with low energy consumption whereas in PNS there are higher population of unmyelinated axons such as the C fibres nociceptors, in comparison to the myelinated (Griffin and Thompson, 2008). However, it is not known whether there is a relevant link between this difference in unmyelinated fibres in intact CNS and PNS versus the regenerative capabilities of both systems following injury.

Post-injury, the denervated SCs respond promptly to create an environment favouring regeneration, however in comparison OLs are sensitive to the toxic environment at the lesion site and undergo apoptosis and necrosis (Li *et al.,* 1999; Lytle and Wrathall., 2007). The toxic environment of the lesion site is caused by many factors. For instance, the secretion of proteolytic enzymes that can digest cells from necrotic cells; ischemia contributing to free radical formation and reactive oxygen which results in oxidative stress and adversely affects OLs (Almad *et al.,* 2011). A CNS injury naturally causes demyelination of OLs resulting in myelin debris, which is not cleared in the CNS and inhibits axonal regeneration. Moreover OLs provide little to no support for axonal growth, thus preventing axonal regeneration and survival (Almad *et al.,* 2011). However, remyelination of axons albeit with thinner myelin does takes place post-injury of the CNS, with studies showing that oligodendrocyte progenitor cells (OPCs) proliferate and migrate to myelinate axons (Watanabe *et al.,* 2002; Blakemore and Keirstead, 1999; Almad *et al.,* 2011). These OPCs, as the name suggest are the progenitor cells for OLs,

36

are abundant in the adult CNS and after demyelination, they proliferate and migrate to the site of demyelination and remyelinate axons.

Another major difference between CNS and PNS is the absence of basal lamina in OLs while in the PNS SCs assemble basal lamina consisting of several extracellular matrices such as laminin, collagen and fibronectin that promote axon growth during development and in regeneration of axons among their many other roles (Colognato and Tzvetanova, 2011).

In terms of inflammatory response post-injury, in the PNS it is crucial that macrophages remove myelin debris by phagocytosis before the initiation of axonal outgrowth. However, in the CNS macrophage recruitment is hindered due to restrictive blood-brain barrier which is only permeable at the injury site (George and Griffin., 1994). In the PNS, the blood nerve barrier, which is damaged at the site of injury also becomes permeable along the distal nerve segment thus allowing the entry of inflammatory molecules. In the CNS, the astrocytes are the main cells involved in inflammation that have been demonstrated to express a high number of phagocytotic receptors (Lutz and Barres, 2014). Astrocytes produce several cytokines and chemokines, however it is not very clear why astrocytes are unable to clear injury-caused debris in the CNS (Lutz and Barres, 2014). It is therefore evident that for successful CNS regeneration in an injury model, it is important to study the environment of not only the CNS but the PNS as well in order

to navigate therapeutic options and strategies for introducing a pro-axon re-growth environment in the CNS.

## 1.5 EVENTS POST TRAUMATIC PERIPHERAL NERVE INJURY

### 1.5.1 Wallerian degeneration

An axonal injury provokes a cascade of non-neuronal cell responses in the peripheral nerve, specifically in the distal end of an injured nerve, termed as Wallerian degeneration (WD) (Waller, 1850). As such both crush and transection injuries trigger WD, with the injured nerve divided into three segments – the injury site, the portion of the nerve proximal to the injury and the segment of the nerve distal to the injury site. As mentioned previously, in a transection injury the distal nerve segment is completely severed from the proximal segment of the nerve (Figure 3A). The degeneration of the detached distal axons is a critical step in WD (Figure 3B). This prompts a well-synchronised non-neuronal cell response for the removal of regeneration-inhibiting myelin debris in the injured nerve as well as regulation of gene expression and secretion of growth factors that promote axonal outgrowth post-injury (Griffin *et al.*, 1995). The degeneration of distal axons is often delayed, which can take anywhere from 24-48h after injury in rodents (Figure 3B) (Miledi and Slater, 1970; Beirowski *et al.*, 2005).

Extensive work done on the Wallerian degeneration slow (Wld$^s$) mice demonstrated a longer survival period of distal axons (2-3 weeks) following nerve transection injury (Lunn

*et al*., 1989). Prior to this, it was thought that WD was initiated due to lack of nourishment of the distal axons from the cell body of the axons following transection injury (Waller, 1850). Wld[s] gene encodes a fusion protein of ubiquitin ligase Ube4b and nicotinamide mononucleotide adenylyltransferase 1 (Nmnat1) (Mack *et al*., 2001). Nmnat1 is an enzyme involved in the synthesis of nicotinamide adenine dinucleotide (NAD). Overexpression of nuclear Nmnat1 in five lines of transgenic mice was not sufficient to protect distal axons from degeneration after sciatic nerve transection in comparison to the Wld[s] mouse (Conforti *et al*., 2007). However, targeting Nmnat1 to axons in transgenic mice prevented degeneration of distal axons for a longer duration than Wld[s] mouse following transection injury (Babetto *et al.,* 2010).

Another mammalian Nmnat isoform - Nmnat2, was shown to be an essential axon survival factor (Gilley and Coleman, 2010; Gilley *et al*., 2013). The half-life of Nmnat2 is very short, and therefore its loss during injury, or any disruption of Nmant2 transport to the axons from the cell body results in quick depletion of Nmant2 in the distal axons (Coleman and Höke, 2020). This loss of Nmnat 2 also leads to a decrease in NAD levels, however NAD degradation is also initiated by Toll-like receptor adaptor protein called sterile-α and Toll/interleukin 1 receptor (TIR) motif containing protein 1 (SARM1), which acts downstream of Nmnat2 loss in WD (Gerdts *et al.,* 2015; Gilley *et al.,* 2015; Essuman *et al.,* 2017). This depletion of NAD might be central to axon degeneration due to a failure in synthesis of ATP. Changes in calcium influx is one alternative mechanism. Other

SARM1 substrates such as ADPR and cADPR that are involved in regulation of calcium could be important for the later stages of WD (Zhao *et al.,* 2019; Coleman and Höke, 2020).

Entry of calcium into the axoplasm (the cytoplasm of the axons) activates calpain, an axonal protease that brings about the granular fragmentation of the cytoskeleton of axons and its degeneration (Figure 3B) (Schlaepfer and Bunge, 1973; George *et al.*, 1995; Touma *et al.*, 2007).

## 1.5.2 Demyelination

In the initial days following an injury involving WD, SCs are key to ensuring the degradation and phagocytosis of the myelin and axon debris (Figure 3B). As discussed previously, during development as well as for mature axons, SCs provide critical trophic support, but this becomes quite obvious during axonal injury.

Early on in WD, SCs in the distal nerve segment convert to repair SCs which is suggested to be facilitated by the ubiquitin-proteosome system. It was shown that inhibition of this system post-injury in mice, supressed this conversion of SCs (Lee *et al.*, 2009). Both myelinating and non-myelinating SCs undergo several gene expression changes to allow the glial cells to shift its function to axon regeneration from maintaining axonal ensheathment (Figure 3B). Myelinating SCs of the injured axons actually respond very early on, prior to axonal degeneration by shifting gene expression (Liu *et al.*, 1995;

Guertin *et al.*, 2005). This involves first downregulating genes that encourage myelination including the early growth response protein 2 (Egr2/Krox20), P0, myelin protein zero (MPZ)/myelin basic protein (MBP), myelin-associated glycoprotein, gap junction protein connexin 32 (Cx32), and periaxin, POU domain class 3 transcription factor 1 (or known as Oct-6) (Topilko *et al.*, 1994; Balakrishnan *et al.*, 2016; Jessen and Mirsky *et al.*, 2008; Ghislain and Charnay, 2006; LeBlanc *et al.*, 2006). This also involves upregulation of genes such as c-Jun and neurogenic locus notch homolog protein (Notch) that inhibit myelination (Parkinson *et al.*, 2008; Arthur-Farraj *et al.*, 2012; Woodhoo *et al.*, 2009). Several of these growth factors and transcription factors are discussed in more detail in future sections.

Gene expression changes allow the SCs to demyelinate the axons distal to the injury site and are converted into repair SCs that significantly contribute to the regeneration of the damaged axons (Nocera and Jacob, 2020). Once the axons degenerate, the breakdown of myelin can take place within 48 hours of injury, with SCs fragmenting their own myelin sheath resulting in myelin ovoids (Figure 3B) (Stoll *et al.*, 1989). Therefore, in the first 4-7 days following PNI, mainly the repair SCs are involved in degrading and clearing the myelin by myelinophagy (Perry *et al.,* 1995; Gomez-Sanchez *et al.,* 2015; Jang *et al.*, 2016; Lutz *et al.,* 2017).

## 1.5.3 Blood-nerve barrier permeability

The blood-nerve barrier (BNB) consists of endothelial cells interconnected by tight junctions and restricts the passage of blood-borne substances (Kanda, 2013). It is situated at the inmost layer of the perineurium and the endoneurial microvessels (Malong *et al*., 2023). Following a peripheral injury, the BNB becomes 'leaky', distal to the injury site thus allowing the entry of molecules from blood into the neural tissue (Weerasuriya and Mizisin, 2011) (Figure 3C).  During this event, the BNB is partially permeable for a period of approximately four weeks after injury (Gray *et al*., 2007).

Even though a breach in the BNB is to be expected at the injury site, the breakdown of the barrier is not observed anywhere else until axon degeneration is initiated. Interestingly, the period of peak immune response in an injured nerve coincides with the maximum permeability of the perineurium, which occurs between four days to a week post-injury (Weerasuriya and Hockman, 1992). The BNB therefore becomes permeable enough to allow critical immune cells in blood circulation to enter the nerve for the purpose of repair. This permeability of the BNB reduces two weeks post PNI and increases again for a second time which is suggestive of the timepoint during which myelin is discharged from the endoneurium (Weerasuriya, and Hockman., 1992).

## 1.5.4 Recruitment of inflammatory factors for myelin debris clearance

In this next stage of WD, macrophages and SCs work in tandem to clear the myelin debris, the clearance of which is key to establishing a permissive milieu for the future regenerating axons (Figure 3C). As mentioned previously, SCs also initiate myelin debris clearance by myelinophagy following peripheral nerve injury (Perry *et al.,* 1995; Gomez-Sanchez *et al.,* 2015). Additionally, these newly formed repair SCs perform a myriad of functions, for instance they produce several trophic factors, cytokines such as leukemia inhibitory factor (LIF), several interleukins and monocyte chemoattractant protein-1 (MCP-1) which works to attract macrophages (Siebert *et al*., 2000; Tofaris *et al*., 2002). Blood derived macrophage recruitment is also dependant on the expression of chemokine receptor CCR2 which binds to MCP-1 secreted by SCs. Siebert *et al.* (2000) demonstrated a reduced influx of macrophages in CCR2-knockout mice post-transection injury.

Within a week of PNI, hematogenous macrophages, recruited by SCs, invade the injury site, due to the leaky blood-nerve barrier, and take on the leading role of clearing myelin and axonal debris by phagocytosis, a process involving engulfment of particles by cells via membrane protrusions (Figure 3C) (Hirata and Kawabuchi, 2002; Hall, 2005). The macrophages are directed to the injured area by local cues and when there is damage to

only a subgroup of axons in a peripheral nerve, they mainly gather around the injured axons (Stoll *et al.*, 1989).

Macrophages have also been shown to produce mitogenic factors which aid in SC proliferation (Figure 3C) (Baichwal *et al.*, 1988). They also upregulate apolipoprotein E (apoE), which is known to be an essential lipid carrier and during WD helps in metabolising lipids post myelin breakdown (Ignatius *et al.*, 1987; Boyles *et al.*, 1989). ApoE also helps in reutilisation of the degraded lipid during axonal regeneration by SCs and axons (Ignatius *et al.*, 1987; Boyles *et al.*, 1989).

Barrette *et al.* (2008) used transgenic mice that expressed a mutant form of the HSV-1 thymidine kinase (TK) regulated by the myeloid-specific CD11b gene promoter (CD11b-TK$^{mt-30}$) wherein delivery of ganciclovir (GCV) to the mice caused the selective deletion of proliferating CD11b positive cells. In their mouse model, 7 days following a sciatic nerve crush injury, the recruitment and proliferation of macrophages and granulocytes distal to the injury site, was significantly reduced (Barrette *et al.*, 2008). The authors showed that this depletion of the two populations of immune cells severely impaired functional recovery, diminished myelin debris clearance in the distal sciatic nerve and angiogenesis or the formation of new blood vessels was significantly reduced following a sciatic nerve crush injury. In another experiment the authors performed a crush injury in the sciatic nerves of the GCV treated CD11b-TK$^{mt-30}$ or saline control mice and 7 days

following injury they cut out and grafted the distal sciatic nerve between the proximal and distal stumps of transected recipient mice to study axon regeneration (Barrette *et al.,* 2008). Their observation on axonal regrowth showed that the axons failed to regenerate within the graft as compared to the control mice, two weeks following the allograft. The work of Barrette *et al.* (2008) was important in elucidating the role of macrophages in myelin clearance, axon regeneration and angiogenesis.

There are a small number of resident macrophages which in an uninjured nerve in the PNS, accounts for 2-9% of all cells and have been shown in rat sciatic nerve explant cultures to not only proliferate post-injury but also phagocytose myelin debris (Shen *et al.*, 2000). Resident endoneurial macrophages begin phagocytosis of neuronal debris at the earliest, two days after a crush injury in rats and proliferate at day 3 and 4 before the recruitment of hematogenous macrophages from across the blood-nerve barrier (Mueller *et al.*, 2001). They constitutively express major histocompatibility complex molecules (MHC), essential for initiating immune responses (Monaco *et al.*, 1992).

Other than macrophages, the lesion site is also infiltrated by inflammatory immune cells such as neutrophils (Perkins and Tracey, 2000), T-lymphocytes (Moalem *et al.,* 2004) and non-inflammatory fibroblasts (during a transection injury) (Parrinello *et al.*, 2010) (Figure 3C). Neutrophils are the earliest inflammatory leukocytes to gain entry with a role in phagocytosis of nerve debris as well as recruiting monocytes and are also involved in

deciding the differentiation of macrophages to a pro- or anti-inflammatory state (Chertov *et al.*, 1997; Lindborg *et al.,* 2017). In a rat injury model, the density of neutrophils was substantial at the site of nerve injury, 8 hours post-surgery peaking at 24 hours after injury before decreasing in numbers by day 3 (Perkins and Tracey, 2000). Another study demonstrated that neutrophils are effective phagocytes and are essential for myelin clearance (Lindborg *et al.*, 2017). As described above, mice with a global knockout of chemokine receptor CCR2, had a reduction in the recruitment of macrophages after PNI (Siebert *et al.,* 2000). Niemi *et al.* (2013), demonstrated that myelin debris clearance was not impeded 7 days after transection injury. Further work done by the same lab group showed that depletion of neutrophils by antibody treatment in the wild-type and the same CCR2 knockout mice, impeded myelin debris clearance 7 days after transection injury (Lindborg *et al.*, 2017).

T-lymphocytes are one of the last immune cells to be recruited (Figure 3C). They were detected on day 3 at the injury site and a lower count detected in the proximal and distal nerve stump post-sciatic nerve constriction injury, peaking at three weeks post-injury, following which their numbers decreased (Moalem *et al.,* 2004). In the first stage of WD, around day 3 after injury, Type 1 helper cells (Th1) cells produce pro-inflammatory cytokines such as IL-18, tumour necrosis factor α (TNF-α) and interferon γ (IFN-γ) that polarise and activate M1 macrophages (associated with acute inflammatory responses), natural killer cells (NK cells) and neutrophils (Fregnan *et al.*, 2012; Bombeiro *et al.*, 2020).

Type 2 helper cells (Th2) produce anti-inflammatory cytokines such as IL-10 and IL-4 after macrophage recruitment, thus promoting M2 polarisation of macrophages and also suppressing pro-inflammatory signalling pathways (Fregnan *et al.*, 2012).

Macrophages can persist in the injured nerve for months after which they either undergo apoptosis or travel to the lymphoid organs via the circulation (Kuhlmann *et al.*, 2001). The exit of phagocytotic macrophages is essential to resolving the inflammatory state of the regenerating nerve (Figure 3F). Study done on macrophage clearance has shown that macrophages express Nogo receptors, NgR1 and NgR2, whose function is to bind myelin-associated inhibitory proteins (Fry *et al.*, 2007). Post-axon regrowth and remyelination, macrophages expressing these receptors are repelled by myelin on the new axons via RhoA activation and leave the nerve via SC basal lamina and enter circulation via the blood-nerve barrier. Therefore, a complex interaction between SCs and various inflammatory cells is required for removal of axonal and myelin debris post-PNI to allow regeneration of injured axons.

### 1.5.5 Control of Schwann cell proliferation and gene regulation post-injury

SC proliferation, early in WD, was previously shown to be modulated by neuregulin and its receptors erbB kinases (erbB2 and 3) in an autocrine or paracrine manner by SCs themselves (Carroll *et al.*, 1997). However subsequent in vivo work has contradicted this finding (Atanasoski *et al.* 2006; Fricker *et al.,* 2013). Atanasoski *et al.* (2006) using adult

mice with Schwann cell-specific ablation of erbB2 showed that this deletion did not affect SC proliferation at 4 and 12-days post-transection injury in the distal sciatic nerve. In another study, deletion of neuregulin 1 in axons using a tamoxifen inducible Cre recombinase mouse did not affect distal SC proliferation following transection injury of the sciatic nerve (Fricker *et al.*, 2013).

Several mitogens promote SC proliferation in vitro such as platelet-derived growth factor (PDGF-B) and fibroblast growth factors (FGFs) and have been shown to be secreted by macrophages (Schubert, 1992; Oya *et al.*, 2002; Brecknell and Fawcett, 1996). Evidently there is an additional SC proliferation phase after the regenerated axons innervate the distal nerve (Pellegrino and Spencer, 1985). These proliferating SCs are restricted to their basal lamina tubes wherein their longitudinal alignment is necessary to form bands of Büngner, which serve as substrate for the growing axons to allow their re-growth to their distal target (Figure 3D) (Stoll *et al.*, 1989).

Kim *et al.* (2000) reported impaired proliferation of SCs in the distal nerve stump, 7 days following a sciatic nerve transection injury in cyclin D1 knockout mice. Interestingly, the axonal outgrowth in the cyclin D1 knockout mice was comparable to the wild-type control mice following a crush injury, despite the inability of SCs to replicate in the knockout model. Atanasoski *et al.* (2008) showed in cyclin-dependent kinase 4 (CDK4) deficient mice, an absence of SC proliferation in the distal nerve stump at a timepoint of

4 and 12-days post sciatic nerve transection injury as compared to the wild-type injured mice. This showed that cdk4 is required for SCs to re-enter the cell cycle following transection injury.

Repair SCs also secrete several inflammatory cytokines including interleukin-1α (IL-1α), interleukin-1β (IL-1β) and the tumour necrosis factor α (TNFα), (Shamash *et al*., 2002). They also upregulate several neurotrophic factors such as the brain-derived neurotrophic factor (BDNF), and its receptor, the low affinity nerve growth factor receptor (NGFR), and the glial cell-line-derived neurotrophic factor (GDNF) among others, many of which are essential for axonal regrowth (Meyer *et al*., 1992; You *et al*., 1997; Chen *et al*., 2007; Höke *et al*., 2002). Several transcription factors such as SRY (sex determining region Y)-box 2 (Sox2), cJun, oligodendrocyte transcription factor 1 (Olig1), paired box gene 3 (Pax3), Runx2, as well as axon guidance molecules and their receptors are also upregulated post-injury such as Roundabout Guidance Receptor 1 (Robo1) and EphB2 (Li *et al*., 2021, Balakrishnan *et al*., 2021). Several of the above mentioned genes, neurotrophins, transcription factors and axon guidance molecules are discussed in detail in the later sections of the introduction.

**A**

Dorsal root (sensory input)

Dorsal root ganglion (DRG)

Injury site

Muscle/ Target organ

Ventral root (motor output)

Spinal cord

Cell bodies

Basal lamina

Epineurium

Perineurium

Node of Ranvier

Myelinated Axons

**B**

Proximal
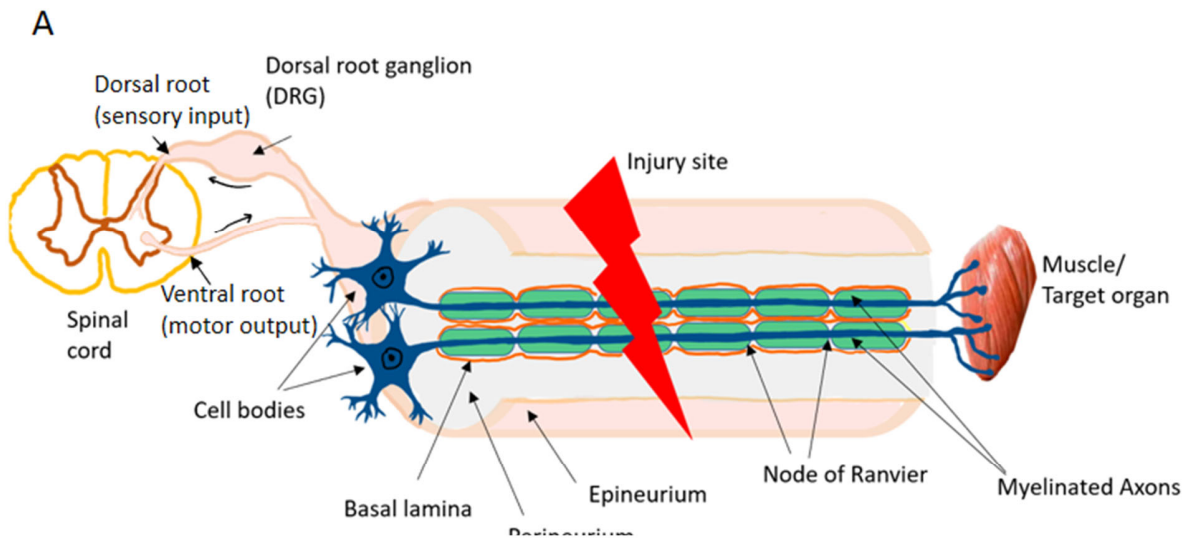
Distal

**Step 1: 24hrs after injury**

**Distal nerve segment – Wallerian degeneration (WD)**

- Swelling in the distal axons, calcium influx and fragmentation of axons by proteases
- Pro-inflammatory cytokines and chemokines are produced
- Downregulation of pro-myelination genes, upregulation of myelin inhibiting genes
- Schwann cell (SC) demyelination forming myelin debris
- SCs convert into a repair phenotype

**Proximal nerve segment**

- Anterograde axoplasmic transport causes swelling of axon ends; cell body swelling and chromatolysis (displacement of nucleus and dissolution of Nissl bodies)
- Die back of axons up to first node of Ranvier

**C**

**Step 2: 3-5 days after injury**

- Blood nerve barrier compromised at injury, partial permeability in the distal nerve
- Neutrophils are first immune responders to be recruited
- SCs begin degrading their myelin, upregulate regeneration associated transcription factors, recruit macrophages across permeable blood nerve barrier for myelin and axonal debris phagocytosis along with resident macrophages
- T-lymphocytes are recruited and produce pro-inflammatory cytokines
- SCs proliferate and macrophages produce mitogens for SC proliferation
- Fibroblasts and perineurial cells begin migration into the lesion site
- Vascularisation is complete before SC migration is initiated.

**D**

**Step 3: 5-7 days after injury**

- Anti-inflammatory cytokines are recruited
- In the distal nerve SCs form Bands of Bungner
- Several daughter axonal sprouts per parent axons are formed
- SC migrate into the lesion site from the proximal and distal nerve stump
- Shrinkage of axon terminals from the target at the end of WD

**E**

Bridge

**Step 4: 1-2 weeks after injury**

- SC cords formed by migrating SCs guide the axons across the nerve bridge
- Axon guidance molecules are secreted or presented by surrounding axons and cells (contact mediated cues) to direct regenerating axons led by the growth cones
- Bands of Bungner formed by SCs direct the axons once they innervate the distal nerve stump.

50

**Step 5: 2 weeks to up to a month after injury**
- Leading axonal sprouts innervate the target and widen
- Other unsuccessful axonal sprouts are atrophied.
- SC myelinate axons, upregulate promyelination genes and transcription factors
- Macrophages exit the nerve via the blood nerve barrier or die

**Unsuccesful regeneration**
Fibroblast scar tissue, large injury gap and any defects during Wallerian degeneration can cause aberrant trajectories of axons and formation of neuroma resulting in atrophy of target tissue.

**Figure Key**

| | |
|---|---|
| Myelinating Schwann cell | Resident macrophage |
| Repair Schwann cell | Recruited macrophage |
| Myelin ovoid | Neutrophil |
| Pro-inflammatory cytokine – e.g IL-1,2,6 TNF | Fibroblast |
| Anti-inflammatory cytokine – e.g IL-10,TGF-β | Axon guidance cues and trophic factors – e.g BDNF,NGF, Netrin-1 |
| Blood vessels/Blood nerve barrier | Axonal sprouts with growth cones |
| | Scar tissue made of fibroblasts and extracellular molecules |
| | Neuroma |

**Figure 3: The steps involved in peripheral nerve repair after an injury**

Steps describing the events following peripheral nerve injury as studied in rodents with a transection injury in the sciatic nerve illustrated as an example. (A) A normal peripheral nerve undergoes a traumatic injury with a complete transection injury as depicted in the figure. The cell body of neurons is located in gray matter in the ventral horn (motor axons) or the dorsal root ganglia (sensory axons). The myelinated axons extend to their target, depicted by an image of a muscle in this instance, where they terminate and synapse to mediate their action. (B-D) The process of Wallerian degeneration is described in detail. (E-F) This is followed by axonal regeneration with the axons innervating their target organ during the outcome of a successful peripheral nerve regeneration. (G) In contrast depicts an unsuccessful regeneration leading to atrophy of the muscle.

## 1.5.6 Axonal Regeneration

Unlike the distal nerve, the proximal segment of the nerve undergoes changes based on the type of injury and its vicinity to the neuronal body. The proximal nerve also exhibits degeneration, typically back up to the first node of Ranvier and is dependent on calcium influx via voltage-dependent ion channels (Stoll *et al*., 2002; Bradke *et al*., 2012). The proximal end also undergoes swelling at the injury site, which can be explained by the blockade of materials such as organelles and proteins that are being transported from the cell body towards their end-targets via the axons (Figure 3B) (Zelená *et al*., 1968; Fu and Gordan, 1997). Nissl's granules are made up of rough endoplasmic reticulum and ribosomes in the cytoplasm of the cell body. Following injury, Nissl's granules are dissolved and become dispersed from the centre to the edge of the cell body along with the nucleus, to increase protein synthesis for regeneration of axons (Figure 3B). This is also accompanied by swelling of the neuronal cell bodies and this process is called chromatolysis (Figure 3B) (Fu and Gordan, 1997)

Axonal regrowth into the distal nerve is initiated only once the myelin debris in the distal nerve segment is cleared. However in the proximal end, the injured parental axons sprout multiple daughter axons with growth cones, located at the tip of the axons, within hours of injury (Figure 3D) (Hall, 2005) Nevertheless, it takes several days before these axonal sprouts that make up the 'regenerating unit,' to emerge from the proximal stump

and enter the nerve 'bridge' (Morris *et al.*, 1972; Hall, 2005). This nerve bridge is made up of perineurial cells, SCs, blood vessels and fibroblasts that migrate from the proximal and distal nerve between the two ends of the transected nerve (Figure 3E) (Schröder *et al.*, 1993; Parrinello *et al.*, 2010; Zochodne, 2012). Initially, the regeneration of the daughter axons is largely dependent on the cystoskeletal materials available in the vicinity of the axons such as actin and tubulin (Tetzlaff *et al.*, 1988). The microtubules serve as a link to transport other specific components needed for axonal growth between parent and daughter axons (Miller *et al*, 1987). Axons regenerate at a pace of 1-3 mm per day as studied in rabbits, rats and humans (Gutmann *et al.*, 1942; Seddon *et al.*, 1943; Sunderland, 1947), which corresponds to the general slow pace of cytoskeletal material transport in the PNS (McKerracher and Hirscheimer, 1992).

The growth cone is capable of clearing its path of any scar tissue that can interrupt the growth of the axons by secreting proteases and plasminogen activators (Siconolfi and Seeds, 2001). Axonal regeneration from the proximal end and past the lesion site is 'staggered' due to the slow and unsynchronised rate at which these axons regenerate also contributing to delayed axonal growth (Al-Majed *et al.*, 2000). In the distal nerve stump, it is critical that the growth cone extends along the bands of Büngner to accurately innervate the peripheral target organ (Figure 3E). Additionally, the growth-permissive environment produced by the SCs in the distal end of the lesion site is also required for further elongation and regeneration of the axons through the distal nerve

(Sulaiman and Gordon, 2013). On entering the distal nerve segment, the number of regenerating daughter axonal branches decreases with time as they begin to compete for the limited SC-lined regeneration tracks (Figure 3F) (MacKinnon *et al.,* 1991). Those axons that do not innervate their targets are atrophied while the axons that do innervate, mature and enlarge in size (Aitken *et al.*, 1947). Nevertheless, this process is quite long, spanning several months in humans.

If the regenerating axons are unable to innervate the distal end of the injured nerve or are misdirected during regeneration, they may form neuromas, a result of disorganised growth of immature axons and connective tissue (Figure 3G) (Battista and Cravioto, 1981). The growth cone's motility during axonal regeneration is reliant on the expression of specific receptors on its membrane which interacts with axon guidance cues that either repels or attracts the growth cone and can be either mediated by contact or chemical signals (Goodman, 1996; Zang *et al*., 2021). Several axon guidance cues and their role in PNR has been studied by my lab group including ephrins, slits and netrins as presented in this thesis.

**1.5.6.1 Role of Schwann cells in axonal regeneration and remyelination**

In mice, SCs begin migrating from the proximal and distal nerve stumps 4-5 days post-injury, while the growing axons start to attach to these migrating SCs, six days post-injury and negotiate their path through the nerve bridge (Chen *et al.,* 2019a) (Figure 3E). As

described previously (refer to Section 1.5.4), Barrette *et al*. (2008) showed that depletion of macrophages in vivo compromised the formation of blood vessels (angiogenesis) following PNI. Additionally, in their study, they observed that several axons regenerated along the trajectory of the growing blood vessels post-PNI. Cattin *et al.* (2015), further showed that at day 3 post-transection injury in rats, there was a significant invasion of blood vessels into the nerve bridge with analysis at day 2 demonstrating that this invasion arose from the proximal and distal nerve segments. Vascularisation of the injured nerve was completed prior to the influx of migrating SCs. In mice similar results were observed but with a slower rate of regeneration as compared to rats. Additionally, they showed that the macrophages in the bridge of the injured nerve secrete vascular endothelial growth factor A (VEGF-A) to aid in the creation of a polarised vascular scaffold that can direct SCs from the nerve stumps and across the bridge thus guiding the regrowing axons (Cattin *et al*., 2015). At around day 7 the migrating SCs form 'Schwann cell cords' that contributes to the nerve bridge, thus allowing the growing axons to cross the site of lesion and innervate the distal nerve segment (Chen *et al.*, 2019a) (Figure 3E).

As mentioned before, repair SCs play a vital role in promoting axonal regeneration. The repair SCs regulate several neurotrophic factors, axon guidance molecules, cytokines, cell adhesion molecules, and extracellular matrix (ECM) proteins like laminin and fibronectin to create a microenvironment promoting axonal regeneration and

remyelination which will be discussed in detail further in the chapter. For axons to regenerate (elongate), repair SCs in the distal nerve stump proliferate and align within the basal membrane of endoneurial tubes to form bands of Büngner or regeneration tracks and provide guidance to the axons for selective reinnervation of the denervated end-target (Bunge, 1987; Nathaniel and Pease, 1963). Gomez-Sanchez *et al.* (2017) by means of lineage tracing, demonstrated that both myelinating and non-myelinating SCs elongate and branch to form the bands of Büngner. Moreover once axonal regeneration is achieved, the SCs that form the bands of Büngner then convert back to the myelinating or non-myelinating SC phenotype (Gomez-Sanchez *et al.*, 2017). Once target innervation by axons is achieved, complete functional recovery is dependent on the redifferentiation of repair SCs into the myelinating and non-myelinating phenotype. However, often the new myelin is thinner than required for an axon of that diameter with shorter internodes (Schröder, 1972).

The axons that require myelin are remyelinated in a 1:1 ratio as observed in uninjured nerves and is initiated when SCs interact with the axolemma, inducing synthesis of galactocerebroside (an important component of myelin) and upregulation of pro-myelination genes in SCs (Gomez-Sanchez *et al.*, 2017; Jessen *et al.*, 1987). LeBlanc and Poduslo (1990) studied the expression of myelin proteins post rat sciatic nerve crush injury  which included myelin basic protein (MBP), myelin protein zero (P0), peripheral myelin protein 2 (P2) and myelin associated glycoprotein (MAG). Their study revealed

that protein levels of all the studied genes decreased post-crush injury however the rate at which they returned to levels comparable to that of normal nerve differed significantly. Post-crush injury, MAG attained normal nerve protein expression at 12 days, P2 at approximately day 14 and for P0 and MBP around day 35 in the distal nerve segment (LeBlanc and Poduslo, 1990). They further suggested a role of MAG in the SC-axon interaction after axonal regeneration and initiating myelin assembly and P2 in the transport of lipids during remyelination. Whereas P0 and MBP's late accumulation after injury suggests their role in maintaing the structure and compactness of myelin sheath (LeBlanc and Poduslo, 1990).

Such a complex repair mechanism post-PNI necessitates a well-coordinated regulation of SC plasticity. It is observed however that mainly post-transection injury, complete regeneration of the axons is often not feasible due to slow regeneration, large nerve gaps or the failure of the repair machinery to sustain a repair-supportive environment for a long time (Gaudet *et al.*, 2011). Therefore, understanding how SCs can be manipulated to aid in axon regeneration can potentially be used as a novel therapeutic strategy to treat PNI. Moreover, such research can also benefit in the discovery of potential correlations with the CNS to improve CNS regeneration following injury.

## 1.6 KEY MEDIATORS AND AFFECTORS OF PERIPHERAL NERVE REGENERATION

### 1.6.1 Cyclic adenosine monophosphate (cAMP)

Post-PNI the injury site is exposed to the extracellular environment. This results in a variety of action potentials being retrogradely transported to the cell body of axons, leading to chromatolysis (Mandolesi *et al.*, 2004). This further triggers an inflow of calcium in the neuronal cell bodies via voltage-dependent ion channels thus promoting the activation of several proteins including adenylyl cyclase responsible for converting adenosine triphosphate (ATP) to cyclic adenosine monophosphate (cAMP). cAMP activates several signal transduction pathways post-PNI which is essential for nerve regeneration including converting the quiescent neurons to a state favouring growth through several downstream signalling pathways (Knott *et al.*, 2014). cAMP in a PKA-dependent manner can facilitate axon regeneration, overcoming inhibitory elements by activating multiple transcription factors including activating transcription factor-3 (ATF3), cyclic AMP responsive element binding protein (CREB) and signal transducer and activator of transcription 3 (STAT3) which are involved in axonal regeneration (Mahar and Cavalli, 2018).

cAMP has also been implicated in regulating the attractive and repulsive axonal guidance cues. For instance in cultured Xenopus spinal neurons, a competitive analogue of cAMP

converted the attractive response in growth cones mediated by neurotrophic factors – nerve growth factor (NGF) and brain-derived neurotrophic factor (BDNF), into that of repulsion (Song *et al.*, 1997). cAMP signalling and downstream effectors also play a vital role in the cellular changes that takes place in SCs post-injury including transition into a repair SC phenotype and SC proliferation (Knott *et al.*, 2014). Forskolin is known to activate adenylyl cyclase, thereby elevating intracellular cAMP levels.  In rat SC cultures, elevation of cAMP was shown to be vital, via secondary agents like forskolin, for the mitogenic activity of platelet-derived growth factors (PDGF), glial growth factor (GGF) and fibroblast growth factors (FGF) in stimulating mitosis and proliferation of SCs (Davis and Stroobant, 1990; Stewart *et al.*, 1991).

## 1.6.2 Transcription factors in peripheral nerve repair

Once axons are severed during injury, several intracellular regulatory pathways within neurons are activated, resulting in the production of various transcription factors that co-ordinate to establish the fate of the damaged neurons (Patodia and Raivich, 2012). Transcription factors are proteins that bind to the DNA with the ability to transcribe DNA into RNA and thus play an important role in activating and suppressing target gene expression (Barnes and Adcock, 1995). Additionally, these proteins can bind to multiple promoter sites, allowing a single transcription factor to turn on or off many genes. In the process of regeneration, transcription factors play an important role by

translating stress signals induced by an injury response into downstream protein expression.

### 1.6.2.1 Transcription factors in neurons that promote regeneration

Using phosphoproteomics and microarray, Michaelevski *et al.* (2010) discovered 400 overlapping axonal signalling networks associated with 39 transcription factors in the sensory neurons of DRGs that were involved in response to a sciatic nerve crush injury in rats. Axonal injury results in the activation of several signalling pathways that can lead to gene transcription. These transcription factors are responsible for regulating several regeneration-associated genes (RAGs) in injured neurons (van Kesteren *et al.*, 2011; Mahar and Cavalli, 2018). As mentioned previously upregulation of cAMP after PNI is required for the activation of several pro-regeneration transcription factors. In relation to this, transcription factors such as c-Jun and activating transcription factor 3 (ATF3) have been widely studied for their involvement in axonal regeneration, among many others (Jenkins and Hunt, 1991; Seijffers *et al.*, 2007). Raivich *et al.* (2004) showed in mice lacking c-Jun in neural cells, a reduced facial nerve reinnervation and a delay in functional recovery. Seiffers *et al.* (2007) observed in transgenic mice that constitutively expressed ATF3 in adult DRG neurons, an increased/earlier regeneration as compared to wild-type mice following PNI. As such several transcription factors are involved in peripheral axonal injury response such as JunD, signal transducer and activator of transcription 1 and 3 (Stat 1 and 3), Myc, interferon regulatory factor 7 (Irf7), p53, cAMP

response element binding protein (CREB), CCAAT/enhancer binding proteins (C/EBPs), suppressor of others against Decapentaplegi 1 (Smad1), X-Box binding protein 1 (XBP1), SRY-Box transcription factor 11 (Sox11 ) among several others (Jenkins and Hunt, 1991; Qin *et al*., 2018; Schwaiger *et al*., 2000; Raivich *et al*., 2004; Saijilafu *et al*., 2013; Nadeau *et al*., 2005;  Di Giovanni *et al*., 2006; Jankowski *et al*., 2009; Lonze *et al*., 2002; Oñate *et al*., 2016).

**1.6.2.2 Transcription factors in Schwann cells that promote peripheral nerve repair**

**1.6.2.2.1 c-Jun**

Schwann cell-derived c-Jun has been extensively studied for its role in PNR. In SCs, the expression of c-Jun is limited to non-myelinating SCs in an adult and has been shown to be an inhibitor to myelination (Shy *et al*., 1996; Parkinson *et al*., 2008).

Single-cell RNA sequencing of the distal nerve stump post-nerve transection injury showed that c-Jun is significantly upregulated in SCs but this upregulation was also observed in endothelial cells and endoneurial fibroblasts, three days after injury with surprisingly the highest expression in mast cells on day nine (Li *et al*., 2021). Using mice with an ablation of c-Jun in SCs, Arthur-Farraj *et al.* (2012) demonstrated c-Jun's function as a 'global regulator' of SC response during Wallerian degeneration and subsequent axon regeneration, following PNI. In their experiments, deletion of c-Jun in SCs caused formation of abnormal bands of Büngner, which is required for axon guidance in the

distal nerve segment, and delayed myelin clearance post-transection injury. Moreover, after crush injury they observed a significant death of sensory DRG axons specifically in the unmyelinated axons and a failure in functional recovery as compared to the control mice (Arthur-Farraj *et al.*, 2012).

In another study, transection injury in mouse model with SC-specific deletion of c-Jun, reduced macrophage recruitment, functional recovery and prevented axonal innervation of peripheral targets (Fontana *et al.*, 2012). Moreover, the same study showed that expression of several neurotrophic genes such as glial cell line-derived neurotrophic factor (GDNF) and brain-derived neurotrophic factor (BDNF) were reduced post-injury in nerves with c-Jun null SCs.

Once axons enter the distal nerve segment post-injury, c-Jun is downregulated as its presence in the distal nerve prevents the myelination of the axons by SCs (Shy *et al.*, 1996). In in vitro studies and in a transection injury model of 5-day old mice with a c-Jun deletion in SCs, Parkinson *et al.* (2008) demonstrated that c-Jun blocks myelination and contradicts the role of Krox-20, a myelin-favouring transcription factor. Fazal *et al.* (2017) generated mice with an overexpression of c-Jun in SCs, wherein there is a 6-fold protein elevation of c-Jun in uninjured sciatic nerve as compared to the wild-type mice. In their mouse model there was a significant delay in remyelination 2 weeks following a crush injury. However, by the 10-week timepoint, myelination of axons that require myelin was

comparable to the control, albeit with thinner myelin sheath. Interestingly, the role of c-Jun was found to be injury dependent, as c-Jun deletion in SCs did not produce any effects in the PNS during development or the normal functioning of the adult mouse nerve (Arthur-Farraj *et al.*, 2012).

**1.6.2.2.2 Sex determining region Y (SRY)-box 2 (Sox2)**

Sex determining region Y (SRY)-box 2 (Sox2) is a transcription factor recognised for its role in sustaining stem cell pluripotency and thus regulating embryonic development (Sarlak and Vincent, 2016). In conjunction with various transcription factors, Sox2 can revert differentiated cells to their pluripotent state (Takahashi and Yamanaka, 2006; Chambers and Tomlinson, 2009). Le *et al.* (2005) showed in in vitro experiments, that SCs treated with Sox2 adenovirus or lentivirus, blocked the expression of the genes involved in myelination including Krox-20 and Mpz but increased the proliferation of SCs when stimulated with β-neuregulin, a SC mitogenic factor.

In peripheral nerves, Sox2 is upregulated in the SCs of the distal nerve post-injury (Le *et al.*, 2005). Previously my research group demonstrated in mice overexpressing Sox2 specifically in SCs, an inhibition of myelination of axons in intact nerve (Roberts *et al.*, 2017). Moreover, the SCs remained in a proliferative and non-differentiated state and was also linked with increased number of macrophages in the nerve. Their work on post-

PNI in these mice also showed reduced functional recovery as well as hypomyelination of axons (Roberts *et al.*, 2017).

In contrast, Sox2 was also reported to be necessary during peripheral injury (Parrinello *et al.*, 2010). In an injured nerve, interaction between ephrin-B expressed in fibroblasts and its receptor EphB2 expressed in SCs results in sorting of SCs into clusters (Parrinello *et al.*, 2010). This ephrin-B/ephB2 cell sorting is mediated by Sox2 through N-cadherin relocalisation to SC cell junctions. Essentially, this cell sorting was shown to be important in the collective migration of SCs tracts across the injury site to guide the regenerating axons (Parrinello *et al.*, 2010). Additionally in in vitro experiments on Sox2 deficient SCs (knockdown by siRNA), soluble ephrin-B2 ligand could not rescue the impaired ephrin-B2-dependent clustering, however when Sox2 was overexpressed in EphB2-knockdown SCs, normal SC clustering was observed implying that EphB2 receptor acts upstream of Sox2 (Parrinello *et al.*, 2010).

Our research group had previously shown in mice with a SC-specific knockout of Sox2, the evidence of aberrant trajectory of axons in the nerve bridge following a transection injury of the sciatic nerve (Dun *et al.*, 2019). This resulted in the formation of an abnormal nerve bridge as observed at 3-months post-injury as well as significant loss of axon innervation in the distal tibial nerve. Using the same mouse model, they also showed that this defect in axon pathfinding is due to ectopic SC migration following transection

injury with the regenerating axons following the same abnormal trajectory (Dun *et al*., 2019). However, a crush injury in the same mouse model showed a small decrease in axon outgrowth and a transient delay in functional recovery, yet remyelination of the nerve was not impaired (Dun *et al.,* 2019).

**1.6.2.2.3 Krox-24, Krox-20, Oct 6 and Sox10**

With an antagonistic role to c-Jun in SCs, the transcription factor - early growth response 2 (EGR2) also known as Krox-20 regulates myelin formation during development (Topilko *et al*., 1994), myelin maintenance in adult peripheral nerves (Decker *et al*., 2006) and remyelination post-injury (Topilko *et al*., 1997). Homozygous deletion of Krox-20 in mice prevented the myelination of axons at postnatal day 15 (P15) and although the SCs had initiated myelination (the promyelin state), full compacted myelin was not formed due to the absence of late myelin genes such as MPZ and MBP as confirmed at postnatal day 10, thus establishing the role of Krox-20 in myelination (Topilko *et al*., 1994).

Post-injury Krox-20 is downregulated in SCs which is consistent with the downregulation of genes favouring myelination during Wallerian degeneration. Whereas Krox-24, normally expressed in non-myelinating SCs in an adult nerve is upregulated post-injury, implying its role in the non-myelinating or proliferative state of SCs (Topilko *et al*., 1997). As mentioned, Krox-20 is an antagonist of c-Jun and Sox2, with Krox-20 driving

myelination whereas the latter two implicated in inhibition of myelination (Parkinson *et al.*, 2004; Le *et al.*, 2005; Parkinson *et al.*, 2008; Fazal *et al.*, 2017; Roberts *et al.*, 2017).

POU domain transcription factor 1 also known as Oct-6 and SRY-box transcription factor 10 (Sox 10) are two other transcription factors other than Krox-20 that have been implicated as SC differentiation and myelin regulators during development. Oct-6's expression is transient during myelination and deletion of Oct-6 in mice resulted in arrested myelination of the peripheral nerve during development, very similar to the results in Krox20 null mice (Bermingham *et al.*, 1996). In adult nerves, Oct-6 is expressed in the myelinated SC cytoplasm whereas it was absent in non-myelinating SCs (Kawasaki *et al.*, 2003).

In comparison, in peripheral nerves undergoing axonal degeneration, Oct-6 expression was identified in denervated SCs, while in nerves experiencing active axonal regeneration peak nuclear expression of Oct-6 was observed. This data implied that during nerve degeneration post-injury or in peripheral neuropathies, myelin breakdown results in the upregulation of Oct-6 in SCs (Kawasaki *et al.*, 2003). Once axon regeneration is initiated, Oct-6 is transported to the nucleus to upregulate the transcription of axon regeneration-related genes including and not limited to those that support remyelination such as Oct-6 itself. Once compact myelin is achieved around the regenerated axons, Oct-6 is again transported to the cytoplasm of SCs and is

downregulated (Kawasaki *et al*., 2003). These results were in agreement with previous work of Scherer *et al.* (1994) wherein they demonstrated that post-injury in mice, Oct-6 mRNA peaked during axonal regeneration with Oct-6 located in the nuclei of SCs associated with regenerating axons. In another study, using Oct6 Δ SC enhancer (SCE) mice, wherein the deletion of the SCE prevents Oct-6 upregulation after injury resulted in an earlier/higher upregulation of c-Jun levels after crush injury as compared to the control mice (Brügger *et al*., 2017).  Additionally, the authors in the same mouse model reported earlier demyelination of SCs and faster axonal regrowth following a crush injury.

Although the role of Sox10 in development of PNS has been widely studied (as discussed previously), very little is known about its role in PNR. Sox10 expression persists in mature SCs and satellite glial cells, long after development is achieved (Kuhlbrodt *et al.,* 1998). Sox10 deletion in SCs of adult mice using Tamoxifen-inducible PLP-Cre (proteolipid protein (myelin) 1 promoter) system, resulted in the development of severe peripheral neuropathy marked by demyelination, axonal degeneration, neurological symptoms and changes in peripheral nerve conduction velocity (Bremer *et al*., 2011). The authors reported the survival of SCs devoid of Sox10 in the sciatic nerve post Tamoxifen injections indicating that Sox10 might not be essential for mature SC survival. However, the demyelination phenotype observed in the mice indicates that Sox10 is important for maintaining the differentiated state of SCs in adult peripheral nerves (Bremer *et al*., 2011).

## 1.6.2.2.4 Runt related transcription factors

The family of evolutionary conserved runt-related transcription factor (Runx) has been studied for their role in regulating several processes during development including apoptosis, proliferation, differentiation and cell growth, and as oncogenic regulators. In mammals, three Runx genes have been defined -Runx1 (CBFα2, AML1), Runx2 (CBFα1, AML3) and Runx3 (CBFα3, AML2). Runx1 is a key regulator of embryogenesis and is required for the differentiation of hematopoietic cells as well as establishing definitive hematopoiesis and thereby its mutation has been studied as the cause of several haematological cancers (Yzaguirre *et al.*, 2017). Runx2 is mainly known as a regulator of bone development and skeletal morphogenesis during development (Otto *et al.*, 1997; Komori *et al.*, 1997). Runx2 regulates the expression of Indian Hedgehog (Ihh), which in turn is essential for proliferation of chondrocytes during skeletal development (Komori *et al.*, 2018). Ihh activates parathyroid hormone-like hormone (Pthlh) which subsequently inhibits Runx2 and maturation of chondrocytes, thus establishing a negative feedback loop (Komori *et al.*, 2018). Runx3 has a role in the growth regulation of the gastrointestinal tract during development and in gastric tumours; (Fukamachi and Ito, 2004), regulating dorsal root ganglia neurons during development (Levanon *et al.*, 2002) as well as a tumour suppressor role (Ito *et al.,* 2005).

Two alternative promoters, namely a proximal (P2) and a distal (P1) to the start codon, transcribe all three mammalian Runx genes, giving rise to several isoforms, with different properties, varying from cell to cell (Geoffroy *et al.,* 1998; Coffman *et al.,* 2003). All of the Runx isoforms have a distinct C-terminus containing both inhibitory and activation domains, as well as a highly conserved 128 amino acid DNA-binding domain at the N-terminus known as the Runt domain (Coffman *et al.,* 2003). Runx proteins form heterodimers with an unrelated beta subunit known as CBF$\beta$ to bind DNA, which explains their alternative nomenclature as core-binding factors (CBF). Although the runt domain binds DNA as a monomer, interaction with CBF$\beta$ (which does not bind DNA by itself) strengthens this binding (Adya *et al.,* 2000).

Until now, Runx1 and Runx3 have been studied to a certain extent for their role in the development of the nervous system (Inoue *et al.,* 2008). Global deletion of Runx1 in mouse embryo reduced a select population of vestibulocochlear and trigeminal ganglion neurons at embryonic day 11.5 (Theriault *et al.,* 2004). Using Runx3 deficient mice, Inoue *et al.* (2002) demonstrated that Runx3 was necessary for axonal projection of proprioceptive DRG neurons during development and its absence caused severe limb ataxia. However, up until recently, limited work was done to study the role of Runx2 during the development of the nervous system as well as its role post-injury.

**1.6.2.2.4.1 Role of Runx2 in peripheral nerve regeneration**

Previously, the activator protein-1 (AP-1) binding site and the runt domain binding site were shown to be located very close to each other in the rat collagenase-3 promoter (D'Alonzo *et al.,* 2002). Moreover, the authors demonstrated that their binding transcription factors — c-Fos.c-Jun (binding to AP-1) and Runx2 (binding to runt domain), physically interact with each other to form ternary structures and regulate the collagenase-3 promoter (D'Alonzo *et al.,* 2002).

Hung *et al.* (2015) using chromatin immunoprecipitation sequencing (ChIP-seq), investigated the transcription factor binding sites that were enhanced after nerve transection injury in rats revealing several related binding sites for transcription factors such as c-Jun that are upregulated post-injury. ChIP-seq, surprisingly showed that the Runt-binding domain was located on injury-enhancers proximal to thirteen c-Jun-dependent, injury-induced genes such as oligodendrocyte transcription factor 1 (Olig1), sonic hedgehog (Shh) and Runx2 itself (Hung *et al.,* 2015).

As previously discussed, c-Jun is essential for regulating several genes following PNI and its interaction with Runx2 (D'Alonzo *et al.,* 2002), as well as the location of the runt binding domain proximal to several genes upregulated post-injury, hinted on a role of Runx2 in PNR (Hung *et al.,* 2015). By immunohistochemistry, the authors showed Runx2 upregulation in the distal nerve SCs 3 days after mouse sciatic nerve transection injury

(Hung *et al.,* 2015). In siRNA analysis of c-Jun and Runx2 in primary rat SCs, Hung *et al*. (2015) showed by RT-qPCR that c-Jun siRNA downregulated the expression of several genes including Runx2, however Runx2 downregulation by siRNA did not alter c-Jun expression.

Arthur-Farraj *et al.* (2017) also showed by RNA sequencing and qPCR, the upregulation of Runx2 mRNA in the distal nerve stump as early as 24hrs after mouse sciatic nerve transection injury. Additionally the authors showed by qPCR that Runx2 was mainly expressed in cultured SCs, with low expression in fibroblasts and none in activated macrophages (Arthur-Farraj *et al.*, 2017). Ding *et al.* (2018) studied the expression of Runx2 post-crush injury in rats. The authors reported an upregulation of Runx2, 3 days post-injury with highest expression observed 7 days post-injury and immunohistochemical analysis showed that Runx2 was mainly expressed by SCs. The upregulation of Runx2 was also confirmed in SCs in in vitro studies, using cAMP to induce differentiation in SCs (Ding *et al.,* 2018). Additionally, reduced SC migration in siRNA mediated knockdown of Runx2 in SCs suggested that Runx2 might be important in SC migration post PNI (Ding *et al.,* 2018). These preliminary results for Runx2 indicated a much larger role of Runx2 in PNR. Also, prior to the work done for this thesis, in vivo knockout of Runx2 had not been previously used to study PNR.

A general lack of information in vivo for the role of Runx2 in regulating gene expression for successful peripheral nerve repair after injury, led us to study it in a mouse model with a SC-specific knockout of Runx2 in mice. Homozygous germline deletion of Runx2 in mice is not viable due to a lack of osteoblast differentiation resulting in absence of ossification and respiratory failure (Otto *et al.,* 1997; Komori *et al.,* 1997). Therefore, in my model the SC-specific knockout of Runx2 was achieved in mice using Cre-mediated deletion regulated by the P0 promoter (described in detail in Chapter 2.1.2).

## 1.7 AXON GUIDANCE

### 1.7.1 Growth cones and their role in axon guidance

The "fan-shaped" growth cone is located at the distal end of an axon continually examining its surroundings by expanding and withdrawing membrane protrusions known as filopodia, a tapering finger-like actin meshwork and lamellipodia, together with a flat sheet-like veil (Figure 4) (Dent and Gertler, 2003). The growth cone consists of three domains: the highly motile and actin-rich peripheral domain made up of the filopodia and lamellipodia; a more stable transition zone rich in myosin that contracts the actin network; and a third central domain which displays significant molecular mobility, including steady organelle and vesicle shuttling and contains microtubules (Figure 4) (Bouquet and Nothias, 2007).
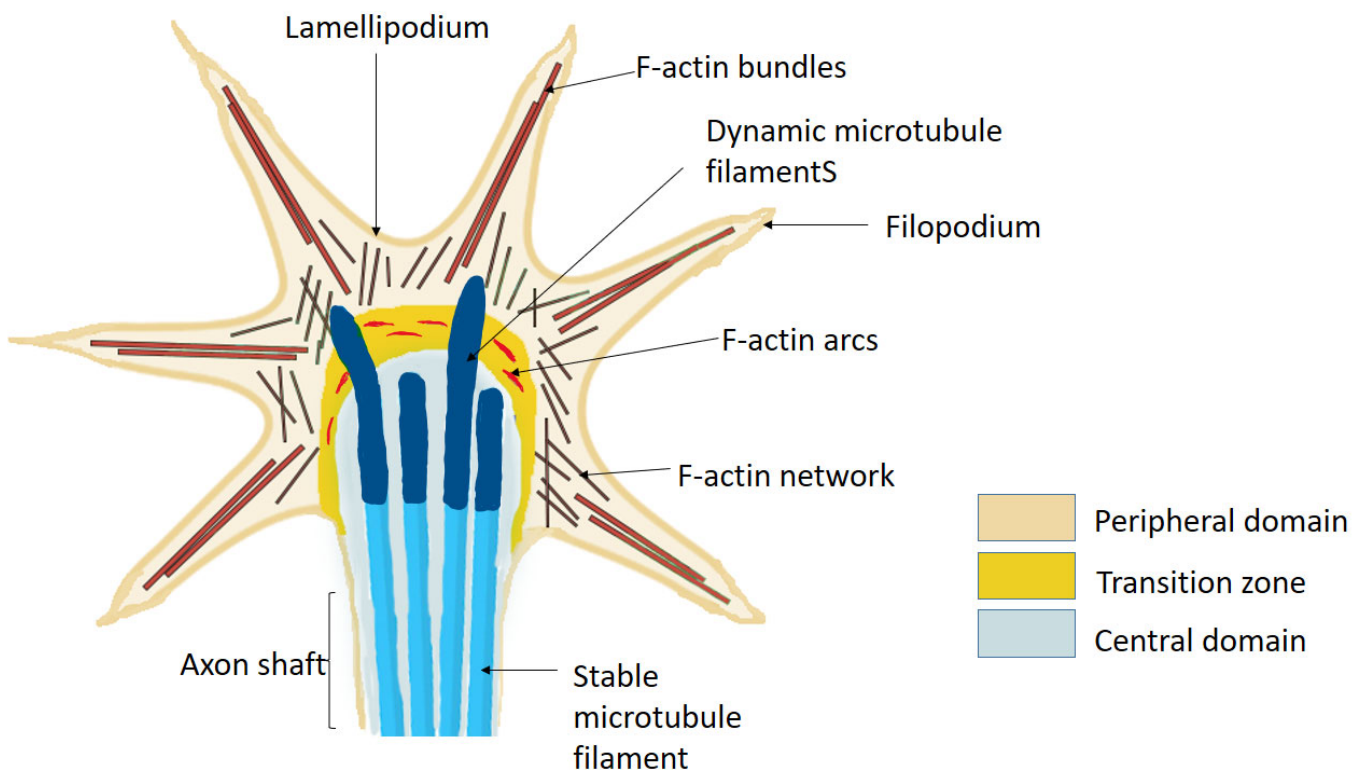
**Figure 4: Structure of the growth cone**

The growth cone is located at the tip of growing axons taking part in pathfinding. It consists of three regions – the peripheral domain, consisting of F-actin network in the sheet-like lamellipodium and the F-actin bundles in the finger-like filopodium; the transition zone, with contractile myosin structures termed as actin arcs (contractile structures) and a central domain, rich in microtubules (with stable and dynamic microtubule populations) that further on make up the axon shaft.

Axon outgrowth is achieved by the growth cone in three steps, namely - protrusion, engorgement and consolidation (Figure 5) (Goldberg and Burmeister, 1986; Dent and Gertler, 2003). The growth cone integrin receptors bind with surrounding permissive substrate such as the extracellular matrix (ECM) at specific adhesion sites thus activating signalling pathways and the generation of a 'molecular clutch' (Figure 5A) (Nichol *et al.,*

2016). During protrusion, the anchoring of the actin to the ECM allows the filopodia and lamellipodia to migrate forward and expand as F-actin polymerisation continues in front of the clutch site (Figure 5B). In the next stage of engorgement, the F-actin flow is reduced in the peripheral domain of the growth cone thus creating an F-actin void between the central domain and the clutch site and allowing the influx of microtubules, vesicles and organelles in the protrusions (Figure 5C) (Lin and Forscher, 1995). During the final stage of consolidation, the microtubules compact to form the new section of the cylindrical axon shaft while the F-actin depolymerises at the base of the growth cone thus allowing the retraction of the membrane protrusions around the microtubule bundle (Figure 5D) (Schaefer *et al.,* 2008). The three concurrent stages of axon growth occur during the production of new axons and axon branching (Dent and Gertler, 2003).
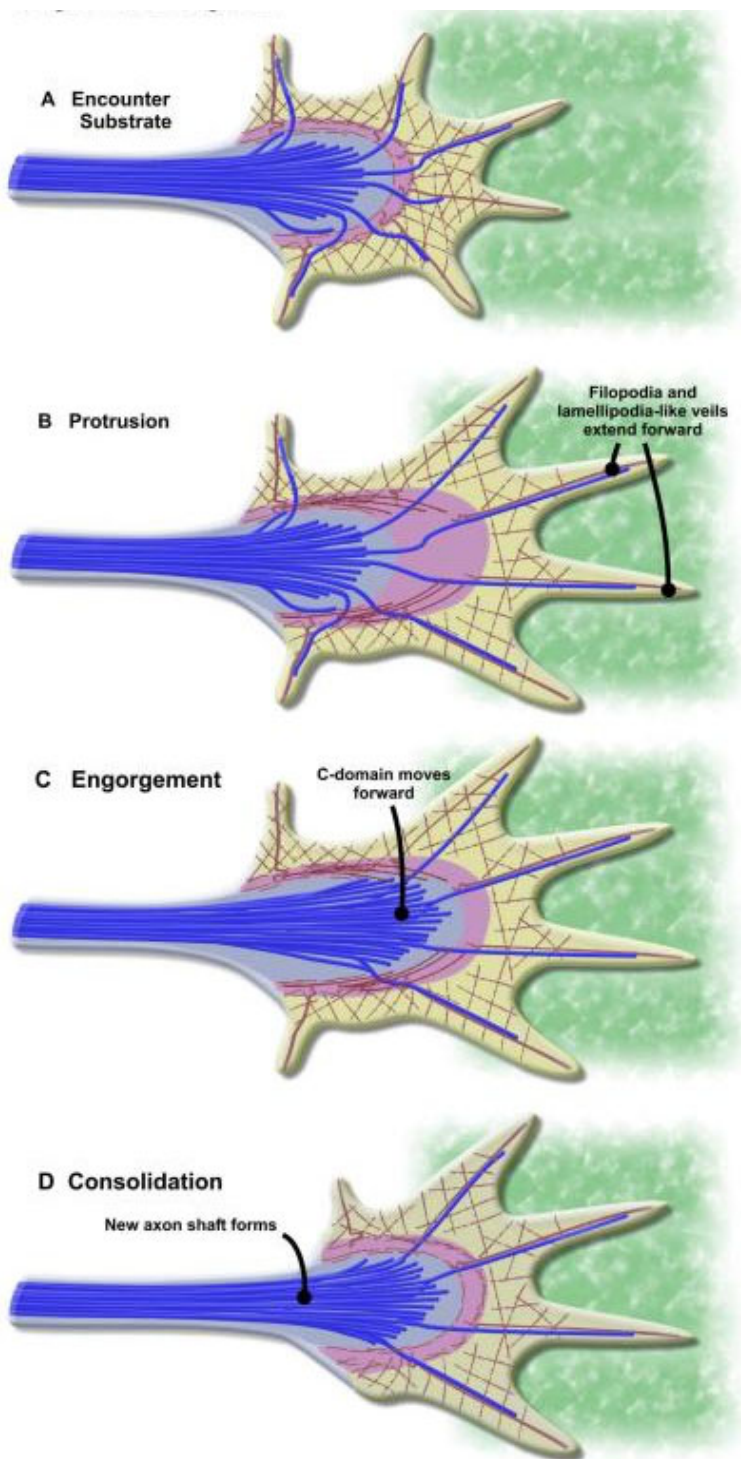
**Figure 5: Goldberg and Burmeister's (1986) description of axon outgrowth**

Goldberg and Burmeister in 1986 described the process of axonal outgrowth that occurs in three stages of protrusion, engorgement and consolidation in response to a permissive/adhesive substrate. (A) The

receptors on the growth cone bind to the available substrate and activates intracellular signalling pathways as well as formation of a 'molecular clutch' through clutch proteins that anchors the actin cytoskeleton to the substrate and reduces F-actin retrograde flow. (B) During protrusion, F-actin polymerisation still persists in front of the clutch site, and this pushes actin-rich finger-like filopodia and the sheet-like lamellopodia projections forward. (C) Once the actin is cleared in the passage between the adhesion site and the central domain, engorgement involves the invasion of microtubules in the extended protrusions guided by actin arcs. (D) Consolidation occurs when the F-actin now depolymersises at the base or the base of the growth cone forming a new segment of the axon shaft (Lowery and Vactor, 2009)

As the growth cone navigates its path, the budding axons also lengthens. At this stage, the microtubules from the central domain are integrated into the newly generated cytoskeleton sustained by microtubule-associated proteins (MAPs) such as growth-associated protein-43 (GAP-43), whose expression is increased during axon growth and is required for stabilising actin filaments (He *et al.,* 1997).

### 1.7.2 Axon growth and axon guidance cues

As discussed previously, the growth cone guides the axons to their end targets also referred to as pathfinding (Tessier-Lavigne and Goodman, 1996). For instance, growth cones can bind noncovalently to permissive/adhesion molecules whose distribution can enable axon growth while presence of inhibitory molecules defines the region wherein the axons do not grow (Letourneau, 2009; Raper and Mason, 2010). Examples of permissive substrates includes the extracellular matrix (ECM) components available in

basement membranes (such as SC basal lamina) as well as cell adhesion molecules (CAMs) localised on non-neuronal or neuronal cell surfaces. On the other hand, several tropic and trophic factors act as cues in 'steering' the migration of growth cones to their target (Letourneau, 2009). Growth cones can thus respond to a gradient of long- and short-range cues that can be attractive or repulsive by a process called chemotaxis. Tropic cues include the Netrin, Slit, Ephrin and Semaphorin families. Whereas trophic factors include several neurotrophic factors. Trophic factors are widely known to stimulate growth cone motility and have been known to orient axonal outgrowth mainly in vitro such as the glial cell line-derived neurotrophic factor (GDNF), hepatocyte growth factor (HGF) and nerve growth factor (NGF) among the many neurotrophic factors (Ye *et al.*, 2019; Onesto *et al.*, 2021).

In the absence of such instructional stimuli, growth cones grow randomly, with a balanced actin polymerisation and depolymerisation thus resulting in a balanced protrusion and retraction of the growth cone with the axons following the same pattern.

During axon outgrowth of developing nerves and post-PNI, the growth cone can come across several cues and its interaction with these cues is important in navigation of axons to their end targets. The majority of the research and literature in axon guidance is centred around development of the nervous system while the processes of axon guidance in PNR is still poorly understood. Ramón y Cajal in 1890 accurately suggested

long-range chemoattraction, which occurs when target cells release diffusible chemoattractant molecules that attract distantly located axons (Figure 7). However, since then it has been shown that axons in vitro can also be repelled by diffusible substances released by tissues demonstrating long-range chemorepulsion (Tessier-Lavigne and Goodman, 1996) (Figure 7). Moreover, short range, contact-based or locally available permissive and inhibitory cues also play a role in axon growth including cell-adhesion molecules such as neural cell adhesion molecule (NCAM), L1CAM and ECMs such as laminin, tenascin, proteoglycans/glycosaminoglycans and fibronectin among others that are presented by neighbouring cells (Figure 6).
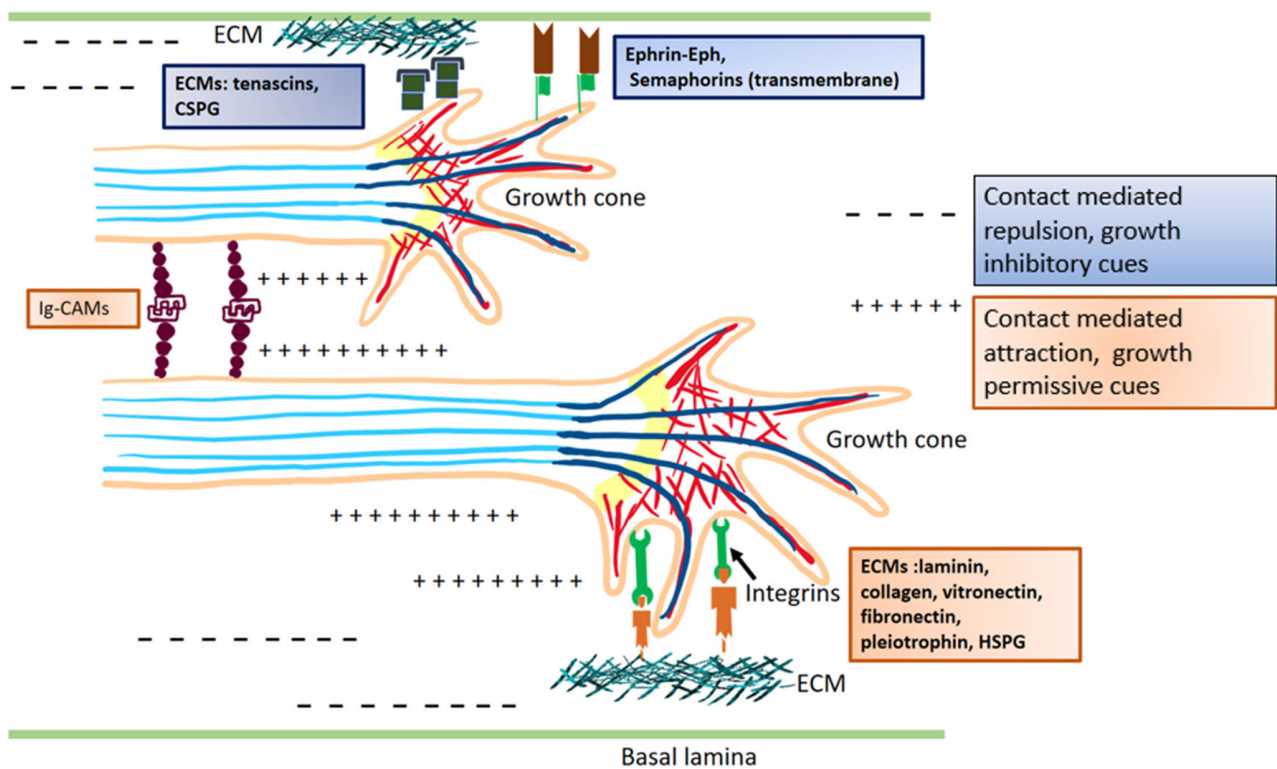
**Figure 6: Adhesion mediated axon growth and contact-mediated axon guidance**

The figure illustrates the mechanism of axon growth in the presence of inhibitory and growth promoting substrates as well as contact-mediated repulsion and attraction of the growth cone. Extracellular matrices, located in the basal lamina, such as laminin, collagen, vitronectin, fibronectin, pleiotrophins and heparin sulfate proteoglycans (HSPG) are known to provide permissive substrates for axon growth upon binding to receptors on the growth cone such as the integrins. Whereas tenascins and chondroitin sulfate proteoglycan (CSPG) are known to be inhibitory or non-permissive to growth, by binding to the growth cone. Immunoglobulin superfamily cell adhesion molecules (IgCAMs) such as neural cell adhesion molecule (NCAM) mediate axon growth via axon-axon adhesion by fasciculation or bundling of axons. The IgCAMs mediate axon growth by homophilic binding or binding to other CAMs and integrins. Whereas the Ephrin/Eph family of axon guidance and receptors as well as membrane bound semaphorins have been shown to mediate contact-based repulsion on the growth cone, with recent evidence also pointing to a contact-mediated attraction function of Ephrin/Ephs. The growth permissive and inhibitory cues as well as the contact-mediated attractive and repulsive axon guidance cues have been extensively studied during development of the nervous system with similar guidance patterns

observed in peripheral nerve regeneration. Some axon guidance cues can mediate both attraction and repulsion. The molecules represented in this image are for explanation purpose only and do not represent the actual structure. For simplicity, Schwann cells have not been defined in the image.

During development, growth cones come across intermediate targets which relay vital axon guidance information for further navigation of the axons but how the intermediate targets are chosen or presented is still not well understood (Tessier-Lavigne and Goodman, 1996; Zang *et al.,* 2021). The presence of a chemoattractant results in a preference of actin-mediated growth cone membrane protrusions towards the chemoattractant and vice-versa when a chemorepulsive cue is encountered (Dent and Gertler, 2003). Although axons can grow towards an intermediate target in the presence of a permissive substrate or growth promoting signals, a synapse formation is prevented by a shift in growth cone relay and axons continue to their intended target (Squarzoni *et al.,* 2015; Stoeckli, 2018). This shift has to be accurately timed to prevent missing the intermediate target or in an opposite scenario, a lag at the intermediate target. During axon guidance in the ventral midline of the spinal cord there is no lag of axons at the floor plate (Wang and Scott, 2000). However in chick embryos, motor axons stop in the plexus region at the base of the limb for approximately 24hrs before invading the limb, although this lag is thought to allow for maturational changes to occur in the limb (Wang and Scott, 2000; Huber *et al.,* 2005).

Originally it was suggested that some axon guidance molecules served as attractive "go" cues and others as repulsive "stop" cues. However, it is now known that it is the particular receptors that are engaged on the growth cone and the subsequent internal signalling pathways in the growth cone that are activated, rather than the integral aspect of the specific cue, that decides the response (Goodman, 1996; Zang *et al.,* 2021). Axonal growth is not synchronised and therefore in theory, if the intermediate targets that produce the guidance cues were to determine the axonal trajectory, the faster growing axons would reach earlier to the intermediate target by attractive signalling (Stoeckli, 2018). To further direct the faster growing axons to its next direction, the intermediate target would have to change its signalling to that of repulsion (Stoeckli, 2018). This would mean that the axons that are lagging behind or are growing at a slower pace would encounter repulsive signalling even before they arrive at their intended intermediate target. Hence it is more likely that the intermediate targets produce only one type of cue (either attractive or repulsive), and it is the growth cone receptors that are responsible for interpreting the signal they receive from external cues (Stoeckli, 2018). However, changes in the intracellular signalling such as regulation of cAMP levels can also be responsible for producing this effect.
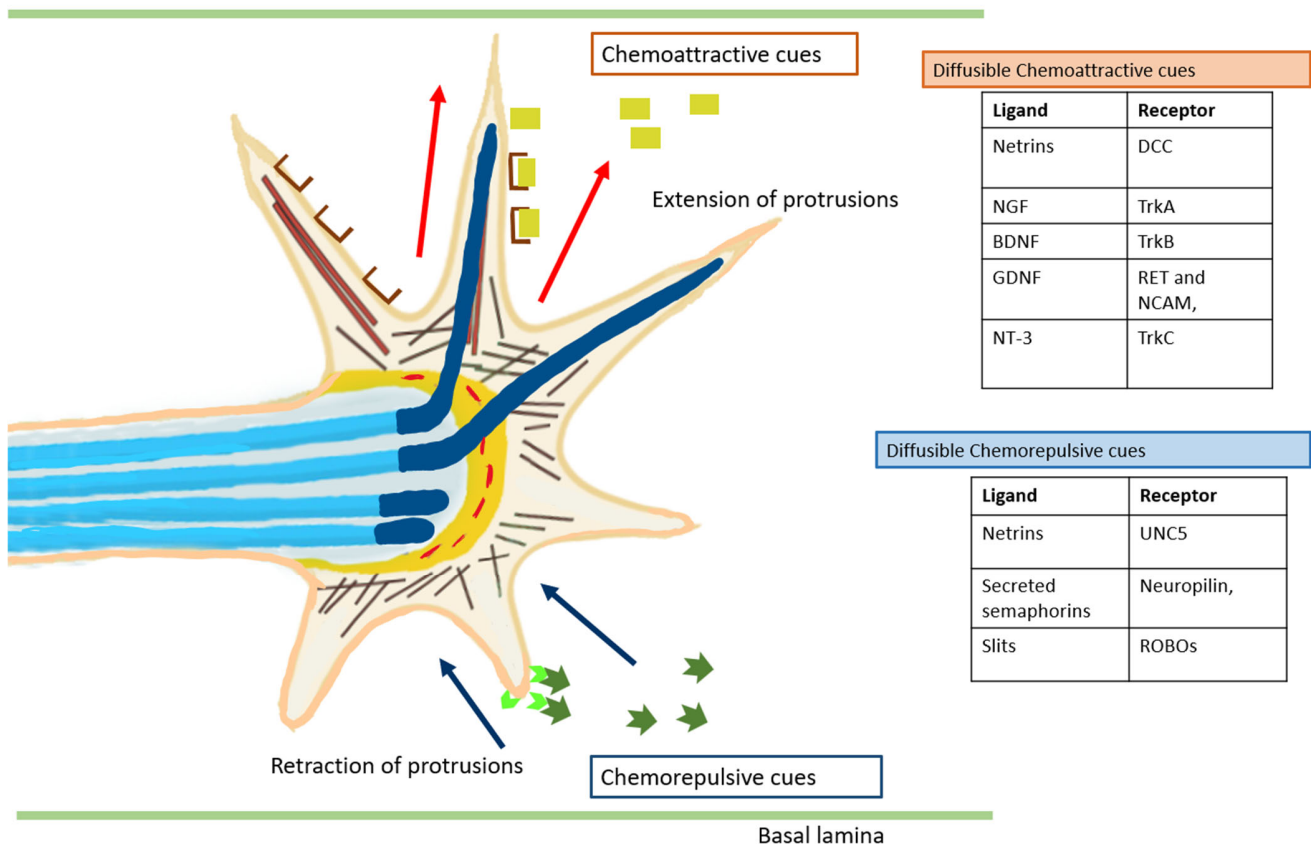
**Figure 7: Axon guidance by secreted molecules**

Several non-neuronal cells such as Schwann cells, epineurial, perineurial cells and other cells as well as neurons themselves secrete diffusible chemoattractants and chemorepellents that can bind to receptors on the growth cones and decide the trajectory of growing axons at a distance from their site of synthesis. Chemorepulsive cues repel growth cones while chemoattractants pull the growth cone towards them thus preventing them from lengthening along an unsuitable projection and guiding them to their end target. Several examples of both cues are presented in the image. Deleted in colorectal carcinoma (DCC), nerve growth factor (NGF), brain-derived neurotrophic factor (BDNF), glial cell line-derived neurotrophic factor (GDNF), rearranged during transfection (RET), neural cell adhesion molecule (NCAM), neurotrophin-3 (NT-3), roundabouts (ROBOs) and tyrosine kinase (Trk) receptors are represented. Several molecules can mediate both attraction and repulsion. These cues have been extensively studied for their role in axon guidance during neural development and few in peripheral nerve regeneration. The shapes used to depict molecules in this figure are not an actual description of their structure. For simplicity, Schwann cells have not been defined in the image.

## 1.7.3 Extracellular matrix and cell adhesion molecules

The extracellular matrix (ECM) is located in the basal lamina of SCs and the endoneurium in peripheral nerve, with the basal lamina ECM consisting of collagen, fibronectin, entactin, heparan sulphate proteoglycan, laminin and nidogens (Bannerman *et al.*, 1986; Baron-Van *et al.*, 1986). ECM molecules are known to act as both promoters and inhibitors of axon outgrowth.

In vitro studies on chicken DRG neurons demonstrated that axonal growth cones are guided by the regulated ratios of axon outgrowth-supporting substrate like laminin, to that of inhibitory substrate such as chondroitin sulfate proteoglycans (CSPG) (Snow *et al.,* 2002). The growth cone's response to the presence of these mixed cues depends on growth cone integrins and consequent activation of signalling pathways in growth cones. In rats, post-crush injury to the peroneal nerve, injected soluble laminin polymer enhanced axon growth and functional recovery compared to a phosphate buffer saline (PBS) injected control (Haggerty *et al.*, 2019). Laminin alpha 2 chain and laminin alpha 3 chain were overexpressed as early as 2 days post-crush injury in rats (Gantus *et al.*, 2006). Moreover, type IV collagen expression progressively increased post-crush injury with maximum expression observed on day 21 post-injury, while CSPG expression was

significantly reduced as early as day 2 post PNI and returned to normal by day 21 (Gantus *et al.*, 2006).

Chen *et al.* (2015) also reported upregulation of Type VI collagen post nerve injury and its expression by macrophages was important for macrophage migration and polarisation during PNR. Their studies on mice lacking Type VI collagen resulted in impaired macrophage migration and delayed PNR. Collagen is present in abundance in the ECM of peripheral nerves and has been studied for its role in development of the PNS and maintenance of normal function in adults. One study showed that in rats, a collagen scar is formed post sciatic nerve injury and thus could potentially block the axonal sprouts from regenerating (Pleasure *et al.*, 1974).

Integrins are a large family of transmembrane receptors and are a type of cell adhesion molecule (CAM) which are responsible for physical interactions of cells with the extracellular matrix (ECM). They associate with cytosolic adaptor and signalling proteins that control cytoskeletal movements of growth cones and have been widely implicated in their role in axonal growth and pathfinding (Bourgin *et al.,* 2007; Schlomann *et al.,* 2009). Several integrins are upregulated post-PNI many of which are overexpressed in the axons and their growth cones post-injury (Werner *et al.,* 2000; Hammarberg *et al.,* 2000; Wallquist, 2004). Deletion or absence of these integrins in vitro and in vivo resulted

in reduced neuronal outgrowth and delay in re-innervation of end targets post-injury (Werner *et al.,* 2000; Gardiner *et al.,* 2005).

**1.7.4 Neurotrophins**

Neurotrophic factors are a family of small proteins extensively investigated for their roles in neuronal differentiation, proliferation, survival, and growth in the CNS and PNS during development as well as in injury and neurological disorders (Lykissas *et al.,* 2007). The neurotrophic factors family can be segregated into neurotrophins, neurotrophic cytokines, glial cell line-derived neurotrophic factor (GDNF) family ligands, and cerebral dopamine neurotrophic factor (CDNF).

Neurotrophins are secreted by neurons and their target tissues, and among their many roles are essential for axon guidance, promoting axonal outgrowth and survival of neurons post PNI. Neurotrophins consist of the nerve growth factor (NGF), brain-derived neurotrophic factor (BDNF), neurotrophin-3 (NT-3) and neurotrophin-4/5 (NT-4/5). They bind to two classes of receptors - tropomyosin kinase family of tyrosine kinase receptors (Trks) as well as the low-affinity nerve growth factor receptor (NGFR) from the tumour necrosis factor superfamily (Lykissas *et al.,* 2007). Neurotrophins exert varied effects on the growth cones, however most studies point to an attractive response rather that a repulsive one (Lykissas *et al.,* 2007). It has been suggested that neurotrophins regulate the actin content in the growth cones in embryonic sensory neurons to mediate

chemoattraction or repulsion (Paves and Saarma, 1997). Moreover, each neurotrophin can mediate both functions on the same growth cone.

Nerve growth factor (NGF) was the first of the family to be discovered with significance in promoting sensory and sympathetic neuron survival, their differentiation, and maintenance during embryonic development and in adults (Levi-Montalcini and Hamburger, 1951). Although NGF and its specific receptor TrkA are highly expressed during development in the peripheral nerves of rats, in intact adult sciatic nerves NGF is not detected. This changes post-injury with approximately 15-fold upregulation of NGF mRNA reported in the proximal and distal nerve stump following rat sciatic nerve transection injury (Heumann *et al.,* 1987a; Heumann *et al.,* 1987b; Meyer *et al.,* 1992). TrkA mRNA was not detected in the proximal or distal sciatic nerve post-injury (Funakoshi *et al.,* 1993). Additionally, for NGFR, the common receptor for the neurotrophins, its mRNA was upregulated post-injury by SCs (Heumann *et al.,* 1987b). To understand the purpose of this gene expression, in vitro cultures of sciatic nerves explants were studied in two separate studies by the same research group (Heumann *et al.,* 1987b; Lindholm *et al.,* 1987). Addition of primary rat peritoneal macrophages or the conditioned media of the cells increased NGF mRNA expression suggesting that NGF expression is stimulated by invading macrophages (Heumann *et al.,* 1987b; Lindholm *et al.,* 1987). The authors also showed that interleukin-1 beta released by macrophages is responsible for the upregulation of NGF (Heumann *et al.,* 1987b; Lindholm *et al.,* 1987).

Post-sciatic nerve transection injury in rats, NGF injected into a silicone nerve conduit improved the regeneration of motor axons (He *et al.,* 1992), although some studies point to a potential role of sensory axon regeneration for NGF (Derby *et al.,* 1993).

Brain derived neurotrophic factor (BDNF) is another widely studied neurotrophin due to its role in axon guidance and PNR. As studied in sciatic nerve transection injury in rats, in the distal sciatic nerve, BDNF mRNA was upregulated at day 3 after injury and peaking at 3-4 weeks (Meyer *et al.,* 1992). BDNF peak mRNA upregulation following injury was ten times higher than the peak mRNA expression of NGF. Additionally, SCs were cited as the source of BDNF expression (Meyer *et al.,* 1992).

Various elegant experiments in mice and rat injury models have demonstrated BDNF's role in promoting survival and elongation of injured motor axons (Sendtner *et al.,* 1992; Yan *et al.,* 1992; Vejsada *et al.,* 1998). BDNF's function in regeneration of motor axons is potentially determined by its receptor, as homozygous NGFR knockout mice showed increased axonal regeneration while trkB heterozygous null mice suffered from reduced regeneration (Boyd and Gordon, 2001). This suggested that NGFR, a common receptor for the neurotrophins might inhibit PNR whereas BDNF binding to trkB enhances it. However, a few studies have conflicting view, for instance, Tomita *et al.* (2007), demonstrated impaired motor axon regeneration and hypomyelination following injury in a mouse model with sciatic nerve graft from mice with an NGFR global knockout. This

model was specifically designed to investigate the role of SC-derived NGRF separate from axonal effect of loss of NGFR, as the nerve graft was devoid of DRGs (no cell bodies of neurons).

NT-3, another neurotrophin binds to TrkC and to a lesser extent, trkA while NT-4/5 binds to trkB similar to BDNF. NT-3 mRNA is expressed in the intact sciatic nerve of adult rats but was reduced immediately in the distal nerve segment post-crush injury and the expression returned to baseline within 2 weeks (Funakoshi *et al.,* 1993). A similar pattern was observed for NT-4/5 mRNA up until two weeks post-injury when the level of NT-4/5 increased significantly as compared to the intact nerve. NT-3 along with NGF promoted axonal outgrowth in cultured DRG neurons while BDNF did not demonstrate such potential (Edström *et al.,* 1996). Sahenk *et al*. (2005) studied the role of NT-3 in three peripheral neuropathy models. First model was using sural nerve grafts from patients with Charcot–Marie–Tooth type 1A (CMT1A) xenografted in nude mice. A second model using TremblerJ (TrJ) mice, with a naturally spontaneous occurring point mutation in the PMP22 gene resulting in abnormal myelination of the PNS. And a third model of patients with CMT1A. In both mouse models, NT-3 improved axonal regeneration whereas in the patient study there were more myelinated fibres in the regenerating unit for patients treated with NT-3 as compared to placebo (Sahenk *et al.,* 2005).

NT-4/5 administration post rat sciatic nerve injury improved axonal regeneration, functional recovery as well as increased myelin thickness (Yin *et al.,* 2001). Simon *et al.* (2003) observed that NT-4/5 carrying conduits in rat sciatic nerve injury model helped in improving the innervation of motoneurons to type 1 muscle fibres.

In one injury model, following sciatic nerve resection injury in rats, lentiviral vectors to overexpress either BDNF, GDNF, NGF, CNTF or NT-3 was injected in the resected sciatic nerve ex vivo and sutured back with the original nerve (Hoyng *et al*., 2014). In their data only BDNF, GDNF or NGF overexpression increased number of axons in the grafted nerve segment, two weeks following resection injury. However, functional recovery studies showed that rats with overexpression of BDNF and GDNF exhibited impaired motor functional recovery while overexpression of NGF showed impaired sensory functional recovery by week 20 following injury. This impairment in rats with elevated levels of BDNF and GDNF was shown to be a result of reduced myelination and impaired muscle innervation distal to injury site, 20 weeks following injury. Sensory functional recovery in NGF-overexpressing rats was shown to be due to extensive growth of sensory axons and increased SC proliferation causing the formation of axon coils in the grafted region (Hoyng *et al.*, 2014)

## 1.7.5 Axon guidance molecules

### 1.7.5.1 Ephrin ligands and their Eph receptors

Erythropoietin-producing human hepatocellular receptors (Ephs) are a large family of tyrosine kinase receptors that mediate contact-dependent cell–cell communication via Eph receptor-interacting proteins (Ephrin ligands) (Lisabeth *et al.*, 2013). Both the ligand and receptor are divided into two classes: A-subclass ephrins, which are attached to the cell membrane by a glycosylphosphatidylinositol (GPI) linkage and bind to EphA receptors; and B-subclass ephrins which have a transmembrane domain and bind to EphB receptors (Gale *et al.*, 1996). The receptor to ligand binding is promiscuous within each A or B class, with certain differences in binding affinities (Gale *et al.*, 1996; Himanen *et al.*, 2004).  Upon cell contact Eph-ephrin can transduce signals bidirectionally into cells expressing Eph (forward signalling) and the cells expressing the Ephrin ligand (reverse signalling) (Huot, 2004).

Although previously Ephrins have been shown to act as growth cone repellents, some studies have also shown that contact mediated attraction is also possible (Holmberg and Frisén, 2002). Eph/Ephrin signalling is known to direct the movement of cells and has been extensively studied during development, for instance in guiding of growth cones of axons and neural crest cells during development (Krull *et al.*, 1997; Wang and Anderson, 1997; Wilkinson, 2001; Lackmann and Boyd, 2008). Although initially it was thought that

each Eph or ephrin family member responded specifically by mediating either attraction or repulsion, current thinking is that the same Eph/Ephrin duo can mediate either response (Halloran and Wolman, 2006; Egea and Klein, 2007)

In the peripheral nerve, EphA4 expression was reported in SC cultures obtained from intact and injured sciatic nerves (Wang *et al.*, 2013). Additionally, the authors also demonstrated the inhibitory effect of EphA4 on SC migration and PNR. By knocking down EphA4 in SCs they observed an increase in SC migration. While in in vivo experiments, EphA4 expression in rats was inhibited by shRNA and four days post-transection surgery, axonal outgrowth increased in the target group as compared to the control (Wang *et al.*, 2013). EphA4 was also shown to inhibit myelination in vitro by inhibiting SC differentiation but increasing SC proliferation (Chen *et al.*, 2019b). The authors also demonstrated an upregulation of EphA4 in SCs post sciatic nerve crush injury in rats up until day 14 which was followed by a decrease until day 28. Additionally, in rats by siRNA-mediated knockdown of EphA4 or an EphA4 overexpression vector injected in the sciatic nerve post-crush, they demonstrated the role of EphA4 as a negative regulator of myelination (Chen *et al.*, 2019b).

In another study, it was reported that ephrin-B/EphB2 signalling between fibroblasts and SCs was crucial for cell sorting (Parrinello *et al.*, 2010). The study demonstrated that SCs and fibroblasts expressed EphB receptors and ephrin-B ligands. However, fibroblasts

expressed much higher levels of ephrin-B2 ligand, which was very low in SCs and vice versa for EphB receptors, with the most significant difference observed for EphB2 expression. Furthermore, deletion of EphB2 in mice and administration of inhibitory EphB2 fusion proteins at the transection site in rats resulted in disorganised migration of SCs from the nerve stumps post-transection injury which also led to misdirection of regenerating axons. Their results demonstrated that EphrinB2/EphB2 interaction between fibroblasts and SCs was needed for regeneration of the nerve bridge and thereby alignment of axons post transection injury.

### 1.7.5.2 Semaphorins

Semaphorins/collapsins are a large family of chemorepulsive proteins that are both secreted and membrane-bound and, similar to Eph/ephrin system, are essential during development of the nervous system as well as organogenesis (Raper, 2000). Among the eight classes of Semaphorins Sema3s (Sema3A-Sema3G) are the most characterised in vertebrates. Sema3s mediate their function by binding to neuronal receptor complexes comprised of neuropilins (NRP) and plexins (Raper, 2000).  Semaphorins are expressed in several neuronal cells of the developing and mature peripheral and central nervous systems (Wright *et al.*, 1995; Giger *et al.*, 1996; Kolodkin, 1996; Giger *et al.*, 1998). In the developing spinal cord Sema3s participate in the correct patterning of sensory projections (Messersmith *et al.*, 1995; Wright *et al.*, 1995; Püschel *et al.,* 1996). Whereas

in the developing peripheral nerves the mesenchymal cells express Sema3 and have been shown to guide growing axons to their targets (Wright *et al.*, 1995; Giger *et al.*, 1996).

Peripheral nerve crush injury in rats resulted in a decrease of Sema3 mRNA in injured motor neurons however its receptor, Neuropilin-1 mRNA's expression in both sensory and motor neurons did not change post-injury (Pasterkamp *et al.*, 1998). The authors hypothesised that downregulation of Sema3 is essential for regeneration of sensory and motor neurons post-PNI. Scarlato *et al.* (2003) demonstrated a significant increase in mRNA of Neuropilin 1 and 2 (NRP1 and NRP2) and NRP2 ligand Sema3F in the distal segment of the sciatic nerve 4 days post-crush and transection injury, with almost a 14-fold increase in NRP2 four days post axotomy. Bannerman *et al.* (2008), using mice with a global knockdown of NRP2 demonstrated that axonal regeneration towards the distal segment post-crush injury in mice was impeded. Moreover remyelination of regenerated axons and functional recovery was significantly impeded in the NRP2 deficient mice, 2 weeks following crush injury thus outlining its role in PNR.

### 1.7.5.3 Slits and Robos

Another family of key axon guidance molecules is the Slit family and its receptors - roundabout (Robo). The Slit/Robo pairing has been widely studied for its repellent signalling in axon pathfinding and neuronal migration during the development of the

nervous system (Kidd *et al.*, 1999; Yuan *et al.*, 1999; Brose and Tessier-Lavigne, 2000; Hammond *et al.*, 2005). Three Slit subtypes – Slit1-3 (Holmes *et al.*, 1998; Yuan *et al.*, 1999) and four Robo receptor subtypes – Robo1-4 (Kidd *et al.*, 1998; Yuan *et al.*, 1999; Huminiecki *et al.*, 2002) have been identified in vertebrates.

In the adult mouse peripheral nervous system, Carr *et al.* (2017) reported that Slit1-3 and its receptors Robo1 and 2 were expressed by the perikarya of dorsal root ganglia (DRG) and ventral spinal cord as well as motor and sensory axons. Their data also showed that Slit2, Slit3, and Robo1 were also expressed by satellite cells of DRGs, fibroblasts and SCs in peripheral nerves while Robo2 and Slit1 are only expressed by axons in the PNS. In an injury model in rats, Slit1 mRNA was found to be weakly expressed in the facial nerve which increased from day 5 up until day 28 post-transection injury (Fujiwara *et al.*, 2008). On the other hand, Slit2 mRNA expression decreased from day 1 of transection injury up until day 7, while Slit 3 expression remain unchanged. In a study carried out on zebrafish, Robo2 was found to be important for preventing erroneous trajectories of the dorsal nerve axons at nerve branch points after transection injury (Murphy *et al.,* 2022). Therefore the authors suggested that Robo2 promotes the regeneration of axons toward their dorsal targets (Murphy *et al.,* 2022).

## 1.7.5.4 Netrin-1 and its receptors

Netrins are a family of extracellular, laminin-related proteins that have been identified as key players in axonal guidance, cell migration and proliferation, inflammation, stem cell maintenance and angiogenesis during neural development (Cirulli and Yebra, 2007; Sun *et al.*, 2011; De Castro, 2003). A significant breakthrough in axon guidance came with the discovery of Netrin-1. In *C.elegans*, unc5 mutants presented a disruption in dorsal migration of pioneer axons and cell migration alongside the body wall of the nematode (Hedgecock *et al.,* 1990). Whereas unc40 mutants showed a disruption in mainly ventral migration but unc6 mutants showed a disruption in either of the directions (Hedgecock *et al.,* 1990). The unc6 protein was identified as a secreted laminin related protein in *C. elegans* (Ishii *et al.,* 1992). Serafini *et al.* (1994) purified Netrin-1 and Netrin-2, homologous to unc6 in *C.elegans* from embryonic chick brain and showed that both Netrins promoted axonal outgrowth in cultured explants of embryonic rat dorsal spinal cord. Deleted in colorectal cancer (DCC) and Neogenin in mammals as well as Frazzled in *D. melanogaster* were identified as homologs of unc40 in *C.elegans* (Chan *et al.,* 1996; Keino-Masu *et al.,* 1996; Kolodziej *et al.,* 1996). All three are transmembrane receptors of the immunoglobulin superfamily. Several UNC5 homologs of unc5 in *C.elegans* have also been identified in vertebrates (Ackerman *et al.,* 1997; Leonardo *et al.,* 1997).

Other than Netrin-1 and -2, Netrin-3, -4,-5,-G1 and -G2 have been identified (Van Raay *et al.,* 1997; Koch *et al.,* 2000; Nakashiba *et al.,* 2000; Nakashiba *et al.,* 2002; Yamagishi *et al.,* 2015). Among the Netrin proteins identified, Netrin-1 is the best-characterised member of the family. Kennedy *et al.* (1994), showed that Netrin-1 was a diffusible chemoattractant, secreted by floor plate cells in rat chick embryo. Their study also showed that recombinant Netrin-1 promoted commissural axon outgrowth and reorientation in in vitro explant cultures of rat dorsal spinal cord. However, Netrin-1 also exhibited repulsion of trochlear motor axons (that innervate the superior oblique muscles of the eye) in vitro thus suggesting the bifunctional guidance role of Netrin-1 as both a chemoattractant and a chemorepulsive cue (Colamarino and Tessier-Lavigne, 1995). Netrin-1 deficient embryos at embryonic day 10.5 and 11.5 (E10.5 and E11.5) exhibited aberrant trajectories of spinal commissural axons and brain development defects with mice homozygous for Netrin-1 mutant allele, dying shortly after birth (Serafini *et al.,* 1996).

DCC was first recognised as a tumour suppressor gene with evidence showing deletion of one DCC allele associated in chromosome 18q in human patients with colorectal cancer (Fearon *et al*., 1990). However, several studies since then were focused on studying DCC as a chemoattractive receptor to Netrin-1 for guidance of commissural axons during development (Keino-Masu *et al.,* 1996). The work of Keino-Masu *et al.* (1996) showed DCC expression by spinal commissural axons in rats. Also, their in vitro

experiments on explant cultures of rat dorsal spinal cord using anti-DCC antibody, blocked Netrin-1-mediated outgrowth of commissural axons (Keino-Masu *et al.,* 1996). Similar to Netrin-1, mouse pups with a homozygous deletion of DCC die shortly after birth (Fazeli *et al.*, 1997). Studying the DCC null mouse embryos at embryonic day 9.5-11.5 showed misdirection of commissural axons in the ventral spinal cord as well as impaired development of the brain with absence of corpus callosum and hippocampal commissure (Fazeli *et al.*, 1997). Unrelated to axon guidance, their data also showed that DCC deletion did not increase or affect tumorigenesis in the mice.

The chemorepellant activity of Netrin-1 is thought to be mediated by the binding of Netrin-1 to the UNC5 family of receptors. In studies on cultured *Xenopus* spinal cord neurons from neural tube tissue of stage 22 embryos, 5 µg/ml of Netrin-1 gradient mediated attraction of growth cones (Hong *et al.,* 1999). Whereas neurons from embryos injected with either mammalian UNC5A, UNC5B or unc5 mRNA (*C.elegans*) mediated repulsion of growth cones of neurons away from the Netrin-1 gradient (Hong *et al*., 2000). Delivery of a monoclonal antibody against the extracellular domain of DCC in cultured *Xenopus* axons from UNC5B mRNA injected embryos, saw neither attraction nor repulsion of axons in the presence of a Netrin-1 gradient (Hong *et al*., 1999). Several studies on Netrin-1's axon guidance bifunctionality showed that to mediate chemoattraction Netrin-1 binds to two neighbouring DCC receptors thus initiating the homodimerisation of DCC on the growth cone (Figure 8). This triggers the recruitment of

several intracellular signalling complexes thus activating Src family kinases which initiate actin cytoskeleton rearrangement (Liu *et al.*, 2004; Finci *et al.*, 2014; Dun and Parkinson, 2017). In the presence of UNC5 receptors, Netrin-1 binds to UNC5 and DCC on two separate receptor-binding sites and this leads to the linkage of DCC and UNC5 resulting in an intracellular signalling pathway that mediates repulsion (Figure 8) (Hong *et al.,* 1999; Finci *et al.,* 2014). However, in *Drosophila* Netrin-1 binding with both Frazzled (mammalian DCC homolog) and UNC5 was shown to facilitate only long-range repulsion, while UNC5-Netrin-1 binding was sufficient to facilitate short-range repulsion of commissural axons (Keleman and Dickson, 2001). This shows that Netrin-1's function in axon guidance is dependent on its binding to the specific receptor on the growth cone.
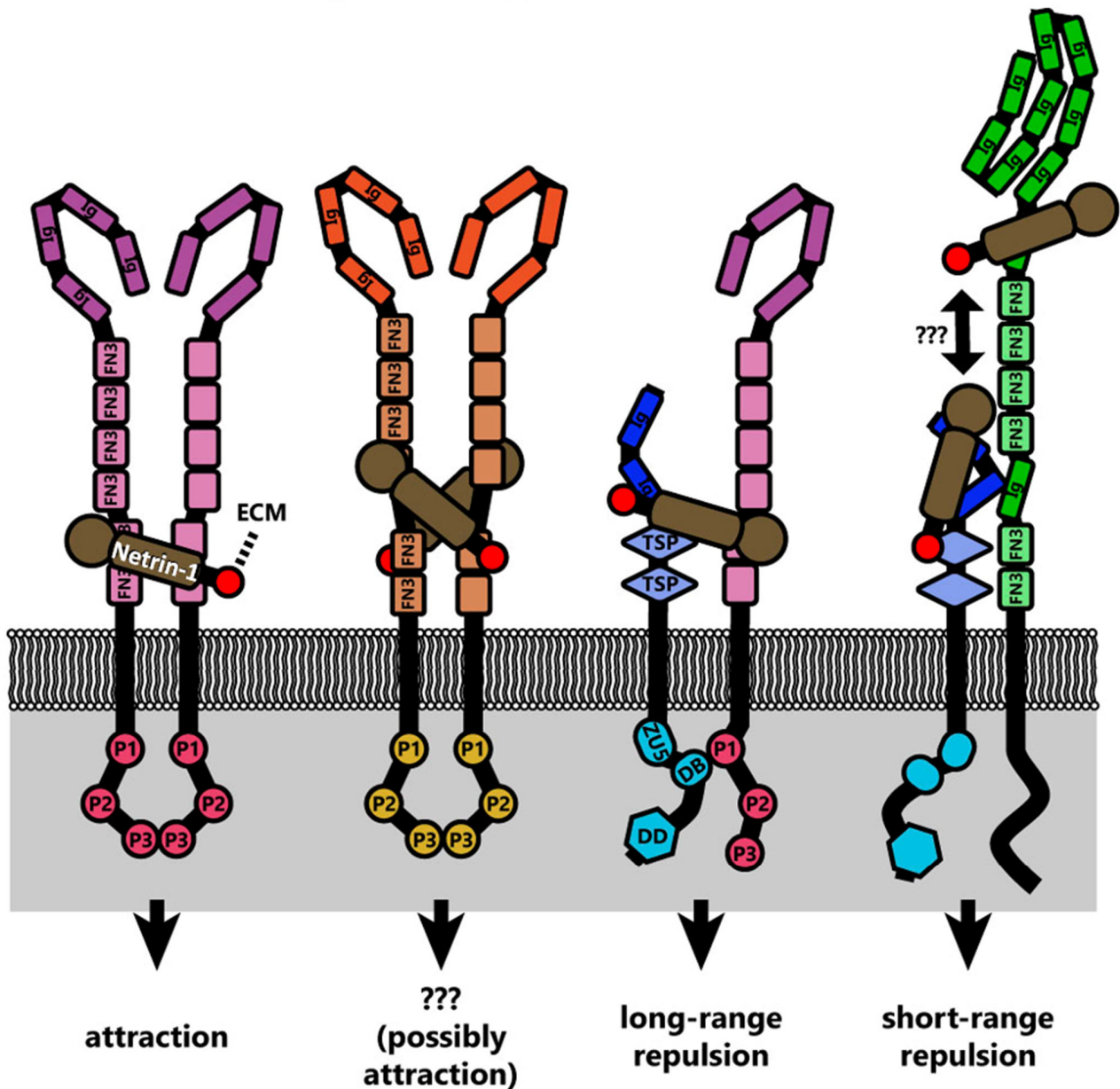
**Figure 8: Netrin-1 mediated chemoattraction and repulsion is dependent on receptor binding**

Netrin-1 binds to two neighbouring DCC receptors presented on the cell membrane resulting in homodimerisation via its P3 intracellular domain. Netrin-1 binding to DCC mediates chemoattraction, involving several intracellular signalling components resulting in the reorganisation of actin cytoskeleton. Substrate-bound Netrin-1 can also potentially link DCC dimers to the extracellular matrix (ECM). The structure of DCC and Neogenin comprises of four Ig domains and six fibronectin type III

domains (FN3), a single-pass transmembrane region and a cytoplasmic tail with three highly conserved sequence motifs called P1-3 motifs. Netrin-1 has been suggested to bind to the FN3 repeats number 4, 5 and 6 in Neogenin and DCC. Two Netrin-1 molecules form an X-shaped dimer and bind to two Neogenin molecules. The function of Neogenin and Netrin-1 complex is yet to be defined but attraction has been suggested. The UNC5 receptors comprises of two extracellular Ig domains and two thrombospondin (TSP) domains while the intracellular domain is composed of a ZU5 domain, a DCC-binding domain (DB) and a death domain (DD). Both Ig repeats are Netrin-1 binding sites in UNC5. For Netrin-1 mediated repulsion, it has been shown that long range repulsion requires Netrin-1 binding to both DCC and UNC5 receptors resulting in a heterodimer and linkage of P1 motif in DCC with DB domain of UNC5 receptors. Short-range repulsion has been suggested to be mediated by Netrin-1 binding to UNC5 and a co-receptor DSCAM. DSCAM consists of ten extracellular Ig domains and six FN3 repeats, a transmembrane domain, and a cytoplasmic domain with Netrin 1 suggested binding to the Ig domain. Structural studies are yet to describe Netrin-1 binding to UNC5 and DSCAM (Boyer and Gupton, 2018).

Other receptors of Netrin-1 have been identified such as the Down syndrome cell adhesion molecule (DSCAM) that is expressed in the mammalian spinal commissural axons. DSCAM was previously suggested to interact with Netrin-1 for guiding of commissural axons across the ventral midline towards the floor plate cells during development in *Drosophila* and in in vitro studies (Andrews *et al.,* 2008; Ly *et al.,* 2008; Liu *et al*., 2009). However subsequent studies have shown that DSCAM is not important for this function. Palmesino *et al.* (2012) in DSCAM null mice observed normal commissural axon trajectory in the spinal cord of embryos. Moreover their in vitro experiments showed that axon outgrowth from dorsal spinal cord explants of the DSCAM knockout embryos was comparable to the control littermates in response to Netrin-1 (Palmesino *et al.,* 2012). DSCAM is expressed by mouse retinal ganglion cells (RGC)

during early development and while Netrin-1 is known to regulate the growth of the RGC axons through the optic disc to exit the eye into the optic nerve, studies performed on several DSCAM mutant mice showed that DSCAM was not required for this function (Bruce *et al*., 2017). These studies showed that DSCAM mutants do not display Netrin-like axon guidance deficits in the spinal cord or retina.

Other than axon guidance, Netrin-1 has also been shown to have a rather contradictory role in the development of the vasculature with studies showing Netrin-1-UNC5B mediated inhibition of angiogenesis (Larrivée *et al*., 2007) and some describing Netrin-1 as a pro-angiogenic factor (Wilson *et al*., 2006). CD146 (also known as melanoma cell adhesion molecule, MCAM) is a recently identified receptor of Netrin-1 implicated in facilitating angiogenesis and vascular development (Tu *et al*., 2015).

## 1.8 NETRIN-1 IN INJURY OF THE NERVOUS SYSTEM

Several studies have also investigated the role of Netrin-1 following CNS injury (Bayat *et al*., 2012; Liao *et al*., 2013; Bai *et al*., 2017). Administration of Netrin-1 improved spatial memory and synaptic dysfunction in rats with global cerebral ischemia (*Bayat et al*., 2012). Exogenous Netrin-1 treatment also attenuated neuronal loss by reducing apoptosis in the ipsilateral ventroposterior thalamic nucleus after focal cerebral infarction in renovascular hypertensive rats (Liao *et al*., 2013). In a model of rat spinal cord injury, Netrin-1 treatment prevented the loss of motor neurons and improved

functional recovery (Bai *et al.*, 2017). This data suggests a neuroprotective role of Netrin-1 in the CNS following injury.

## 1.8.1 Netrin-1 and DCC expression in intact peripheral nervous system and after injury

Major research on Netrin-1 and its receptors has been focused on studying its role in neural development as well as in CNS injury yet very few studies have been carried out to understand its potential role in PNR. Madison *et al.* (2000) reported a 40-fold upregulation of Netrin-1 mRNA two weeks post-transection injury in the distal sciatic nerve but no change in the mRNA levels following a crush injury. Their data also showed that Netrin-1 was undetectable in intact nerves but was expressed by not all but several SCs of the distal nerve segment (Madison *et al.*, 2000). Therefore, it was hypothesised that SCs could be one of the main sources of Netrin-1 upregulation in the distal nerve segment post-injury. In agreement with this, in a recent study on a model of chronic restriction injury on rat sciatic nerves, the authors reported as much as a 2.6-fold increase in Netrin-1 mRNA in the sciatic nerve. This upregulation was observed as early as 6 hours post-injury and a peaked at 21 days post-injury, which was the maximum time-point analysed in this study (Chen *et al.*, 2021b). However, the same study showed that despite upregulation of Netrin-1 mRNA, the protein expression by immunohistochemistry was reduced by 58% in the sciatic nerve 7 days following injury.

Lee *et al.* (2007) reported no expression of DCC mRNA in RT4 schwannoma cells (rat schwannoma cell line) and primary rat SCs by RT-PCR. Immunoblotting to detect DCC and Neogenin also showed that both proteins were not expressed in RT4 and iSC schwannoma cell lines (immortal Schwann cell line) (Lee *et al.*, 2007). Lv *et al.* (2015) by RT-qPCR showed that RSC96 cells (an immortalised rat SC line) expressed Netrin-1 mRNA whereas DCC mRNA was not detected. Webber *et al.* (2011) studied the expression of Netrin-1 and DCC in rat dorsal root ganglia, with no variation in Netrin-1 mRNA levels post-transection injury while there was a significant upregulation of DCC protein and mRNA level at 7 days post-injury. Their data also showed that DCC was expressed robustly in both the proximal nerve stump and distal nerve segment 7 days following a transection injury in some regenerating axons, but more importantly in the leading migrating SCs immediately distal to the injury site (Webber *et al.*, 2011).

## 1.8.2 Role of Netrin-1 and DCC in peripheral nerve regeneration

Netrin-1 is thought to be involved in regulating SC proliferation and migration post nerve transection injury (Lee *et al.*, 2007; Lv *et al.*, 2015). When treated with exogenous Netrin-1 (50 ng/ml), cell proliferation was induced in RT4 schwannoma cells, however this proliferation was inhibited by knocking down UNC5B using UNC5B specific RNAi, indicating that UNC5B might be the receptor involved in stimulating SC proliferation (Lee *et al.*, 2007). Yet another study carried out on RSC96 cells saw that Netrin-1 at a

concentration ranging from 0 to 500 ng/ml had no effect on the proliferation of the RSC96 cells yet significantly promoted SC migration only at a dose of 100 ng/ml (Lv *et al.*, 2015). The authors stated that Netrin-1 promoted SC migration in a dose-depended manner by activating p38 mitogen activated protein kinase (MAPK) and PI3K-Akt. They hypothesised that at lower dosage, Netrin-1 was responsible for increase in the phosphorylation of p38 MAPK and PI3K-Akt and promoted migration of RSC96 cells whereas the exact opposite effect was observed at a higher dosage of Netrin-1 (500ng/mL). UNC5B was described as the receptor involved with Netrin-1 in migration of RSC96 cells as 100 ng/ml of Netrin-1 also increased UNC5B protein expression, explained by the authors, as a way to adapt to a higher Netrin-1 concentration (Lv *et al.*, 2015). However, Netrin-1 physiological concentration varies between 50 – 150 ng/ml in vertebrates (Castets and Mehlen, 2010; Serafini *et al.,* 1994). Moreover, several studies have shown the dose-dependent function of Netrin-1 with evidence pointing to an inhibitory role of Netrin-1 at higher concentrations for its role in angiogenesis, axon guidance and migration (Serafini *et al*., 1994; Lu *et al.,* 2004; Larrivee *et al*., 2007).

Very little has been done to study the role of Netrin-1 and DCC in PNR in in vivo models. Previously, Jaminet *et al.* (2013) observed a significantly slower functional recovery in grasping tests post-median nerve transection and repair in Netrin-1 heterozygous mice (50% reduction in mRNA and protein expression), with reduced grasping strength even 50 days following injury as compared to pre-injury. In zebrafish, DCC mutants (90%

reduction of DCC mRNA), exhibited aberrant trajectories of motor axons at the injury site, 48hrs post-motor nerve transection injury (Rosenberg *et al.*, 2014).

Despite Netrin-1 and its receptors such as DCC gaining attention for its potential to mediate PNR, not much is known about the underlying molecular mechanisms involved or their function in vivo. This might be in part owing to the difficulties in generating an appropriate mouse model lacking Netrin-1 or DCC.  As described previously, mice with global deletion of either Netrin-1 or DCC causes abnormal commissural axon extension towards the floor plate; several brain developmental defects and in both cases death of mouse pups shortly after birth (Serafini *et al.*, 1996; Fazeli *et al.*, 1997). However, recently several lab groups have successfully generated Netrin-1 and DCC conditional knockout mouse models (Dominici *et al.*, 2017; Krimpenfort *et al.*, 2012).

In this study to circumvent embryonic lethality after the deletion of DCC or Netrin-1 during embryonic development, I employed the use of a Cre-lox system to generate conditional mutants. Breeding Ntn1$^{loxP/loxP}$ mice (Dominici *et al.*, 2017), with SC-specific Cre recombinase mice P0-Cre (mP$_0$-TOTACRE) (Feltri *et al.*, 1999), I generated SC-specific Netrin-1 knockout mice (Ntn1 KO) to investigate if Netrin-1 is a key signalling  molecule produced by SCs to direct axon regeneration. I also bred DCC$^{loxP/loxP}$ (Krimpenfort *et al.*, 2012) with ROSA-26-Cre/ERT2 mice and induced global DCC knockout in adult mice by Tamoxifen injection to study a possible Netrin-1/DCC signalling after peripheral nerve

injury in adult mice. However, I could not generate a global deletion of Netrin-1 after Tamoxifen dosing in adult mice on breeding the Ntn1$^{loxP/loxP}$ mice (Dominici *et al.*, 2017) with ROSA-26-Cre/ERT2 mouse line (Hameyer *et al.*, 2007) for further experiments to study the effect of complete Netrin-1 ablation on PNR.

My hypothesis, based on the data available in literature, was that SCs express Netrin-1 to guide both motor and sensory regenerating axons across the nerve gap after an injury by interacting with DCC expressed on the regenerating axons. Thus, one aim of this study was to confirm the regulation and expression of Netrin-1 and its receptor DCC in intact PNS and following injury. But importantly I was interested in investigating the role of Netrin-1 and DCC in PNR following injury in the described mouse models.

# CHAPTER 2: MATERIALS AND METHODS

## 2.1 Generation of transgenic mouse strains

All animal work was performed following Home Office regulations under the UK Animals (Scientific Procedures) Act, 1986. Ethical consent for the work carried out in this study was approved by Plymouth University Animal Welfare and Ethical Review Board. All mouse lines were kept in a dedicated animal facility under a 12hr light and 12hr dark cycle. Food and water were provided *ad libitum* to the mice with daily cage checks, periodical change of cage bedding and humane sacrifice of the animals by a Schedule 1 procedure at appropriate time points.

### 2.1.1 Netrin-1 and DCC mice strains

Breeding pairs for C57BL/6 mice were previously procured from Charles River Laboratories (Wilmington, Massachusetts). The Ntn1$^{loxP/loxP}$ mice having two unidirectional loxP sites flanking the exon 3 of the Netrin-1 gene (Dominici *et al*., 2017) and DCC$^{loxP/loxP}$ mice having two loxP site insertions flanking exon 23 of DCC (Krimpenfort *et al*., 2012) were obtained from Professor Alain Chedotal (Institut de la Vision, Paris, France). The P0-Cre (mP0-TOTACRE) strain has been described previously (Feltri *et al*., 1999), wherein P0-Cre expression is controlled by the myelin protein zero promoter and is expressed specifically in the SCs. Mice with SC-specific knockout of Netrin-1 (P0-Cre$^{+}$ Ntn1$^{loxP/loxP}$) were generated by crossbreeding floxed Netrin-1 (Ntn1$^{loxP/loxP}$) mice with the

P0-Cre[+] line. Ntn1[loxP/loxP] mice were cross-bred with ROSA-26-Cre/ERT2^{+} mice (R26-CreERT2) (Hameyer *et al.*, 2007), provided by Professor Karen Blyth (University of Glasgow, U.K), to produce Netrin-1 global knockout mice (R26-CreERT2^{+} Ntn1[loxP/loxP]). Here, R26-CreERT2 transgene is driven by the endogenous mouse Gt (ROSA)26Sor promoter which is ubiquitously expressed in mouse embryos and is active in most cells. The PLP-GFP transgenic mice express GFP in oligodendrocytes in the CNS and in myelinating and non-myelinating SCs of the peripheral nerve (Mallon *et al.*, 2002; Chen *et al.*, 2019a) and were crossed with P0-Cre[+] Ntn1[loxP/loxP] mice to generate SC-specific Netrin-1 knockout mice expressing GFP in SCs (P0-Cre[+] Ntn1[loxP/loxP] PLP-GFP[+]). Global knockout of DCC was generated in mice (R26-CreERT2^{+} DCC[loxP/loxP]) by breeding DCC[loxP/loxP] mice with R26-CreERT2^{+} mice . For all experiments, age and sex matched littermates having the floxed allele but negative for Cre were used as controls. All mice were kept on a C57BL/6 background.

**2.1.2 Runx2 mouse strain**

The Runx2 [loxP/loxP] mouse (having two loxP site insertions flanking exon 3 of Runx2) were described previously (Ferrari *et al.*, 2015). Similar to Netrin-1 mice, deletion of Runx2 in Schwann cells was achieved by breeding the Runx2 [loxP/loxP] mice with P0-Cre mice (mP0-TOTACRE) (Feltri *et al.*, 1999) to get mice with SC-specific knockout of Runx2 (P0-Cre[+] Runx2[loxP/loxP]). These mice were bred with PLP-GFP mice to obtain SC-specific Runx2

knockout mice that expressed GFP in SCs (P0-Cre[+] Runx2[loxP/loxP] PLG-GFP[+]) (Mallon *et al.*, 2002). For all experiments, age and sex matched littermates having the loxP inserts but lacking the Cre transgene were used as controls. All mice were maintained on an FVB background.

## 2.2 Genotyping and Polymerase Chain reaction (PCR)

For mouse genotyping, newly weaned mice were ear notched and genomic DNA was extracted using hot sodium hydroxide and tris (HotSHOT) technique (Truett *et al.*, 2000). Briefly, 75 μL of alkaline lysis reagent (For recipe refer to Table 10) was added to the ear notches and heated to 95°C in a PTC-100 Peltier Thermal Cycler (M.J. Research, Waltham, USA) for 90 minutes followed by cooling to 4°C. The samples were vortexed briefly and 75μl of neutralisation reagent (For recipe refer to Table 10) was added followed by another round of vortexing and storage at -20˚C. 2 μl of DNA was used for genotyping in a typical PCR mix as described in Table 1 and the PCR program was setup on G-Storm GS0004M PCR machine as described in Table 2.

Agarose gel electrophoresis was used to resolve the PCR products. 15ul of the PCR product was loaded onto a 1-2% agarose gel (For recipe refer to Table 10) and electrophoresed in 1X Tris-acetate-EDTA (TAE) buffer (For recipe refer to Table 10) at 120V for 30-60 minutes with a Bio Rad Power Pac 300 and a BioRad Sub-Cell GT tank

(Hercules, California, USA). The gel was imaged on Pxi Genesys gel imaging system (NI, Austin, Texas, USA).

**Table 1: Optimised concentration of polymerase chain reaction (PCR) components for genotyping of mice**

| Reaction Components | Volume | Final Concentration |
|---|---|---|
| 5X Green GoTaq® Flexi Buffer (Promega, M891A) | 5 µl | 1X |
| dNTP mix (Promega, U120A-U123A) | 0.5 µl | 200 µM each |
| MgCl$_2$ (Promega, A351H) | 1.5 µl | 1.5mM |
| Forward and reverse primers (Eurofins, Germany) | 1 µl | 0.5 µM each |
| Nuclease free water (Invitrogen, 750023) | 14.9 µl | |
| GoTaq® G2 Hot Start Polymerase (Promega, M740B) | 0.1 µl | 1.25U |
| DNA template | 2 µl | |
| **Total volume** | 25 µl | |

**Table 2: Polymerase chain reaction (PCR) program. Annealing temperature and time were modified for different primer pairs.**

| Steps | Temperature ˚C | Time | Cycles |
|---|---|---|---|
| Initial Denaturation | 95˚C | 5 minutes | 1 |
| Denaturation | 95 ˚C | 30 seconds | 35 |
| Annealing | 55-62˚C | 40 seconds | |
| Extension | 72 ˚C | 40 seconds | |
| Final Extension | 72 ˚C | 5 minutes | 1 |

For mice with SC-specific knockout of Netrin-1 (P0-Cre$^+$ Ntn1$^{loxP/loxP}$), genotyping was carried out to check the presence of P0-Cre, loxP sites and the deletion of exon 3 of Netrin-1 (Table 3). The PCR for loxP sites would show a single band of 458bp for the presence of homozygous loxP sites, a single band at 312bp for wild-type Netrin-1 and two bands of both sizes if heterozygous for loxP site. PCR for presence of P0-Cre would show a single band of 492 bp. For mice with global knockout of Netrin-1 (R26-CreERT2$^+$ Ntn1$^{loxP/loxP}$ ), genotyping was done for the presence of homozygous loxP sites (as described above) and to detect presence of R26-CreERT2 transgene with the primers designed to amplify a 300bp product if the transgene was present (Table 3). For both the mouse lines I could also confirm the knockout of Netrin-1 by genotyping. Primers for confirming deletion of exon 3 of Netrin-1 were designed by GenOway (Lyon, France) who generated the Netrin-1 floxed mouse line for Professor Alain Chedotal (Table 3).

Genotyping would give a band of 498bp only after deletion of exon 3 of Netrin-1 whereas the product size was too large to be amplified by PCR for the control mice with no deletion of Netrin-1 (Table 3).

For DCC global knockout mice (R26-CreERT2$^+$ DCC$^{loxP/loxP}$) genotyping was required to determine the presence of R26-CreERT2 transgene (as described above) and loxP sites and was genotyped as previously described (Krimpenfort *et al.*, 2012). PCR for loxP sites in DCC showed a single band of 300bp for insertion of two loxP sites, a single band of 200bp for presence of wild-type DCC gene and two bands of both sizes if they were heterozygous for the loxP sites (Table 3). After Tamoxifen injections, the DCC mice were again genotyped as previously described (Krimpenfort *et al.*, 2012), with a band of 400bp only after deletion of exon 23 of DCC and no band observed for the control mice (Table 3).

In mice with SC-specific knockout of Runx2 (P0-Cre$^+$ Runx2$^{loxP/loxP}$), genotyping was performed for the presence of loxP sites and P0-Cre (as mentioned above). PCR for loxP sites amplified a band of 203bp for the presence of loxP, a band of 169bp for wild-type genotype and double bands of both sizes for mice heterozygous for loxP (Table 3). To confirm the presence of heterozygous GFP in mice, primers were designed to amplify a 173bp product (Table 3).

**Table 3: List of primers for the amplification of target genes by PCR with their individual sizes**

| Gene | Forward Primer 5'- 3' | Reverse Primer 5'- 3' | Size (bp) |
|------|----------------------|----------------------|-----------|
| P0-Cre mouse | CCACCACCTCTCCATTGCAC | GCTGGCCCAAATGTTGCTGG | 492 |
| R26Cre mouse | CGATGCAACGAG TGATGAGGTTC | GCACGTTCACCGGCATCAAC | 300 |
| GFP mouse | AAGTTCATCTGCA CC ACCG | TCCTTGAAGAAGATGGTGCG | 173 |
| DCC loxP site | CAAGACACATGGAAGGTGAAA TG | GACCTCACTTACATATCAAAAT GG | WT:200 loxP :300 |
| Netrin1 loxP sites | CACCTCTGAACTCTGGCTG | GGATACAGTAATCTGGGCTC | WT:312 loxP: 458 |
| Runx2 loxP sites | GACCTCCTCCCTACAGCTTC | CCCTCGCGTTTCAAGGTGCC | WT:169 loxP:203 |
| DCC KO mouse | CAAGACACATGGAAGGTGAAA TG | CCCAAATCTTCTATATTACAATA TC | 400 |
| Netrin-1 KO | AACTGGTTCCAAGCTGC AAGGAGCT | AAGGAAGCCCTTGGGCCAGA AT | 498 |

## 2.3 Tamoxifen Injections

To induce Cre recombination, 5-7 week old floxed DCC or Netrin-1 mice with ROSA-26-Cre/ERT2 (R26-CreERT2$^+$ DCC$^{loxP/loxP}$ or R26-CreERT2$^+$ Ntn1$^{loxP/loxP}$) were intraperitoneally injected with Tamoxifen (Sigma-Aldrich, T-5648) once a day for 5 consecutive days at a

dosage of 75 mg Tamoxifen/kg per day. For R26-CreERT2$^+$ Ntn1$^{loxP/loxP}$ mice, gavaging of

Tamoxifen was also attempted using the same dosage of Tamoxifen. The Tamoxifen was

dissolved in corn oil at a concentration of 20 mg/ml by shaking overnight at 37°C and

stored at 4°C. Two weeks after the last injection the mice were re-genotyped to detect

DCC and Netrin-1 deletion as previously described (Krimpenfort *et al.*, 2012; Dominici *et*

*al.*, 2017).

## 2.4 Peripheral nerve surgery

Six to eight-week-old male and female mice were selected and anesthetised with

isoflurane. The mice were subcutaneously injected with nonsteroidal anti-inflammatory

drug Meloxicam (Metacam Boehringer Ingelheim 5mg/ml) as an analgesic at a dosage of

5mg/kg for adult mice. Either nerve transection or crush injury protocols was performed

on the mice. After a longitudinal incision, nerve transection was performed on the

exposed right sciatic nerve, 0.5 cm distal to the sciatic notch and the two disconnected

nerve ends were not sutured or joined back together. To induce nerve crush injury, the

right sciatic nerve was compressed for 30 seconds using delicate forceps, and again for

30 seconds at the same location but orthogonal to the initial crush. The left sciatic nerve

was left uninjured.  Following either transection or crush injury, the overlying muscle

covering the nerve was sutured. Post suturing, analgesia (0.025% bupivacaine solution),

was topically administered above the muscle suture and the skin was closed with an auto

clip applier. The animals were monitored daily and depending on the experiment, at necessary time points post-surgery, the mice were euthanised humanely according to UK Home Office regulations and the required tissue was dissected out.

## 2.5 Immunofluorescence

### 2.5.1 Antigen Retrieval for immunohistochemistry

Dorsal root ganglia (DRGs), spinal cord (SC) or injured and uninjured sciatic nerves were dissected out from the experimental mice at required time points and fixed for minimum 5 hrs in 4% paraformaldehyde (For recipe refer to Table 10). The tissue was washed twice in 1X PBS and incubated in pre-heated 10mM sodium citrate buffer with 0.05% Tween20 (For recipe refer to Table 10) in a 12-well plate. The plate was placed in a water bath pre-heated to 80°C for 30 minutes. The tissue was removed from the water bath, washed twice with 1X PBS and left for 48 hrs in 30% sucrose at 4°C. Following this, each tissue was embedded in OCT embedding matrix (Cell Path, KMA-0100-00A) and cut into 10μm transverse sections using a Leica CM1860 Cryostat (Leica Microsystems, Wetzlar, Germany) and placed onto SuperFrost Plus microscope slide (VWR, 631-0448) for immunohistochemistry.

### 2.5.2 Immunohistochemistry

DRGs, spinal cord, and injured and intact sciatic nerves were dissected out after euthanisation of mice. The tissue samples were fixed in 4% paraformaldehyde for 5 hrs

at 4°C followed by three times wash with 1X PBS. The samples were immersed in 30% sucrose at 4°C overnight to cryoprotect the tissues. The tissue was then put in a plastic embedding mould (VWR, 720-0820-22) and OCT embedding matrix (Cell Path, KMA-0100-00A) was poured to cover the tissue. The moulds were then placed in a box with liquid nitrogen to freeze the tissue in OCT. 10μm sections of the tissue was cut from the solid OCT blocks using the Leica CM1860 Cryostat and the sections were picked onto a SuperFrost Plus microscope slide (VWR, 631-0448) and left to dry.

For staining a hydrophobic barrier was drawn around the sectioned tissue on the slides using a PAP pen (Vector laboratories, H-4000). Once the barrier was dry, the slides were washed with 1X PBS to remove the OCT and the tissue permeabilised with 0.25% Triton X-100 (Sigma, T9284) in PBS (PTX) diluted in 1% bovine serum albumin (BSA) (Fisher Scientific, BP9702-100) for an hour (For recipe refer to Table 10). The permeabilisation solution was removed and the tissue blocked with a solution containing 3% BSA with 0.05% Triton X-100 in PBS (PTX) for an additional hour (For recipe refer to Table 10). Following the removal of the blocking buffer, primary antibodies (diluted in blocking buffer) were added to the slides and left overnight at 4°C (Refer to Table 4 for a list of primary antibodies). Following three washes with 1X PBS (ten minutes each), sections were incubated with the secondary antibody (Refer to Table 4 for a list of secondary antibodies) and Hoechst dye (Thermo fisher Scientific, 62249) for an hour at room temperature. Again after three 1X PBS washes, a drop of CitiFluor mounting solution

(Agar Scientific, R1320) was added to each slide and the tissue was covered with a coverslip (VWR, 631-0135). The edges of the coverslip were sealed with nail varnish and the slides were imaged on a Leica SPE confocal microscope (Leica Microsystems, Wetzlar, Germany).

## 2.5.3 Whole nerve staining

The whole nerve staining protocol was previously described by my research group (Dun and Parkinson, 2018). At the described time points after surgery, the sciatic nerve was dissected out and fixed in 4% paraformaldehyde (PFA) for 5 hrs at 4°C. They were then washed in 1X PBS three times for ten minutes each and incubated overnight in permeabilisation solution - 1% PTX in 10% foetal bovine serum (FBS, Sigma, F7524) (For recipe refer to Table 10) overnight at 4°C on a shaker. The next day, the tissue was kept in a solution containing 0.1% PTX in 10% FBS along with the primary antibody (Refer to Table 4) and incubated for 72hrs at 4°C. After the incubation with primary antibody, nerves were again washed with 1X PBS three times for 15 minutes for each wash. This was followed by continuous washes in 1X PBS for 6 hrs at room temperature, with a change of the PBS every 1 hr. The nerves were then immersed in a solution of 0.1% PTX in 10% FBS with secondary antibody (Refer to Table 4), for 48hrs at 4°C on a shaker. This was again followed by the 1X PBS washing steps as mentioned after removal of primary antibody. The nerves then underwent three stages of tissue clearing in 25%, 50% and

75% glycerol (Sigma-Aldrich, G6279) diluted in 1X PBS for 24hrs for each glycerol concentration. Mounting solution (Agar Scientific, R1320) was added to the slides and covered with a coverslip. Coverslip edges were sealed using nail varnish and slides were imaged on a confocal microscope.

**Table 4: Primary and secondary antibodies**

| Antibody | Host Species | Supplier | Cat. No | Dilution | Analysis |
|---|---|---|---|---|---|
| **PRIMARY ANTIBODIES** | | | | | |
| **Anti-neurofilament heavy chain polyclonal** | Rabbit | Abcam | ab8135 | 1:50(WM), 1:500 (IHC) | Whole nerve staining, IHC |
| **Anti-neurofilament heavy chain polyclonal** | Chicken | Abcam | Ab4680 | 1:50(WM) 1:600(IHC) | Whole nerve staining, IHC |
| **Anti-DCC polyclonal** | Goat | Santa Cruz Biotechnology | sc-515834 | 1:100 | IHC |
| **Anti-Netrin-1 monoclonal** | Rabbit | Abcam | ab126729 | 1:500 | WB, IHC |
| **Anti-Netrin-1 monoclonal** | Rat | R&D systems | MAB1109 | 1:100 | IHC |
| **Anti-GAPDH monoclonal** | Mouse | Abcam | ab8245 | 1:8000 | WB |

| Anti-NeuN monoclonal | Rabbit | Abcam | ab177487 | 1:500 | IHC |
|---|---|---|---|---|---|
| Hoechst dye | | Thermo fisher Scientific | 62249 | 1:500 | IHC |
| Anti-S100 polyclonal | Rabbit | Agilent | GA50461-2 | Ready to use | IHC |
| Anti-CD34 monoclonal | Rabbit | Abcam | ab198395 | 1:400 | IHC |
| Anti-GFP polyclonal | Chicken | Abcam | ab13970 | 1:400 | IHC |
| Anti-myelin basic protein polyclonal | Rabbit | Abcam | Ab40390 | 1:400 | IHC |
| Anti-Glucose Transporter GLUT1 polyclonal | Rabbit | Abcam | ab652 | 1:200 | IHC |
| Anti-Runx2 (D1H7) monoclonal | Rabbit | Cell Signaling Technology | 8486 | 1:1000(WB) 1:400 (IHC) | WB, IHC |
| Recombinant Alexa Fluor® 488 Anti-p75 NGF Receptor monoclonal | Rabbit | Abcam | ab195179 | 1:200 | IHC |
| Anti-Cre Recombinase (D7L7L) monoclonal | Rabbit | Cell Signaling Technology | 15036 | 1:1000 | WB |

| | | | | | |
|---|---|---|---|---|---|
| **Anti-Vinculin monoclonal** | Mouse | Sigma-Aldrich | V9131 | 1:2000 | WB |
| **Anti-CD31 monoclonal** | Rabbit | Cell Signaling Technology | 77699T | 1:200 | IHC |
| **SECONDARY ANTIBODIES** | | | | | |
| **Donkey Anti-rabbit Rhodamine (TRITC) polyclonal** | Donkey | Jackson Immuno Research | 711-025-152 | 1:200 | Whole nerve staining |
| **Donkey Anti-Rabbit Fluorescein (FITC) polyclonal** | Donkey | Jackson Immuno Research | 711-095-152 | 1:200 | Whole nerve staining |
| **Donkey Anti-Chicken Fluorescein (FITC) polyclonal** | Donkey | Jackson Immuno Research | 703-095-155 | 1:200 | Whole nerve staining |
| **Donkey Anti-Chicken Rhodamine (TRITC) polyclonal** | Donkey | Jackson Immuno Research | 703-025-155 | 1:200 | Whole nerve staining |
| **Donkey Anti-Goat IgG Rhodamine (TRITC) polyclonal** | Donkey | Jackson Immuno Research | 705-025-147 | 1:200 | IHC |
| **Alexa Fluor 633 goat anti- rat IgG (H+L) polyclonal** | Goat | Invitrogen | A21094 | 1:200 | IHC |

| | | | | | |
|---|---|---|---|---|---|
| **Alexa Fluor 488 donkey anti-Rat IgG (H+L) polyclonal** | Donkey | Invitrogen | A-21208 | 1:200 | IHC |
| **Alexa Fluor 488 goat anti-Chicken IgY (H+L) polyclonal** | Goat | Invitrogen | A-11039 | 1:200 | IHC |
| **Alexa Fluor 568 goat anti-chicken IgY (H+L) polyclonal** | Goat | Invitrogen | A-11041 | 1:200 | IHC |
| **Alexa Fluor 488 goat anti-Rabbit IgG (H+L) polyclonal** | Goat | Invitrogen | A-11008 | 1:200 | IHC |
| **Alexa Fluor 568 goat anti-Rabbit IgG (H+L) polyclonal** | Goat | Invitrogen | A-11011 | 1:200 | IHC |
| **Goat Anti-Rabbit IgG (H + L)-HRP Conjugate** | Goat | Bio-Rad | 1706515 | 1:5000 | WB |
| **Goat Anti-Mouse IgG (H + L)-HRP Conjugate** | Goat | Bio-Rad | 1706516 | 1:5000 | WB |

## 2.6 Edu labelling and cell proliferation assay

At appropriate time points post-peripheral nerve injury, the mice were injected intraperitoneally with EdU (Invitrogen, C1033), at a concentration of 1mg per 10g body weight. To make the solution, 100 mg/ml stock solution of EdU was made in dimethyl sulphoxide (DMSO) and then diluted 1 in 10 in PBS and injected followed by euthanisation of animals 3 hrs later. The nerves were dissected followed by fixation, cryoprotection, embedding in OCT compound, cryosectioning, permeabilisation and blocking steps (Refer to Section 2.5.2). The slides with the adhered tissue were incubated with the EdU Click-iT reaction cocktail (Invitrogen, C10339) for 30 min at room temperature. The slides were then washed with 1X PBS, three times for ten minutes each. If staining for other proteins, the slides were then incubated with the necessary primary antibody (Refer to Table 4) diluted in a blocking solution (3% BSA and 0.05% PTX) overnight at 4°C. The following day, after three washes with 1X PBS for ten minutes each, the sections were incubated with the secondary antibody (Refer to Table 4) diluted in 3% BSA and 0.05% PTX and Hoechst dye for 1hr at room temperature. The slides were again washed three times with 1X PBS and mounted in CitiFluor (Agar Scientific, R1320) for confocal imaging.

## 2.7 Western blotting

Sciatic nerves were dissected out and lysed in 1x SDS lysis buffer (Alfa Aesar, J61337) using a Fisherbrand™ Model 120 Sonic Dismembrator (Fisher Scientific, Waltham,

Massachusetts, USA). The samples were centrifuged down to 14,000 xg for 5 minutes to confirm absence of any remnant tissue particles and then heated at 95°C for 5 minutes for protein denaturation.

The lysates were loaded onto polyacrylamide gels (For recipe refer to Table 10) with gel percentage determined based on the size of the protein to be detected or on 4–20% Mini-PROTEAN® TGX™ Precast Protein Gels (BioRad, 4561094). SDS-PAGE was carried out in 1X Running buffer (For recipe refer to Table 10) using a Bio-Rad PowerPac Basic (Hercules, California, USA) with voltage kept constant at 120V until the bands have migrated from stacking to running gel and then at 150V for 60-90 minutes until the loaded protein size markers have separated sufficiently and the bromophenol blue has reached the bottom of the gel. The separated proteins were then transferred onto a 0.45μm polyvinylidene fluoride (PVDF) transfer membrane (Bio-Rad, 4561086) in 1X transfer buffer (For recipe refer to Table 10) at constant 250mA for 90 minutes with an ice pack submerged in the electrophoresis chamber to prevent generation of excess heat. Post-transfer the membrane was blocked either with 5% skimmed milk in Tris buffered saline with 0.1% Tween-20 (TBST; for recipe refer to Table 10) or with 5% BSA (w/v) in 1X TBST for 1hr at room temperature. The membrane was then incubated with primary antibodies (Refer to Table 4) diluted in 5% skimmed milk (in TBST) overnight at 4°C. The next day, the membranes were washed three times in 1X TBST for 10 min each followed by incubation with HRP conjugated secondary antibody (Refer to Table 4) in 5%

milk (in TBST) for 1hr at room temperature. The membrane was washed in 1X TBST three times for ten minutes for each wash and Pierce ECL western blotting substrate (Thermo Fisher Scientific, 32106) was added onto the membrane to develop the chemiluminescent signal. The intensity of the chemiluminescent signal was captured on Pxi Genesys gel imaging system (NI, Austin, Texas, USA). Western blot results were analysed using grayscale with Image J1.52a (National Institutes of Health, Bethesda, MD, USA).

## 2.8 mRNA extraction and cDNA synthesis

Sciatic nerves were dissected out from euthanised mice and kept in RNALater solution (Invitrogen, AM7020) overnight at 4 ˚C. The following day, the sciatic nerves were transferred to 500 µl of QIAzol lysis reagent (QIAGEN, 79306) and lysed using a Fisherbrand™ Model 120 Sonic Dismembrator (Thermo Fisher Scientific, Waltham, Massachusetts, USA). Extraction of total RNA was performed using miRNeasy Mini Kit (QIAGEN, 217004) following manufacturer's protocol and RNA was eluted in 30µl of RNase free water. Concentration and purity of the RNA was measured using a Nanodrop 2000 spectrophotometer (Thermo Fisher Scientific, Waltham, Massachusetts, USA) and the RNA samples were stored at -20 ˚C.

As RNA cannot be amplified by PCR, the RNA template was first reverse transcribed to a single strand cDNA template using M-MLV reverse transcriptase (Promega, M368) as

recommended by the manufacturer. For first stand cDNA synthesis, the RNA template, nuclease free water (Invitrogen, 750023) and random hexamer primers (Promega, C1181) were made up as detailed in Table 5 and maintained at 70˚C for 5 minutes in a PTC-150 Thermal MiniCycler (MJ Research, Waltham, Massachusetts, USA) after which the samples were kept on ice for 5 minutes. In the next step, the rest of the reaction mixture was added (Table 5) and reverse transcription was carried out in the PTC-150 Thermal MiniCycler as described in Table 6 to synthesise the cDNA. The cDNA was then stored at -20°C for future analysis.

**Table 5: Reaction mixture for cDNA synthesis.**

| Reaction Components | Volume | Final Concentration |
|---|---|---|
| mRNA template | As required | 2µg |
| Nuclease free water (Invitrogen, 750023) | As required | |
| Random hexamer primers (Promega, C1181) | 1µl | 0.5µg |
| M-MLV reverse transcriptase 5X reaction buffer (Promega, M368) | 10 µl | 1X |
| dNTP mix (Promega, U120A-U123A) | 2.5 µl | 500µM |
| RNAse inhibitor (Promega #N2111) | 1.25 µl | 50U |
| M-MLV reverse transcriptase (Promega, M368) | 1 µl | 200U |
| **Final Volume** | 50 µl | |

**Table 6: Protocol for single strand cDNA synthesis from mRNA template.**

| Steps | Purpose |
|---|---|
| Nuclease free water, random hexamer primers and mRNA template is incubated at 70˚C for 5 minutes | To denature secondary structure within the mRNA template |
| Cool on ice for 5 minutes | To prevent the reformation of the secondary structures and anneal the random primers. |
| Add the remaining reaction mixture and incubate at 25˚C (room temperature) for 10 minutes | For extension of random primers |
| 55 ˚C for 50 min | For cDNA synthesis. Higher temperatures reduce RNA secondary structure formation and improves cDNA synthesis. |
| 70 ˚C for 15 min | Enzyme inactivation |

## 2.9 Quantitative polymerase chain reaction

Quantitative polymerase chain reaction (qPCR) was carried out in the PCR LightCycler480 Real-Time PCR Instrument (Roche Applied Science, Penzberg, Germany) using The LightCycler 480 SYBR Green I Master (Roche Applied Science, 04707516001) with the reaction mixture detailed in Table 7 and the qPCR program cycles detailed in Table 8. The primers used for qPCR are described in Table 9. Relative gene expression

was performed by using the $2^{-\Delta\Delta CT}$ method with GAPDH as the reference gene. Three technical replicates for each sample was carried out for statistical analysis.

**Table 7: Reaction mixture for quantitative polymerase chain reaction (qPCR)**

| Reaction Components | Volume | Final Concentration |
|---|---|---|
| 2X SYBR green (Roche, 04707516001) | 5 µl | 1X |
| RNase-free water (QIAGEN) | 2 µl | |
| Primers (Forward and Reverse) (Eurofins, Germany) | 2 µl | 0.25 µM each |
| cDNA | 1 µl | |
| **Total volume** | **10 µl** | |

**Table 8: Standard program for quantitative polymerase chain reaction (qPCR)**

| Program | Temperature and hold time | Number of cycles |
|---|---|---|
| Hotstart | 95°C for 3 min | 1 |
| Amplification | 95°C for 10 sec | |
| | 58°C for 20 sec | 40 |
| | 72°C for 10 sec | |
| Melting curve | 65°C for 1 min | 1 |
| Cooling | 40°C for 30 sec | 1 |

**Table 9: List of qPCR primers for the amplification of target genes with their individual sizes.**

| Gene | Forward Primer 5'- 3' | Reverse Primer 5'- 3' | Size (in bp) |
|------|----------------------|----------------------|--------------|
| OLIG1 | AAGCGCATGCAGGACCTGAACT | AGCGTGGCAATCTTGGAGAGCT | 116 |
| SHH | GGATGAGGAAAACACGGGAGCA | TCATCCCAGCCCTCGGTCACT | 129 |
| NGFR | ACCGCTGATGTTCTAGCCCC | TGGTCCTATCTCTCGCCGGA | 181 |
| GAPDH | CATCACTGCCACCCAGAAGACTG | ATGCCAGTGAGCTTCCCGTTCAG | 153 |

## 2.10 Electron Microscopy

### 2.10.1 Tissue preparation

Following dissection, injured and uninjured sciatic nerves were fixed in 2.5% (w/v) glutaraldehyde diluted in 0.1M sodium cacodylate buffer (pH 7.2) for 24 hrs .The samples were then processed, sectioned and imaged for electron microscopy (EM) by microscopy senior technician Mr. Glenn Harper at Plymouth Electron Microscopy Centre (PEMC, Plymouth, UK). Briefly, sciatic nerves were washed two times with 0.1M sodium cacodylate buffer (For recipe refer to Table 10) followed by a second fixation step with 1% omium tetroxide (in sodium cacodylate buffer) for 1 hr. The nerves were washed twice again with sodium cacodylate buffer for 5 minutes and the tissue was dehydrated through an ascending series of alcohol concentrations - first with 30% ethanol, 50%, 70%, 90% and finally 100% ethanol. The nerves were washed twice with 100% ethanol for 15

minutes each time. Following alcohol dehydration, the nerves were kept in agar low viscosity resin (Agar Scientific, U.K). The nerves went through increasing concentrations of resin (diluted in ethanol) - 30%, 50%, 70% and 100% resin, each concentration left on overnight.  To allow the resin to thoroughly penetrate the tissue, the 100% resin step was repeated twice.  The nerves were then embedded in Beem capsules and moved into a TAAB embedding oven (Agar Scientific, UK), at 60$^o$C overnight where the resin was polymerised.

## 2.10.2 Tissue Sectioning and Imaging

Tissue sectioning and imaging was kindly carried out by Mr Glenn Harper at the Plymouth Electron Microscopy Centre however the methodology is briefly described. Following embedding, 0.5 micron semithin sections were cut using an Ultramicrotome Reichert-Jung Ultracut E (Leica Microsystems, Wetzlar, Germany) using a glass knife (Agar Scientific). The sections were collected on slides in water droplets. The slides were dried on a hot plate and the myelin stain methylene blue was added for 1 minute to stain the sections and then washed off with double distilled water. The slides were then imaged using a Leica IM8 microscope (Leica Microsystems, Wetzlar, Germany).

For Transmission Electron Microscopy (TEM), the embedded tissue blocks were cut on a Leica EM UC7 ultramicrotome (Leica Microsystems, Wetzlar, Germany) using a diatome diamond knife (Agar Scientific) to a thickness of 80nm. The sections were then transferred onto copper grids and counterstained with first a saturated solution of uranyl

acetate followed by staining with Reynold's lead citrate for about 15 minutes each with a water wash between the two staining steps. Finally, the sections were imaged using a JEOL 1400 transmission electron microscope (Jeol, Welwyn Garden City, UK). For analysis, 200 myelinated axons per mouse were analysed for g-ratio using Adobe Photoshop software (Adobe Systems, San Jose, CA, USA). For each genotype, a minimum of three mice were used for the measurements.

### 2.10.3 Myelin sheath thickness and g-ratio calculation

For calculating the g-ratio, the images were opened on photoshop on a touch screen laptop and a stylus was used to draw around the inner circumference of the axon to calculate the area and the same was repeated with the outer circumference to get the area of the myelinated axon. This was done for all 200 myelinated axons per mouse while blinded to the genotype of the sample analysed. The area of the myelin and the axon was used to calculate the diameter which was then used to calculate the g-ratio as previously described (Rushton, 1934). The g-ratio was calculated as inner axon diameter/outer myelin diameter.

### 2.11 Static sciatic index

Static sciatic index (SSI) measurements (Bozkurt *et al.*, 2008) was used to study functional recovery post-sciatic nerve crush injury. The animals were placed in a transparent ventilated acrylic box (15cm x15cm x 15cm) which restricted their movement within the

camera's field of view. A camera was placed below the box and a video of the mouse's movements were captured. The captured videos were then analysed on a computer and chosen frames were utilised to measure the toe spread and intermediate toe spread. The calculation for the toe spread factor (TSF) and intermediate toe spread factor (ITSF) was carried out as previously described (Bozkurt *et al.*, 2008). SSI was calculated using the formula SSI = (108.44 × TSF) + (31.85 × ITSF) − 5.49.

## 2.12 Imaging

The tissue samples for immunohistochemistry were scanned by a Leica SPE confocal microscope (Leica Microsystems, Wetzlar, Germany). For whole nerve staining, several Z-series were captured of the area of interest and each separate series was then merged into a single image by Adobe Photoshop (Adobe Systems, San Jose, CA, USA).

## 2.13 Data Analysis and statistics

The accession numbers for the Affymetrix gene chip microarray data sets reported in this study are GEO: GSE22291 (Barrette *et al.*, 2010); GSE74087 (Pan *et al.*, 2017); GSE30165 (Li *et al.*, 2013) and GSE38693 (Arthur-Farraj *et al.*, 2012) and for RNA sequencing data it is GSE103039 (Clements *et al.*, 2017). Additionally, GSE147285 (Toma *et al.*, 2020); GSE120678 (Carr *et al.*, 2019) and GSE137870 (Gerber *et al.*, 2021) datasets were reported for single-cell RNA sequencing. The microarray data was accessed on Gene Expression Omnibus (GEO) (https://www.ncbi.nlm.nih.gov/geo/), a public repository of

gene expression profiles. The data was then analysed by NCBI online tool GEO2R (https://www.ncbi.nlm.nih.gov/geo/geo2r/) for fold change expression of genes in injured tissue relative to the uninjured tissue. The data was checked to ensure it was normalised and that the data was log2 transformed (by looking at the box plots). For the single-cell RNA sequencing (scRNA-seq) datasets GSE147285 and GSE120678, Dr Matthew Banton previously analysed them using the R package Seurat and created an interactive R shiny app that provided a graphical method to interrogate the scRNA-seq data sets. Dr Xin-peng Dun used this app to examine the clustering and gene expression of the cells in my recent publication (Chen *et al.*, 2021a). This interactive R shiny application was then used to look at the gene expression patterns for the target genes presented in this thesis.

The experiments that required measurements such as length, area or counting points in an image, were all carried out on Adobe Photoshop (Adobe Systems, San Jose, CA, USA). For quantification of number of regenerated axons, all axons in a transverse section of the sciatic nerve or its tibial branch were counted. The area of each cross section was calculated, and data was represented as total number of axons per total area of cross section of the nerve.

The data for each experiment was first analysed for normal distribution using GraphPad Prism 8.4.3 software (GraphPad Software, La *Jolla*, CA, USA). With data being normally

distributed, a Student's two-tailed t-test was carried out using the same software to determine the statistical significance.  When data was not normally distributed including data derived from g-ratio analysis a nonparametric Mann Whitney U test was performed. For comparison across multiple groups, one way ANOVA was used to determine statistical significance.   $P<0.05$, $P<0.01$, $P \leq 0.001$ were considered as statistically significant and labelled with one, two and three asterisk, respectively, in the figure. If no significant difference was observed between the control and the sample groups, the graphs were not labelled with any asterisks. All data is represented as mean values ± SEM in the figures. The sample size (n) for each experiment has been described in the figure legends. Sample size was determined by carrying out a pilot experiment with $n < 3$ and using G*power software (Faul *et al.*, 2009) to determine the sample size required to achieve full statistical significance.

**Table 10: Detailed list of reagents and recipes**

| Reagents | Recipe | Source |
|---|---|---|
| 1. Alkaline lysis buffer | • 25 mM NaOH | Sigma |
| | • 0.2 mM Disodium EDTA (pH12 dissolved in water without adjusting pH) | Sigma |

| | | |
|---|---|---|
| 2. Neutralising buffer | • 40 mM Tris-HCl (pH5 dissolved in water without adjusting pH) | Sigma |
| 3. 50X Tris-acetate-EDTA (TAE) | • 242.0g Tris Base<br>• 18.6g EDTA<br>• 57.1ml Glacial acetic acid<br>• Made up to 1L with water (pH 8.0) | Fisher bioreagents<br>Sigma<br><br>Fisher Chemical |
| 4. 2% Agarose gel (for small gel) | • 1.4g Agarose<br>• Boiled in 70mL of water<br>• 1.4 µl of GelRed nucleic acid stain | Sigma<br><br>Millipore |
| 5. 10X Phosphate Buffered Saline (PBS) | • Ready to use | Fisher BioReagents |
| 6. Laemmli SDS sample buffer, reducing(6X) | • Ready to use | Alfa Aesar |
| 7. 10X Tris Buffered Saline (TBS) | • 80g Sodium chloride<br>• 24.4g Tris base<br>• Made up to 2L with water<br>• pH to 7.6 with HCl | Sigma<br>Fisher bioreagents |
| 8. 1X Tris Buffered Saline in 0.1% Tween 20 (TBST) | • 100mL of 10X TBS<br>• dissolved in 900mL of water<br>• 1mL of Tween 20 | Fisher BioReagents |

| | | |
|---|---|---|
| 9. 10% Polyacrylamide Running gel | • 4.8ml water | |
| | • 2.5ml Trizma®-HCl 1.5M (pH 8.8) | Sigma |
| | • 2.5ml 40% acrylamide/Bis Solution | Bio-Rad |
| | • 100µl 10% SDS | Sigma |
| | • 75µl 10% ammonium persulphate (APS) | Sigma |
| | • 10µl Tetramethylethylene diamine (TEMED) | Fisher Chemical |
| 10. 5% Polyacrylamide Stacking gel | • 2.95mL water | |
| | • 1.4mL Trizma-HCl 1.5M(pH 6.8) | Sigma |
| | • 0.625 mL 40% acrylamide/ Bis Solution | Bio-Rad |
| | • 50µl 10% SDS | Sigma |
| | • 37.5µl 10% ammonium persulphate (APS) | Sigma |
| | • 5µl Tetramethylethylene diamine (TEMED) | Fisher Chemical |
| 11.1X Running Buffer | • 3g Tris base | Fisher BioReagents |
| | • 14.4g Glycine | Fisher BioReagents |
| | • 10mL 10% SDS | Sigma |
| | • Made up to 1L with water | |
| 12.1X Transfer Buffer | • 3g Tris base | Fisher BioReagents |

| | | |
|---|---|---|
| | • 14.4g Glycine | Fisher BioReagents |
| | • 200mL methanol | VWR Chemicals |
| | • Made up to 1L with water | |
| 13. 5% (w/v) milk powder in TBST | • 2.5g skimmed milk <br> • Dissolved and made up to 50 mL in TBST | Sigma |
| 14. 5% (w/v) Bovine Serum Albumin in TBST | • 2.5g bovine serum albumin (BSA) <br> • Dissolved and made up to 50mL in TBST | Fisher BioReagents |
| 15. Sodium Citrate Buffer | • 2.94g Trisodium citrate (dihydrate) <br> • 0.5mL Tween 20 <br> • Made up to 1L with water <br> • pH to 6.0 with HCl | Sigma <br><br> Fisher BioReagents |
| 16. 4% PFA | • 40g Paraformaldehyde <br> • Dissolved and made up to 1L in 1X PBS, stirring overnight at 60 °C (pH 7.4) | Sigma |
| 17. 30% Sucrose | • 15g Sucrose <br> • Dissolved and made up to 50mL with 1X PBS | Sigma |
| 18.1% Triton in PBS | • Dissolve 100 µl of TritonX-100 in 900 µl of 1X PBS | Sigma |

| | | |
|---|---|---|
| 19.1% BSA in PBS with 0.25% Triton X-100 | • 0.5g of Bovine Serum Albumin (BSA)<br>• 125 µl of TritonX-100<br>• Dissolved and made up to 50mL in 1X PBS | Fisher Scientific<br><br>Sigma |
| 20.3% BSA in PBS with 0.05% Triton X-100 | • 1.5g of BSA<br>• 2.5mL of 1% Triton in PBS<br>• Dissolved and made up to 50 mL in 1X PBS | Sigma |
| 21. 1% PTX in 10% FBS | • 5mL Fetal bovine serum (FBS)<br>• 500 µl 1%Triton in PBS<br>• Dissolved and made up to 50ml in 1X PBS | Sigma |
| 22.0.1% PTX in 10% FBS | • 5mL FBS<br>• 5ml 1% Triton in PBS<br>• Dissolved and made up to 50 mL in 1X PBS | Sigma |
| 23. 2.5%Glutaraldehyde in 0.1M sodium cacodylate buffer | • 10mL 25% Glutaraldehyde<br>• 50 mL 0.2M Cacodylate buffer at required pH<br>• • Made up to 100mL with distilled water. | Sigma |

# CHAPTER 3: EXPRESSION AND ROLE OF NETRIN-1 IN PERIPHERAL NERVE REGENERATION

## 3.1 Preliminary work done on Netrin-1 expression in peripheral mouse sciatic nerve before and after injury.

Prior to the start of this project, my research group carried out preliminary experiments to study the expression of Netrin-1, 3, 4 and 5 by RT-PCR in the adult mouse sciatic nerve both before and after injury. They observed that Netrin-4 and 5 are not expressed in the peripheral nerve both before and after injury (Dun *et al.*, 2018, unpublished). Netrin-3 mRNA was detected in the 7-day transected, proximal, bridge and distal sciatic nerve segments however not in cultured rat Schwann cells (SCs) (Figure 9A). In contrast, Netrin-1 mRNA was present in intact and injured peripheral nerves, and cultured SCs (Figure 9A). They also performed RT-qPCR analysis to study Netrin-1 mRNA expression in intact (control) and injured nerves 4-, 7-, 10- and 14-days post-transection injury (Figure 9B). The results surprisingly showed that Netrin-1 mRNA was significantly downregulated as compared to the uninjured control, contrary to the literature available (Madison *et al.*, 2000; Chen *et al.*, 2021b). Additionally, immunohistochemical analysis of the intact sciatic nerve in PLP-GFP mice that express endogenous GFP in SCs of the peripheral nervous system (Mallon *et al.*, 2002; Chen *et al.*, 2019a), showed Netrin-1 expression in mainly non-myelinating SCs (Figure 9 C-F). The antibody used for this immunostaining was later found to be non-specific (Please refer to Section 3.3 and Figure 14 E-L).
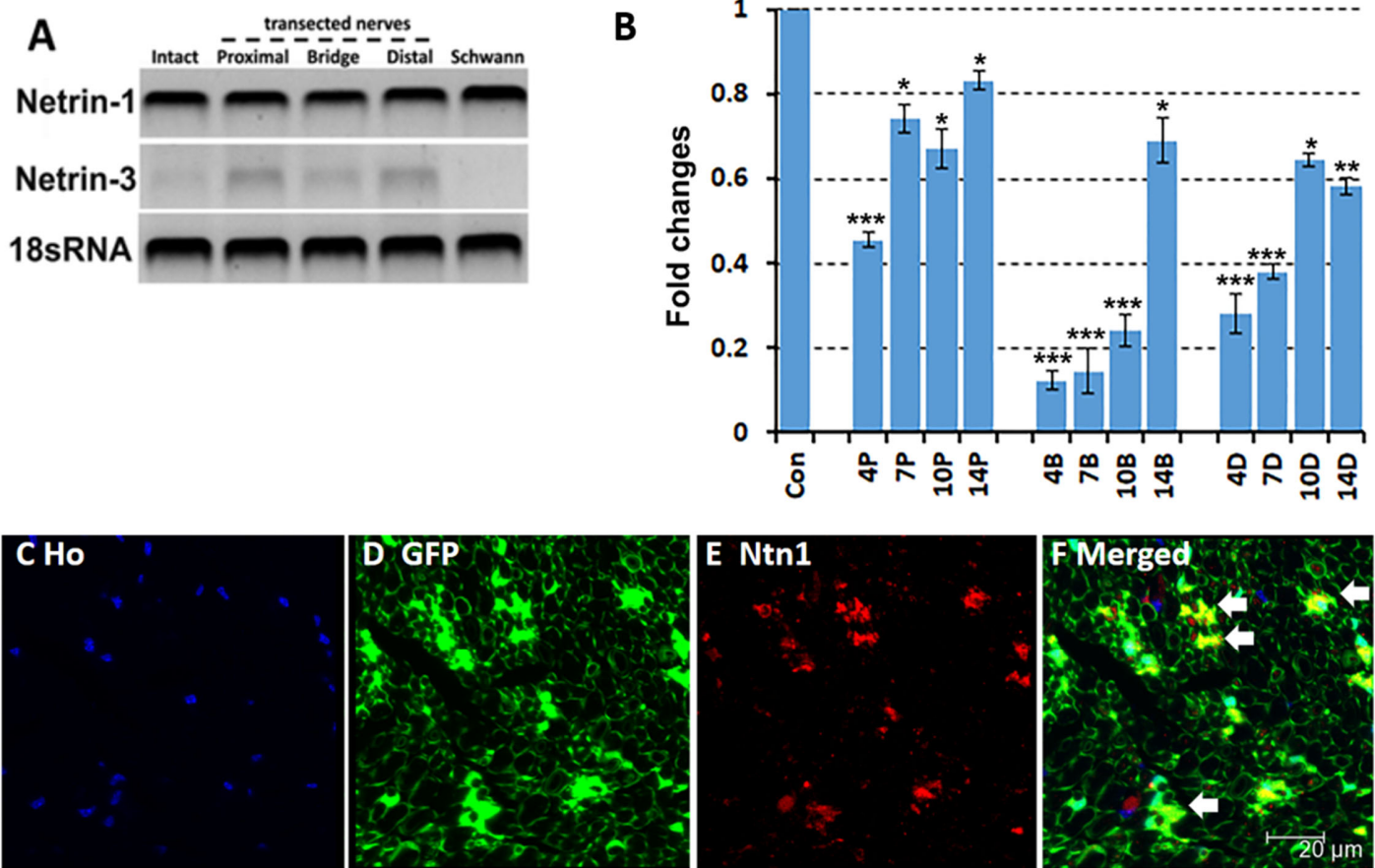
**Figure 9: Netrin-1 mRNA is downregulated post-peripheral nerve transection injury and Netrin-1 is expressed in Schwann cells**

Preliminary data for Netrin-1 as investigated by my research group. (A) RT-PCR of Netrin-1 and Netrin-3 mRNA in the intact and separate segments of the transected (7 days post-injury) mouse sciatic nerve (labelled as proximal, bridge and distal) and in cultured rat SCs. 18S ribosomal RNA is used as a reference RNA (B) RT-qPCR of Netrin-1 mRNA depicted in fold changes relative to the control intact sciatic nerve (Con) for different segments of the nerve - proximal (P), nerve bridge (B) and the distal nerve stump (D) at 4, 7, 10 and 14 days post sciatic nerve transection injury (n=3 for each time point). (C-F) Intact transverse sections of PLP-GFP sciatic nerve with endogenous expression of GFP (green) in Schwann cells of the peripheral nervous system, immunolabelled for Netrin-1 (Ntn1, red). (F) Co-localisation of Netrin-1 in mainly non-myelinating Schwann cells that have a brighter expression of GFP and are marked by white arrows. Note: The staining depicted in C-F was later found to be non-specific and immunohistochemistry with another antibody was repeated in Figure 14. $*P<0.05$, $**P < 0.01$, and $***P$

< 0.001. Error bars represent (±) SEM of triplicates (Dun, 2019, unpublished)

## 3.2 Netrin-1 mRNA regulation following peripheral nerve injury.

Data mining and analysis to study Netrin-1 gene expression in rodent dorsal root ganglia (DRGs), intact and injured sciatic nerve as well as in SCs was carried out. Different published datasets for microarray were obtained from the NCBI Gene Expression Omnibus (GEO). First, I looked at microarray data sets GSE22291 and GSE74087 to study Netrin-1 gene expression in the distal nerve stump of wild-type mouse sciatic nerve post-injury (Barrette *et al*., 2010; Pan *et al*., 2017). For both datasets C57BL/6 mice underwent sciatic nerve crush injury and the injured distal stump of the sciatic nerve was collected at day 3, 7 and 14 post-injury along with the uninjured sciatic nerve. The distal nerve stumps were pooled by group and RNA extracted by the authors. The log2 transformed normalised values were downloaded for each biological replicate at the mentioned time points using NCBI online tool GEO2R and expression of Netrin-1 mRNA analysed relative to the uninjured control.  The data was then plotted in terms of fold changes relative to the expression of uninjured sciatic nerve.

Both datasets, in agreement with the data produced by my research group (Figure 9B) showed that Netrin-1 mRNA was downregulated post-crush injury at all the recorded time points (Figure 10 A,B) and does not recover to the expression levels of uninjured nerve even at 14-days post-injury. Next, I analysed the microarray dataset GSE38693, which looked at total RNA expression from distal nerve stump of transected mouse

sciatic nerve 7 days post-injury (Arthur-Farraj *et al*., 2012). In a similar pattern to the previous two datasets, Netrin-1 mRNA expression was significantly downregulated in the distal nerve stump 7 days post sciatic nerve transection injury (Figure 10 C).
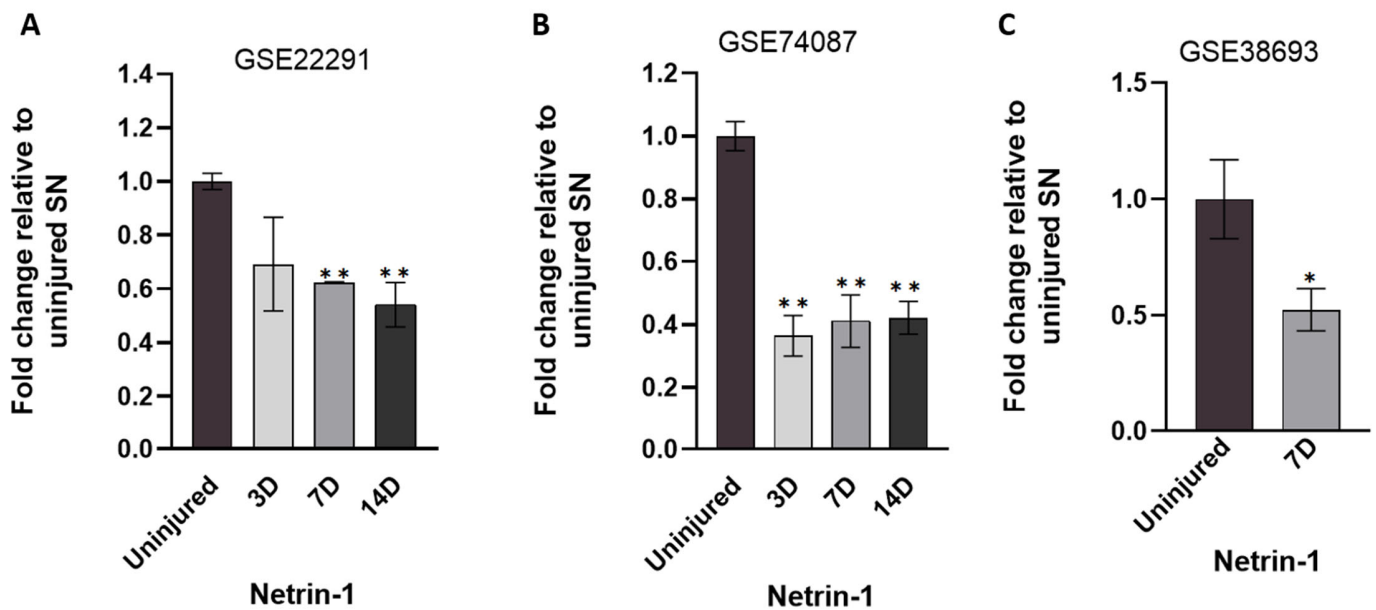


**Figure 10: Netrin-1 mRNA expression is downregulated in the distal sciatic nerve of mice following injury**

(A, B) Time course of fold change Netrin-1 downregulation in the distal nerve stump at day 3, 7 and 14 (3D, 7D, 14D, respectively) following sciatic nerve crush injury in mouse, relative to uninjured sciatic nerve (SN). The data was analysed from microarray datasets GSE22291 (n=2 for each time point) and GSE74087 (n=3 for each time point). (C) Netrin-1 mRNA downregulation in the distal sciatic nerve 7 days post-nerve transection injury, relative to the uninjured sciatic nerve, from microarray dataset GSE38693 (n=2). *p<0.05, **p<0.01. Error bars represent (±) SEM.

Previously, Webber *et al.* (2011) reported that there was no significant Netrin-1 mRNA expression change in the dorsal root ganglia (DRG) at day 3 and day 7 following rat sciatic

nerve transection injury. Therefore, I analysed another microarray dataset - GSE30165 to study Netrin-1 mRNA expression changes in proximal nerve segments and L4-L6 DRGs of Sprague-Dawley rats at day 1, 4, 7 and 14 post-sciatic nerve transection (Li *et al.*, 2013). On analysing this data, I confirmed no change in Netrin-1 mRNA expression in the DRGs at all the time points when compared to the uninjured DRGs (Figure 11 A). However significant downregulation of Netrin-1 mRNA was observed in the proximal stump of the sciatic nerve at day 1, 4 and 7 post-injury with the expression level at day 14 approximate to that of uninjured nerve (Figure 11 B)
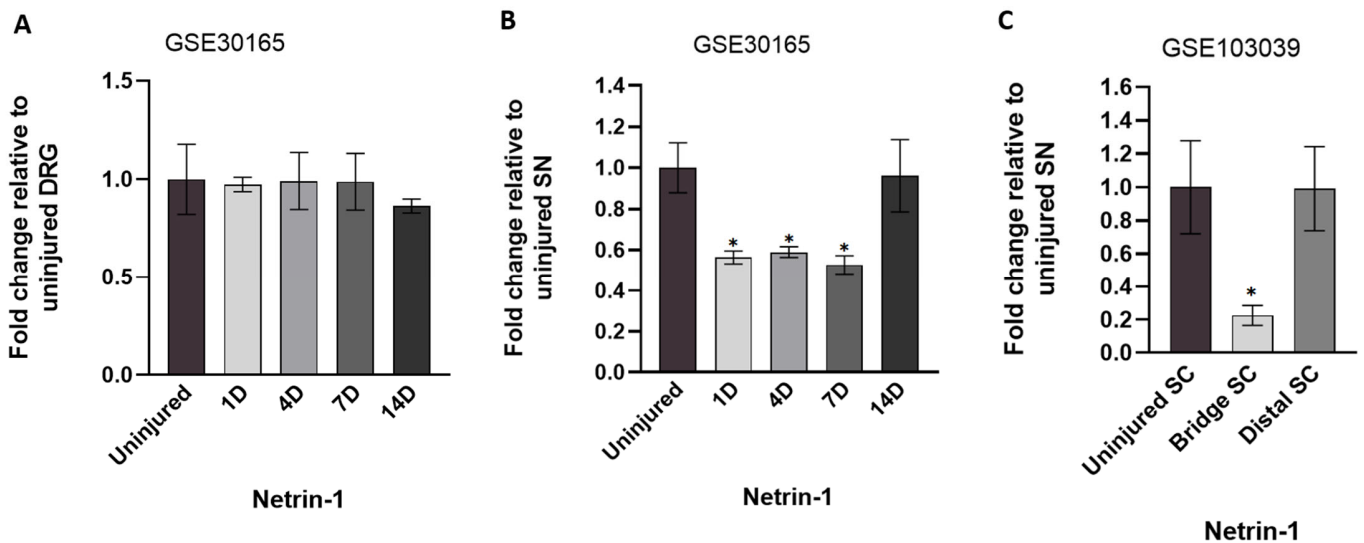


**Figure 11: Netrin-1 mRNA expression in dorsal root ganglia, proximal sciatic nerve and Schwann cells after sciatic nerve injury**

(A) Netrin-1 transcript expression in the L4-L6 dorsal root ganglia (DRG) of adult Sprague-Dawley rats in terms of fold change relative to uninjured DRG as analysed from microarray studies at day 1, 4, 7 and 14 (1D, 4D, 7D and 14D respectively) following sciatic nerve (SN) transection injury. Data analysed from GSE30165 microarray dataset (n=3 for each time point) with no change in expression levels in the DRGs.

(B) Netrin-1 mRNA downregulation in the proximal sciatic nerve at day 1, 4, and 7 post-nerve transection injury with upregulation at day 14, relative to the uninjured SN from GSE30165 microarray dataset (n=3 for each time point). (C) Netrin-1 mRNA downregulation in the Schwann cells (SC) purified from the bridge segment of the sciatic nerve but no change observed in the SCs of the distal nerve stump 6 days after mouse sciatic nerve transection injury analysed from high throughput RNA sequencing dataset GSE103039 (n=4). The expression is relative to the SCs purified from uninjured SN. *p<0.05. Error bars represent (±) SEM.

Finally, as SCs have been described as the main source of Netrin-1 expression in the peripheral nerve (Madison *et al.,* 2000), I studied Netrin-1 mRNA in SCs after transection injury. I looked at the dataset GSE103039, wherein the authors performed sciatic nerve transection on adult mice with a tdTomato reporter expression in SCs. In their study, injured and the contralateral uninjured nerve were dissected and collected 6 days post-injury (Clements *et al*., 2017). In their experiment, the bridge and distal segment of the nerve were separated and the tissue from three mice was pooled for each segment separately as well as for the intact nerve. SCs were sorted from other cells based on tdTomato expression by fluorescence activated cell sorting (FACS) and RNA extracted followed by high throughput RNA sequencing (Clements *et al*., 2017). Data analysis from this dataset for Netrin-1 mRNA expression showed significant downregulation in the SCs derived from the nerve bridge in comparison to the SCs extracted from the intact nerve (Figure 11 C). However, six days post-transection injury, surprisingly the distal SCs express Netrin-1 mRNA almost at the level of the SCs from the intact nerves.

In the intact nerves, the SCs exist as myelinating and non-myelinating SCs whereas post-injury they assume a repair phenotype more prevalent in the distal nerve stump responsible for Wallerian degeneration (Arthur-Farraj *et al*. 2012; Nocera and Jacob, 2020; Balakrishnan *et al*., 2021). While at around day 6 post-transection injury, the nerve bridge is invaded by migratory and proliferating SCs that guide regenerating axons across the lesion site (Chen *et al*., 2019a). Therefore, it was interesting to note that the level of Netrin-1 mRNA expression by the SCs of the distal segment did not change despite the change in the phenotype of the SCs. Although observing a marked downregulation of Netrin-1 mRNA in the distal sciatic nerve from datasets GSE22291, GSE74087 and GSE38693 (Figure 11) as well as RT-qPCR (Figure 9B) performed by my research group prior to this project, it was surprising to note that SCs that were described as the main source of Netrin-1 expression in the peripheral nerve did not show the expected downregulation of Netrin-1 in the distal nerve stump six days after transection injury (Figure 11 C). However, it is to be noted that Clements *et al.* (2017) described in their methodology the dissociation of the sciatic nerves – "Nerves were digested for a total of 20 min at 37°C with trituration after 10 min," and therefore the effects of artefactual gene expression in their data cannot be ruled out (Adam *et al*., 2017; Marsh *et al.,* 2022).

## 3.3 Generating Schwann cell-specific knockout of Netrin-1 in mice

Preliminary work on Netrin-1 expression in the sciatic nerve by my research group and as reported in literature (Madison *et al.*, 2000; Lv *et al.*, 2015) showed that Netrin-1 expression was primarily localised to SCs. Based on this data and the concept that SCs are responsible for guiding regenerating axons to innervate their end target following traumatic injury, I had initially generated SC-specific Netrin-1 knockout mice to study whether SC-derived Netrin-1 was involved in peripheral axon regeneration by interacting with its attractive receptor Deleted in colorectal carcinoma (DCC).

Schwann cell-specific Netrin-1 knockout mice (Ntn1 KO) were generated by breeding Ntn1 $^{loxP/loxP}$ mice (Dominici *et al.*, 2017) with P0-Cre$^+$ mice (mP0-TOTACRE) (Feltri *et al.*, 1999) (Figure 12). The P0-Cre expression is controlled by the myelin protein zero promoter and is expressed specifically in the SCs in the peripheral nervous system (Ogawa *et al.*, 2015). P0-Cre mice have been used extensively by my research group and have been well characterised (Roberts *et al.*, 2017; Mindos *et al.*, 2017; Laraba *et al.*, 2022). Offsprings generated from a cross between a strain with a floxed gene sequence and a strain with P0-Cre$^+$, results in Cre-mediated recombination and deletion of the flanked sequence in the SCs between embryonic days 13.5-14.5.
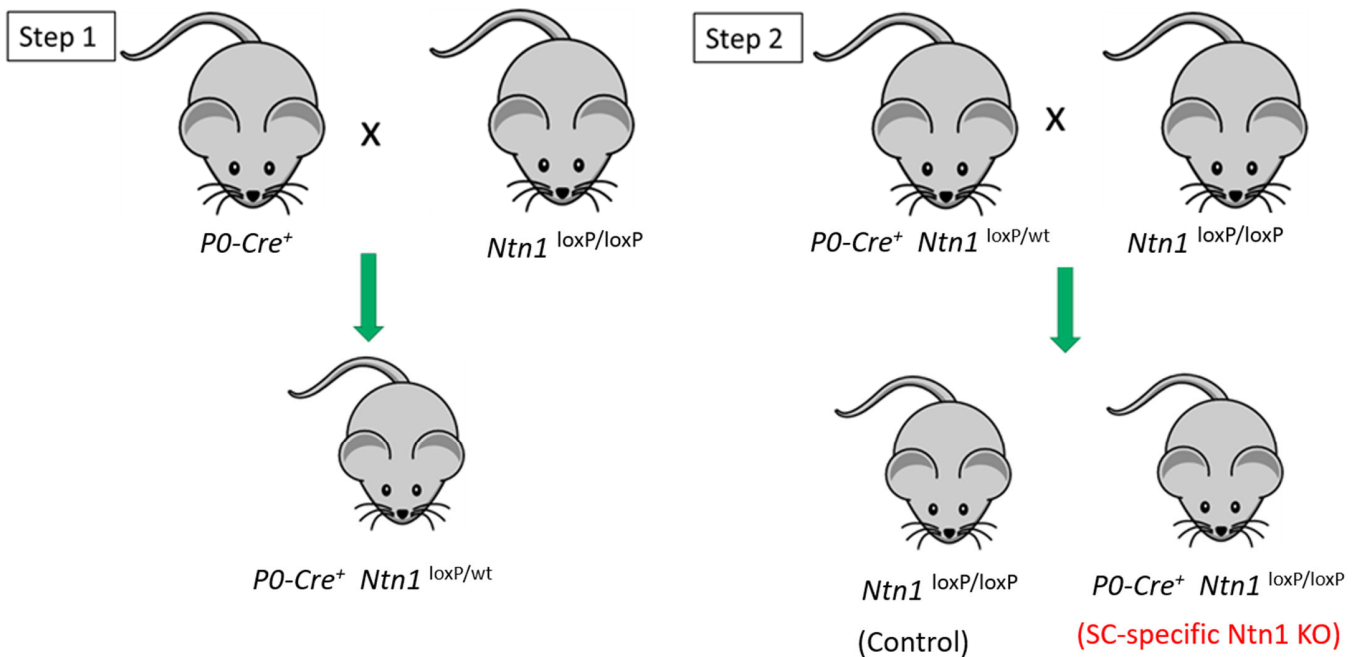
**Figure 12: Breeding scheme to generate Schwann cell-specific Netrin-1 knockout mice.**

Illustration of the necessary breeding steps taken to produce Netrin-1 knockout in SCs. In step 1, homozygous mouse with loxP sites flanking exon 3 of Netrin-1 (Ntn1$^{loxP/loxP}$) was bred with mice carrying the Cre transgene regulated by the myelin protein zero promoter in Schwann cells (P0-Cre). The resulting offspring was heterozygous for loxP sites and was back crossed in step 2 with Ntn1$^{loxP/loxP}$ mouse. The resulting progeny that was homozygous for Netrin-1 loxP sites and had the P0-Cre transgene (P0-Cre$^{+}$ Ntn1$^{loxP/loxP}$) were used as the Schwann cell-specific knockout mice in my experiments and mice without P0-Cre but homozogyously floxed for Netrin-1 were used as controls.

No significant phenotypic differences were observed when comparing the Netrin-1 knockout mice to the control including the body weight at the two-month time point (Figure 13 A). Transmission electron microscopy (TEM) studies also showed that in the sciatic nerve of postnatal day 60 mice there was no difference in the g-ratio (a measure of myelin thickness) compared to the control (Figure 13 B-D). These results suggested

that Netrin-1 is not required by SCs for myelination of myelinating axons during development. Although minor developmental changes in myelin thickness, if any, cannot be excluded, however, by postnatal day 60 they appear to have been corrected.
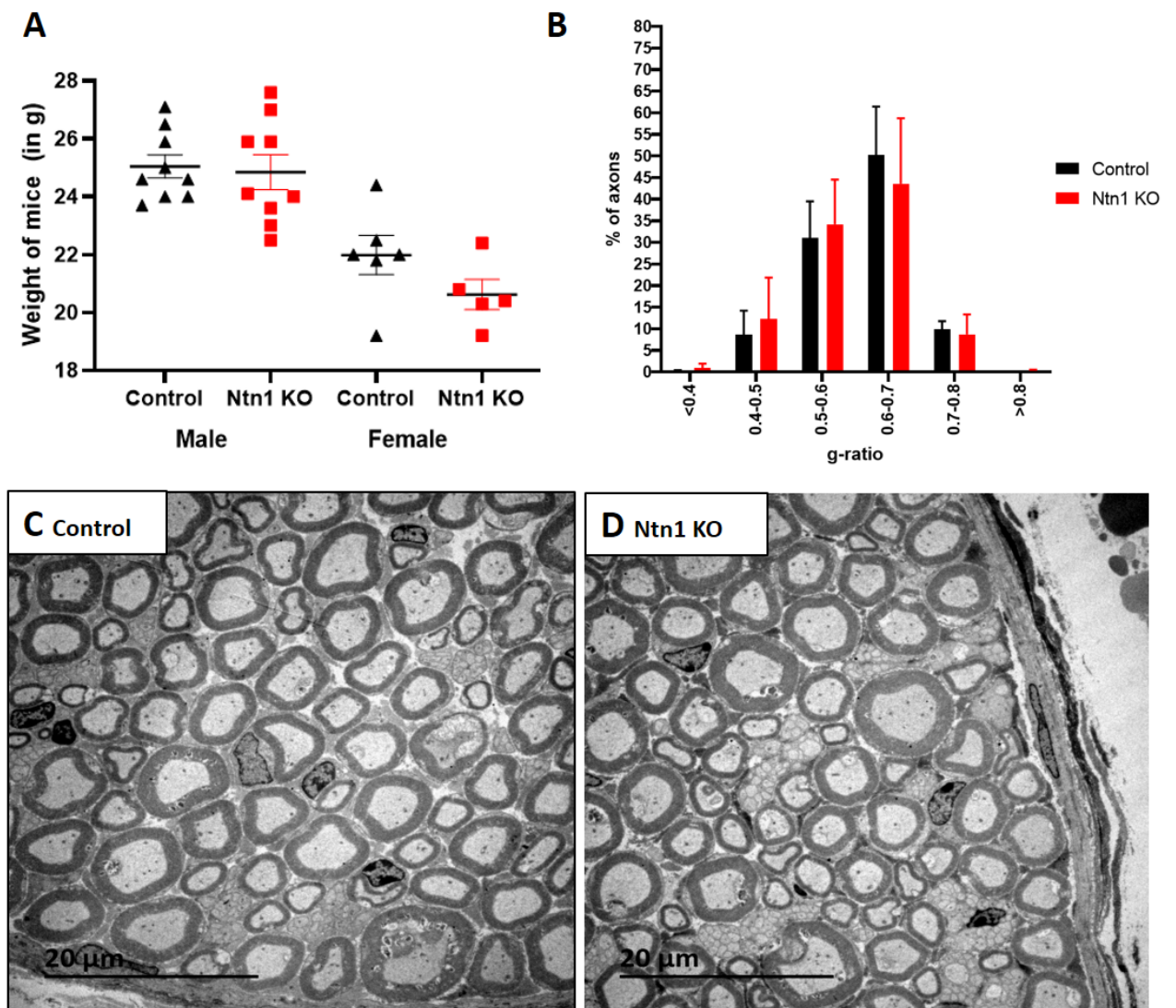


**Figure 13: Schwann cell-specific Netrin-1 knockout does not affect the myelin thickness of myelinated axons during development**

(A) Weight comparison of control and Schwann cell specific Netrin-1 knockout (Ntn1 KO) mice for both

males and females at postnatal day 60 (n=9 for control or Ntn1 KO males; n= 6 for control females; n=5 for Ntn1 KO females). (B) No difference in g-ratio of Ntn1 KO mice as compared to control. (C-D) Transmission electron microscopy (TEM) representative images of the structure of sciatic nerve in transverse sections of control and Ntn1 KO mice (n=3). (A, B) There was no statistically significant difference ($p > 0.05$) between the two groups. Error bars represent (±) SEM.

To confirm the knockout of Netrin-1 in SCs I performed a western blot using the Netrin-1 Abcam antibody (Cat no: ab126729) on intact sciatic nerves from control and Netrin-1 knockout mice, however surprisingly I did not observe the expected reduction of Netrin-1 levels (Figure 14 A, B). Immunohistochemistry carried out with the same Netrin-1 Abcam antibody (Cat no: ab126729) previously used by my research group to show Netrin-1 expression in SCs of sciatic nerves (Figure 9 C-F) also showed inconclusive results (data not shown). Therefore, I used PCR to confirm Netrin-1 gene deletion. I used primers as designed by GenOway (Lyon, France) located outside the two loxP sites that flanked exon 3 of Netrin-1 gene. The forward primer was located at the 5' end of the first loxP site and the reverse primer was located at the 3' end of the second loxP site (Figure 14 C). In a normal polymerase chain reaction (PCR), these primers would only amplify a 498bp sequence if recombination was successful and exon 3 of Netrin-1 was deleted while for the control mice, no band would be observed as the exon 3 of wild-type Netrin-1 sequence is too large to be amplified (3.8 kbp) under normal PCR conditions. I observed the expected 498bp band only for Netrin-1 mice that had the P0-Cre[+] transgene indicating that recombination and Netrin-1 gene deletion was successful (Figure 14 D). I

also sent the PCR product from Netrin-1 knockout mice for sequencing and the results showed deletion of exon 3 sequence along with one loxP site confirming Netrin-1 gene deletion (data not shown). However, this did not confirm absence of Netrin-1 protein in the SCs.
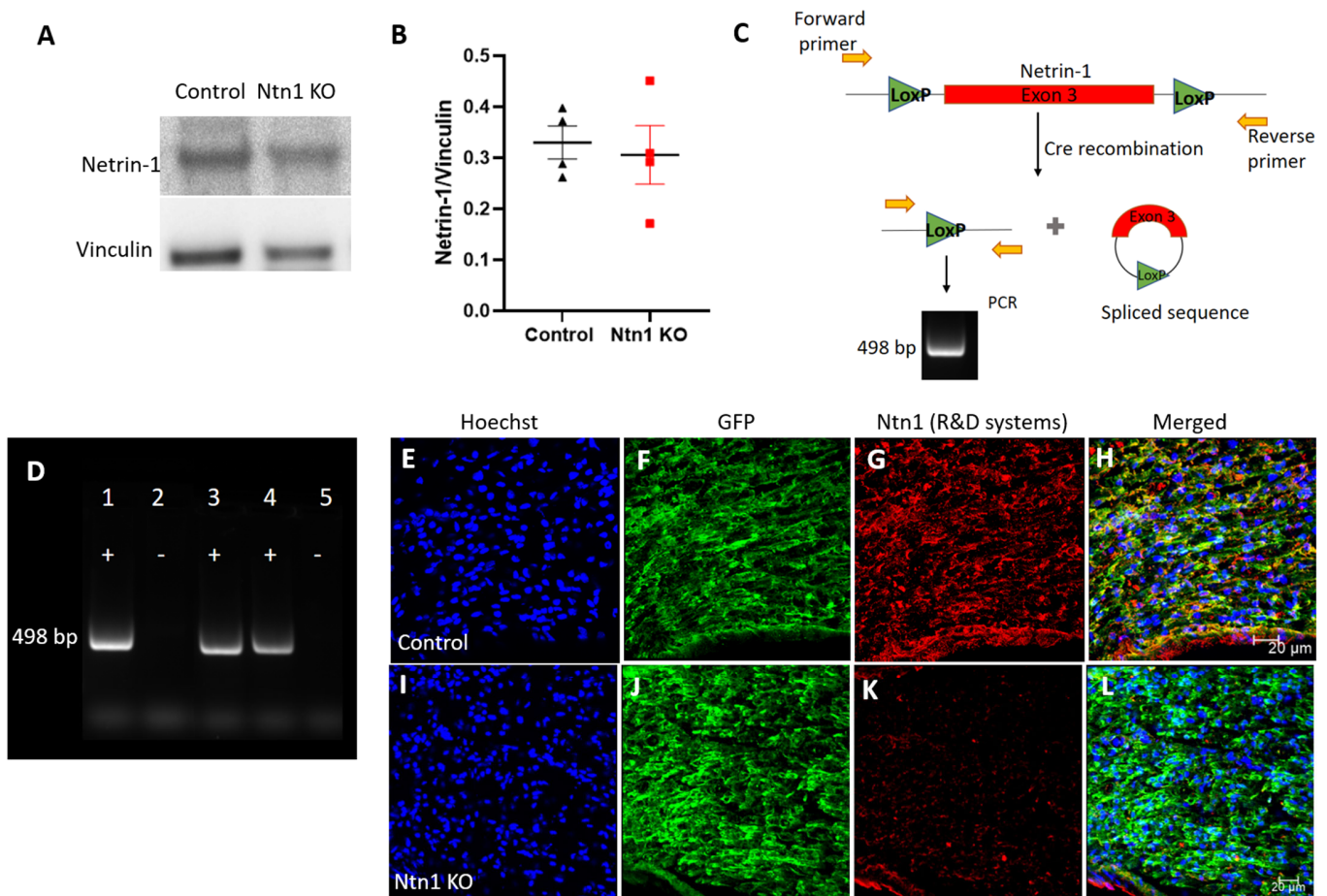


**Figure 14: Confirming Netrin-1 knockout in Schwann cells of Netrin-1 P0-cre mice**

(A) Intact sciatic nerves were immunoblotted for Netrin-1 in control and Schwann cell-specific Netrin-1 knockout mice (Ntn1 KO) with vinculin used as a loading control. (B) Quantification of Netrin-1 expression in intact sciatic nerves relative to Vinculin showed no difference when comparing Ntn1 KO to control mice (n=4 per group). (B) There was no statistically significant difference ($p > 0.05$) between the two groups. Error bars represent (±) SEM. (C) Primers (yellow arrows) were located on either end

of the two loxP sites (flanking exon 3 of Netrin-1) to perform a polymerase chain reaction (PCR) and confirm deletion of Netrin-1 after Cre-mediated recombination. A 498bp amplified product would be observed if deletion was successful in Ntn1 KO mice. (D) PCR performed on lysates from Ntn1 KO (+) and control (-) mice showed a 498bp band observed only for Ntn1 KO mice. (E-L) Distal sciatic nerves were dissected from mice 7-days after sciatic nerve transection injury and longitudinal sections were used for immunohistochemistry. These mice carried a PLP-GFP transgene thus expressing endogenous GFP in Schwann cells (green) and were immunostained for Netrin-1 (red). Absence of Netrin-1 in GFP expressing cells confirmed Netrin-1 knockout in SCs. Hoechst (blue) labels the nuclei. Scale bar is 20 μm.

After testing several Netrin-1 antibodies (data not shown), on the recommendation of another lab group, I procured a Netrin-1 antibody from R&D systems (Cat no: MAB1109). Immunohistochemistry on the distal sciatic nerves after a 7-day transection injury with the new Netrin-1 antibody allowed the confirmation of Netrin-1 knockout in SCs (Figure 14 E-L). But more importantly, the antibody showed a different Netrin-1 protein expression pattern as compared to what was previously shown by Madison *et al.* (2000) and my research group (Figure 9 C-F). In light of this new information, I decided to re-characterise the expression of Netrin-1 in the peripheral nervous system with the Netrin-1 antibody from R&D systems. Western blotting using both antibodies showed similar results and a band at 75kDa (data not shown).

## 3.4 Expression of Netrin-1 in dorsal root ganglia and spinal cord.

Sciatic nerve comprises both sensory and motor axons, with the cell body of sensory axons located in the DRGs and some in the dorsal horn of the spinal cord while the cell bodies for motor neurons are located in the ventral horn of the spinal cord. Therefore, when there is an injury to sciatic nerve both populations of axons can get damaged. As mentioned previously, Webber *et al.* (2011) observed Netrin-1 mRNA expression both before and after sciatic nerve axotomy, in adult rat DRG neurons however there was no change in netrin-1 mRNA levels after injury.

I therefore first examined the expression of Netrin-1 before and after mouse sciatic nerve transection injury using the new Netrin-1 antibody from R&D systems (Cat no: MAB1109). From here on, I used only the Netrin-1 R&D systems (Cat no: MAB1109) antibody for all immunohistochemistry work presented for Netrin-1 in this thesis. L4-L5 DRGs were dissected out before and after a 7-day transection injury to the sciatic nerve from wild-type C57BL/6 mice. Double staining of NeuN, a well-known neuronal marker and Netrin-1 on transverse sections of the DRGs showed that Netrin-1 was expressed by sensory neurons both before and after injury (Figure 15 A-H). Although not quantified the staining performed at the same time and under the same conditions, did not show any observable changes in Netrin-1 expression in DRGs before and after injury (Figure 15 A-H). In a similar manner, L4-L5 spinal cord was dissected out and double stained for

NeuN and Netrin-1. It was observed that majority of the NeuN positive neuronal cell bodies of the ventral horn, that are the source of motor axons, expressed Netrin-1 before and 7-days after a transection injury to the sciatic nerve (Figure 15 I-T). Cell bodies of dorsal horn of the spinal cord were also positive for Netrin-1 (Figure 15 I-L).

| Hoechst | NeuN | Netrin-1 | Merged |
|---------|------|----------|--------|



Ventral horn

Dorsal horn

Uninjured

7D injury

50 μm

100 μm
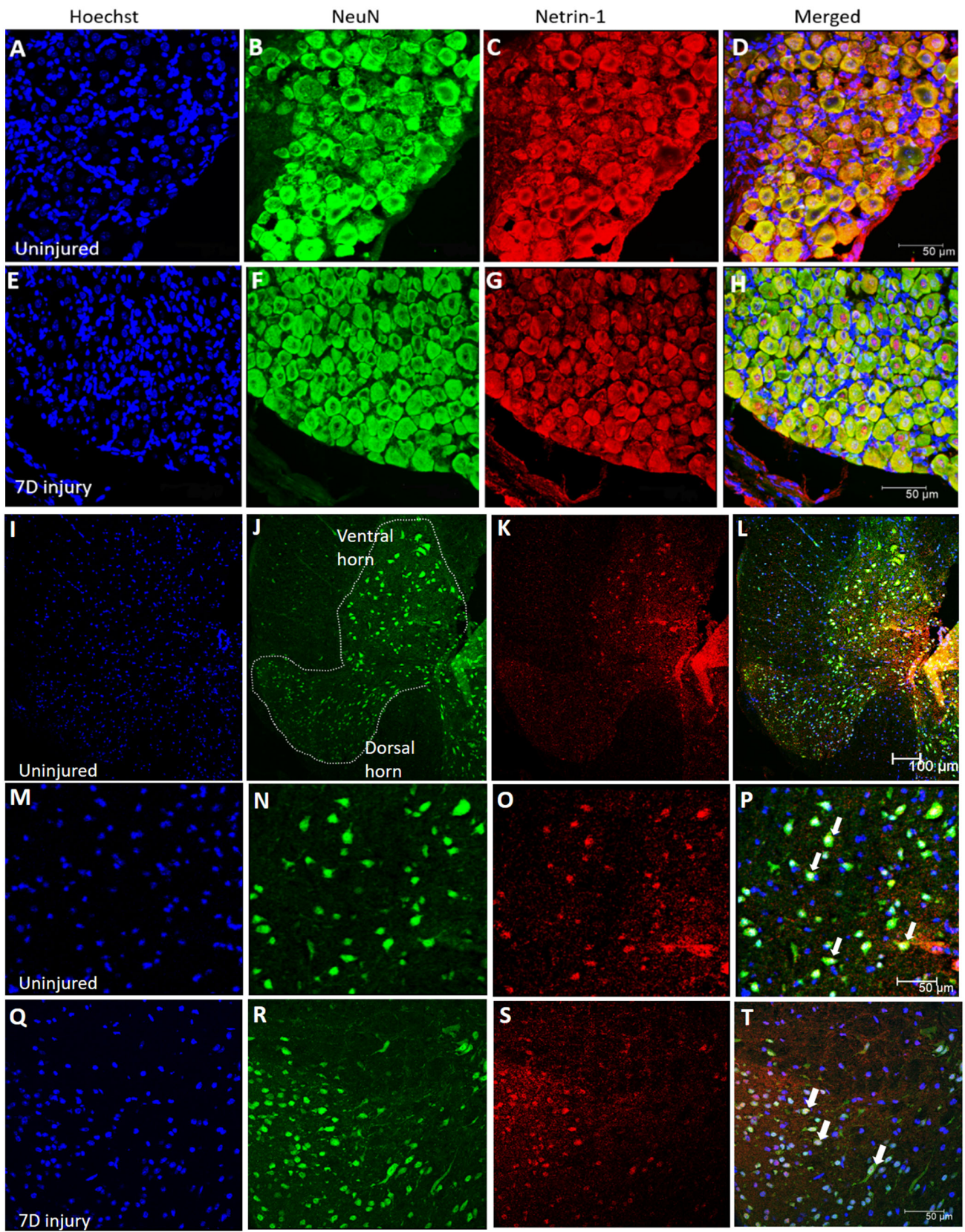
**Figure 15: Expression of Netrin-1 in the neuronal cell bodies of dorsal root ganglia and the spinal cord**

(A-H) Double staining of dorsal root ganglia (DRGs) from C57BL/6 mice before (A-D) and 7 days (7D) post sciatic nerve axotomy (E-H) of C57BL/6 mice labelled by Netrin-1 (red), and NeuN (green), a neuronal marker to label cell bodies. (D, H) Merged images show co-localisation of Netrin-1 in sensory cell bodies (yellow). (I-L) NeuN and Netrin-1 staining of uninjured spinal cord with white dashes demarcating the ventral and dorsal horns of the spinal cord. The ventral and dorsal horns are distinguishable by the large diameter sized cell bodies for ventral motor neurons and smaller diameter for dorsal sensory neurons. Netrin-1 co-localisation observed in both ventral and dorsal horns. (M-P) Magnified image of the ventral horn of the spinal cord before injury with NeuN labelling (green) of motor axons. (Q-T) Ventral horn of the spinal cord 7-days after sciatic nerve transection injury with Netrin-1 expression observed in NeuN positive motor neurons. (P, T) White arrows depicts the co-localisation of Netrin-1 in cell bodies of motor neurons. Hoechst (blue) labels the nuclei. (A-H and M-T) Scale bar is 50 μm and 100 μm for (I-L).

## 3.5 Expression of Netrin-1 in uninjured and regenerating axons following injury

Preliminary immunohistochemical examination of the sciatic nerve carried out by my research group showed that Netrin-1 was expressed mainly by SCs (Figure 9 C-F). Madison *et al.* (2000) also had previously shown that Netrin-1 expression was not observed in uninjured or crushed sciatic nerves in rats however following a transection injury there was evident expression of Netrin-1 associated with several, but not all, SCs. However, I observed Netrin-1 expression in DRGs and the spinal cord which suggested

that Netrin-1, like other transported proteins and membranous organelles (Guillaud *et al.*, 2020), could also be anterogradely transported to the axons of the peripheral nerves.

Therefore, I re-investigated the expression of Netrin-1 in uninjured and injured sciatic nerves of C57BL/6 mice. Sciatic nerve transection injury was performed on mice and 7 days post-injury the injured nerve with the muscle (to stabilise the nerve bridge) was dissected out as well as the contralateral uninjured side. The nerves were processed for immunohistochemistry and double stained for Netrin-1 and a neurofilament heavy chain antibody (NF) to label axons. I observed evident expression of Netrin-1 in the axons of the intact sciatic nerve (Figure 16).
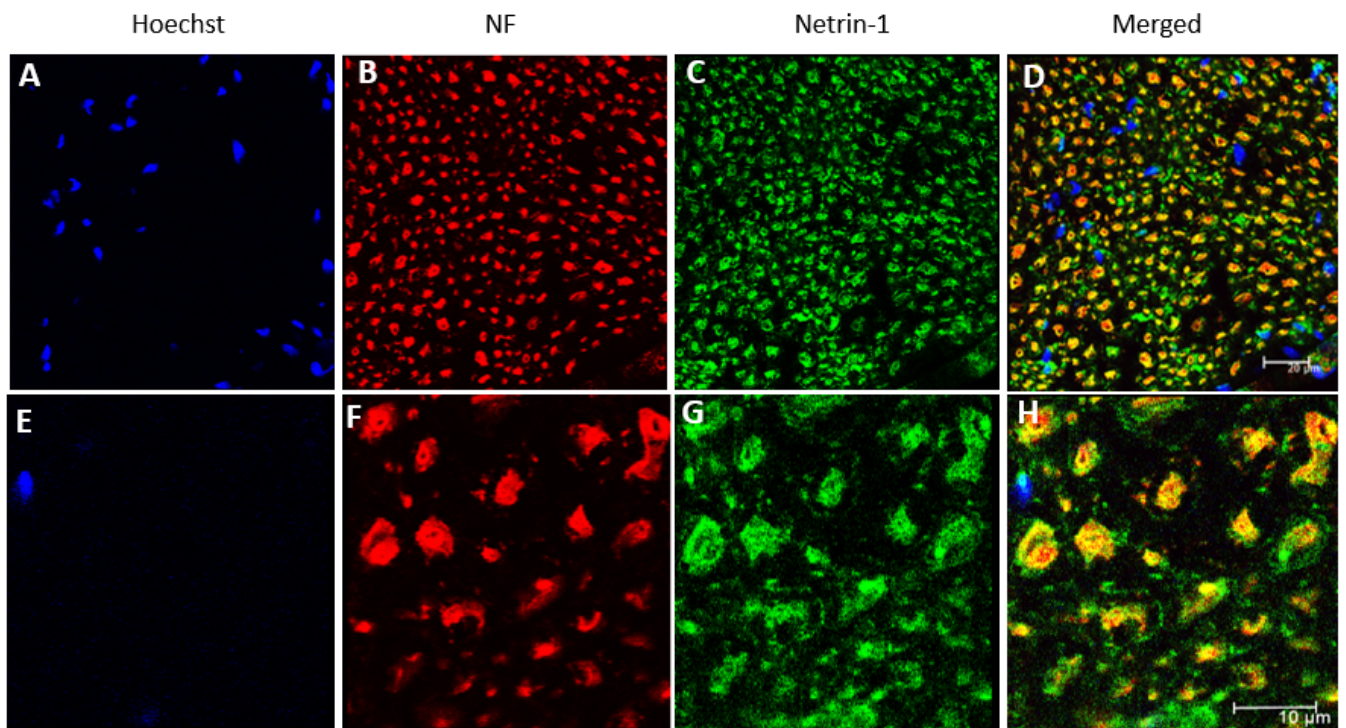
**Figure 16: Netrin-1 expression in the axons of intact mouse sciatic nerve**

(A-H) Netrin-1 (green) staining on transverse sections of intact sciatic nerve colocalises with neurofilament heavy chain (NF, red) depicting Netrin-1 expression in axons. (D, H) The area of co-localisation appears in yellow. (E-H) Magnified image of (A-D). Hoechst (blue) staining labels the nucleus. (A-D) Scale bar is 20 μm and for (E-H) its 10μm.

In the 7-day transected nerves, a timepoint at which the regenerating axons have only just crossed the nerve bridge with the distal nerve stump still devoid of axons (Figure 17 A), Netrin-1 expression was observed in the proximal nerve segment where axonal degeneration is less pronounced (Figure 17). Moreover, the intensity of Netrin-1 immunofluorescence appeared to be more prominent in the nerve bridge. However, interestingly in the distal part of the sciatic nerve, Netrin-1 expression was observed in

what appears to be the axonal debris, formed as a result of axonal degeneration after injury (Figure 17 B, D, F).
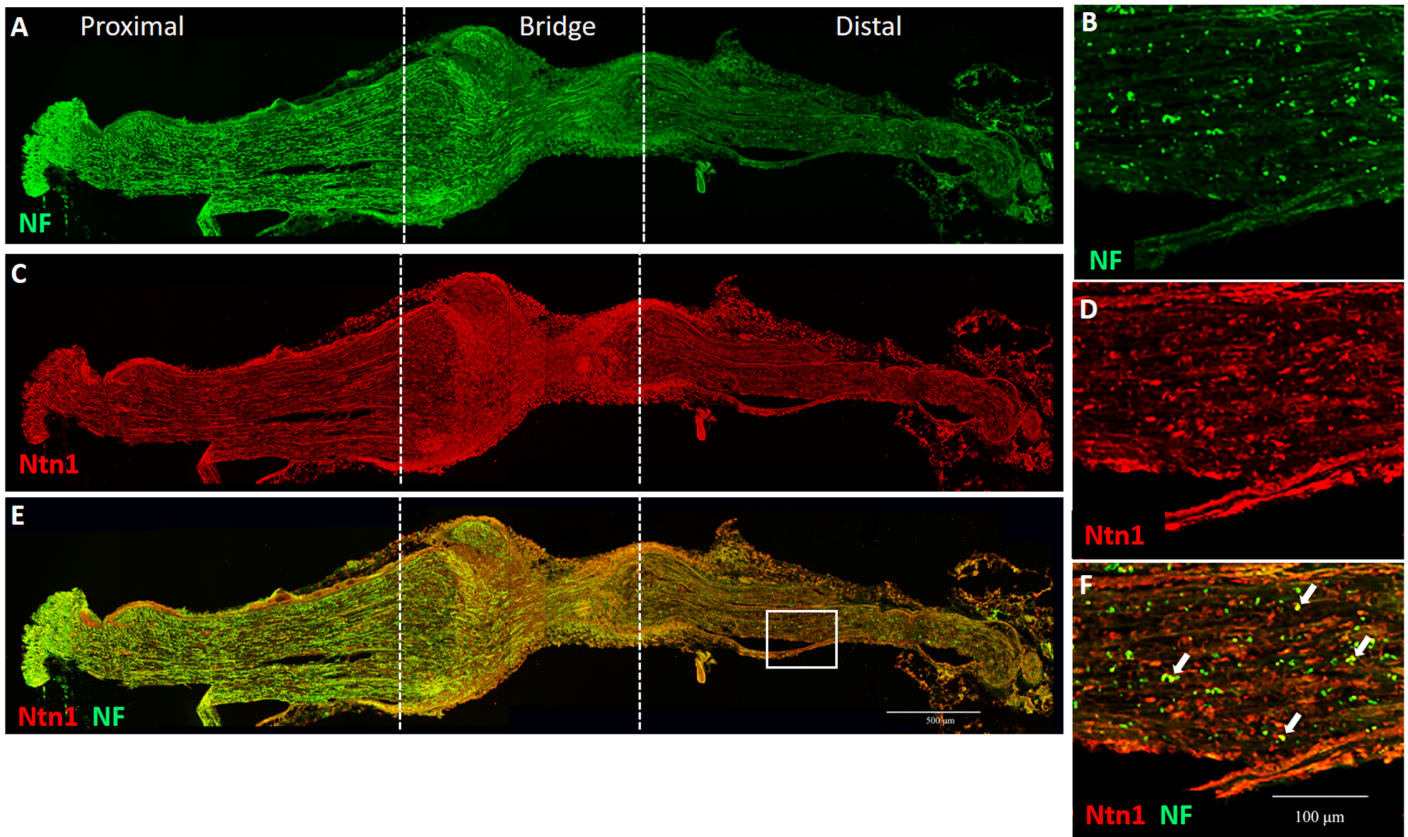


**Figure 17: Netrin-1 expression in axons of mouse sciatic nerves seven days post-transection injury**

(A, B) Neurofilament (NF, green) and (C, D) Netrin-1 (Ntn1, red) double staining in longitudinal sections of sciatic nerve 7-days after mouse sciatic nerve transection injury. (E, F) Axons of proximal and bridge sections of the injured sciatic nerve express Netrin-1 as well as axon debris of the distal stump. (B, D, F) Magnified image of the box in (E) with the white arrows depicting axon debris and Netrin-1 co-localisation. (A, C, E) Scale bar is 500 µm and for (B, D, F) it is 100µm.

I also examined Netrin-1 expression in the sciatic nerves 14-days after a transection injury, a timepoint in mice at which axons have innervated the distal nerve segment but peripheral nerve repair is still not complete. I looked at transverse sections of the proximal, bridge and distal nerve stump, immunostained for Netrin-1 and neurofilament heavy chain antibodies. Netrin-1 expression was robustly seen in the three nerve segments (Figure 18).
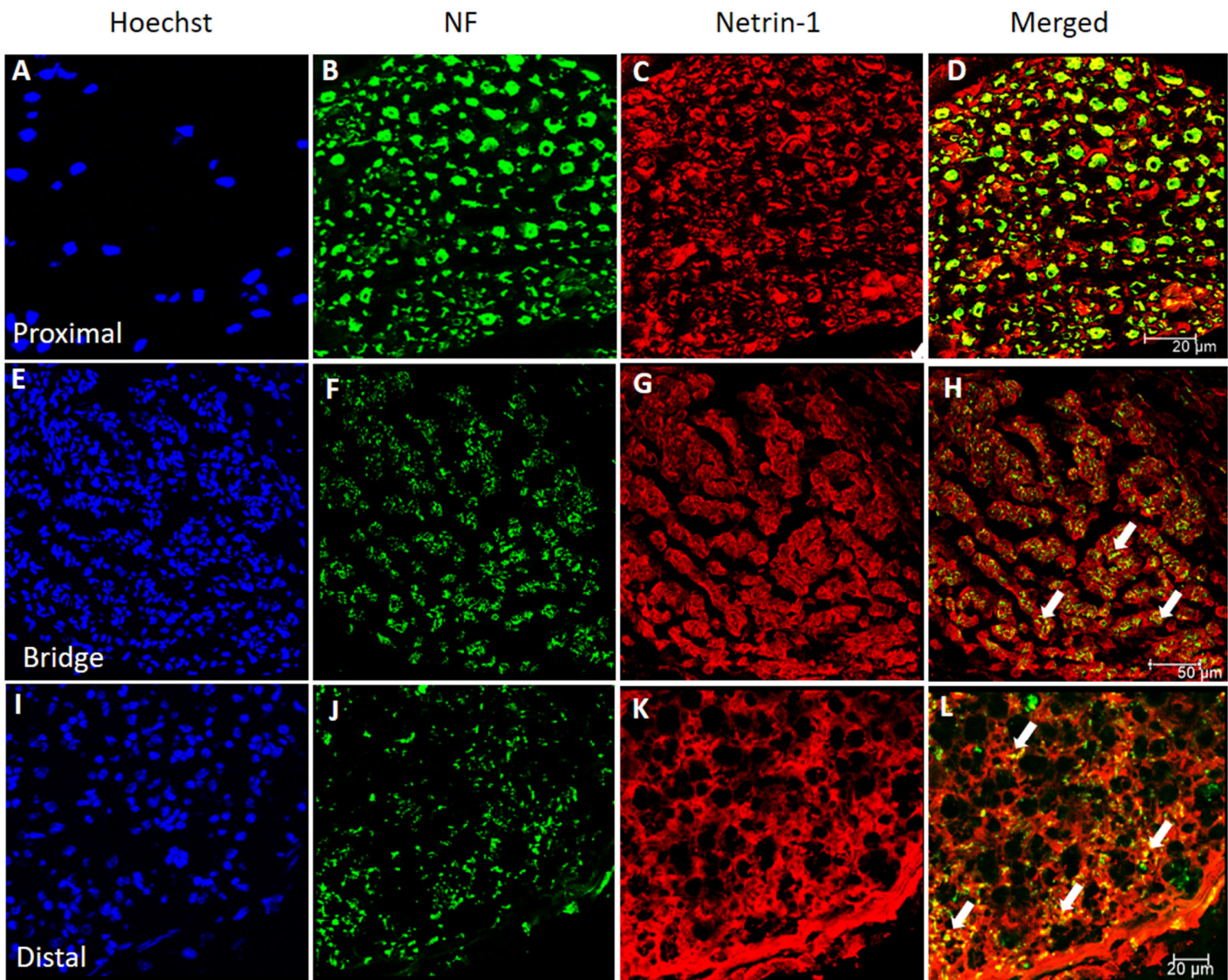
**Figure 18: Netrin-1 expression in axons 14 days following sciatic nerve transection injury**

Netrin-1 (red) and neurofilament heavy chain (NF, green) immunostaining of transverse sections of mouse sciatic nerve 14 days after sciatic nerve transection injury. (A-D) Netrin-1 colocalises with NF in the proximal nerve segment of the sciatic nerve depicting expression of Netrin-1 in axons. (E-H) Netrin-1 expression in regenerating axons of the nerve bridge and (I-L) and the distal sciatic nerve. White arrows depict Netrin-1 colocalisation with NF (D, H, L). Netrin-1 staining is observed in surrounding cells as well. Hoechst (blue) staining labels the nucleus of cells. (A-D and I-L) Scale bar is 20 μm and for (E-H) it is 50μm.

## 3.6 Netrin-1 expression in the Schwann cells of injured and uninjured sciatic nerve.

Madison *et al.* (2000) showed in their histochemical analysis that two weeks post-transection Netrin-1 was robustly expressed by SCs in the rat peripheral nerve and suggested that Netrin-1 could be strategically situated in the SCs to regulate axon regeneration post-injury. Rosenberg *et al*. (2014) also reported that in zebrafish, Netrin-1b mRNA colocalises with SCs along the motor nerve prior to and post-transection injury of the motor nerve. Moreover, I had already observed Netrin-1 expression in SCs when validating my knockout model 7-days post-injury (Figure 14 E-L). However, I further wanted to study the expression of Netrin-1 in SCs in intact sciatic nerves and at 14 days post-injury.

Therefore, I used PLP-GFP transgenic mice that express GFP in oligodendrocytes in the CNS and in myelinating and non-myelinating SCs of the peripheral nerve (Mallon *et al*., 2002). The mice underwent transection surgery on the right sciatic nerve followed by dissection at 14 days whereas the left uninjured sciatic nerve was used to study Netrin-1 expression in intact nerve. My research group's extensive work with the PLP-GFP mice has shown that GFP expression is more prominent in non-myelinating SCs and comparatively dull or weaker in the myelinating SCs (Chen *et al.,* 2019a; Li *et al.,* 2021). Similar to the results of my research group using the Abcam Netrin-1 antibody (Cat no: ab126729) (Figure 9 C-F), my immunohistochemical analysis with Netrin-1 antibody from

R&D systems (Cat no: MAB1109) showed that Netrin-1 was expressed mainly in non-myelinating SCs of intact sciatic nerves (Figure 19).
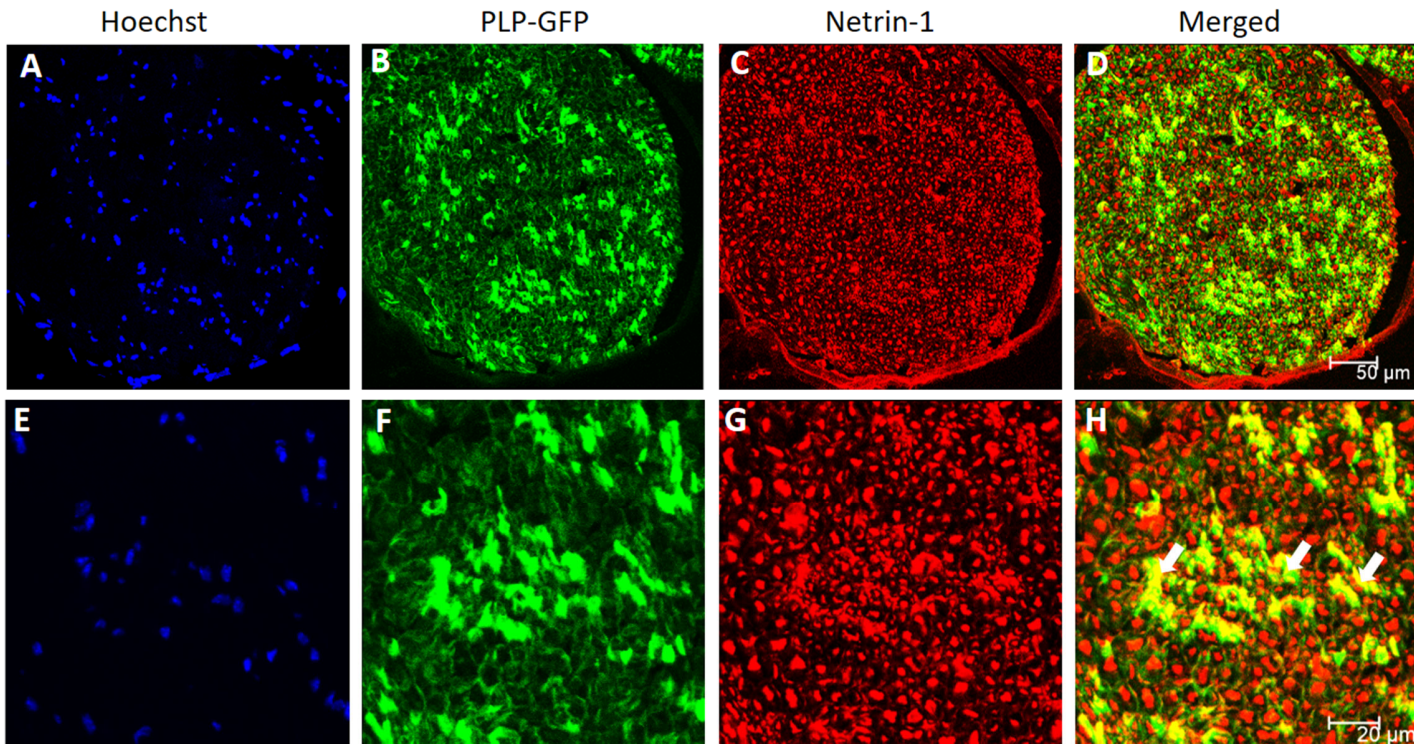


**Figure 19: Netrin-1 expression in Schwann cells of intact mouse sciatic nerve**

(A-H) Colocalisation of Netrin-1 (red) with endogenous GFP expressed in Schwann cells in transverse sections of intact sciatic nerve from PLP-GFP mice. (E-H) is a magnified image of (A-D). The white arrows in (H) show colocalisation of Netrin-1 mainly in bright green (non-myelinating) Schwann cells. Hoechst (blue) staining labels the nucleus. (A-D) Scale bar is 50 µm and for (E-H) it is 20µm.

At 14-days post-transection injury, Netrin-1 staining on transverse sections of PLP-GFP sciatic nerve showed that Netrin-1 colocalised with GFP expressing SCs in the proximal, bridge and distal nerve segments (Figure 20). However, I did observe Netrin-1 expression in cells other than SCs in all three nerve segments (Figure 20).
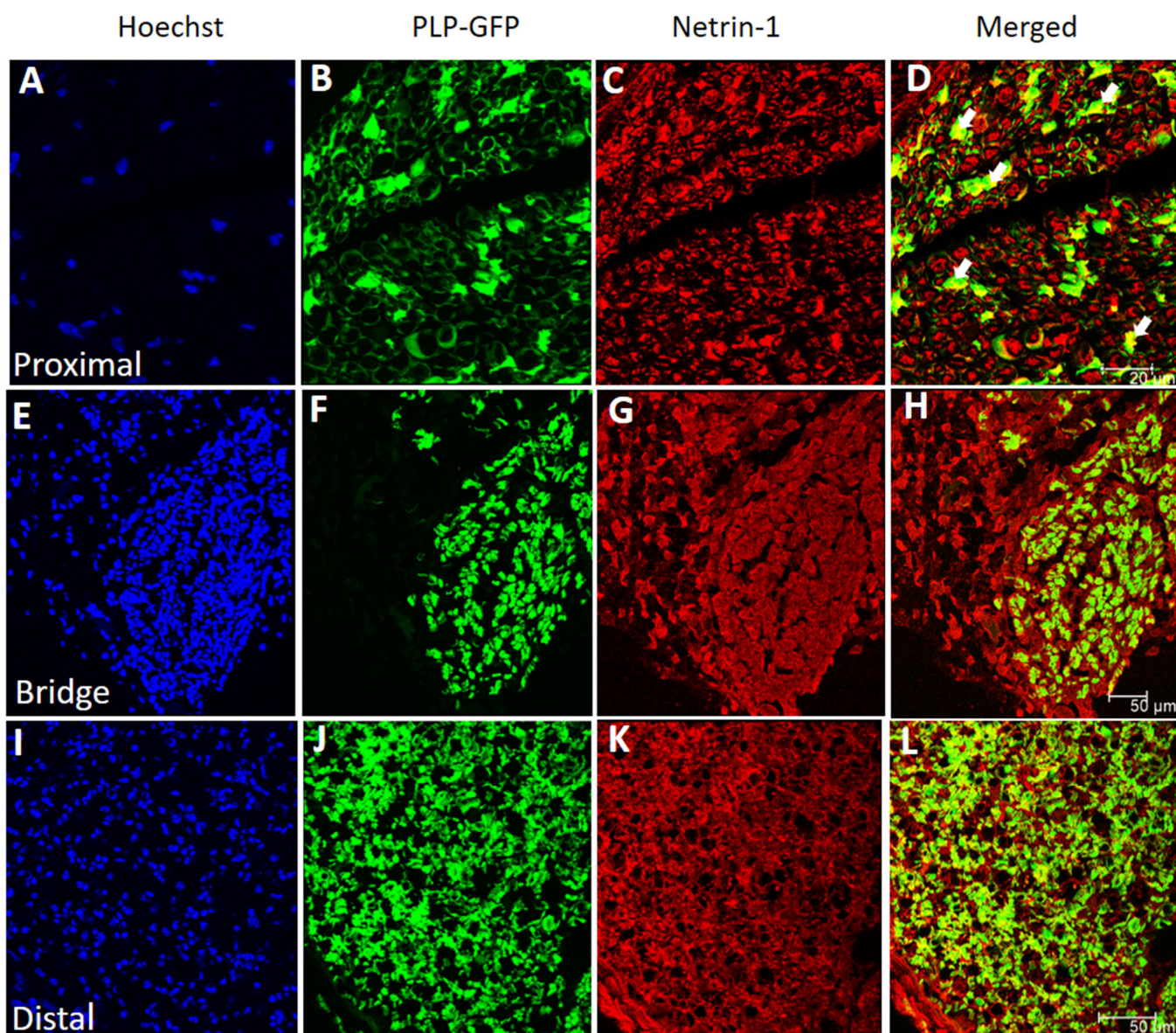
**Figure 20: Netrin-1 expression in Schwann cells 14 days post-transection injury in transverse PLP-GFP mouse sciatic nerve sections.**

Netrin-1 (red) staining colocalises with Schwann cells (green) in transverse sections of the proximal (A-D), bridge (E-H) and the distal (I-L) nerve segments of the sciatic nerve 14 days after a transection injury. The white arrows in (D) show co-localisation of Netrin-1 mainly in bright green (non-myelinating) Schwann cells. Netrin-1 staining is observed in surrounding cells as well. Hoechst (blue) staining labels the nucleus. (A-D) Scale bar is 20 µm and for (E-L) its 50µm.

## 3.7 Axon guidance defect in Netrin-1 knockout mice following nerve transection injury

My immunohistochemical examination of the sciatic nerve showed expression of Netrin-1 both in SCs and axons among the identified cell-types. However, it was still important to study whether SC-derived Netrin-1 had a role in peripheral nerve regeneration.

To study the role of SC-derived Netrin-1 in regeneration of axons, I performed a transection injury on the sciatic nerve in control and SC-specific Netrin-1 knockout mice to assess whether Netrin-1 was required for SCs to guide regenerating axons across the sciatic nerve gap. At 2 weeks post-transection injury, the sciatic nerve was harvested for whole mount staining (Dun and Parkinson, 2018). Briefly, unsectioned nerves were fixed and incubated with neurofilament heavy chain (NF) primary antibody for 48hrs to label axons followed by a secondary Alexa fluor antibody and stages of clearing in 25%, 50% and 75% glycerol. It was observed that in the Netrin-1 control animals, the majority of the axons crossed the bridge 14 days post-injury with a few axons showing aberrant trajectories (Figure 21 A). However, I observed a severe disruption in the trajectory of axons in the Netrin-1 knockout mice with the axons extending to the left and right of the transection site (Figure 21 B) rather than following the normal path to the distal segment of the nerve. From all animals, I also harvested the right tibial nerve which was processed for immunohistochemistry and cut transversally to quantify the number of axons that had effectively crossed the nerve bridge and entered the distal nerve stump 14 days

post-injury (Figure 21 C, D). All axons per fascicle were counted and depicted as total number of axons per total area of cross section of the tibial nerve. However, I did not observe any significant difference in the number of axons that had regenerated into the tibial nerve (Figure 21 E).

These results suggested that SC-derived Netrin-1 might be important for the initial guidance of the axons across the nerve bridge after a transection injury. However, no comparable difference in the number of axons that innervate the tibial nerve suggested that Netrin-1 expression by other neuronal and non-neuronal cells in the sciatic nerve such as the axons themselves could compensate for the loss of Netrin-1 in SCs. This compensation could be sufficient to correct the aberrant axon trajectories.
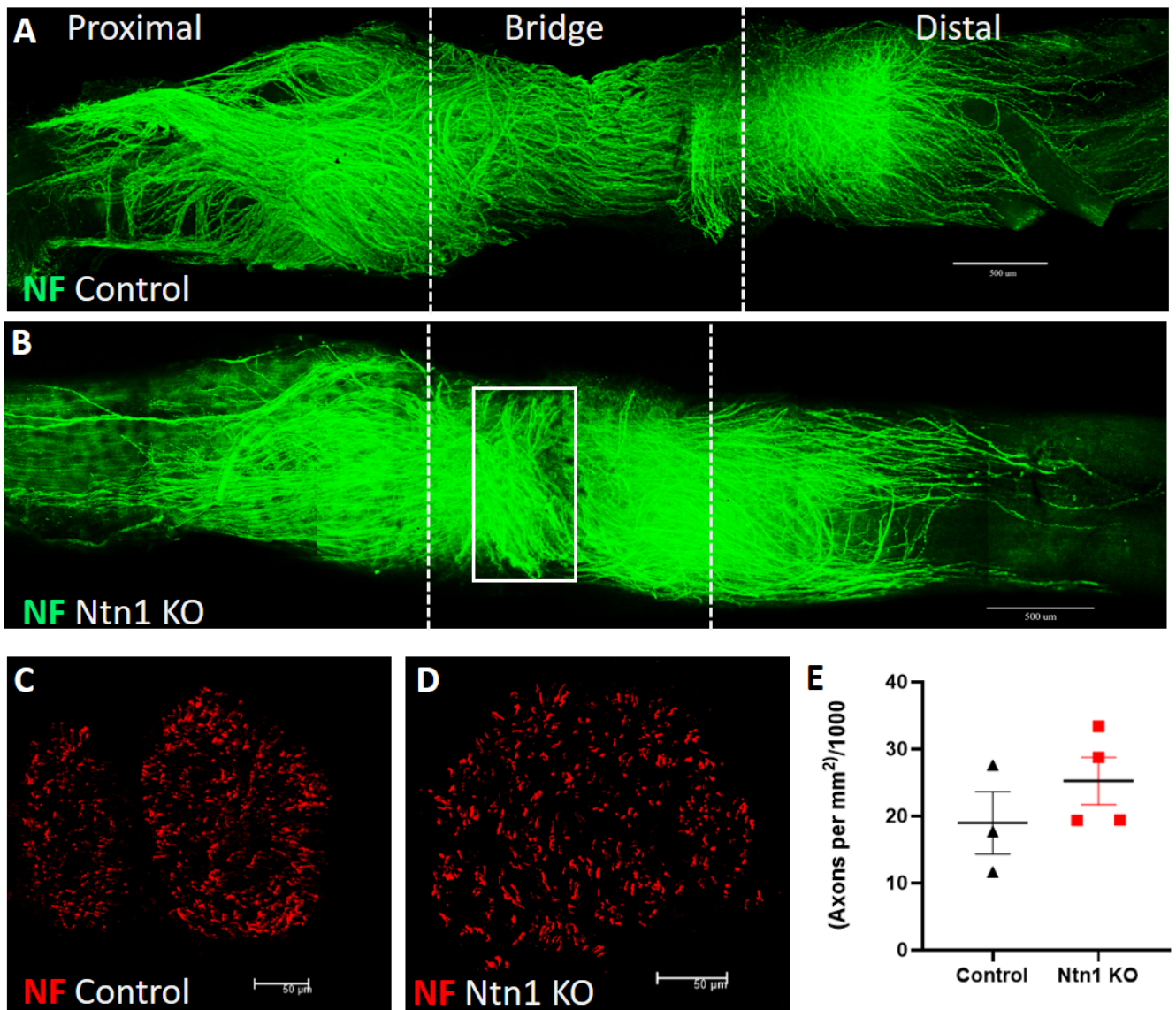
**Figure 21: Axon guidance defect in the nerve bridge of Schwann cell-specific Netrin-1 knockout mice**

(A and B) Whole mount nerve staining of sciatic nerve with antibody for neurofilament heavy chain (NF, green) depicting axonal regeneration in the nerve bridge of (A) control (n=3) and (B) SC-specific Netrin-1 knockout mice (Ntn1 KO) (n=4), 14 days post-nerve transection injury. The dotted lines depict the segregation of the proximal, the nerve bridge and the distal end of the nerve. (C and D) Transverse section of the tibial branch of the sciatic nerve immunolabelled with neurofilament heavy chain (NF, red) antibody shows axon density in the distal nerve stump in control (C) and Ntn1 KO mice (D) 14 days

post nerve transection injury. Scale bars in (A and B) represents 500 μm and in (C and D) represents 50 μm. (E) Quantification of total number of axons per total area of cross section of the tibial nerve in control (n=3) and Ntn1 KO mice (n=4), 14 days post-transection injury. There was no statistically significant difference (p > 0.05; not significant) between the two groups. Error bars represent (±) SEM.

## 3.8 Normal axon outgrowth in Netrin-1 knockout mice post-nerve crush injury.

In comparison to a transection injury, sciatic nerve crush results in a break of axons but SCs basal laminae are preserved which significantly improves the chances of regeneration (Amado *et al*., 2008; Luís *et al*., 2008). This facilitates the precise study of the ability of a regenerating axon to interact with both the SC and basal lamina (Luís *et al*., 2008).

To study whether axon outgrowth was affected post-crush injury in my mouse model, SC-specific Netrin-1 knockout and control mice were subjected to nerve crush injury in the right sciatic nerve and the whole length of the nerve including the tibial branch was harvested 7 days post-injury. The nerves were fixed in 4% paraformaldehyde (PFA) for a minimum of 5 hrs and the epineurium was carefully removed with sharp forceps followed by whole mount staining (Dun and Parkinson, 2018). The speed of axon regrowth was examined with whole nerve neurofilament heavy chain (NF) antibody staining as described previously. Under a confocal microscope, I assessed the neurite outgrowth from the crush site up until the leading axon (Figure 22 A-D). Despite observing off-trajectory axons after a transection injury in the Netrin-1 knockout mice,

in the crush injury where the basal lamina is still intact, the axons regenerated at a pace close to that of the control indicating that probably in a crush injury SC-derived Netrin-1 does not influence axon outgrowth. However, it is to be noted that axon outgrowth at time-points earlier than 7 days following crush injury was not studied. Therefore, the possibility that in SC-derived Netrin-1 knockout mice, there can be a lag in axon outgrowth earlier than 7 days post-crush injury, cannot be ruled out.
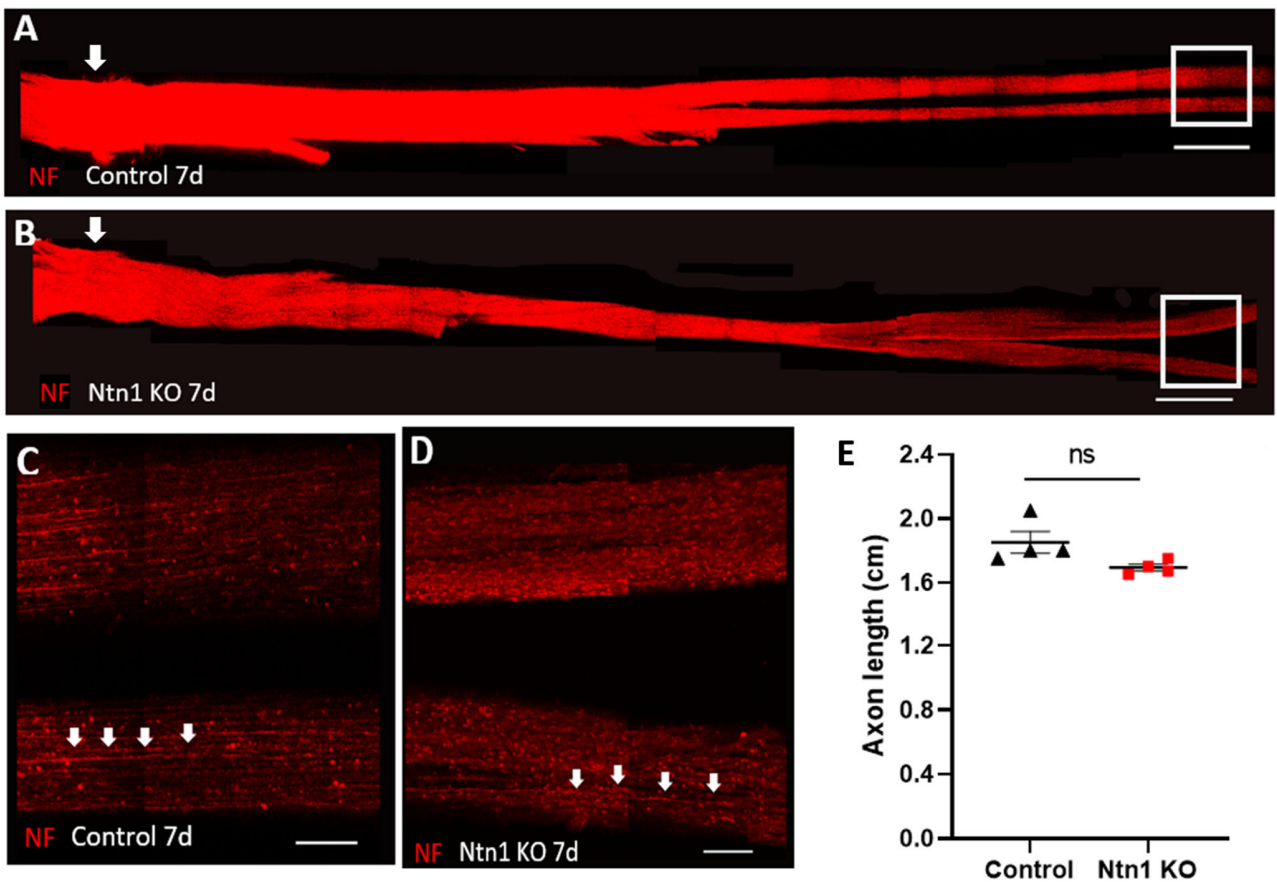
**Figure 22: Normal axon outgrowth in Schwann cell-specific Netrin-1 knockout mice 7 days post-crush injury**

(A-D) Whole nerve preparation labelled for neurofilament heavy chain (NF, red) antibody 7 days post-sciatic nerve crush injury in (A) control and (B) Schwann cell-specific Netrin-1 knockout mice (Ntn1 KO) to depict axonal outgrowth. Multiple serial micrographs were captured from the site of crush injury (shown by a white arrow) up until the leading axon (white box) and tiled into a single composite image. (C, D) Magnified views from the boxed area depicting the leading axons are shown for (C) control and (D) Ntn1 KO mice as shown by small arrows. Scale bar in (A and B) is 1000µm and in (C and D) is 100 µm. (E) Quantification of the length (in cm) of the leading axon from the crush site 7 days post-injury in control and Ntn1 KO mice (n=4 per group). There was no statistically significant difference ($p > 0.05$; not significant) between the two groups. Error bars represent (±) SEM.

## 3.9 Netrin-1 is not essential for functional recovery post-crush injury

As no significant differences were observed in the SC-specific Netrin-1 knockout mice compared to the control in terms of axon outgrowth post crush injury, I wanted to confirm whether the same was true in terms of functional recovery. For this purpose, a crush injury on the right sciatic nerve was performed in mice followed by static sciatic index (SSI) measurements to study functional recovery (Bozkurt *et al.*, 2008). Each mouse was kept in a plastic transparent box and a camera was positioned below the box to record the toe spread of the right (injured) and left (uninjured) paw (Figure 23 A-D). The data was collected from each mouse prior to injury on day 0 and every alternative day from 7 days post-injury (when the mouse could fully place its paw down on a surface) up until day 21.

Prior to surgery as expected no difference in the SSI between the mouse groups was observed. Following surgery for crush injury on the right sciatic nerve of both control and Netrin-1 knockout mice, the SSI decreased from -5.49 (pre-operative condition for normal posture) to -60 ± 5 in both groups (Figure 23 E). There was no statistically significant difference in the SSI score when comparing both groups from day 7 up until day 21, when a mean score of -5.49± 5 was recorded for both groups indicating complete functional recovery (Figure 23 E).Thus, the data from axon outgrowth and functional

recovery suggested that SC-derived Netrin-1 was not required for axonal regeneration after a crush injury. However, it is to be noted that the SSI does not assess the regeneration of small unmyelinated axons such as the C-fibre nociceptors which is better evaluated by tests such as Hargreaves test. Therefore, role of SC-derived Netrin-1 in the regeneration of small unmyelinated fibres cannot be ruled out.
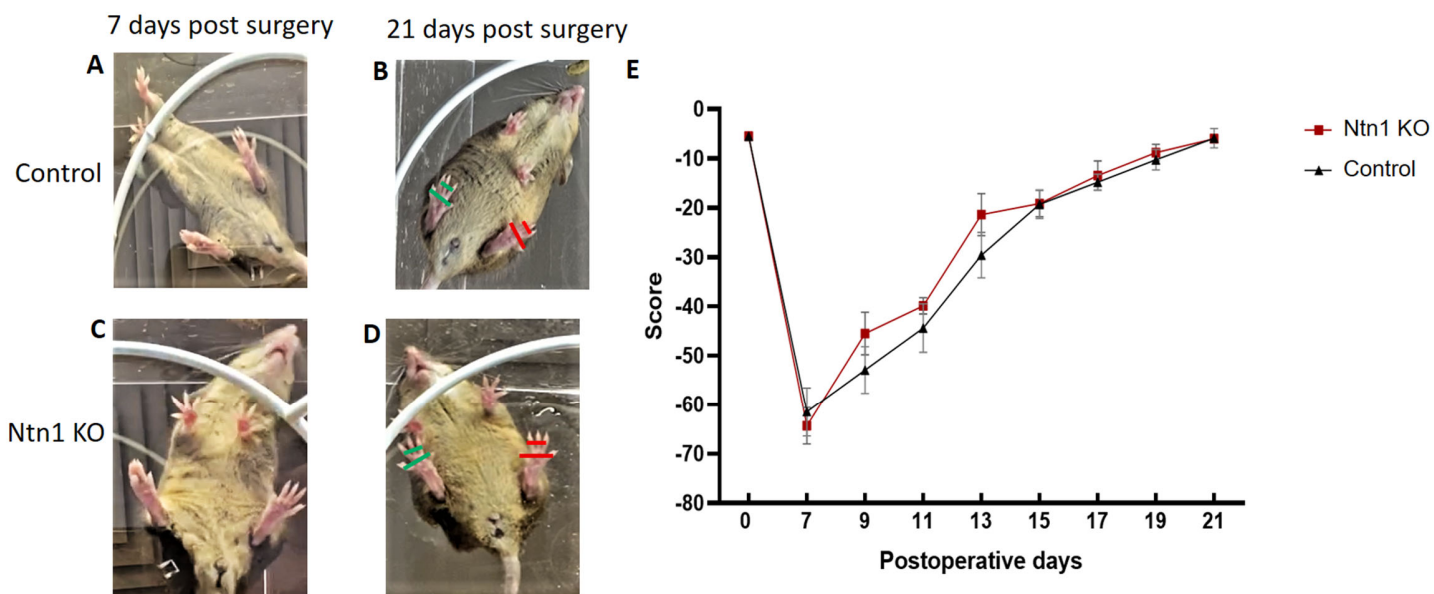


**Figure 23: Functional recovery is not affected in Schwann cell-specific Netrin-1 knockout mice post-crush injury.**

(A, C) Representative images for control and SC- specific Netrin-1 knockout (Ntn1 KO) mice 7 days post-crush injury with the right paw unable to spread all digits when in static position. (B, D) The same mice 21 days post-crush injury with paw spread of the right foot (green) almost equal to that of uninjured left foot (red). (E) The course of Static Sciatic Index (SSI) for control and Ntn1 KO mice following nerve crush injury. In the plotted graph, values approaching zero imply a trend to recovery of function (n=9 for each group). There was no statistically significant difference ($p > 0.05$) for SSI between the two groups. Error bars represent ($\pm$) SEM.

**3.10 Netrin-1 does not affect Schwann cell proliferation post-transection injury**

Wallerian degeneration post-traumatic PNI triggers a cascade of glial cell responses such as SC proliferation and migration important for successful peripheral nerve repair (Koeppen, 2004; Guertin, 2005). Therefore, I wanted to study whether proliferation of SCs post-injury was affected by the absence of Netrin-1 in SCs.

Both control and SC-specific Netrin-1 knockout mice were crossed with, PLP-GFP mice to generate control (Ntn1 $^{loxP/loxP}$ GFP$^+$) and knockout (P0-Cre$^+$ Ntn1 $^{loxP/loxP}$ GFP$^+$) mice that had endogenous expression of green fluorescent protein (GFP) in SCs and can be detected on a confocal microscope (Mallon *et al.*, 2002; Dun *et al.*, 2019). These mice then underwent sciatic nerve transection surgery and 7 days post-injury they were injected with Edu followed by dissection of the sciatic nerve distal to the site of injury, 3hrs after injection. The tissue was then fixed in 4% PFA, cryopreserved in 30% sucrose, embedded in OCT followed by 10 μm longitudinal cryosectioning of the nerve. Immunohistochemistry was carried out with Hoechst to label nuclei and EdU Click-iT reaction cocktail to label EdU-positive cell. Images were taken on confocal microscope, and I counted the number of EdU positive nuclei in GFP positive SCs in the distal nerve segment (Figure 24 A-H). Quantification of the GFP-labelled proliferating cells revealed

that there was no significance in the rate of proliferation of SCs in the distal sciatic nerve in the SC-specific Netrin-1 knockout mice compared to the control (Figure 24 I).
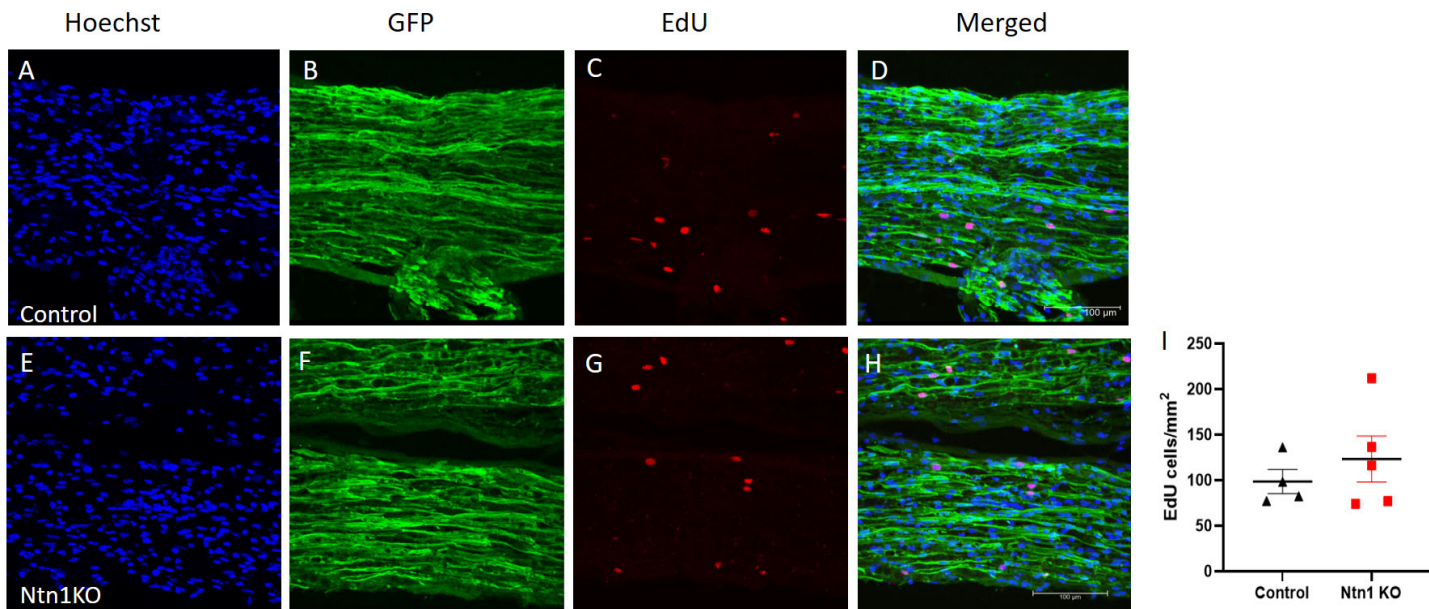


**Figure 24: Loss of Netrin-1 in Schwann cells does not affect Schwann cell proliferation after peripheral nerve transection injury**

(A-H) Confocal microscope images of longitudinal sections of the distal sciatic nerve labelled with EdU (red), and endogenous Schwann cell-specific GFP (green), 7 days post nerve transection injury in control (A-D) and Schwann cell-specific Netrin-1 knockout mice (Ntn1 KO) (E-H). The merged images demonstrate the colocalisation of Schwann cells (SCs) and EdU labelled proliferating cells in control and Ntn1 KO mice. Scale bar is represented as 100 μm. Hoechst (blue) staining labels the nucleus. (I) Quantification of the number of proliferating SCs in the distal nerve stump 7 days post-transection injury (n=4 for control and n=5 for Ntn1 KO mice). (I) There was no statistically significant difference (p > 0.05) between the two studied groups. Error bars represent (±) SEM.

**3.11 Netrin-1 does not affect Schwann cell migration post-nerve transection.**

Torigoe *et al.* (1996), established a film sandwich model, wherein a mouse peroneal nerve was fitted in between two thin plastic fluorine resin films after nerve transection injury. This model was used to study early axon regeneration up to a 6-day time point. In their study, they showed that SCs migrate near the transection site at day 3 post-injury that gradually increases by day 4 (Torigoe *et al.*, 1996). My research group had previously used the PLP-GFP mouse model and whole mounting of the sciatic nerve to study SC migration and similarly observed the appearance of first migrating SCs 4 days post mouse sciatic nerve transection injury (Dun and Parkinson, 2018; Chen *et al.*, 2019a). They demonstrated that SCs migrating from the proximal stump of the nerve go beyond the regenerating axons on day 5 post PNI and form 'SC cords' within the nerve bridge by 7 days. Their study also showed that SC migration and guiding the regenerating axons across the nerve injury site, is essential for preventing misdirection of regenerating axons.

Therefore, to study SC migration in my model, I again used the GFP expressing SC-specific Netrin-1 knockout and control mice and performed nerve transection injury. Ideally, I wanted to observe the rate of SC migration in the nerve bridge of my model before the formation of the SC cords and therefore based on the timeline for SC migration as observed by my research group (Chen *et al.*, 2019a), I sacrificed the mice 6 days post-

transection injury. After dissection of the sciatic nerve, fixation in 4% PFA, the nerves went through clearing stages in glycerol for a period of 24hrs for each concentration of glycerol (25%, 50% and 75%). The nerves were then mounted and imaged. A series of z stack images were taken along the nerve on a confocal microscope and were stitched together using Adobe Photoshop. However, I observed that the SCs had already crossed the bridge to form a SC cord at day 6-post-injury connecting the proximal and distal nerve stumps in both, the control and SC-specific Netrin-1 knockout mice (Figure 25 A, B).

Thus, the experiment was repeated again this time with the nerves dissected at 5 days post-transection injury. I observed that at 5 days, the SCs had just initiated migration both from the proximal and the distal stumps of the nerve (Figure 25 C, D). When measuring the distance of the leading processes of the SCs from the proximal end of the nerve and the same from the distal end of the nerve no significant difference was observed between the two groups (Figure 25 E). Similarly, no major difference was observed in the area covered by the migrating SCs from both the proximal and distal stump of the nerve when comparing the control and SC-specific Netrin-1 knockout mouse groups (Figure 25 F).
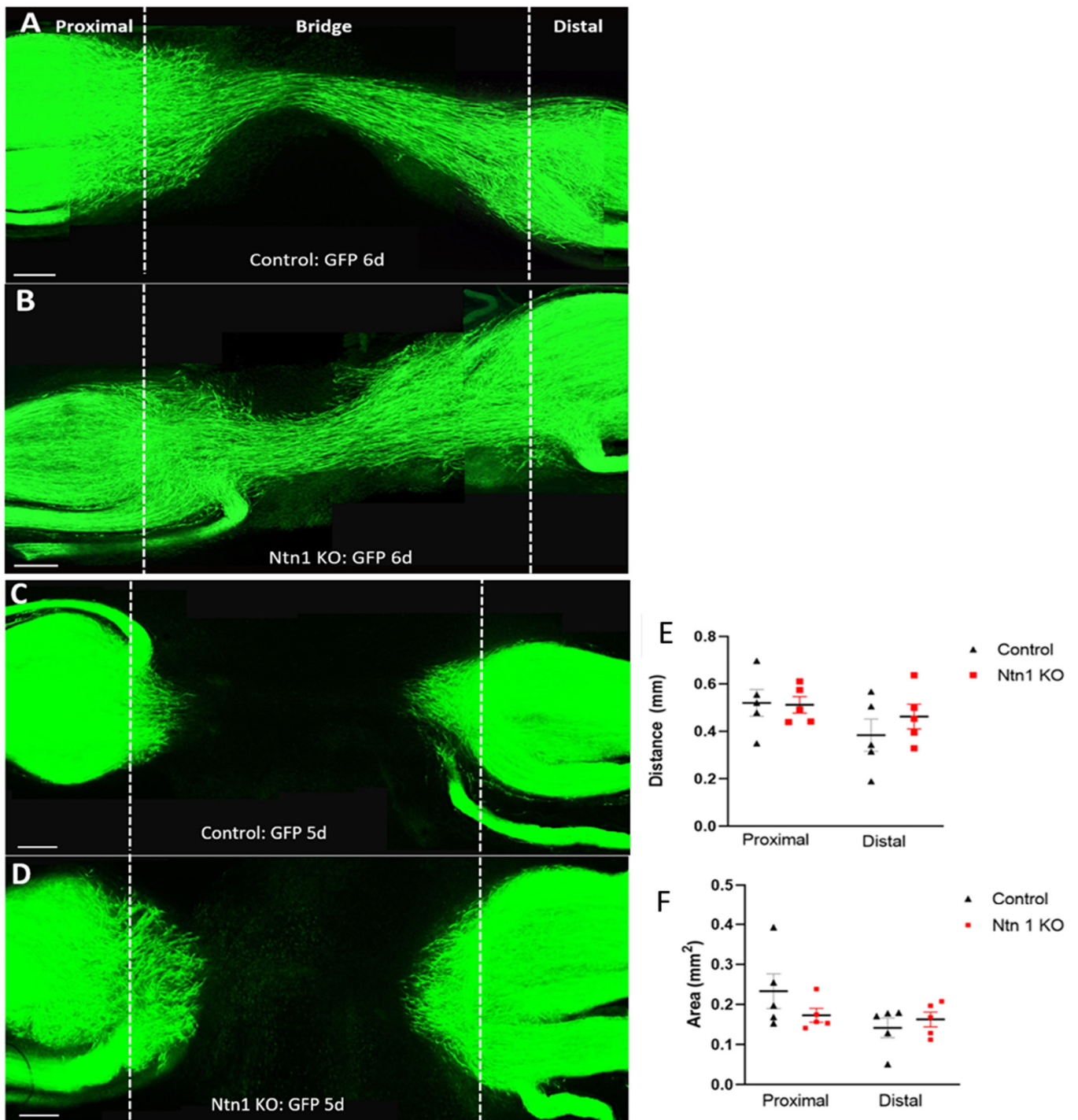
**Figure 25: Schwann cell migration in the nerve bridge is not affected in Schwann cell-specific Netrin-1 knockout mice after a transection injury**

(A and B) Whole mounted sciatic nerve 6 days post-transection injury depicting Schwann cell (SC) cord formation (GFP, green) in (A) control and (B) SC-specific Netrin-1 knockout mice (Ntn1 KO). The mice

express endogenous GFP in Schwann cells. White dashes depict the segregation between the proximal, bridge and distal nerve stump. (C and D) Whole mounted sciatic nerve 5 days post-transection injury shows SC migration (GFP) in the nerve bridge of (C) control and (D) Ntn1 KO mice. Scale bars in (A-D) represented as 200 μm. (E) Graph showing the distances (in mm) of the leading migrating SCs from either the proximal or distal end in the nerve bridge of control and Ntn1 KO mice 5 days post-transection injury. (F) Graph depicts the area (in mm$^2$) covered by the migrating SCs from the proximal and distal stump of the sciatic nerve in the nerve bridge of control and Ntn1 KO mice 5 days post-transection injury (n= 5 for each group). Error bars represent (±) SEM. There was no statistically significant difference (p > 0.05) between the two studied groups for either the distance (E) or the area covered (F).

## 3.12 Schwann cell derived Netrin-1 is not important for remyelination of axons following injury

In the process of nerve repair, another important mechanism is remyelination of regrown axons. Despite the possibility of spontaneous remyelination post-injury in the PNS, the remyelinated axons often have thinner myelin sheaths as well as a reduced internodal length thus resulting in slower nerve conduction (Schröder, 1972; Sherman and Brophy, 2005).

To determine whether absence of SC derived Netrin-1 was capable of affecting myelination post-injury in the peripheral nerves, I performed a crush injury on the right sciatic nerve of the SC-specific Netrin-1 knockout and control mice. The tibial nerve was dissected at two time points, an earlier 28 day and a later 60-day time point and fixed in 2.5% (w/v) glutaraldehyde diluted in 0.1M Sodium cacodylate buffer (pH 7.2). The

176

samples underwent the long process of further fixation, dehydration in alcohol, resin permeation and embedding to prepare the samples for transmission electron microscopy (TEM). The embedded tissue samples were cut using a diamond knife and imaged on the TEM. The g-ratio were then calculated from several images taken for each sample.

TEM data revealed that 28 days post-injury, there was no significant difference in the g-ratio when comparing the control and SC-specific Netrin-1 knockout mice nerves (Figure 26 A-D). A Mann-Whitney U test also showed no significant difference in the average g-ratio between the two groups (Figure 26 D). For both mouse groups, almost 50% of the axons had a g-ratio between 0.6 to 0.7 (Figure 26 C). This is indicative of optimal axonal myelination from Rushton's theoretical estimate of 0.6 as the optimal g-ratio based on speed of nerve fibre conduction (Rushton, 1934).
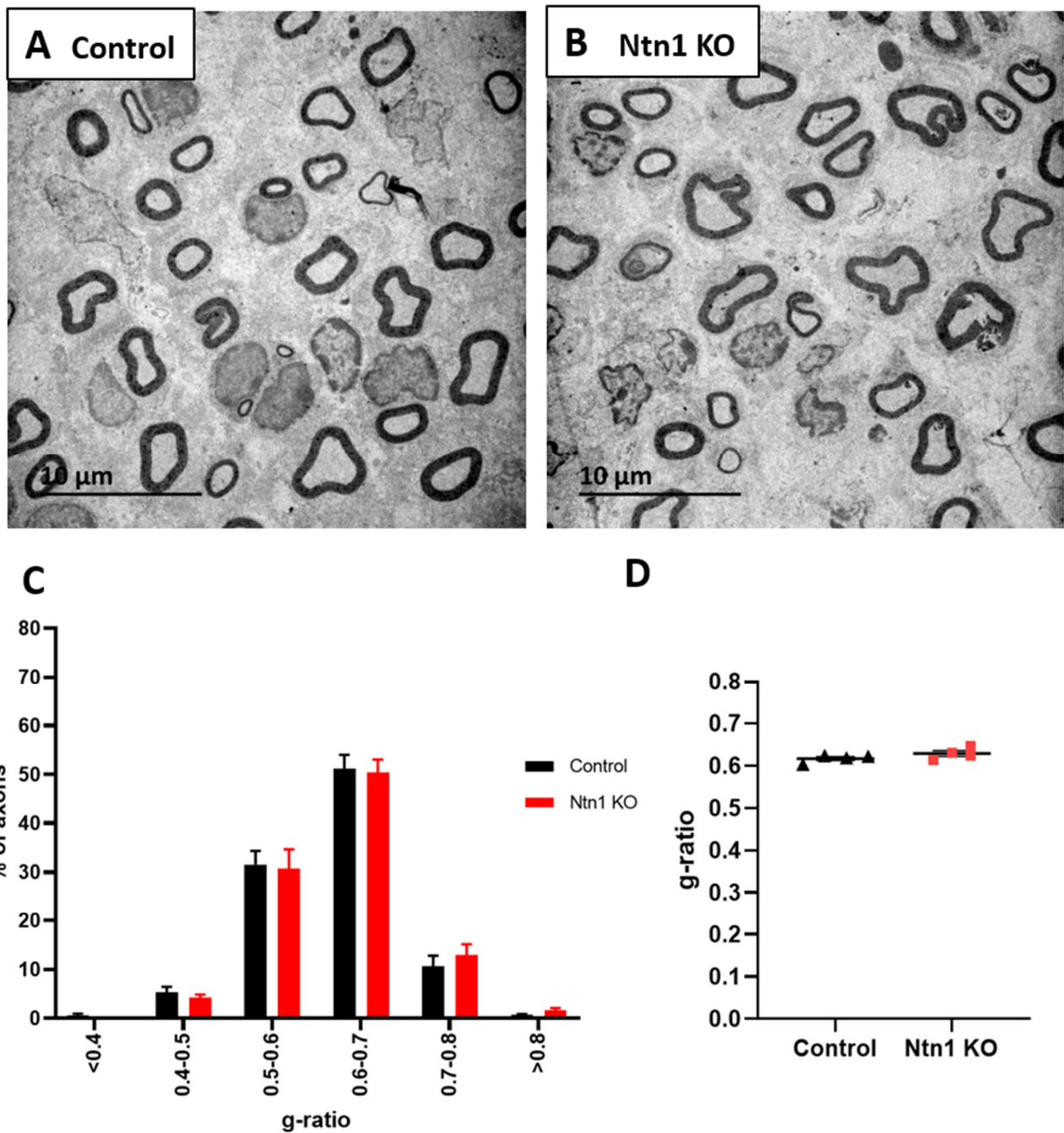
**Figure 26: Schwann cell deletion of Netrin-1 has no affect on remyelination of axons following injury**

(A, B) Transmission electron micrographs of transverse sections of the tibial nerve taken from (A) control and (B) Schwann cell-specific Netrin-1 knockout mice (Ntn1 KO), 28 days post peripheral nerve crush injury. (C) Graph depicting the percentage distribution of axons relative to their g-ratio in the two

groups. (D) Graph comparing the average g-ratio of the two groups (n=4 per group). Error bars represent (±) SEM. There was no statistically significant difference (p > 0.05) between the two studied groups for g-ratio.

TEM data for 60 days post-crush injury was carried out to observe whether this myelination trend continues in the later time point of peripheral nerve repair. Again, I did not observe any difference for g-ratio between the control and the Netrin-1 knockout group (Figure 27). Similar to the data for 28-day time point majority of the axons had a g-ratio ranging between 0.6-0.7 for both the studied groups, however, for this time point the percentage of axons having a g-ratio ranging between 0.7-0.8 went up from 10% to almost 25% (Figure 27 C). A Mann-Whitney U test did not show any significant difference in the average g-ratio between the two groups (Figure 27 D). These results confirmed that loss of Netrin-1 in SCs does not affect the remyelination of axons post-crush injury.
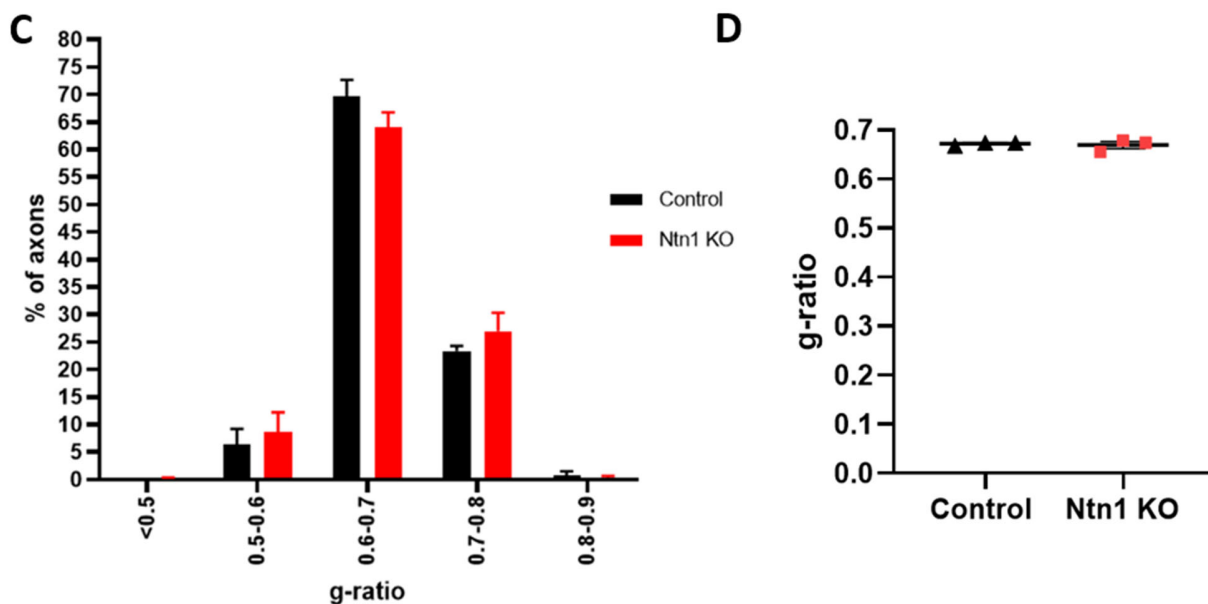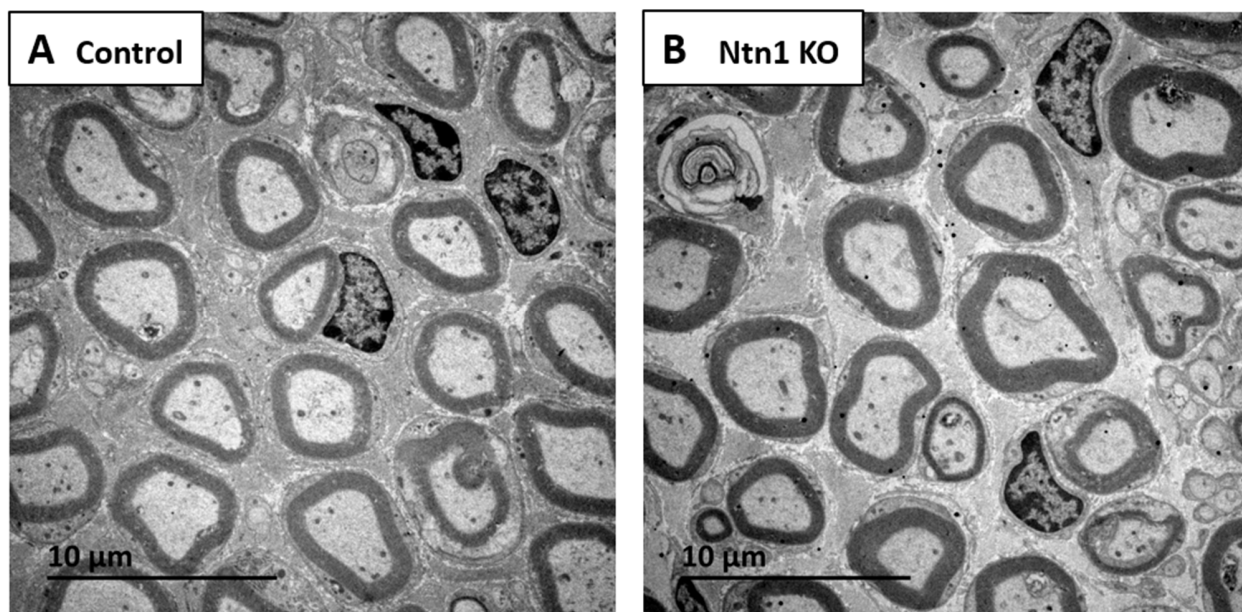
**Figure 27: Schwann cell derived Netrin-1 deletion does not affect remyelination 60 days post-crush injury**

(A, B) Transmission electron micrographs of transverse sections of the tibial nerve taken from control and Schwann cell specific Netrin-1 knockout mice (Ntn1 KO), 60 days post peripheral nerve crush injury. (C) Graph depicting the percentage distribution of axons with reference to their g-ratio in the two groups. (D) Graph comparing the average g-ratio of the two groups (n=3 per group). Error bars

represent (±) SEM. There was no statistically significant difference (p > 0.05) between the two studied groups for g-ratio.

## 3.13 Transcriptomic profiling of Netrin-1 from single cell RNA sequencing data

The work carried out on the Netrin-1 SC-specific knockout mice did not show any significant defects in the absence of Netrin-1 in SCs post-transection and crush injury in terms of peripheral nerve repair. Coincidentally, as I neared the end of the experiments for my Netrin-1 conditional knockout mouse model, two papers were published describing the transcriptomic profiles of injured and uninjured rodent sciatic nerves. Gerber *et al.* (2021) published a paper describing the transcriptional profiles of intact mouse sciatic nerve from embryonic day 13.5 (E13.5) to postnatal day 60 (P60) using single-cell RNA sequencing technology. Additionally, their results were formulated into a useful resource called the Sciatic Nerve ATlas available at SNAT: https://www.snat.ethz.ch. Using this resource to run a search query for Netrin-1 in intact P60 sciatic nerve revealed high Netrin-1 mRNA expression in perineurial and epineurial cells and comparatively lower expression in endoneurial cells and in a few populations of endothelial cells. Most importantly, in SCs, Netrin-1 mRNA expression was quite low in P60 sciatic nerve (Figure 28).

**A**

Ntn1

0: Epineurial cells (EpC)
1: Perineurial cells (PnC)
2: Immune cells (IC)
3: Pericytes and vascular smooth muscle cells (Per/VSMC)
4: Schwann cells (SC) – non-myelinating (Remak) Schwann cells (nm(R)SC ) and myelinating Schwann cells (mSC)
5: Endoneurial cells (EnC)
6,7: Endothelial cells (EC1,EC2)
8: Pericytes/Endothelial cells (Per/EC)

**B**

Ntn1
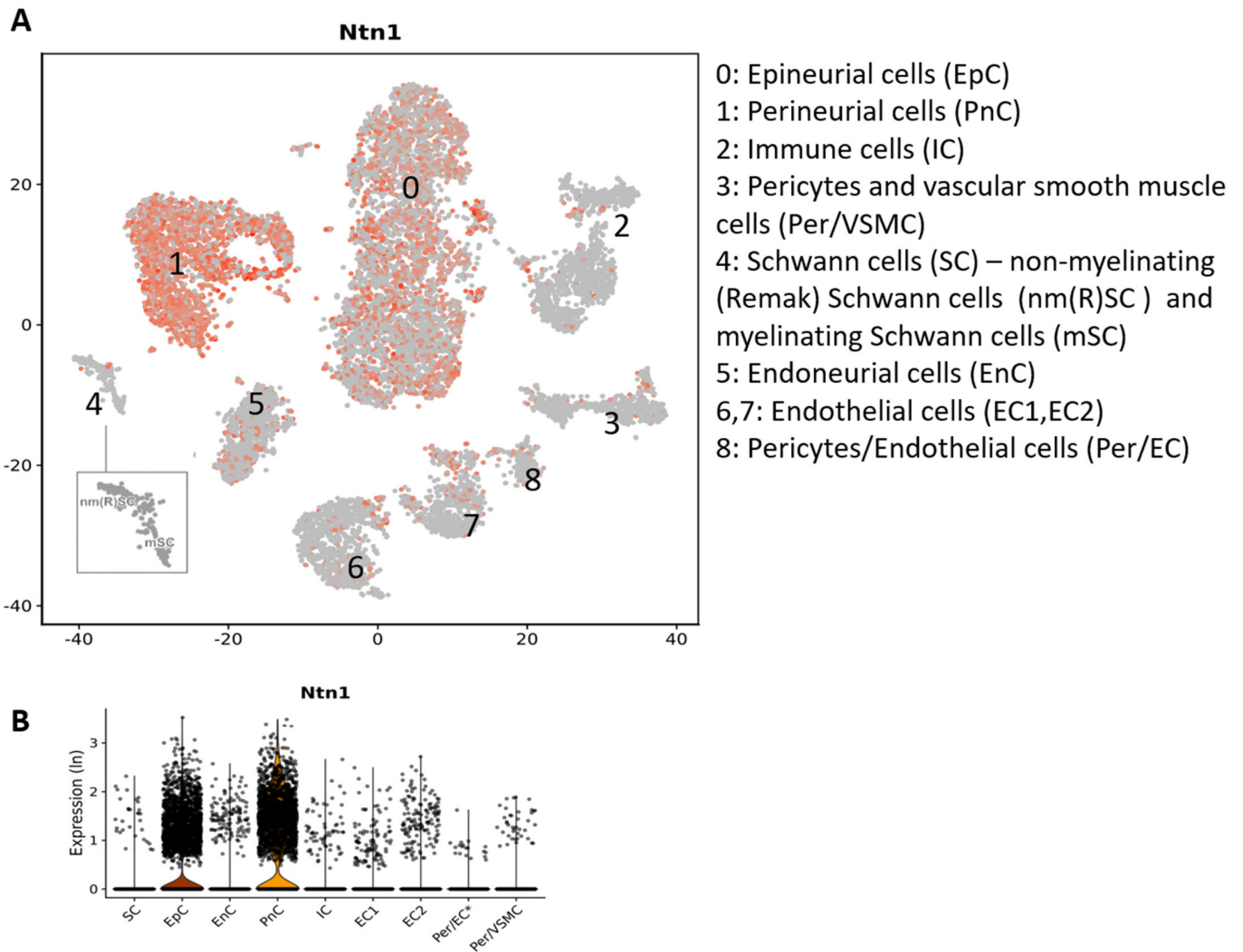
**Figure 28: Netrin-1 single cell transcriptome profiling in mouse sciatic nerve cells at postnatal day 60 from the Sciatic nerve ATlas**

(A) A t-SNE plot showing cell clusters for single cell transcriptomic analysis (GSE137870) of uninjured postnatal day 60 (P60) mouse sciatic nerve with Netrin-1 expression (orange) superimposed on non-Netrin-1 expressing cells (grey) after running a search query on the resource Sciatic nerve ATlas (https://snat.ethz.ch/). (B) Violin plot from the same resource depicting Netrin-1 expression levels in uninjured sciatic nerve of P60 mouse. (A, B) The figure key 1-8 describes the identity of the clusters as determined by the authors.

The second publication of interest was by Toma *et al.* (2020) that also looked at single-cell transcriptional profiling of distal sciatic nerve from CD1 mice 3 days post-transection injury. Their aim was to describe the sciatic nerve ligand environment following injury in rodents (Toma *et al.*, 2020). To analyse the cell-specific expression of Netrin-1 before and after injury from this publication, raw data was obtained from Gene Expression Omnibus (GSE147285). Additionally, an earlier publication by Carr *et al.* (2019), performed a similar study in mice on the distal sciatic nerves 9 days post transection injury (GSE120678). These two datasets were combined and re-analysed as described in the recently published paper by my research group (Chen *et al.*, 2021a). Using the interactive R shiny app developed by Dr Banton, I further studied the combined data sets for Netrin-1 expression in the intact and distal sciatic nerve post-injury.

My analysis revealed that in uninjured sciatic nerve, Netrin-1 is not expressed in myelinating SCs and the expression in non-myelinating SCs is low (Figure 29, Table 11). Instead, Netrin-1 mRNA showed highest expression in perineurial cells followed by epineurial fibroblasts (Figure 29, Table 11) in terms of percentage of cells expressing as well as average expression of Netrin-1 (Figure 29, Table 11). Netrin-1 expression was also observed in endoneurial fibroblasts and endothelial cells (Figure 29, Table 11). This expression pattern in uninjured sciatic nerves was very similar to that of the data obtained from the ATlas search query published by Gerber *et al.* (2021).

**A** Ntn1

0: Endoneurial fibroblasts
1: Non-myelinating Schwann cells (nmSCs)
2,6,7: Epineurial fibroblasts
3, 4: Epineurial endothelial cells
5: Endoneurial endothelial cells
8: Pericytes
9: Vascular smooth muscle (VSM) cells
10: Myelinating Schwann cells (mSCs)
11: Perineurial cells
12: Immune cells (resident macrophages, mast cells, T/NK cells)
13: Lymphatic endothelial cells.

**Figure 29: Single cell transcriptomic profiling of Netrin-1 in uninjured nerves**

Data published for single cell transcriptomic (GSE147285) of intact mouse sciatic nerve was re-analysed and a t-SNE cluster generated, annotated for cell types as identified by marker gene expression. (A) Netrin-1 (Ntn1) mRNA expression (in blue) superimposed on the segregated cell clusters of the dataset. (B) Dot plot showing Netrin-1 expression in the clustered cell types in the intact sciatic nerve. (A, B) The figure key describes the identity of the 14 clusters.

**Table 11: Netrin-1 mRNA expression in uninjured sciatic nerve and 3 days and 9 days post-transection injury in the distal mouse sciatic nerve segment from published transcriptomic data GSE147285 and GSE120678 (Carr *et al.,* 2019; Toma *et al.,* 2020; Chen *et al.,* 2021a).**

| Ntn1 in intact nerve cell types | Percentage of cells | Average expression | Ntn1 in day 3 nerve cell types | Percentage of cells | Average expression | Ntn1 in day 9 nerve cell types | Percentage of cells | Average expression |
|---|---|---|---|---|---|---|---|---|
| Endoneurial fibroblasts | 8.9 | 0.1 | Endoneurial fibroblasts | 14.91 | 0.17 | Endoneurial fibroblasts | 5.22 | 0.06 |
| Perineurial cells | 54.93 | 0.64 | Differentiating fibroblasts and perineurial cells | 13.66 | 0.23 | Differentiating fibroblasts | 5.53 | 0.07 |
| Epineurial fibroblasts | 22.73 | 0.26 | Epineurial fibroblasts | 24.89 | 0.335 | Perineurial cells | 50.56 | 0.66 |
| Non-myelinating Schwann cells (nmSC) | 0.73 | 0.01 | Schwann cells | 2.21 | 0.02 | Epineurial fibroblasts | 18.57 | 0.23 |
| Myelinating Schwann cells (mSCs) | 0 | 0 | Endothelial cells | 2.43 | 0.03 | Schwann cells | 2.1 | 0.02 |
| Arterial endothelial cells | 6.25 | 0.06 | VSM/pericytes | 3.53 | 0.06 | Endothelial cells | 2.48 | 0.02 |
| Capillary endothelial cells | 1.36 | 0.02 | Macrophages | 1.98 | 0.03 | VSM/pericytes | 0 | 0 |
| Venous endothelial cells | 4 | 0.04 | T, NK and mast cells | 1.12 | 0.01 | Macrophages | 0 | 0 |
| Lymphatic endothelial cells | 10.34 | 0.22 | Neutrophils | 0 | 0 | Mast cells | 2.78 | 0.03 |
| Pericytes | 0 | 0 | B cells | 0 | 0 | Neutrophils | 0 | 0 |
| Vascular smooth muscle (VSM) cells | 0 | 0 | | | | B cells | 0 | 0 |
| Immune cells (resident macrophages, mast cells, T/NK cells) | 0 | 0 | | | | NK cells | 0 | 0 |
| | | | | | | T cells | 0 | 0 |

The re-analysed single cell RNA-seq dataset GSE147285 for 3-days post-injury showed Netrin-1 mRNA expression was slightly upregulated in epineurial fibroblasts as compared to the uninjured sciatic nerve (Figure 30, Table 11). In comparison, the expression of Netrin-1 was notably downregulated in perineurial cells and endothelial cells as compared to intact sciatic nerve. For endoneurial fibroblasts, the average expression was comparable to the expression in the intact nerve, but more cells were expressing Netrin-1 mRNA. In the case of SCs, although I did observe a slight increase in the number of SCs

expressing Netrin-1 however the increase in average expression was still very low (Figure

30, Table 11).



**A**

Ntn1

0: Differentiating fibroblasts and perineurial cells
1: Macrophages
2: Endoneurial fibroblasts
3,5: Epineurial fibroblasts
4: Endothelial cells
6: Schwann cells
7: T, NK and mast cells
8: VSM/pericytes
9: Neutrophils
10: B cells

**B**
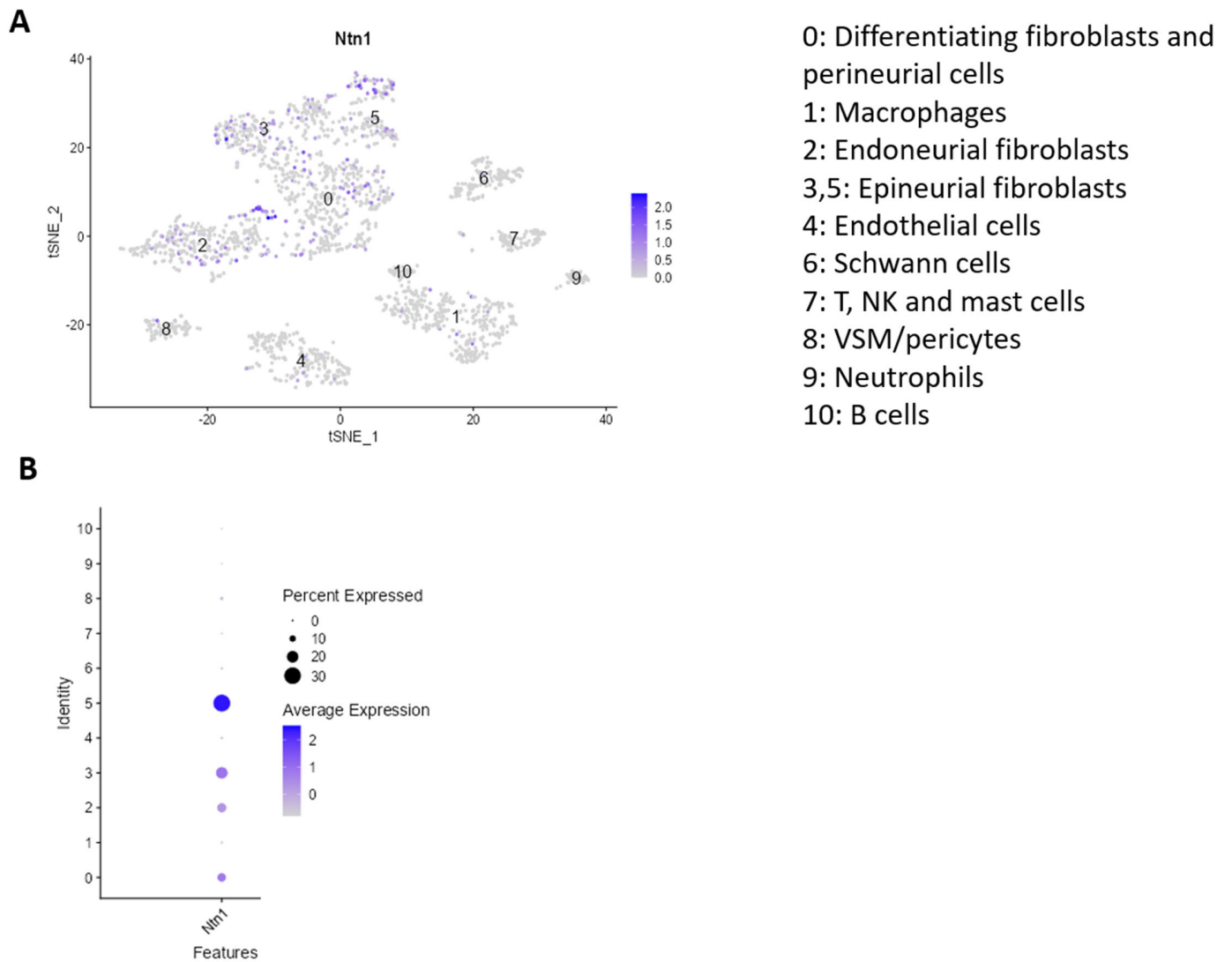
**Figure 30: Single cell transcriptomic profiling of Netrin-1 in day 3 post-transection injury distal mouse sciatic nerve.**

Data published for re-analysis of single cell transcriptomic dataset GSE147285, 3 days post mouse sciatic nerve transection injury from the distal stump of the nerve. A t-SNE cluster was generated, annotated for cell types as identified by marker gene expression. (A) Netrin-1 (Ntn1) mRNA expression (in blue) superimposed on the segregated cell clusters. (B) Dot plot showing Netrin-1 expression in the clustered

cell types in the distal stump of the injured nerve. (A, B) The figure key describes the identity of the 11 clusters.

In the distal mouse sciatic nerve segment at day 9 post-injury, Netrin-1 expression in perineurial cells and epineurial cells was almost comparable to intact sciatic nerve. In endoneurial fibroblasts, I observed a downregulation in average expression of Netrin-1 compared to both intact and 3-days post-injury. Interestingly, Netrin-1 expression in endothelial cells was still quite low in comparison to the intact sciatic nerve, while in SCs the expression of Netrin-1 was the same as 3 days post-injury (Figure 31, Table 11).
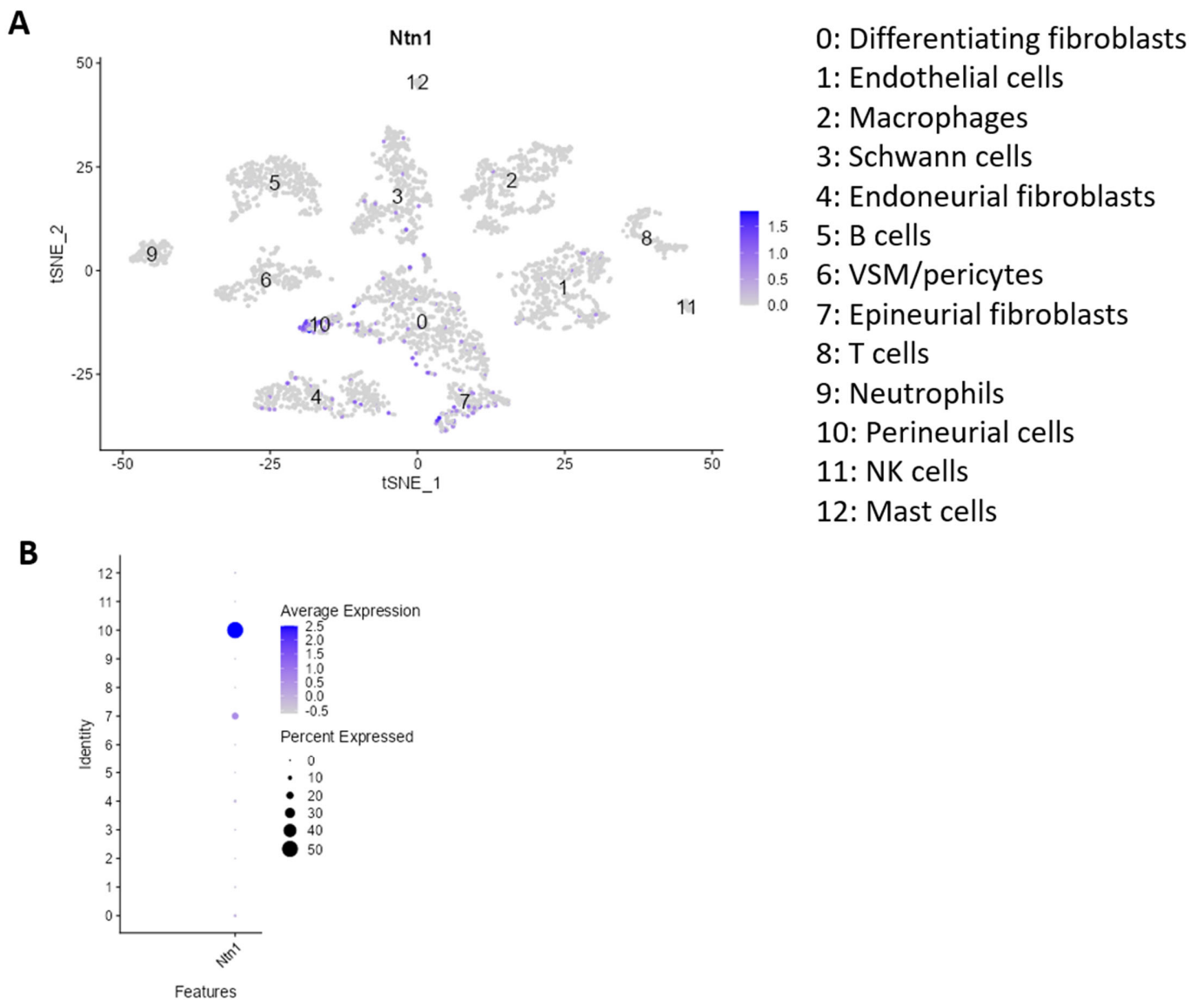
**Figure 31: Single cell transcriptomic profiling of Netrin-1 in day 9 post-transection injury distal mouse sciatic nerve**

Published single cell transcriptomics (GSE120678) data for 9 days post mouse sciatic nerve transection injury from the distal stump of the nerve was re-analysed and a t-SNE cluster generated, annotated for cell types as identified by marker gene expression. (A) Netrin-1 (Ntn1) mRNA expression (in blue) depicted in the cell clusters. (B) Dot plot showing Netrin-1 expression in the clustered cell types in the distal stump of the injured nerve. (A, B) The figure key 1-12 describes the identity of the clusters.

As shown previously, data derived from the high throughput RNA sequencing dataset-GSE103039 showed Netrin-1 mRNA expression in SCs derived from intact, bridge and distal sciatic nerve stump (Figure 11C). Additionally, there was downregulation of Netrin-1 in the SCs from the nerve bridge 6 days post-transection injury (Figure 11C). Moreover RT-PCR for Netrin-1 in cultured rat SCs (Figure 9A) and immunohistochemical examination of the sciatic nerve showed Netrin-1 expression in the SCs (Figure 19, 20). Contradictory to this, the above-described single cell transcriptomic analysis showed that Netrin-1 mRNA expression is quite low in SCs before and after injury.

However, it is to be noted that in most protocols for tissue processing for single-cell RNA sequencing (including the datasets analysed in this thesis), the tissue is incubated at 37° C with enzymes such as trypsin. This step required for the dissociation of the tissue sample and has been suggested to induce alterations in transcription, a variable that cannot be ruled out when analysing mRNA expression for the gene of interest (Adam *et al*., 2017; Marsh *et al*., 2022).

### 3.14 Netrin-1 expression in epineurial fibroblasts, tactocytes and perineurial cells

The single cell transcriptomic profiling of Netrin-1 showed for the first time that Netrin-1 is highly expressed by the connective tissues of the sciatic nerve – namely the perineurial, endoneurial and epineurial cells and additionally in endothelial cells. This data did not include Netrin-1 expression for axonal RNA, which is mainly synthesised in

the cell body (Lasek *et al*. 1973) and the translated proteins are transported to the axons (Droz and Leblond, 1963).

I wanted to observe whether the expression pattern of Netrin-1 protein would follow that of the transcriptomic profiling data in the newly identified cell types. CD34 (Hematopoietic progenitor cell antigen CD34), a transmembrane glycoprotein is expressed on surface of hematopoietic progenitor cells and previously the marker has been reported to be expressed in epineurial cells and endoneurial fibroblast-like cells (Richard *et al*., 2012; Sidney *et al*., 2014; Richard *et al*., 2014; Manong *et al*., 2023). In addition, the previously poorly studied endoneurial fibroblast-like cells, have been studied for their interaction with endothelial cells along the length of endoneurial blood vessels in the endoneurium, and were recently named as tactocytes (Stierli *et al.,* 2018; Manong *et al*., 2023). From here on, the endoneurial fibroblasts will be described as tactocytes.

To study Netrin-1 expression, C57BL/6 mice underwent a transection injury, and the injured and contralateral uninjured sciatic nerves were dissected out at 7 or 14 days post-injury, fixed in 4% PFA, cryosected and double stained for Netrin-1 and CD34. In intact transverse sections of the sciatic nerve, CD34 labelled the epineurium as observed by the morphology, and the tactocytes. Netrin-1 expression was observed in the CD34 positive cells (Figure 32).
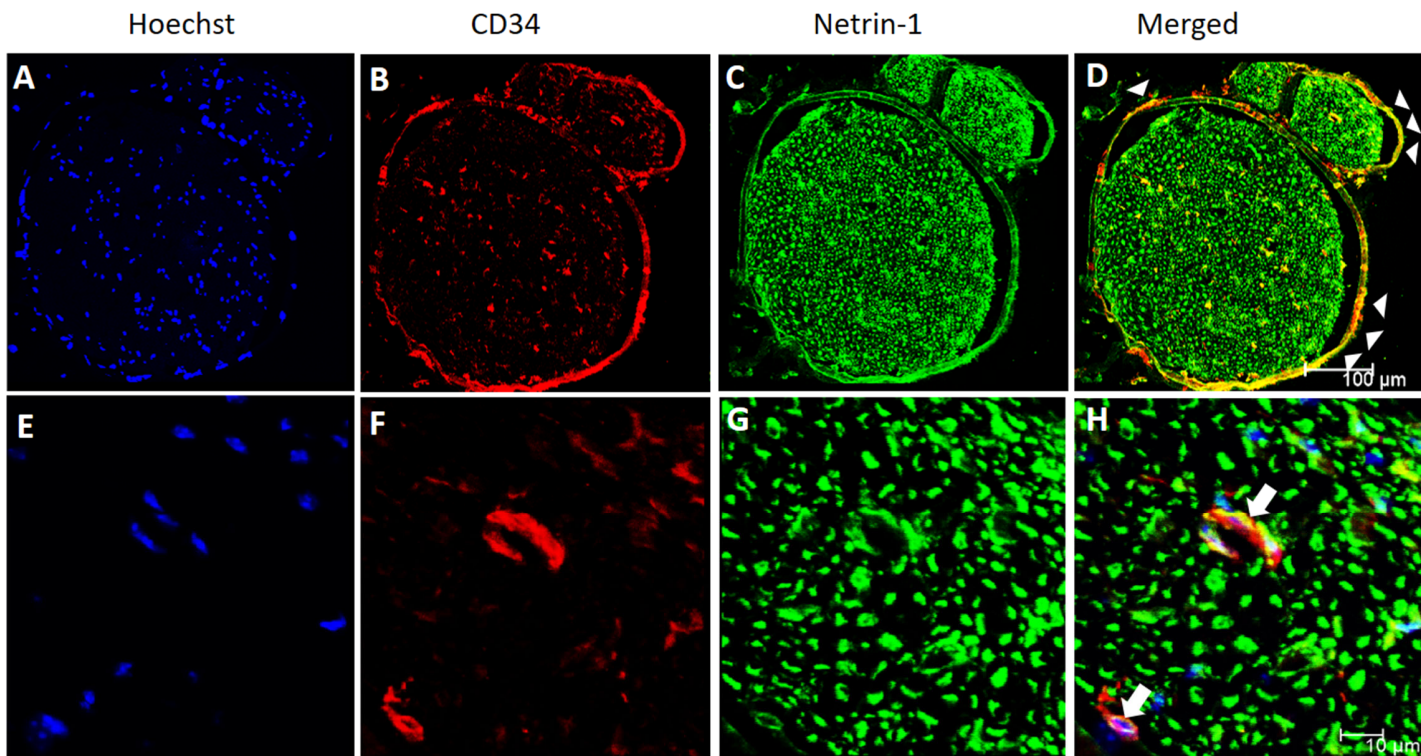
**Figure 32: Netrin-1 expression in the epineurium and tactocytes of an uninjured mouse sciatic nerve**

(A-H) Immunofluorescent staining of transverse sections of uninjured sciatic nerve dissected from C57BL/6 mice. CD34 (red) labels epineurial fibroblasts and tactocytes. (D) Netrin-1 (green) staining colocalises with CD34 in the uninjured sciatic nerve with evident immunoreactivity in the epineurium as shown by white triangles. (E-H) Magnified image of (A-D). White arrows show co-labelling of tactocytes and Netrin-1. Hoechst (blue) staining labels the nucleus. (A-D) Scale bar is 100 μm and for (E-H) its 10μm.

For 7-days post-injury I observed the colocalisation of Netrin-1 with CD34 in the proximal and the distal stump of the sciatic nerve, with the specificity of CD34 in the outer

membrane of the nerve section showing that the region is the epineurium (Figure 33). I

also observed an influx of both epineurial cells and tactocytes in the nerve bridge positive

for Netrin-1 however the two cell types could not be differentiated in the region.
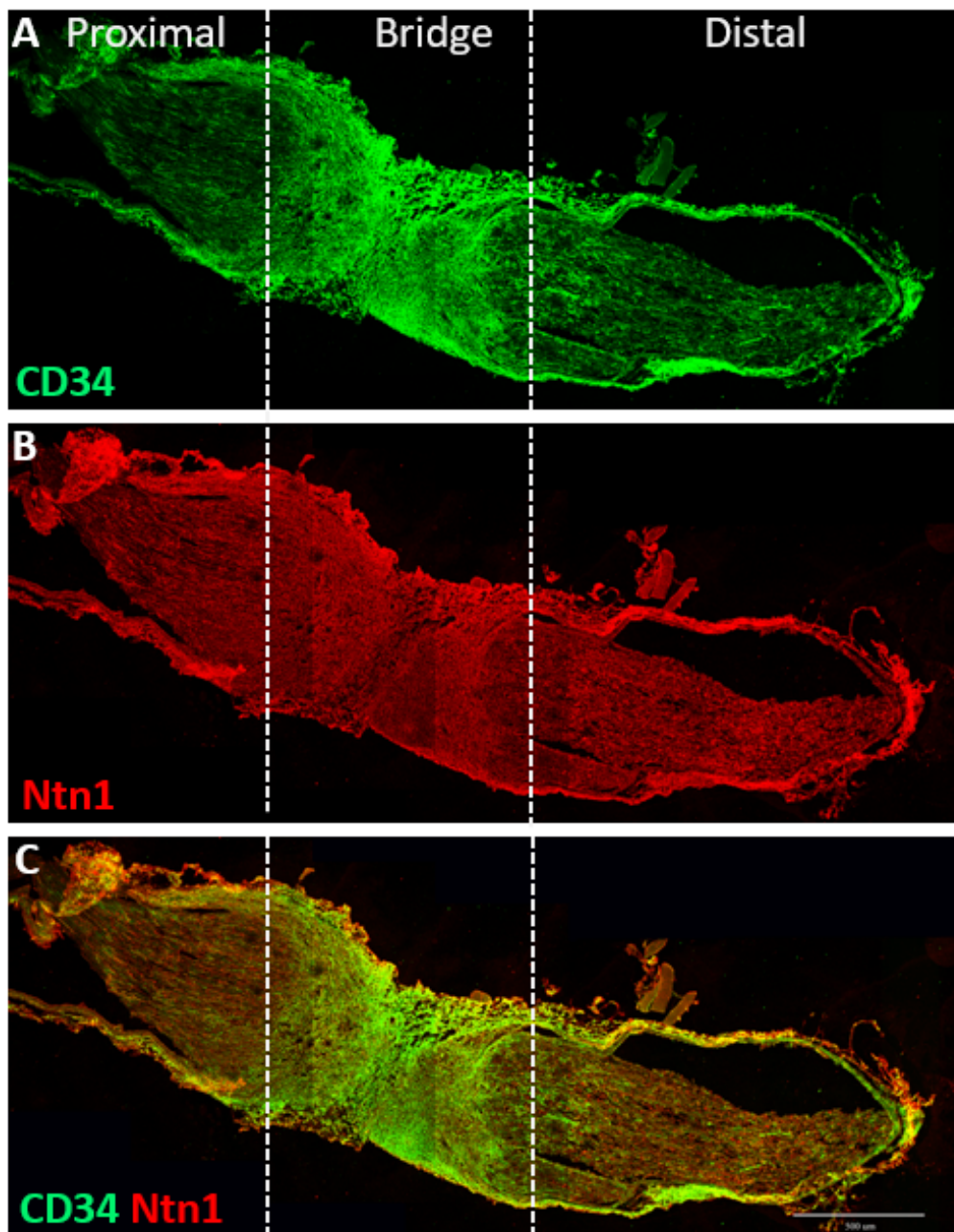
**Figure 33: Netrin-1 is expressed in the epineurial cells and tactocytes 7-days post sciatic nerve transection injury**

(A-C) Longitudinal sections of the sciatic nerve immunolabelled for CD34 (green) and Netrin-1 (Ntn1, red). CD34 labels epineurial fibroblasts and tactocytes. Based on sciatic nerve morphology, the proximal and distal epineurium shows a high expression of CD34 and additionally it is expressed by a mix of both cell types in the nerve bridge. (A-C) Scale bar is 500μm.

In the 14 days post-injury mice, I used transverse sections of the sciatic nerve to look at Netrin-1 expression and observed a similar pattern with Netrin-1 staining clearly observed in the epineurium of the nerve (Figure 34 A-D and I-L). In the proximal stump and distal nerve stump I also observed Netrin-1 expression in the tactocytes (Figure 34 A-D and I-L). Similar to the 7-day injury model, I detected Netrin-1 expression in the bridge with a similar influx of CD34 positive cells, however I could not differentiate between the epineurial fibroblasts and the tactocytes (Figure 34 E-H).
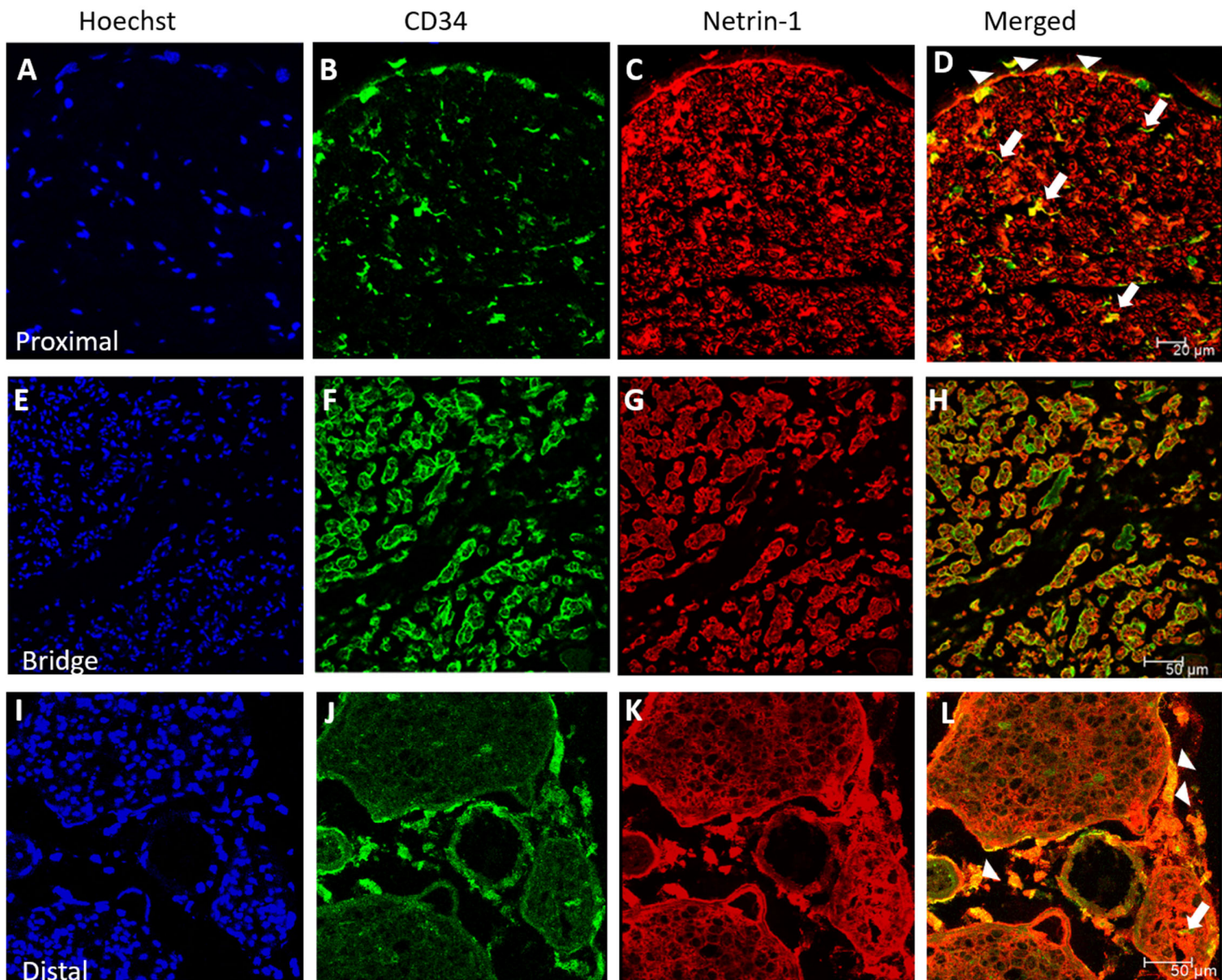
**Figure 34: Netrin-1 expression in epineurial cells and tactocytes 14-days post transection injury**

Transverse sections of the sciatic nerve of C57BL/6 mice 14 days following transection injury. CD34 (green) labels the epineurial fibroblasts and tactocytes in the proximal (A-D), bridge (E-H) and distal (I-L) nerve segments. White arrows and triangles in the proximal and distal nerve depict colabelling of Netrin-1 with tactocytes and epineurial cells, respectively. (E-H) Netrin-1 colocalises with CD34 positive cells in the nerve bridge however the cell types present cannot be differentiated. Hoechst (blue) staining labels the nucleus. (A-D) Scale bar is 20 µm and (E-L) 50µm.

Next, I wanted to study the expression of Netrin-1 in perineurial cells as the single-cell RNA sequencing data for Netrin-1 showed that perineurial cells have the highest expression of Netrin-1 before and after injury (Table 11). I therefore used glucose transporter 1 (Glut-1), an erythrocyte glucose transporter, that is expressed in perineurial cells and endoneurial blood vessels whereas CD34 seems to be immunoreactive to endoneurial fibroblasts/tactocytes and the epineurium (Tserentsoodol *et al.*, 1999; Hirose *et al.*, 2003; Manong *et al.*, 2023). I used C57BL/6 mice to study Netrin-1 expression in the perineurium in intact and injured sciatic nerves. In the uninjured sciatic nerve, Netrin-1 showed robust expression in the perineurium and appeared to colocalise with the endoneurial blood vessels (Figure 35).
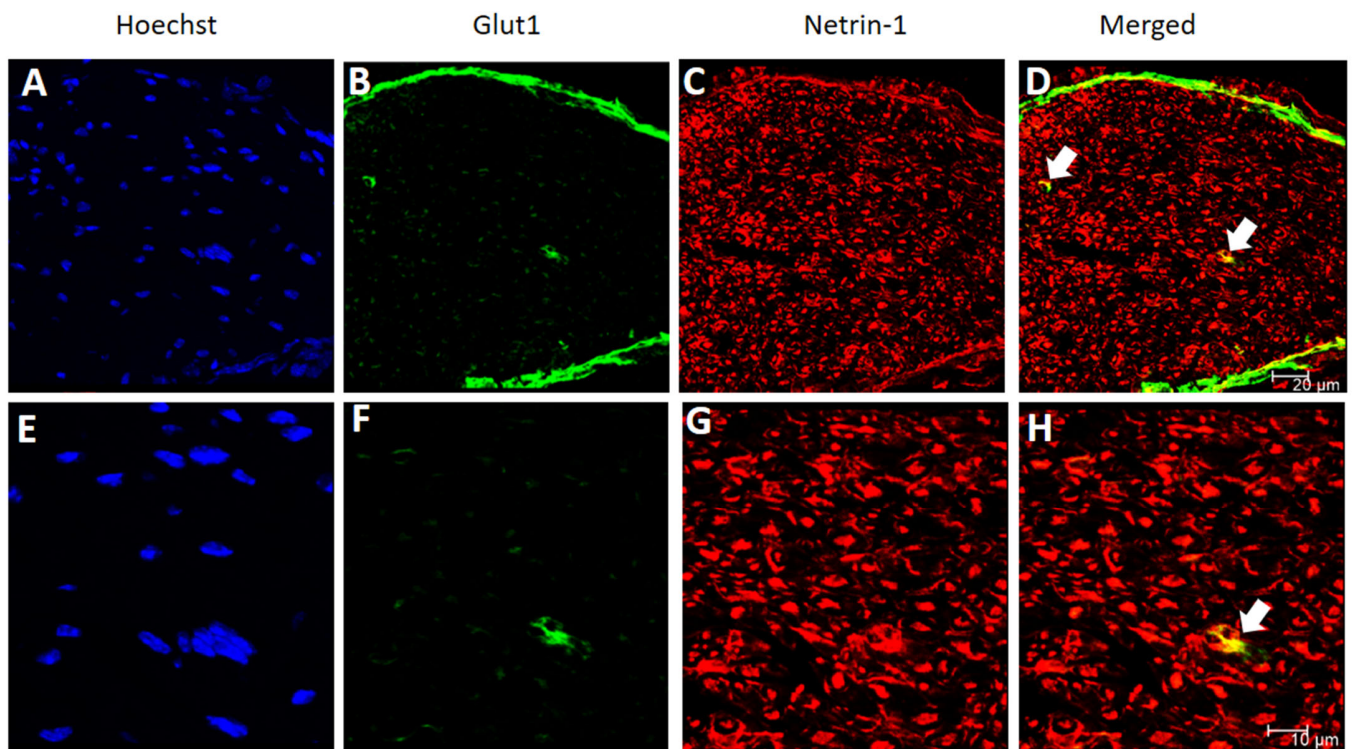
**Figure 35: Netrin-1 is expressed in the perineurium and endoneurial blood vessels of uninjured mouse sciatic nerve.**

(A-H) Transverse sections of uninjured sciatic nerve from C57BL/6 mice were co-stained for Glut-1 (green) and Netrin-1 (red) antibodies. Glut-1 labels the perineurium and endoneurial blood vessels (shown by white arrows) and co-localisation with Netrin-1 (D, H) is observed in both the cell types. Hoechst (blue) labels the nuclei of the cells. (E-H) Magnified image of (A-D). (A-D) Scale bar is 20 μm and (E-H) 10 μm.

Glut-1 staining on the longitudinal sciatic nerve sections 7 days after injury clearly labels the perineurium (Figure 36). Netrin-1 colocalisation was observed in the proximal and distal nerve stump and appears to be more robustly expressed in the bridge of the transected nerve in the area negative for Glut-1 (Figure 36). This indicated that although Netrin-1 expression might be high in the perineurium, it is still expressed by several cell

types such as endoneurial and epineurial fibroblasts, endothelial cells, SCs and regenerating axons as observed in the previous immunohistochemical analysis of injured sciatic nerve.
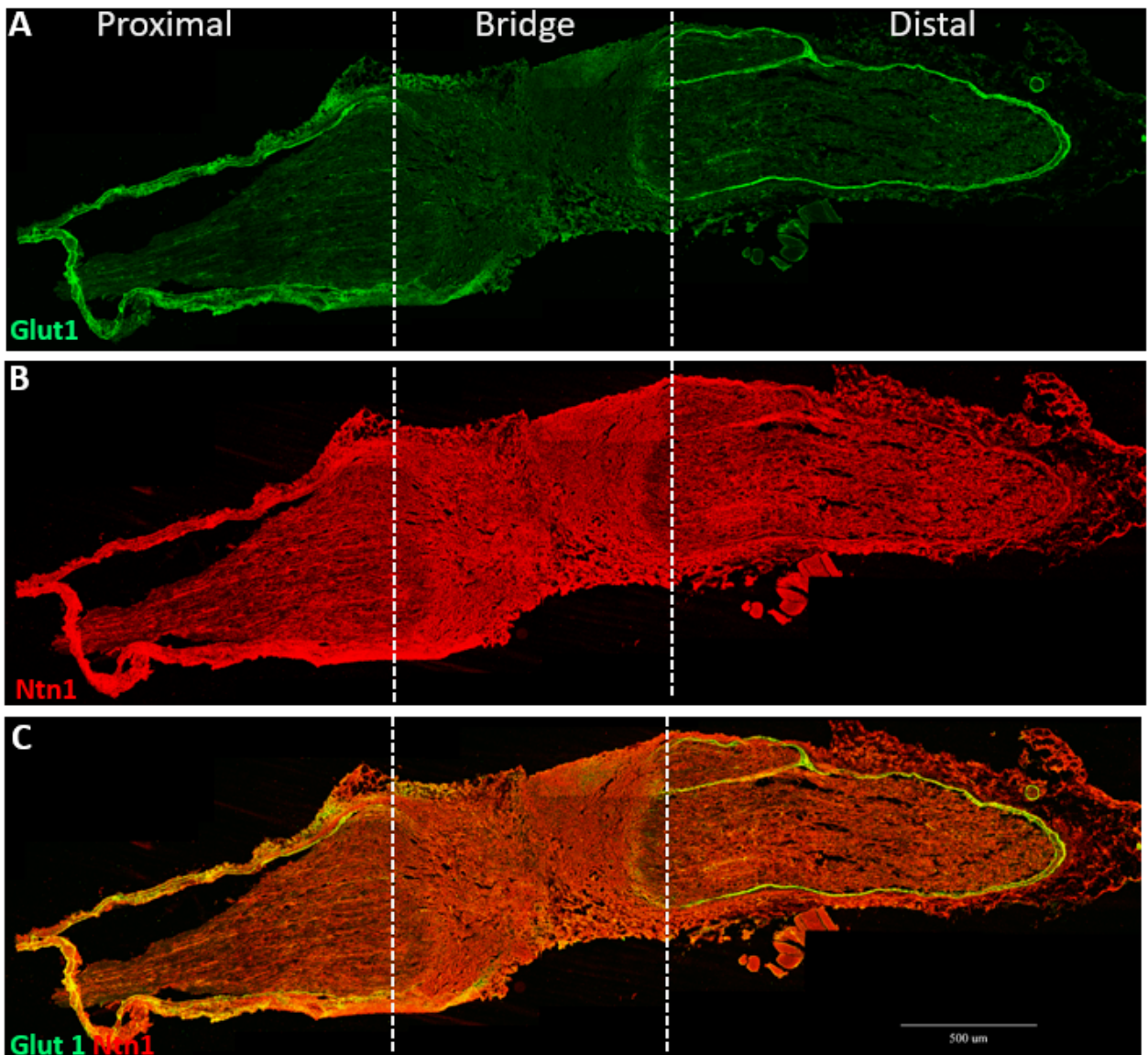


**Figure 36: Netrin-1 is expressed in the perineurium 7 days following transection injury**

(A-C) Glut1 (green) labels the perineurium in longitudinal section of mouse sciatic nerve 7 days post-transection injury. Netrin-1 (Ntn1, red) co-localises with Glut1 in the perineurium however its

expression can be seen in several other cell types. (A-C) Scale bar is 500µm.

Netrin-1 staining in the 14-day time point post mouse sciatic nerve transection revealed similar results, with Netrin-1 showing costaining with Glut-1 in the perineurium of the proximal, bridge and distal nerve segments of the sciatic nerve (Figure 37 A-L). I also observed Netrin-1 in the endoneurial blood vessels along the sciatic nerve (Figure 37 A-D and M-P) This immunohistochemical analysis of Netrin-1 in the perineurium and endoneurial blood vessels correlates with the data from the single-cell sequencing analysis of the sciatic nerve before and after injury.
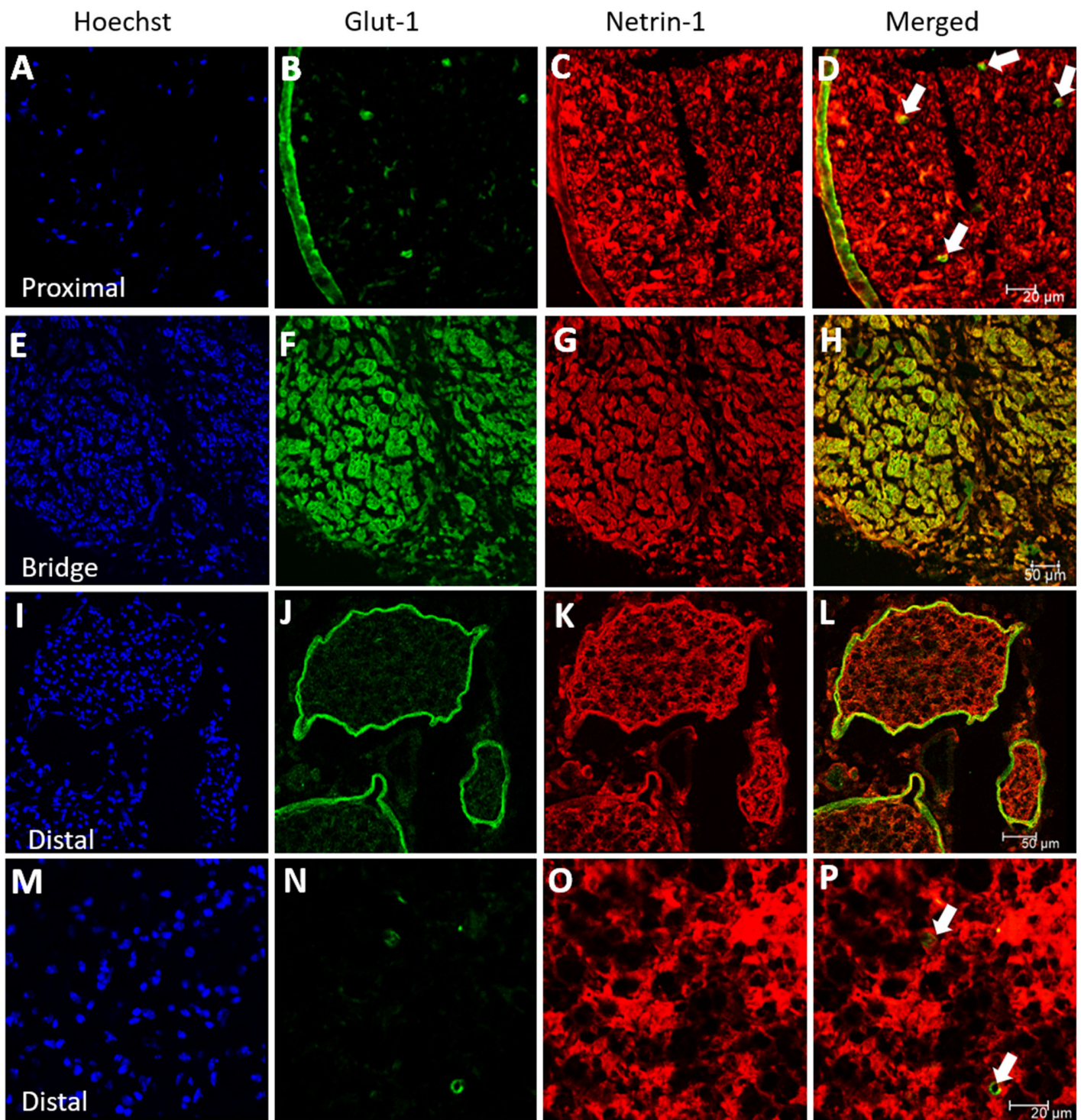
**Figure 37: Netrin-1 expression in the perineurium and endoneurial blood vessels in sciatic nerves 14 days after transection injury**

Netrin-1 (red) double staining with Glut1 (green) in the transverse sections of the proximal (A-D), bridge

(E-H) and the distal (I-P) segment of the sciatic nerve 14-days post-transection injury of C57BL/6 mice. Glut1 labels the perineurium, based on the morphology of the sciatic nerve and the endoneurial blood vessels (shown by white arrows) and Netrin-1 colocalised with Glut1 in all three segments of the sciatic nerve. (M-P) Magnified region with endoneurial blood vessels in the distal nerve segment. Hoechst (blue) labels the nuclei of cells. (A-D and M-P) Scale bar is 20µm, for (E-L) it is 50 µm.

## 3.15 Netrin-1 expression in blood vessels/endothelial cells of the peripheral nerve

Single cell RNA-seq data showed that Netrin-1 was expressed in endothelial cells with the highest average expression observed in lymphatic endothelial cells before injury (Table 11). Following injury, Netrin-1 mRNA expression in endothelial cells was downregulated even on day 9 (Table 11). Therefore, I wanted to study Netrin-1 expression in intact and injured sciatic nerves using a marker only for endothelial cells. For this purpose, I used transverse sections of intact sciatic nerve or 6-day injured sciatic nerves from C57BL/6 mice double stained for Netrin-1 and CD31, a well-known endothelial cell marker.

The staining results confirmed that Netrin-1 is expressed in endothelial cells of the intact mouse sciatic nerve (Figure 38). Moreover, as Netrin-1 is expressed prominently in the perineurium, which can be used to demarcate between endoneurial and epineurial blood vessels, my staining showed Netrin-1 expression in endoneurial blood vessels. The size/diameter of the endoneurial blood vessels suggest that these are mainly small

arteries and capillaries that have been implicated in blood nerve barrier function (Malong *et al.*, 2023).
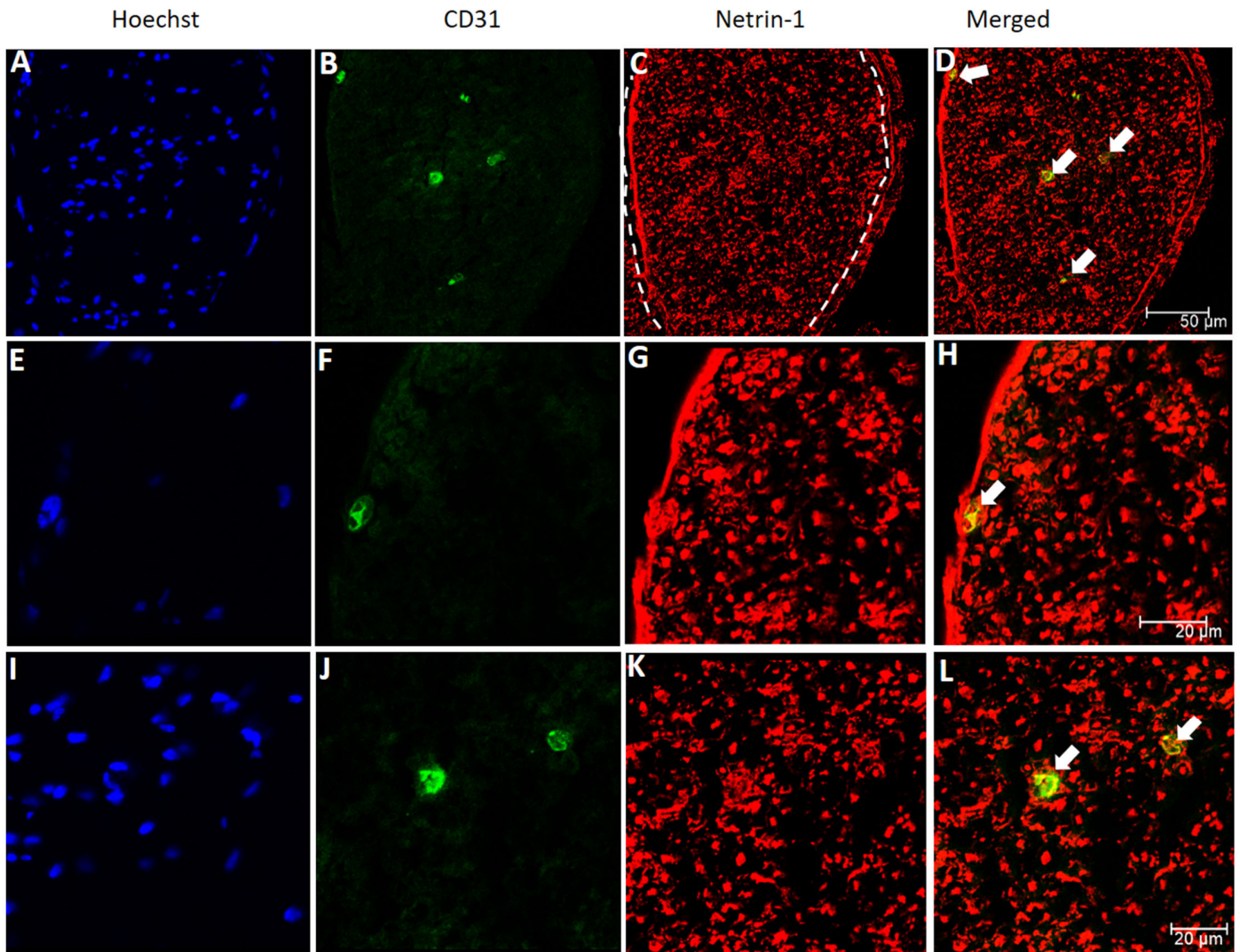


**Figure 38: Netrin-1 expression in endothelial cells in the intact sciatic nerve**

(A-D) Immunofluorescent images of transverse sections of the uninjured sciatic nerve dissected from C57BL/6 mice. CD31 (green) labels endothelial cells. Netrin-1 (red) staining colocalises with CD31 in the uninjured sciatic nerve (shown by white arrows) depicting Netrin-1 expression in endoneurial blood vessels as demarcated by the perineurium (C; depicted by white dashes). (E-L) Magnified image of (A-D) showing Netrin-1 expression in several CD31 positive cells. Hoechst (blue) staining labels the nucleus. CD31 (A-D) Scale bar is 50 µm and for (E-I) its 20µm.

Next, I transected the sciatic nerve in C57BL/6 mice to reveal Netrin-1 expressing cells in the nerve bridge and in the distal nerve stump at day 6 post-transection injury, a timepoint at which the sciatic nerve is known to be fully vascularised in mice (Cattin *et al*., 2015). Staining for CD31 on transverse sections of nerve bridge tissue revealed that several blood vessels in the nerve bridge expressed Netrin-1 (Figure 39 A-H). Blood vessels in the distal nerve stump continue to express Netrin-1 (Figure 39 I-P). Moreover, I could clearly see Netrin-1 expression in the small sized endoneurial and in the heterogenous epineurial blood vessels (Figure 39 I-P). The epineurial blood vessels consist of mainly large diameter vessels such as venules and arterioles (Malong *et al*., 2023). Thus, my immunohistochemical analysis revealed that Netrin-1 is expressed in endothelial cells/blood vessels of intact and injured mouse sciatic nerve.
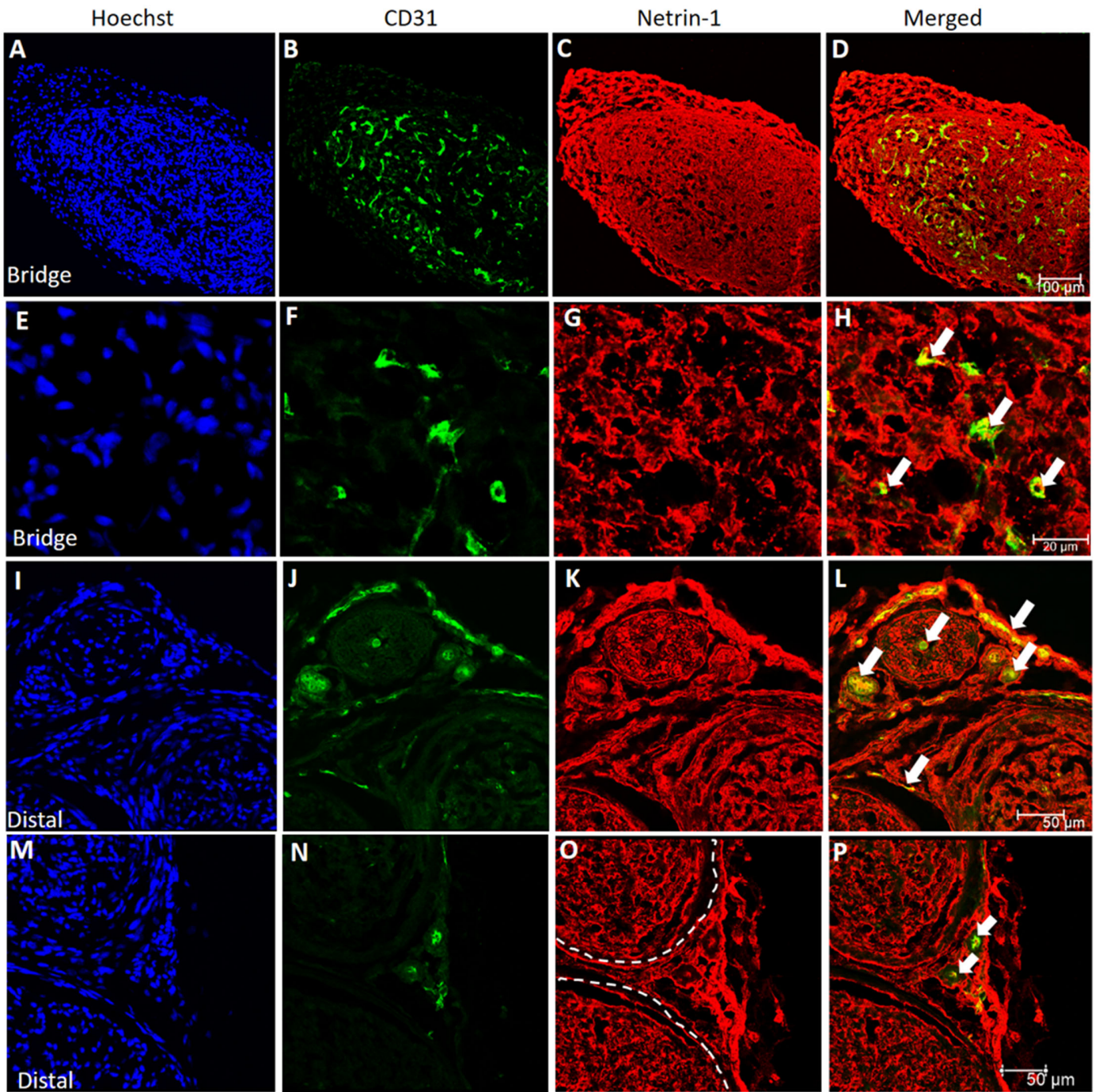
**Figure 39: Netrin-1 expression in blood vessels of mouse sciatic nerve 6-days after transection injury**

Double staining of Netrin-1 and CD31 endothelial cell marker on transverse section of C57BL/6 mice 6-days after a transection injury. (A-H) Blood vessels and vascularisation of the nerve bridge can be

observed by CD31 staining. Netrin-1 is expressed in CD31 positive cells as depicted by white arrows. (E-H) Magnified image of (A-D). (I-) Netrin-1 expression in CD31 positive cells in the distal sciatic nerve shown by white arrows and depicting expression in inner endoneurial blood vessels and epineurial blood vessels as demarcated by the perineurium (shown in white dashes). (M-P) Image specifically depicts Netrin-1 expression in epineurial blood vessels. Hoechst (blue) labels cell nuclei. Scale bar for (A-D) is 100 µm, (E-H) is 20 µm and (I-P) is 50 µm.

## 3.16 Failure to generate a global knockout of Netrin-1 in mice

My data for Netrin-1 including analysis of single-cell RNA sequencing data and immunohistochemical analysis of the mouse sciatic nerve before and after injury revealed that several cells express Netrin-1 and not just SCs. Therefore, I wanted to generate a global knockout of Netrin-1 in mice. The objective was to perform the experiments carried out on SC-specific Netrin-1 knockout mice such as axon guidance and outgrowth; impact on SC migration, proliferation and remyelination. Additionally, as I observed Netrin-1 expression in endothelial cells and in the membranes of the sciatic nerve such as the perineurium, I wanted to study angiogenesis, effects upon regeneration of the perineurium and the blood nerve barrier function after global loss of Netrin-1.

As mentioned previously, knocking out Netrin-1 in mouse embryo causes death of the pups within 24hrs of birth (Serafini *et al.*, 1996). Therefore I employed the use of ROSA-26-Cre/ERT2 (R26-CreERT2) mice, wherein Cre-mediated deletion of a floxed gene is induced by the presence of Tamoxifen and the expression of CreER is regulated by the

endogenous mouse Gt(ROSA)26Sor promoter (Hameyer *et al*., 2007). In these mice, the ligand-binding domain of a mutated estrogen receptor (ERT2) is fused to Cre. The ligand-binding domain does not bind to its natural ligand at physiological concentrations but will bind to the non-steroidal estrogen analog – 4-hydroxytamoxifen (Tamoxifen). This fusion product (CreERT2) is restricted to the cytoplasm of the cell and its translocation to the nucleus, to mediate recombination, is only feasible in the presence of Tamoxifen. Therefore, in my model, I bred Ntn1 $^{loxP/loxP}$ mice with the transgenic R26-CreERT2$^+$ mice to delete Netrin-1 globally in adult mice on delivery of Tamoxifen either via gavaging or intraperitoneal injections. I had successfully generated mice with a deletion of Deleted in colorectal carcinoma (DCC) in adult mice (P35) after gavaging with Tamoxifen using the same R26-CreERT2$^+$ mice (Refer to Chapter 4.2)

Briefly, Ntn1 $^{loxP/loxP}$ mice were crossed with R26-CreERT2$^+$ mice and their offspring bred with Ntn1 $^{loxP/loxP}$ mice to produce R26-CreERT2$^+$ Ntn1$^{loxP/loxP}$ mice (Figure 40 A). Five- to seven week-old mice were then intraperitoneally injected with Tamoxifen made up in corn oil at a concentration of 75 mg Tamoxifen/kg per day for five consecutive days. To confirm the global knockout of Netrin-1, mice were sacrificed four weeks after the last injection of Tamoxifen.  L4-L5 DRGs from control (Ntn1 $^{loxP/loxP}$) and R26-CreERT2$^+$ Ntn1$^{loxP/loxP}$ tamoxifen-treated mice were dissected, fixed in 4% PFA and cryosected transversally. The sections of DRGs were immunolabelled for Netrin-1 and NeuN, to label

axons (Figure 40 B-I). However, surprisingly, I observed no change in Netrin-1 expression when comparing both groups.
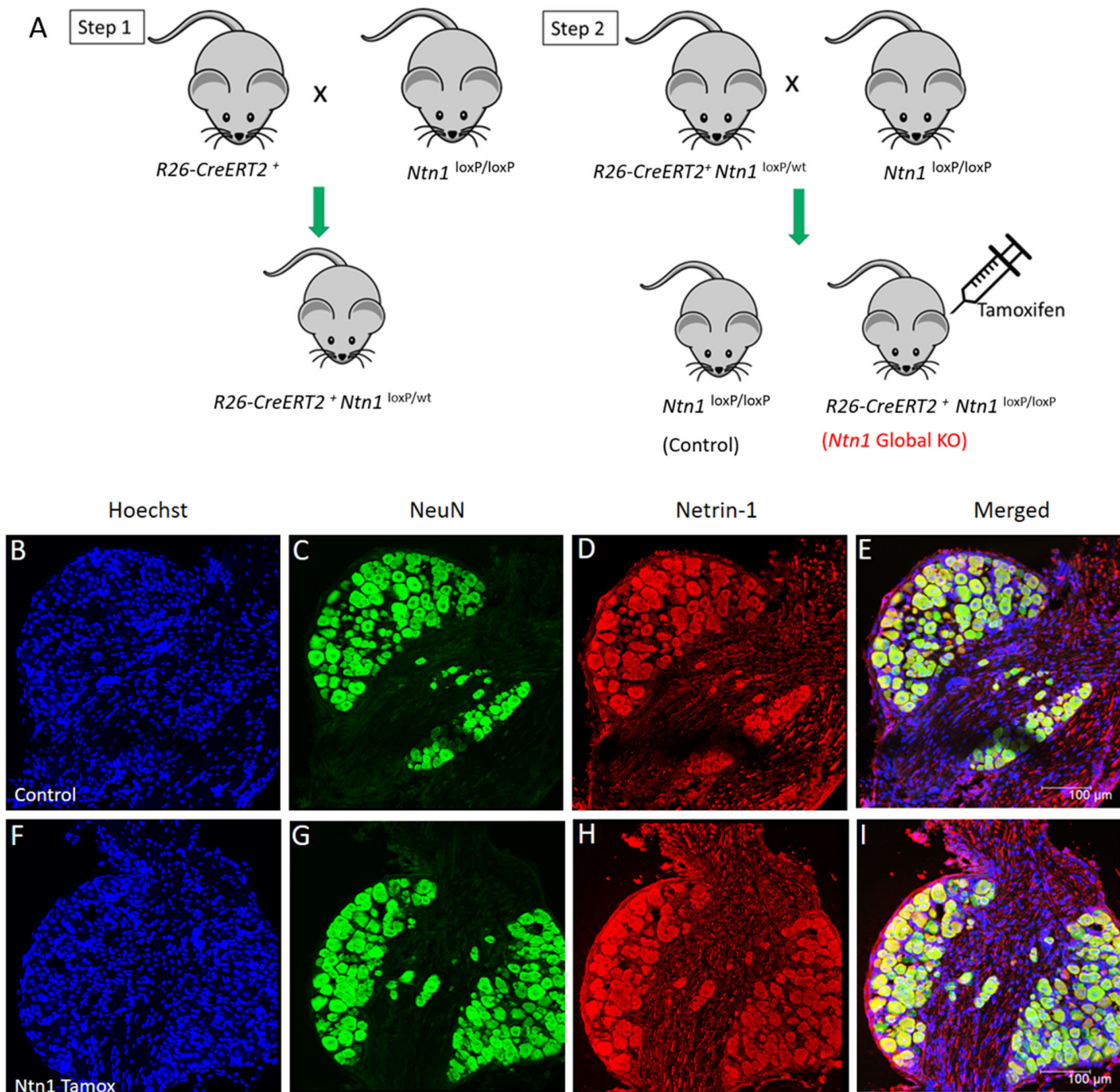


**Figure 40: Attempt to generate Netrin-1 global knockout in mice**

(A) Breeding steps carried out to generate Netrin-1 global knockout mice (Ntn1 global KO). In step 1,

homozygous mouse with loxP sites flanking exon 3 of Netrin-1 (Ntn1$^{loxP/loxP}$) was bred with R26-CreERT2$^+$ mouse carrying the Cre transgene regulated by the constitutively and ubiquitously expressed Gt(ROSA)26Sor promoter. The Cre protein is fused to a mutated estrogen receptor (ERT2) and is restricted to the cytoplasm of the cell. Its translocation to the nucleus, to mediate recombination and target gene deletion, is only feasible in the presence of Tamoxifen. The progeny obtained from step 1 (R26-CreERT2$^+$ Ntn1$^{loxP/wt}$) was back-crossed with Ntn1 $^{loxP/loxP}$ mice to generate mice that were homozygous for Netrin-1 loxP sites and had the R26-CreERT2 transgene (R26-CreERT2 $^+$ Ntn1 $^{loxP/loxP}$). These mice were intraperitoneally injected with Tamoxifen, 5-7 weeks after the birth of the mouse pups to facilitate Cre mediated recombination and deletion of Netrin-1. Mice without the Cre transgene were used as controls. (B-I) Immunostaining of dorsal root ganglia (DRGs) from control and unsuccessful Netrin-1 global knockout mice (Ntn1 Tamox) four weeks after the last dose of Tamoxifen injection. NeuN (green) labels the cell bodies of neurons in DRGs colabelled with Netrin-1 (red). Hoechst (blue) labels the nuclei. No change in Netrin-1 expression was observed comparing the two groups. Scale bar is 100μm.

As I did not observe recombination in the Tamoxifen injected Netrin-1 mice (R26-CreERT2 $^+$ Ntn1 $^{loxP/loxP}$) on the first attempt, I repeated the Tamoxifen treatment several times. Once by increasing the wait time after the last Tamoxifen injection; once by increasing the number of days of Tamoxifen injections from 5 to 7 and; once by changing the technique of Tamoxifen delivery from injection to gavaging. I also performed western blots on the intact sciatic nerve to probe for Netrin-1 as well as the presence of Cre recombinase after Tamoxifen delivery (Figure 41 A-C). I observed Netrin-1 expression comparable to the control. Although Cre recombinase was only present in mice with the

R26-CreERT2^{+} transgene, it was not indicative of the activity of the enzyme (Figure 41 A-C).
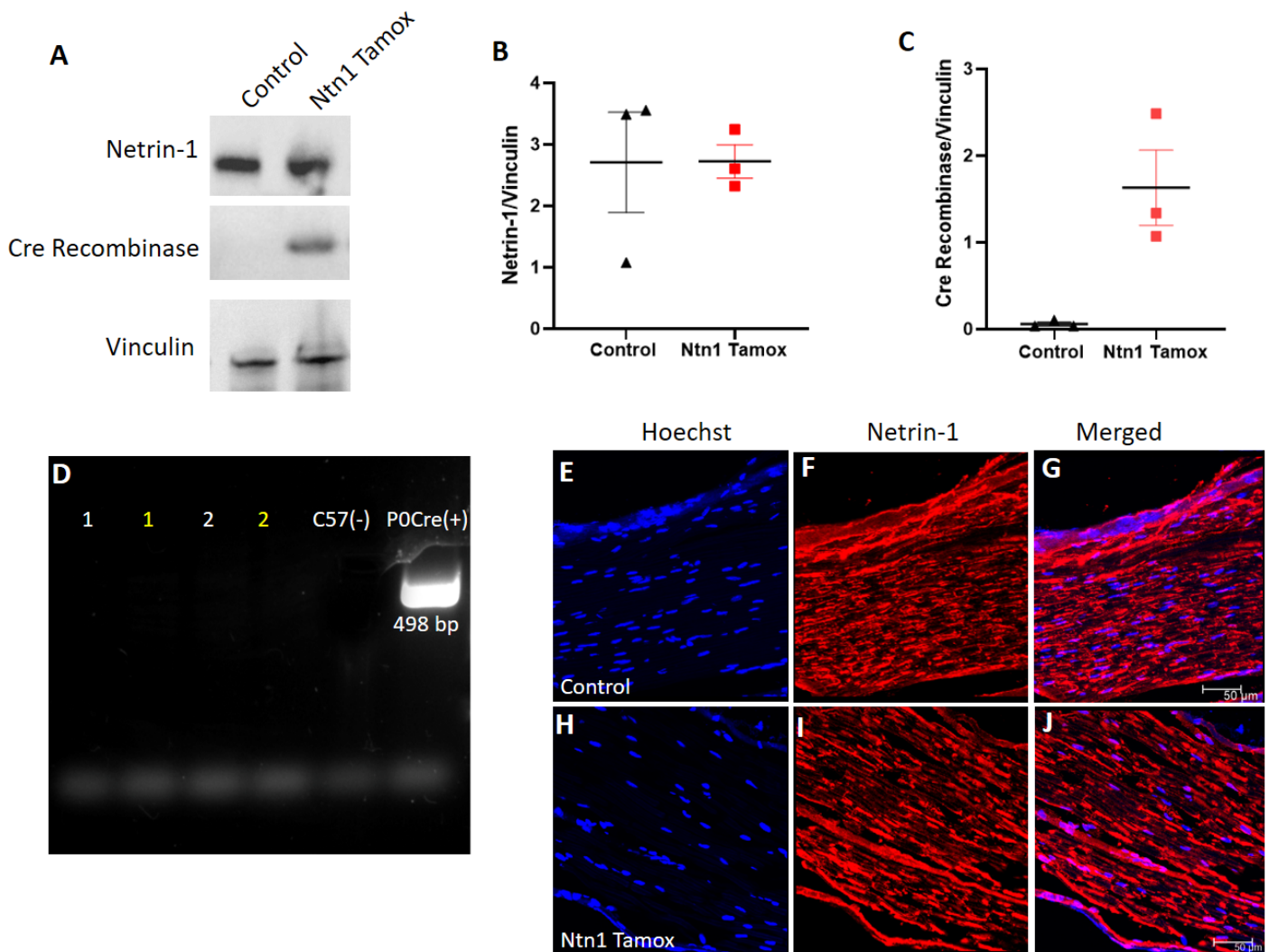


**Figure 41: Gavaging of Tamoxifen in R26-CreERT2^{+} Ntn1[loxP/loxP] for five consecutive days did not induce Cre mediated recombination.**

(A) Western blots probing for Netrin-1 and Cre Recombinase on intact sciatic nerves obtained from Tamoxifen treated control (Ntn1 [loxP/loxP]) and R26-CreERT2^{+} Ntn1[loxP/loxP] mice (Ntn1 Tamox) five days after gavaging the mice with Tamoxifen. Vinculin was used as a loading control. (B) Netrin-1 expression relative to vinculin and (C) Cre recombinase expression relative to vinculin for control and Ntn1 Tamox mice. (A-C) Netrin-1 expression in Ntn1 Tamox mice was relative to control however Cre recombinase

was only present in the Ntn1 Tamox mice after Tamoxifen treatment. (D) PCR to confirm excision of exon-3 of Netrin-1 before (samples in white) and two weeks after (samples in yellow) Tamoxifen treatment. DNA from C57BL/6 mice (C57) was used as negative controls and DNA from P0-Cre[+] Ntn1[loxP/loxP] was used as positive control. The expected band size after excision is 498 bp. (E-J) Intact transverse sections of sciatic nerves dissected out four weeks after last day of Tamoxifen treatment and stained for Netrin-1 (red). Confocal images showed Netrin-1 expression in control (E-G) and Ntn1 Tamox (H-J) mice indicating that the knockout was not successful. Hoechst (blue) labels nuclei of cells. Scale bar is 50 μm.

I also performed PCR on DNA extracted from the Tamoxifen injected mice before and after injections (Figure 41 D). However, my results did not show the expected 498bp band after deletion of exon 3 of Netrin-1 (Figure 41 D), as observed in the P0-Cre[+] Ntn1[loxP/loxP] mice (Figure 14 D). Finally, immunohistochemical analysis of the uninjured sciatic nerve showed no difference in Netrin-1 expression between the control and Tamoxifen treated R26-CreERT2^{+} Ntn1[loxP/loxP] mice (Figure 41 E-J).  Therefore, as I was unable to determine the cause of lack of recombination in this mouse model, I could not perform any experiments to confirm the role of Netrin-1 in peripheral nerve repair in Netrin-1 global null mice.

## 3.17 Discussion and conclusions

In this study, I looked to study the role of SC-derived Netrin-1 in peripheral nerve regeneration (PNR), with the main objective of studying effect of Netrin-1 global ablation, on PNR. The concept that Netrin-1 was involved in PNR, came from several

studies that showed Netrin-1 upregulation following PNI. Madison *et al.* (2000) reported low levels of Netrin-1 mRNA expression in uninjured rat sciatic nerve, with no change in expression two weeks after a crush injury. However, 2-weeks following sciatic nerve transection and repair, by quantitative competitive PCR of the distal sciatic nerve, they reported a 40-fold increase in Netrin-1 mRNA (Madison *et al.*, 2000).

In agreement with this report, Jaminet *et al.* (2013), by RT-PCR reported a 1.9-fold and a 2.4-fold upregulation of Netrin-1 mRNA 2- and 3-weeks, respectively, in the distal nerve segment after mouse median nerve transection and repair. Their western blot data also showed that Netrin-1 was upregulated at day 14 post-injury in the distal nerve segment followed by a massive drop in protein expression by day 21 (Jaminet *et al.,* 2013). The authors inferred that the sudden peak in protein expression coincided with the timepoint at which the regenerating axons are elongating in the distal nerve segment surrounded by SCs expressing Netrin-1. Chen *et al.* (2021b) in a chronic constriction injury model of the sciatic nerves in wild-type Wistar rats also reported a 2.6-fold increase in Netrin-1 mRNA by RT-qPCR of sciatic nerve, starting 6 hrs after injury with the highest upregulation observed 3-weeks post-injury. Albeit the immunohistochemical analysis of the sciatic nerve showed a 58% drop in protein expression as compared to control, 7-days after injury.

Contradictory to this, my research group showed Netrin-1 mRNA downregulation starting from 4 days after injury up until 14 days (the last studied timepoint) in the proximal, bridge and distal nerve segments, following sciatic nerve transection in mice. This data was also validated by three microarray datasets for the distal (two datasets for crush and one for transection), and one for the proximal sciatic nerve (transection injury) confirming the downregulation of Netrin-1 in injured nerves. Additionally, my analysis of high throughput RNA sequencing data of Netrin-1 expression in SCs derived from injured mouse sciatic nerves showed downregulation of Netrin-1 in the SCs of the nerve bridge but surprisingly not in the distal sciatic nerve. This meant that possibly the downregulation of Netrin-1 mRNA after injury in the distal sciatic nerve was not contributed to by SCs.

The transcriptomic profiling of Netrin-1 revealed that Netrin-1 is downregulated in perineurial cells at day 3 following transection injury in the distal sciatic nerve and upregulated to normal uninjured levels by day 9. However, Netrin-1 was also downregulated in endothelial cells persisting even on day 9 in the distal sciatic nerve. This suggested that endothelial cells and perineurial cells are the main source of the initial drastic downregulation of Netrin-1 following injury in the distal sciatic nerve. In later stages of peripheral nerve regeneration, perineurial cells quickly upregulate Netrin-1 to normal levels by day 9 but endothelial cells do not, possibly explaining why even at

day 14 Netrin-1 mRNA is not upregulated to the expression levels that of the uninjured sciatic nerve.

However, as mentioned previously the datasets that were reanalysed and presented in this thesis, obtained from high throughput RNA sequencing (Clements *et al.,* 2017), and single cell sequencing (Gerber *et al.,* 2021; Carr et al., 2019; Toma *et al.,* 2020) have certain drawbacks. Namely, the element of artefactual changes in gene expression that is induced by the process of single-cell dissociation. To obtain single-cell suspensions the tissue is usually incubated at 37° C with enzymes such as trypsin, a step that has been suggested to induce alterations in transcription (Adam *et al.*, 2017; Marsh *et al.,* 2022). Another limitation is the possibility of low-quality data obtained from damaged or dead cells which hamper the downstream analysis and can result in misinterpretation of data (Ilicic *et al.*, 2016).

During embryonic development, Netrin-1 is known to regulate angiogenesis and is expressed in endothelial cells (Larrivée *et al.*, 2007). Netrin-1 stimulated the production of endothelial nitric oxide in a dose-dependent manner in cultures of mature aortic endothelial cells and this was additionally shown to be DCC dependent (Nguyen and Cai, 2006). The study also showed that Netrin-1 was responsible for promoting proliferation and migration of endothelial cells in vitro. In a previous study however, Lu *et al.* (2004) showed that Netrin-1 was an inhibitor of endothelial cell migration, a role mediated by

its interaction with UNC5B receptor. Their studies in vitro, via transwell migration and wound-healing assay showed that Netrin-1 reduced the migration of UNC5B-expressing primary human umbilical artery endothelial cells (HUAECs). In vivo, by intraocular injection of 1 µg/ml of Netrin-1 into postnatal day 5 mice, they observed a reduction in filopodial extension particularly at the tip cell (Lu *et al*., 2004). However, it is to be noted that Netrin-1 physiological concentration varies between 50 - 150 ng/ml (Castets and Mehlen, 2010; Serafini *et al*., 1994), and 1 µg/ml Netrin-1 is much higher than the physiological range. In a recent publication, vascularisation of sciatic nerve was significantly reduced in Netrin-1 deficient mice at embryonic day 17.5 as compared to control thus suggesting a role in blood vessel formation in the developing nerve (Taïb *et al.,* 2022).

My data showed expression of Netrin-1 in blood vessels of injured and intact sciatic nerves and no role of Netrin-1 has been described in angiogenesis following a peripheral nerve injury (PNI). Cattin *et al.* (2015) reported an influx of blood vessels into the nerve bridge of transected rat sciatic nerve at day 3 following injury also suggesting a role of blood vessels in directing SC migration. Considering the single-cell RNA-seq data, and the downregulation of Netrin-1 in day-3 transected sciatic nerves, it is possible that Netrin-1 inhibits the invasion and regeneration of the vasculature following PNI. Therefore, it can be suggested that at later stages of PNR, endothelial cells again upregulate Netrin-1 once the vasculature is established.

The perineurium is thought to be derived from fibroblasts of the mesodermal origin unlike the SCs that are derived from neural crest cells (Bunge *et al.,* 1989; Joseph *et al.*, 2004; Ma *et al.,* 2018). The perineurium surrounds nerve fascicles and protects the endoneurium against mechanical forces and is an important component of the blood nerve barrier (BNB) (Weerasuriya and Mizisin, 2011; Malong *et al.*, 2023). However, unlike the endoneurial microvessels, which also make up the BNB, the perineurium is a more restrictive diffusion barrier (Weerasuriya and Mizisin, 2011). The role of perineurial cells in PNR is yet to be fully elucidated. However, it is known that the BNB is damaged at the injury site after a transection injury, but it also becomes 'leaky', distal to the injury site allowing immune cells to infiltrate the peripheral nerve (Gray *et al*., 2007; Weerasuriya and Mizisin, 2011; Malong *et al*., 2023). Using Evans blue dye tracer in rats following crush injury, Gray *et al*. (2007) showed that the BNB integrity is compromised by day 7 post-injury and persisted till day 28. There is no known function of Netrin-1 in maintaining the BNB, however its high expression by perineurial cells in intact nerves and endoneurial blood vessels (as shown in this thesis), can be suggestive of maintaining the BNB in intact peripheral nerves. Whereas its downregulation on day 3 in both perineurial and endothelial cells/ endoneurial blood vessels and consequent upregulation on day 9 by perineurial cells, as shown by my transcriptomic analysis, indicate a possible involvement of Netrin-1 in the regulation of BNB, distal to the injury site.

Previously, Schröder *et al.* (1993) demonstrated in transection studies of rat sciatic nerve, using a silicone tube inserted between the proximal and distal nerve stump, that perineurial cells were the first cells to invade the nerve bridge post-injury. The authors also stated that the perineurium acts as a guiding structure for other cells during regeneration (Schröder *et al.*, 1993). Parrinello *et al.* (2010) in elegant experiments conducted in vitro and in vivo on rats and mice, after a transection injury, showed that fibroblasts were responsible for clustering of SCs in the nerve bridge. This clustering was shown to be mediated by receptor tyrosine kinase Ephrin B2 (EphB2) on SCs interacting with ephrin-B on fibroblasts leading to sorting of SCs. This sorting was essential for SC migration out of the proximal and distal nerve stumps into the nerve bridge. Moreover, in rats upon inhibiting EphB2 signalling using inhibitory EphB2-Fc fusion proteins and in EphB2 null mice, the authors observed that in the proximal nerve stumps 4 days after partial transection, axon regrowth was less organised and there were more fragmented axons, in the rat and mouse models, respectively. Although, the authors did not specify the identity of the fibroblasts (endoneurial or epineurial), my data showed that Netrin-1 was expressed by all fibroblasts in the nerve bridge. It is possible that Netrin-1, which like Eph/Ephrins is an axon guidance molecule, whose expression by fibroblasts and perineurial cells could potentially be involved in mediating SC migration and axonal regeneration by interacting with any one of its several receptors expressed on SCs or directly with receptors expressed on the axons.

Madison *et al.* (2000) showed Netrin-1 expression in several SCs of the distal sciatic nerve of rats 2 weeks after transection injury, which was not observed in uninjured or crushed nerves at the same timepoint. The authors further stated that the increase in Netrin-1 is not attributed to proliferation of SCs that are expressing Netrin-1 following transection injury because such an increase would have been observed after a crush injury as well (Madison *et al.*, 2000). My analysis of high throughput RNA sequencing dataset derived from purified SCs of the bridge and distal segment of the sciatic nerve 6 days after mouse sciatic nerve transection injury showed Netrin-1 expression in intact sciatic nerve as well as downregulation in the nerve bridge. Immunohistochemical analysis of the sciatic nerve carried out by my research group showed Netrin-1 expression in mainly non-myelinating SCs and in cultured rat SCs by RT-PCR for Netrin-1. Previously Lv *et al*. (2015) also demonstrated Netrin-1 expression in immortalised rat SCs by qRT-PCR. However, on re-analysing sciatic nerve tissue with a different antibody (R&D systems; Cat no: MAB1109), I was surprised to observe Netrin-1 expression in several other cell types including robust expression in axons as well as in non-myelinating SCs. However, the single cell RNA-seq data for Netrin-1 in uninjured and the distal nerve stump of mouse sciatic nerve contradicts the previous data. The analysis showed low expression of Netrin-1 mRNA only in non-myelinating SCs before injury with a marginal increase at day 3 and day 9 in the distal nerve after injury. One explanation is that possibly Netrin-1

translation in SCs is high resulting in a higher copy number of Netrin-1 protein molecules from low levels of mRNA.

Previously Webber *et al.* (2011) reported no change in Netrin-1 mRNA expression in the dorsal root ganglia (DRGs), the location of cell bodies of sensory neurons, following sciatic nerve transection injury in rats. My analysis of a microarray dataset for the expression of Netrin-1 mRNA in the DRG's after sciatic nerve transection injury in rats also showed no change in Netrin-1 expression. Moreover, I showed expression of Netrin-1 in the DRGs and the ventral horn of the spinal cord (location of cell bodies of motor neurons) both before and after injury re-affirming the expression of Netrin-1 observed in axons. This new evidence was only gathered once I had established and had begun experiments on the SC-specific Netrin-1 knockout mice. Contradictory evidence for Netrin-1 expression is probably due to lack of reliable commercially available Netrin-1 antibodies that are compatible with immunohistochemical staining of the mouse tissue.

Therefore, I had aimed to complete the work on describing the role of SC-derived Netrin-1 with future experiments planned for Netrin-1 global knockout mice. Previous studies on PNR had worked with either heterozygous Netrin-1 knockdown mice (Jaminet *et al*., 2013) or by adding recombinant Netrin-1 to neuronal cultures or injecting Netrin-1 in sciatic nerves of rats (Park *et al.*, 2007; Webber *et al.*, 2011) . This was the case due to the embryonic defects and lethality in Netrin-1 global knockout mouse pups (Serafini *et*

*al*., 1996). Therefore, in this study by using conditional mutants regulated by the Cre-lox system I generated Netrin-1 knockout in SCs however was unable to generate global knockout of Netrin-1.

Netrin-1 is capable of mediating both attractive and repulsive signalling which is dependent on its interaction with its receptors. Netrin-1, if bound to an attractive DCC receptor on both binding sites, mediates attractive cues during axon guidance whereas presence of UNC5 receptor at only one binding site is sufficient for switching the attractive cue to a repulsive one when both DCC and UNC5 are present (Hong *et al*., 1999; Finci *et al*., 2014; Dun and Parkinson, 2017). Moreover, this bi-functionality of Netrin-1 has been shown to be dose dependant, as previously mentioned (Serafini *et al.,* 1994; Larrivée *et al*., 2007; Tu *et al*., 2015). Park *et al*. (2007) observed Netrin-1 mediated inhibition of neurite outgrowth of sensory neurons at a concentration of 500ng/mL in DRG explants and dissociated DRG cultures, therefore, suggesting Netrin-1 as an inhibitor of axon regeneration of adult sensory neurons. They also suggested that this inhibition was attributed to the UNC5 repulsive receptors. Contradictory to this, Webber *et al.* (2011), performed sciatic nerve transection injury in rats and injected 100μg/mL of exogenous Netrin-1 for 7 days using a T-chamber with a microinjection port. They did not find any comparable difference to the saline control in terms of SC migration or axon regrowth past the injury site. In pre-conditionally lesioned DRG cultures, addition of recombinant Netrin-1 at either low (5 ng/mL) or high concentrations (200 ng/mL) did not

alter the outgrowth of DRG neurites (Webber *et al.*, 2011). This indicated that Netrin-1 might not be important for axon outgrowth however as described above, normal physiological concentrations of Netrin-1 are much lower, and these studies did not take into account the dose-dependent bi-functionality of Netrin-1.

The contradictory evidence available in literature for role of Netrin-1 in axon guidance following PNI, led me to investigate the SC-derived Netrin-1 in axon outgrowth following a crush injury and the more traumatic transection injury using SC-specific Netrin-1 knockout mice. Following crush injury, functional recovery was achieved at the same rate as the control mice. However, in Netrin-1 heterozygous mice (50% reduction in mRNA and protein expression), Jaminet *et al.* (2013) showed a significantly slower functional recovery in grasping tests after median nerve transection and repair, and the mice did not regain their pre-injury grasping strength even 50 days following injury. A transection injury usually results in a few aberrant axon trajectories not observed after crush injuries where the basal lamina is still intact (Amado *et al.*, 2008; Luís *et al.*, 2008). However, in the SC-specific Netrin-1 knockout mice, I observed several axons displaying incorrect trajectories in the nerve bridge in comparison to the few axons observed in the control mice. Nevertheless, there was no significant difference in the number of axons re-innervating the tibial nerve. It is possible that although SC deletion of Netrin-1 causes an initial disruption in axon pathfinding, expression of Netrin-1 by other cells including axons themselves in the absence of any axon growth, compensates for such loss, thus

guiding the axons along their intended path and further preventing straying of rogue axons.

For a successful peripheral repair, changes in the phenotype of SCs is essential which includes transition to a repair SC phenotype, proliferation, migration and redifferentiation of SCs into myelinating and non-myelinating cells (Chen *et al.*, 2007). Treating RT4 schwannoma cells with exogenous Netrin-1 (50 ng/ml), induced proliferation and this was inhibited by a knockdown of UNC5B implying that UNC5B is the receptor involved in promoting SC proliferation (Lee *et al.*, 2007). My in vivo data showed no difference in SC proliferation of the distal sciatic nerve, 7 days after transection injury in the SC-specific Netrin-1 knockout mice. This data was in agreement with that of Lv *et al.* (2015), wherein in RSC96 cells (an immortalised rat SC line), recombinant Netrin-1 (varying doses from 0 to 500 ng/ml) produced no effect on proliferation of the cells. However, in the same study, 100 ng/ml of Netrin-1 increased SC migration of the RSC96 cells but not other doses, again demonstrating dose-dependent activity of Netrin-1. They also suggested UNC5B as the main receptor involved with Netrin-1 in migration of RSC96 cells as 100 ng/ml of Netrin-1 also increased UNC5B protein expression, explained by the authors as a way to adapt to a higher Netrin-1 concentration (Lv *et al.*, 2015). My results however showed that a SC-specific knockout of Netrin-1 had no significant effect on SC migration 5 days post-PNI with migrating SCs forming a cord in the nerve bridge of the Netrin-1 knockout mice 6 days post-injury.

Regenerating axons attach to these migrating SCs to navigate their path to the end organ, and a failure or disruption in the formation of the SC cord can also indicate a disruption in axon growth (Chen *et al.*, 2019a). My data for axon guidance and SC migration when considered together show that a SC-specific Netrin-1 knockout is not important for either of these functions.

Previous work carried out on oligodendrocytes cultured in vitro by addition of 100 ng/ml Netrin-1 for 24hrs, demonstrated a significant increase in the production of myelin-like membrane sheets (Rajasekharan *et al.*, 2009). However, Tepavčević *et al.* (2014) in mice showed that in induced spinal cord lesions, antibody-facilitated disruption of Netrin-1 led to an increase in the recruitment of oligodendrocytes precursor cells, which further promoted remyelination. Additionally, the authors also showed that lentiviral-induced Netrin-1 expression prior to the recruitment of oligodendrocyte precursor cells led to a decrease in the number of cells recruited and subsequently inhibited remyelination (Tepavčević *et al*., 2014). As there is no data available in literature for a function of Netrin-1 in SC remyelination of axons after injury, I examined the same in the SC-specific Netrin-1 knockout mice. My results showed that SC-specific Netrin-1 deletion is dispensable for SC remyelination at the timepoints I studied.

Finally, I had intended on generating a mouse model with a Tamoxifen induced global knockout of Netrin-1 using the R26-CreERT2 mice (Hameyer *et al*., 2007). However,

despite success of the use of this system to knockout DCC in mice (Refer to Chapter 4.2), I was unsuccessful in the Netrin-1 mouse model. I made several attempts to generate the knockout in these mice by modifying the protocol including initially injecting Tamoxifen (75 mg/kg of animal) for five days or seven days and using intraperitoneal injections as well as gavaging as method of Tamoxifen delivery. However, these modifications were not successful in knocking out Netrin-1 in my mouse model. I attempted to identify the issue and based on my PCR results I believe that Cre mediated recombination and deletion of floxed Netrin-1 exon 3 did not occur. Although, I observed recombination in mice with P0-Cre transgene, as shown by PCR and immunohistochemistry, I could not determine the reason behind the recombination failure in the mice with the R26-CreERT2 transgene. Sequencing of the PCR product from the SC-specific Netrin-1 knockout mice (P0-Cre$^+$ Ntn1 $^{loxP/loxP}$) confirmed the deletion of Netrin-1 exon 3 along with the expected one loxP site. Additionally, PCR for the presence of two loxP sites (homozygous) in all Netrin-1 mice was also confirmed (data not shown). This lack of Netrin-1 deletion in my mouse model might be due to the size of the target deletion between the two loxP sites, mosaic expression of CreERT2 or incomplete deletion of the floxed loci (Sandlesh *et al.,* 2018) However, ultimately, I could not study the effects of Netrin-1 global deletion on peripheral nerve injury in this thesis.

Taken together, in this study, SC-derived Netrin-1 was shown to be dispensable for successful axonal regeneration and functional recovery; SC proliferation, migration and

remyelination of axons following nerve injury. Contrary to literature, the work done by my research group and as shown by my transcriptomic data, demonstrated downregulation of Netrin-1 following injury. I have also described novel expression of Netrin-1 in the perineurium, blood vessels, tactocytes, epineurial fibroblasts and axons, whereas previously Netrin-1 expression was thought to be mainly SC-derived in the peripheral nerve.

# CHAPTER 4: EXPRESSION AND ROLE OF DELETED IN COLORECTAL CARCINOMA (DCC) IN PERIPHERAL NERVE REGENERATION

## 4.1 Expression of DCC in the peripheral nervous system before and after peripheral nerve injury

Deleted in colorectal carcinoma (DCC) has been widely studied as a chemoattractive receptor of Netrin-1 for axon guidance during development (Keino-Masu *et al.,* 1996), however its role in peripheral nerve regeneration has yet to be fully elucidated. To study DCC expression in mice, my research lab previously performed immunohistochemistry on adult mouse L4-L5 DRGs, spinal cord and the sciatic nerve before and after a 7-day transection injury. The cell bodies of sensory neurons in the DRGs and motor axons in the ventral horn as well as sensory axons in the dorsal horn of the spinal cord of mice showed expression of DCC both before and after sciatic nerve injury (Figure 42). Moreover, there was no detectable difference in DCC expression in the injured versus uninjured DRGs for sections stained and imaged under same conditions, however this was not quantified.
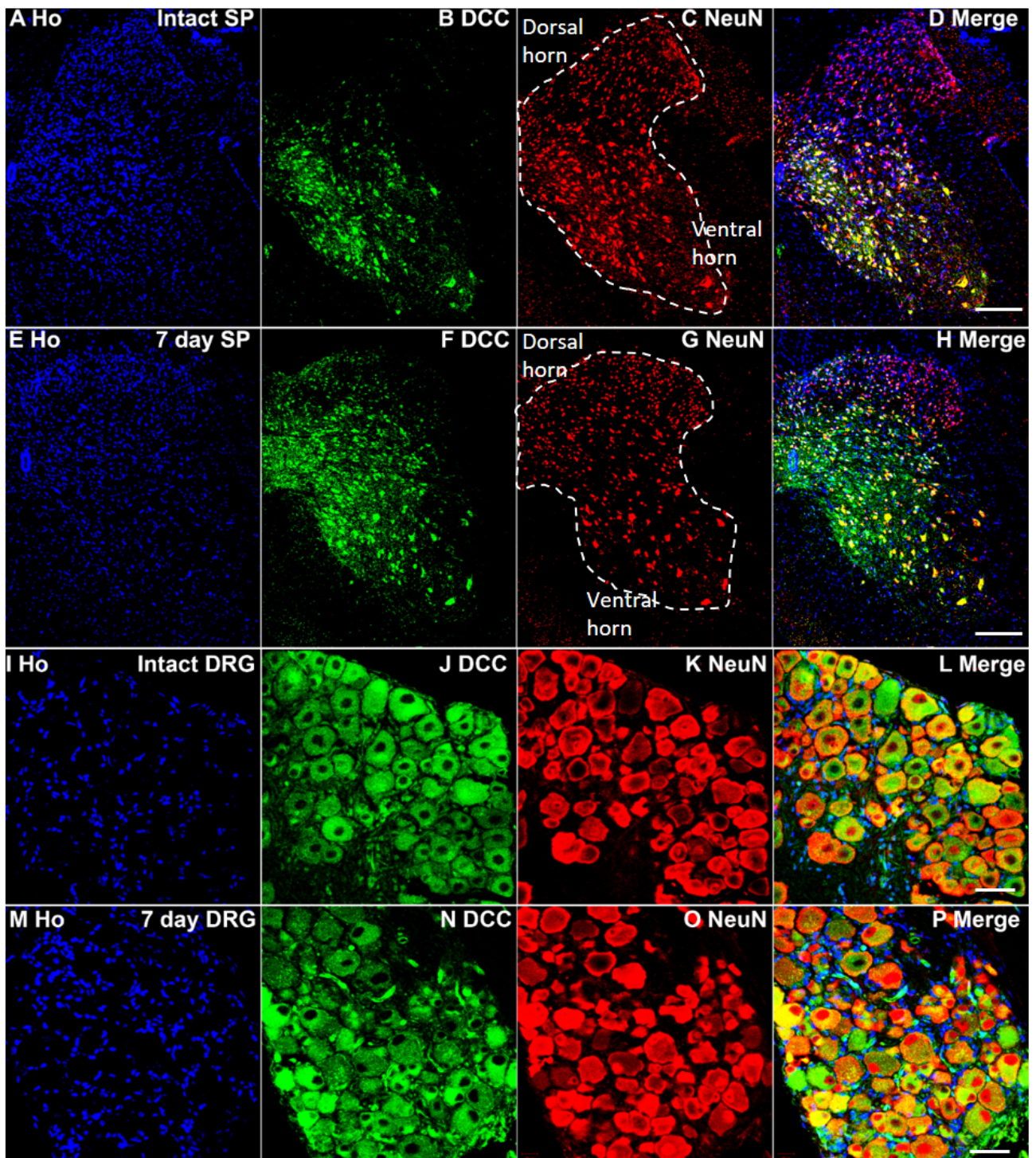
**Figure 42: Expression of DCC in dorsal root ganglia and ventral horn of the spinal cord before and after peripheral nerve injury in adult mice.**

(A-H) Immunostaining to label DCC (green) and neuronal cell bodies (NeuN, red) in the L4-L5 spinal

cord (SP) before (A-D) and 7 days after sciatic nerve cut injury (E-H). White dashes demarcate the dorsal and ventral horn of the spinal cord. (I-P) DCC expression in the cell bodies of sensory neurons in the L4-L5 dorsal root ganglion (DRG) before (I-L) and 7 days after sciatic nerve injury (M-P). The merged image shows co-localisation (in yellow) of neurons and DCC. Scale bar is 100 μm in (A-H) and 50 μm in (I-P) (Dun, 2018, unpublished).

I immunostained adult PLP-GFP intact mouse sciatic nerve with DCC antibody to study DCC localisation in the intact sciatic nerves (Mallon *et al.,* 2002). Confocal microscopy showed no expression of DCC in the SCs of PLP-GFP mice (Figure 43 A-H). Localisation of DCC in the neuronal cell bodies of DRGs and ventral spinal cord suggested that DCC, like Netrin-1, is anterogradely transported to the axons of the peripheral nerves. Therefore, intact sciatic nerves were double stained for neurofilament heavy chain, to label axons along with DCC antibody. My staining showed DCC localisation in axons. (Figure 43 I-L).
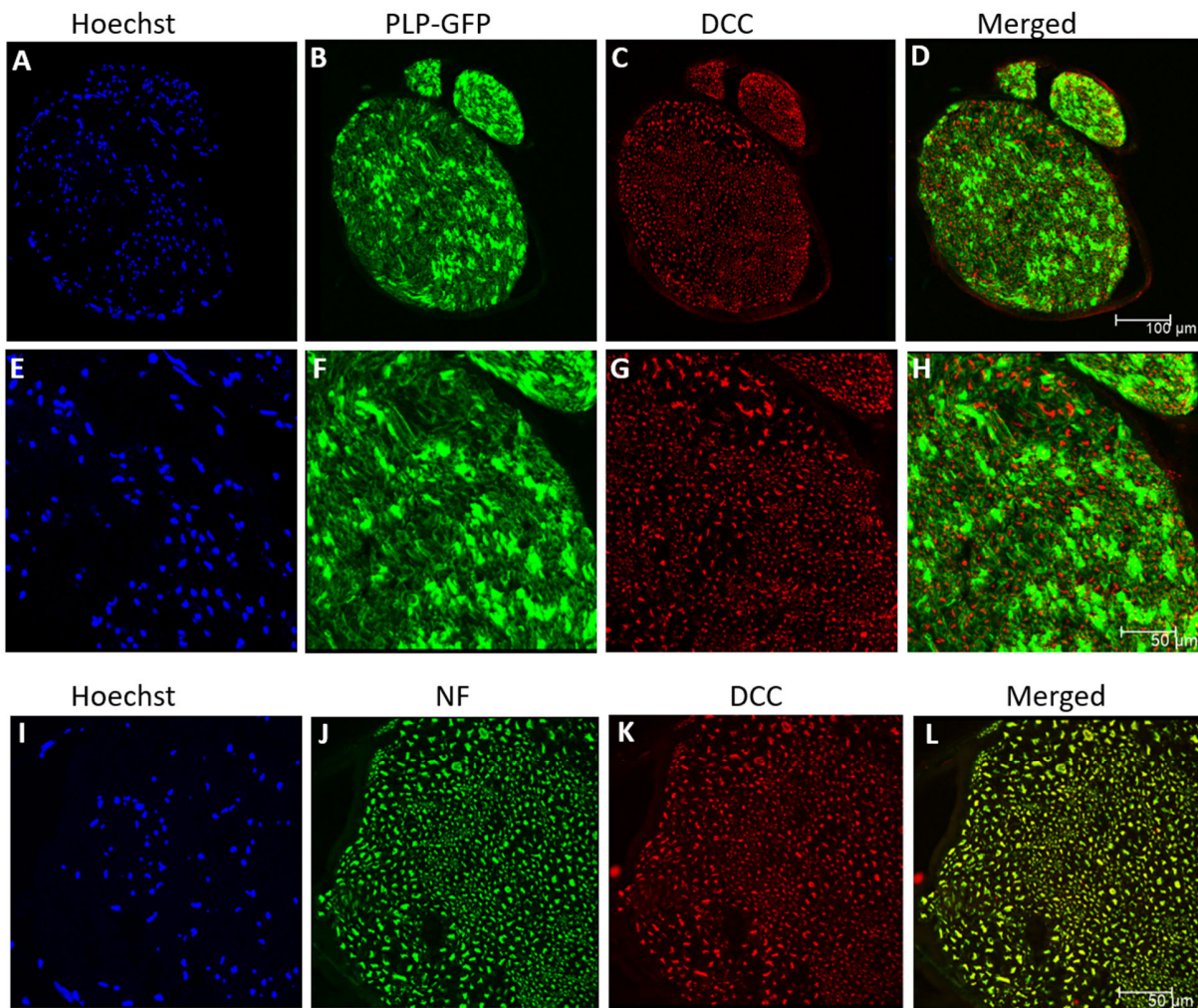
**Figure 43: Expression of DCC only in axons of the intact peripheral mouse sciatic nerve**

(A-H) DCC (red) staining on transverse sections of intact sciatic nerve from PLP-GFP mice showing absence of DCC in endogenous GFP-expressing SCs. (E-H) Magnified image of (A-D). (I-L) DCC (red) and neurofilament heavy chain (NF, green) double staining on intact mouse sciatic nerve depicting DCC expression only in axons. (L) The area of colocalisation appears in yellow. Hoechst (blue) staining labels the nuclei of cells. (A-D) Scale bar is 100 µm and for (E-L) its 50µm.

Previously, my research group had looked at DCC expression 7-days after transection injury in C57BL/6 mice (Figure 44). Following injury, DCC expression appeared to be quite

low in the nerve bridge in comparison to the proximal nerve segment. In the distal nerve,

DCC expression appears to be localised to axonal debris/degenerated axons (Figure 44).

This showed that DCC expression before and after injury is restricted to axons.
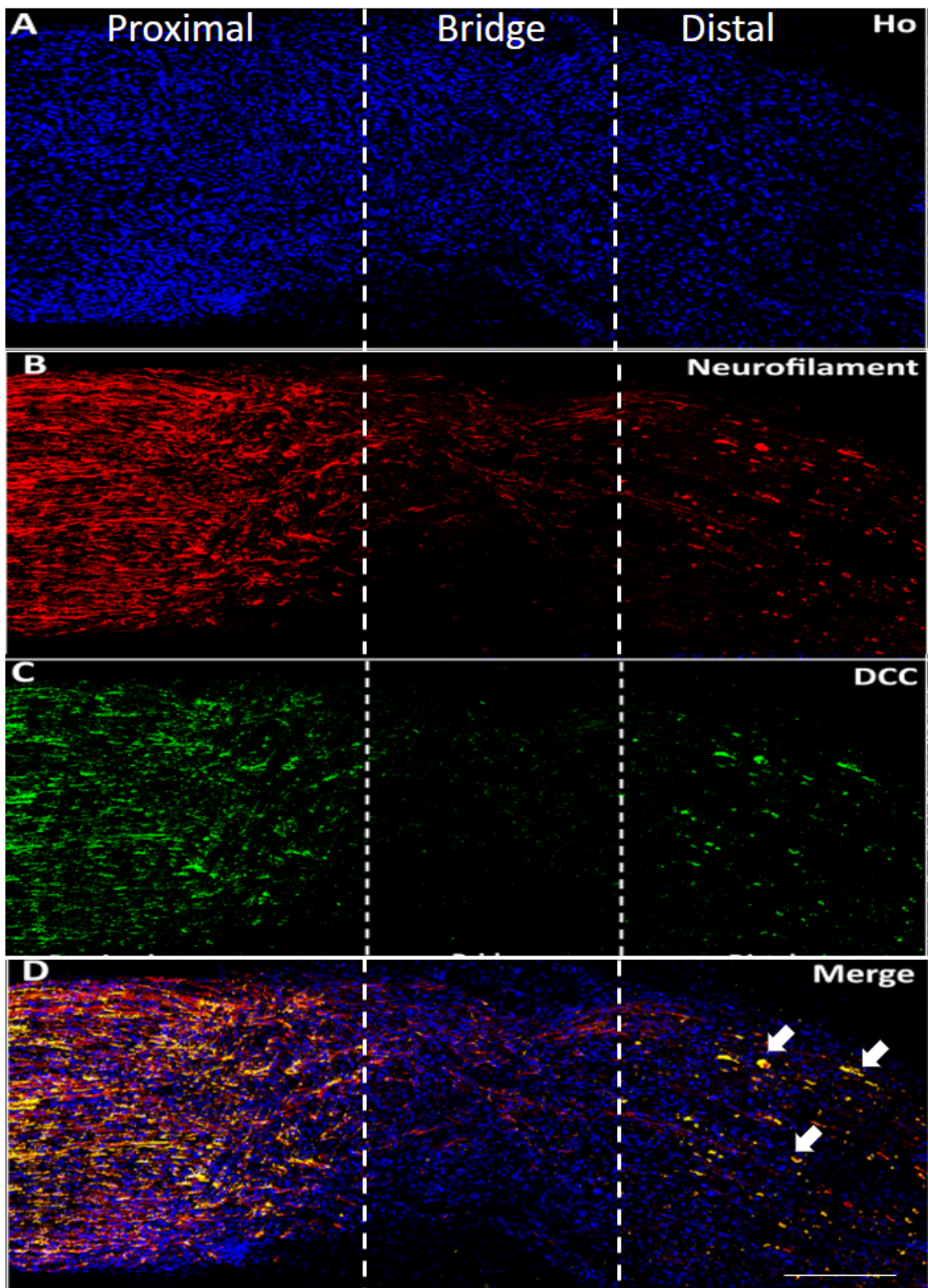
**Figure 44: Expression of DCC in 7-day injured sciatic nerve**

(A-D) Longitudinal section of sciatic nerve from C57BL/6 mouse labelled for DCC (green) and neurofilament (red), 7 days after a transection injury. (D) DCC colocalises with neurofilament in the proximal nerve segment indicating DCC expression in regenerating axons. DCC staining in the bridge is almost negligible with low expression in the distal nerve segment of the sciatic nerve that appears to be colocalising with only axonal debris (shown in arrows). Scale bar is 500 µm. (Dun, 2018, unpublished).

My research group had also previously investigated DCC mRNA expression by RT-qPCR in the spinal cord and DRG at day 4, 7, 10 and 14 after mouse sciatic nerve transection injury and did not observe any significant changes compared to uninjured contralateral spinal cord and DRG, respectively (Dun *et al.*, 2018, unpublished). No DCC expression was detected from the combined single-cell RNA seq data in the distal sciatic nerve at day 3 and day 9 following injury (data not shown) (Carr *et al.*, 2019; Toma *et al.*, 2020; Chen *et al.*, 2021a). Likewise, there was no DCC mRNA expression detected on running a search query on the previously mentioned single cell RNA-seq resource for intact sciatic nerve called the Sciatic Nerve Atlas (Gerber *et al.*, 2021). The lack of mRNA data for DCC in the sciatic nerve suggested that my immunohistochemistry results showing DCC expression only in axons was accurate. This is because axonal RNA is located in the perikaryon of the neurons, which is in the L4-L5 DRGs and the L4-L5 spinal cord for the sciatic nerve of mice and would not be detected by RNA sequencing of the sciatic nerve. Although, some mRNAs are also transported to the axons to be translated locally (Yoon *et al.,* 2009).

Therefore, at the start of this project, before discovering expression of Netrin-1 in other cells besides SCs, I hypothesised that migrating SCs in the nerve bridge expressed Netrin-1 to guide both motor and sensory regenerating axons across the nerve gap after an injury by interacting with DCC on the regenerating axons.

## 4.2 Generating global knockout of DCC in adult mice

DCC was previously known to only act as a receptor for Netrin-1 (Keino-Masu *et al.*, 1996; Fazeli *et al.*, 1997), and therefore I hypothesised that any role of DCC in peripheral nerve repair after global ablation of the gene, would also be observed in the Netrin-1 null mice. However, the opposite wouldn't be accurate as Netrin-1 can interact with several other receptors besides DCC. Therefore, while studying SC-specific Netrin-1 null mice, I also began experiments in mice with a global deletion of DCC.

To generate a global knockout of DCC and circumvent embryonic lethality (Serafini *et al.*, 1996), I used the previously mentioned Tamoxifen-inducible ROSA-26-Cre/ERT2 (R26-CreERT2) mice driven by the endogenous mouse Gt(ROSA)26Sor promoter which is constitutively and ubiquitously expressed in mouse embryos and adult mice (Hameyer *et al.,* 2007). The R26-CreERT2$^+$ mice were crossed with DCC $^{loxP/loxP}$ mice wherein the loxP sites flanked exon 23 of mouse DCC gene (Krimpenfort *et al.*, 2012) to generate R26-CreERT2$^+$ DCC $^{loxP/wt}$ mice (Figure 45 A). These offspring were back crossed with DCC$^{loxP/loxP}$ mice to produce R26-CreERT2$^+$ DCC $^{loxP/loxP}$ mice (Figure 45 A). Five consecutive days of

Tamoxifen (75mg/kg) injections were given intraperitoneally to the R26-CreERT2$^+$ DCC

$^{loxP/loxP}$ mice once they were about five to seven weeks of age. I did not observe any

Tamoxifen induced weight loss, measured at postnatal day 56 (P56) (Figure 45 B). It is

worth noting that DCC has been widely studied as a tumour suppressor (Fearon *et al*.,

1990). However, in the span of experiments performed on the DCC null mice, I did not

observe any increased occurrence of tumours.
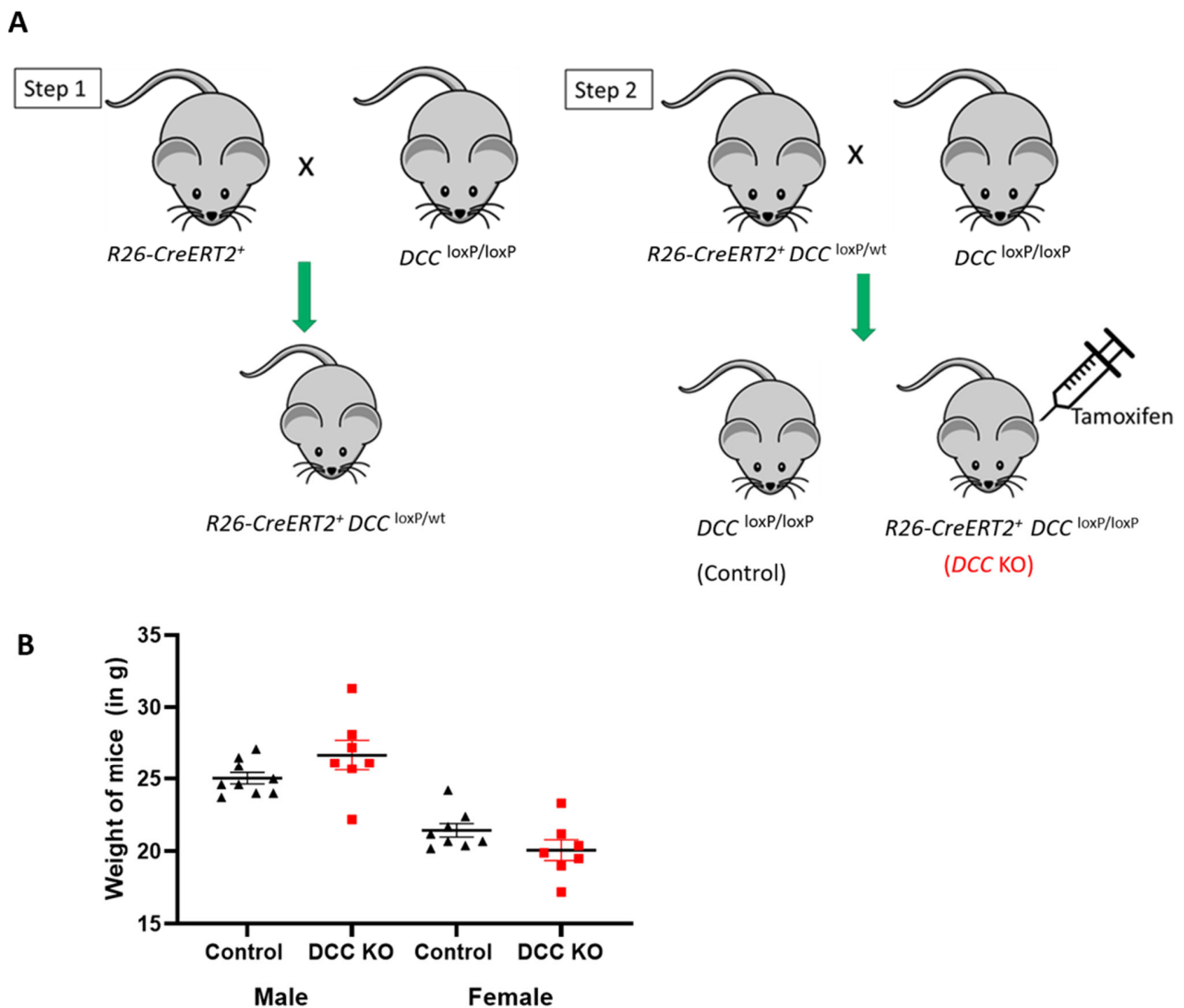
**Figure 45: Generating global knockout of DCC in adult mice**

Illustration of the necessary breeding steps taken to generate a complete knockout of DCC (DCC KO) in adult mice. (A) Homozygous mouse with loxP sites flanking exon 23 of DCC (DCC loxP/loxP) was bred with R26-CreERT2+ mouse carrying the Cre transgene regulated by the constitutively and ubiquitously expressed Gt(ROSA)26Sor promoter. The Cre protein is fused to a mutated estrogen receptor (ERT2) whose ligand binding domain when bound to Tamoxifen allows for translocation of the fusion protein to the nucleus for Cre-mediated recombination and target gene deletion. The resulting offspring from step 1 (R26-CreERT2+ DCCloxP/wt) were back-crossed with DCC loxP/loxP to generate homozygously floxed DCC mice that had the R26-CreERT2 transgene (R26-CreERT2+ DCCloxP/loxP). These mice were intraperitoneally injected with Tamoxifen 5-7 weeks after birth to induce Cre mediated recombination

234

and deletion of DCC. (B) Weight of mice approximately at day 56 post-birth (P56) plotted for control and Tamoxifen-treated DCC KO male and female mice (n=9 for control males; n=7 for DCC KO males; n=8 for control females; n=7 for DCC KO females). No significant weight difference (p > 0.05) was observed.

Two weeks post Tamoxifen injection, I re-ear notched the mice and genotyped them with primers designed to detect deletion of exon 23 of DCC gene. DNA recombination in DCC knockout mice was confirmed in experimental mice with PCR as previously described (Krimpenfort *et al*., 2012), which detects a 400bp amplified DNA band after Cre-mediated recombination and gene deletion (Figure 46 A). As expected, this amplified band was not detected in control mice that were negative for R26-CreERT2^{+} transgene as well as for the mice positive for R26-CreERT2^{+} but prior to Tamoxifen injections (Figure 46 B). To validate deletion of DCC at protein level, I dissected the DRGs of control and knockout DCC mice four weeks after the last Tamoxifen injection. The DRGs were double stained with neurofilament heavy chain and DCC antibodies. Confocal imaging showed DCC expression in the cell bodies of DRGs in control mice but was seemingly absent in the Tamoxifen-treated R26-CreERT2^{+} DCC [loxP/loxP] mice thus confirming knockout of DCC (Figure 46 C-J).
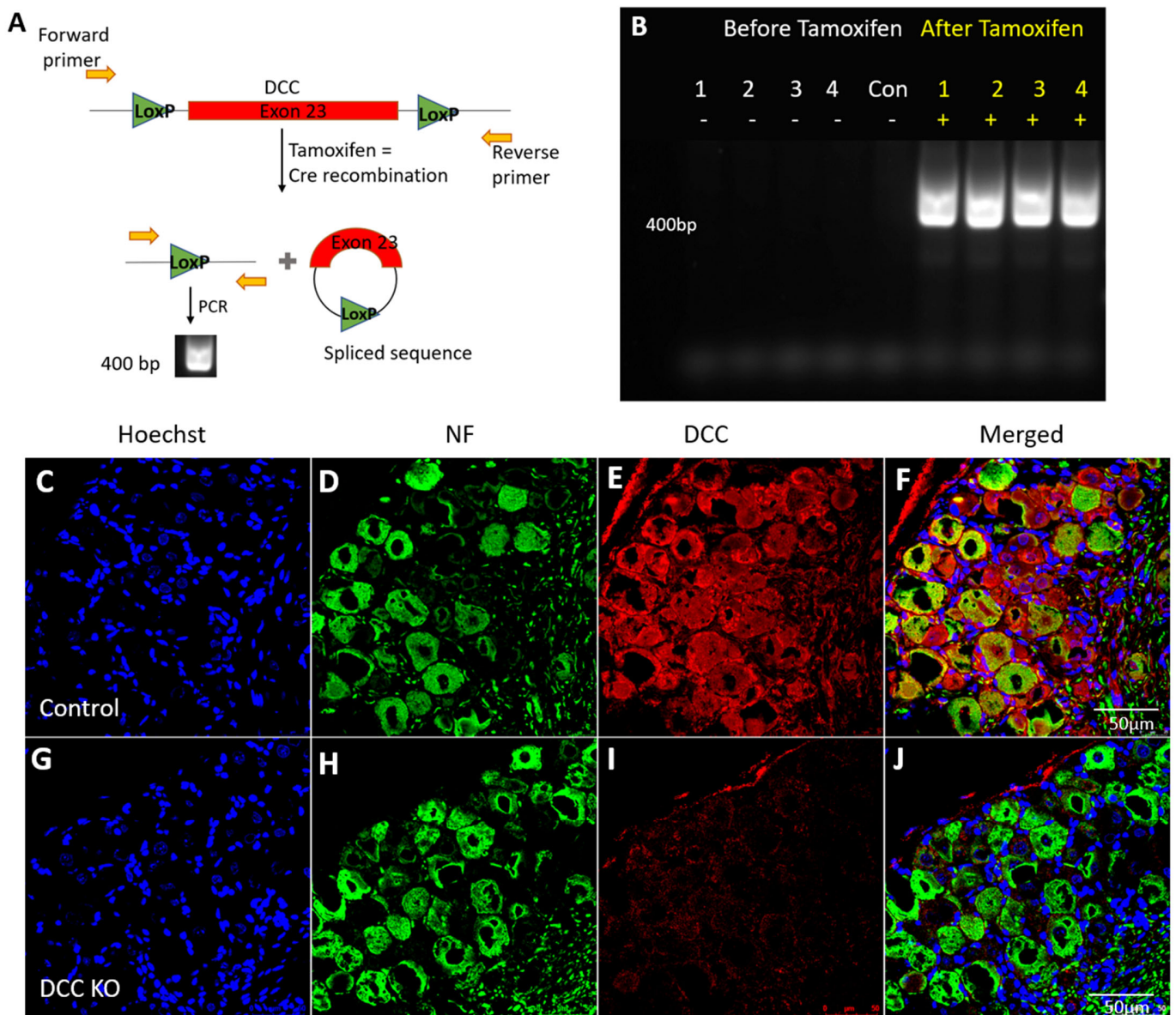
**Figure 46: Confirming global deletion of DCC in Tamoxifen injected R26-CreERT2+ DCCloxP/loxP mice**

(A) Primers (yellow arrows) on either end of the two loxP sites (flanking exon 23 of DCC), amplify a 400bp product by PCR after Tamoxifen treatment of R26-CreERT2+ DCCloxP/loxP (DCC KO) mice to confirm deletion of DCC after Cre-mediated recombination. A 400bp amplified product would be observed if deletion was successful in DCC KO mice. (B) PCR for DCC confirming gene deletion post-Tamoxifen

injection. The 400bp band was only observed after Tamoxifen treatment (sample numbers in yellow) and no band was detected for the same samples before Tamoxifen injection (sample numbers in white) or in control mice (con; DCC [loxP/loxP]). (C-J) Immunohistochemistry of transverse sections of dorsal root ganglia (DRGs) double labelled for neurofilament heavy chain (NF, green) to label neurons and DCC (red) in control (C-F) and DCC knockout mice (G-J) four weeks after the last Tamoxifen injection. DCC expression only in control DRGs. Hoechst (blue) labels cell nuclei. Scale bars in (B-I) represented as 50 μm.

## 4 .3 Axon Guidance defect in DCC knockout mice following nerve transection injury

Our hypothesis was that Netrin-1 mediates axon regeneration by interacting with its receptor DCC post PNI. Whole mount immunolabelling of injured sciatic nerve showed abnormal trajectory of axons of the nerve bridge in SC-specific Netrin-1 knockout mice 14-days after a transection injury. However counting the number of axons that had innervated the tibial branch of the sciatic nerve, did not show any loss of axons in the target mice (Figure 21). I therefore wanted to examine if similar results are obtained upon global deletion of DCC in adult mice.

As previously described, the control and DCC knockout mice underwent sciatic nerve transection injury and 14 days later, the animals were sacrificed, and the sciatic nerve was dissected along with the surrounding muscle for whole mount staining (Dun and Parkinson, 2018). I used neurofilament heavy chain antibody to label axons in the sciatic nerve. Several axons in the nerve bridge seemingly grew into surrounding tissues (Figure 47 A, B). The aberrant trajectory of axons also appeared to be more severe in comparison

to the control mice. However, again on quantifying the total number of axons in a cross section of the tibial nerve no difference in the number of axons that had innervated the tibial nerve was observed (Figure 47 C, D). This suggested that although Netrin-1/DCC signalling might be important for guiding some populations of axons, the majority of axons can regenerate into the distal nerve in the absence of DCC.
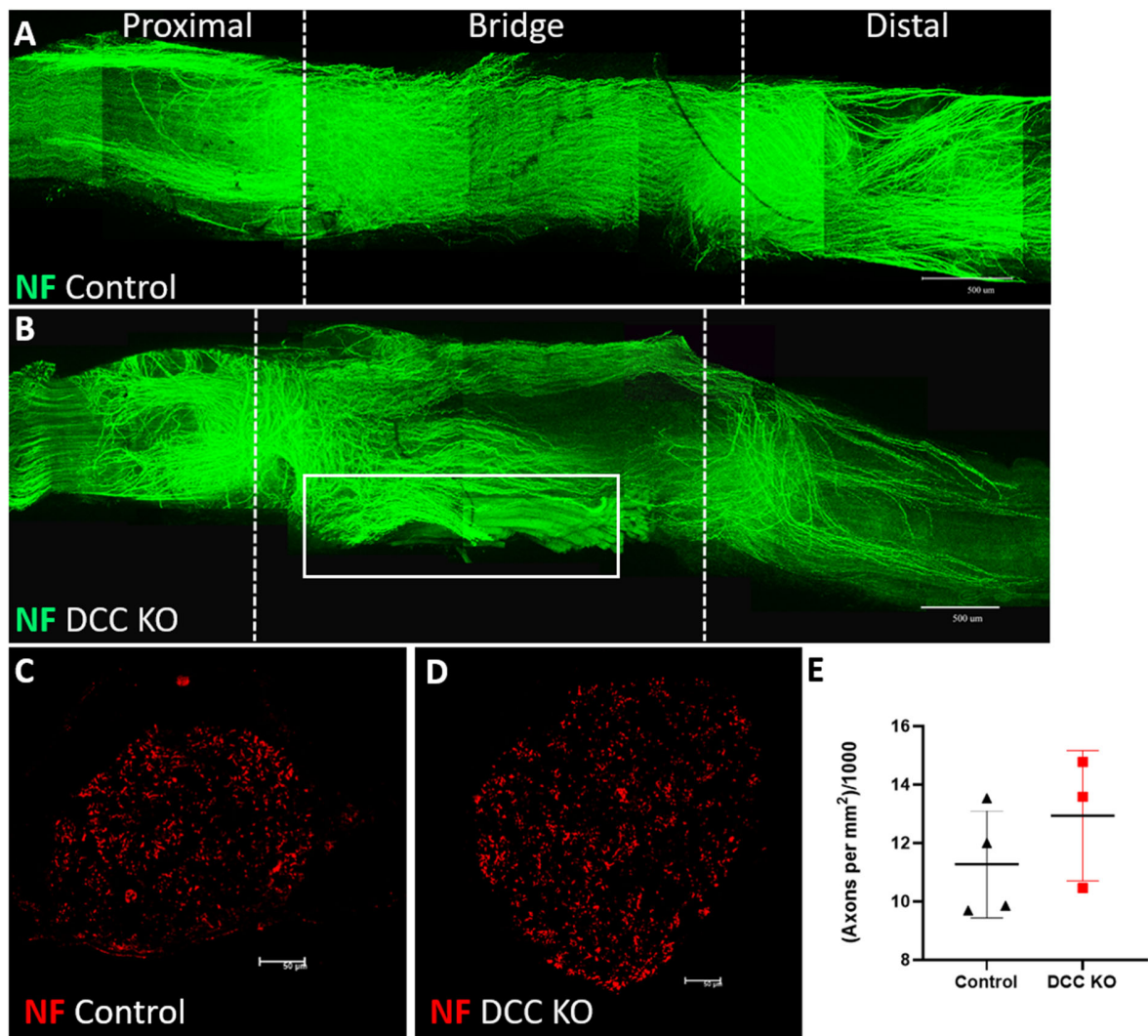
**Figure 47: Axon guidance defect in the nerve bridge of DCC knockout mice**

(A and B) Whole nerve staining of sciatic nerve labelled for neurofilament heavy chain (NF, green) depicting axonal regeneration in the nerve bridge of (A) control (n=4) and (B) DCC knockout mice (DCC KO) (n=3), 14 days post-nerve transection injury. The dotted lines depict the segregation of the proximal, the nerve bridge and the distal end of the nerve. The white box shows regenerating axons that appear to be innervating surrounding tissues and leaving the nerve bridge. (C, D) Transverse section of the tibial branch of the sciatic nerve immunolabelled for NF (red) shows axon density in the tibial nerve in control (C) and DCC knockout mice (D) 14 days post-nerve transection injury. Scale bars in (A and B) represents 500 µm and in (C and D) represents 50 µm. (E) Quantification of axon numbers

in the tibial nerve of control and DCC knockout mice 14 days post-transection injury (n= 4 for control and n=3 for DCC KO mice). All axons per fascicle were counted and depicted as total number of axons per total area of cross section of the tibial nerve. There was no statistically significant difference (p > 0.05; not significant) between the two studied groups. Error bars represent (±) SEM.

## 4.4 Normal functional recovery in DCC knockout mice post-crush injury

With no significant role apparent for DCC in axonal regeneration I wanted to study whether I would observe similar results after a sciatic nerve crush injury. Therefore, I looked at functional recovery after a sciatic nerve crush injury in the DCC knockout mice. As described previously, images of mice were captured before injury and from day 7 onwards following right sciatic nerve crush injury. The mice were kept in a transparent box and the camera was positioned below it (Figure 48 A-D). The toe spread function was measured from the images and static sciatic index (SSI) was calculated as previously described by Bozkurt *et al*. (2008).

I recorded a mean preoperative SSI score of -5.49 ± 5 for both control and DCC knockout mice (Figure 48 E). Seven days post-injury, by measuring the toe spread of the right paw, I recorded a mean SSI score of -95 ± 5 for both groups (Figure 48 E). I recorded an SSI score of –9 ± 5 for both groups 21 days post-injury indicating full functional recovery (Figure 48 E). This showed that DCC was not important for functional recovery after a crush injury by this measure thus suggesting that deletion of DCC does not affect the

speed of axonal regrowth and re-innervation following peripheral nerve crush injury. However, as my experiment on functional recovery did not include tests for regeneration of unmyelinated small diameter axons, such as the Hargreaves test, any potential role of DCC in the regeneration of these axons could not be ruled out.
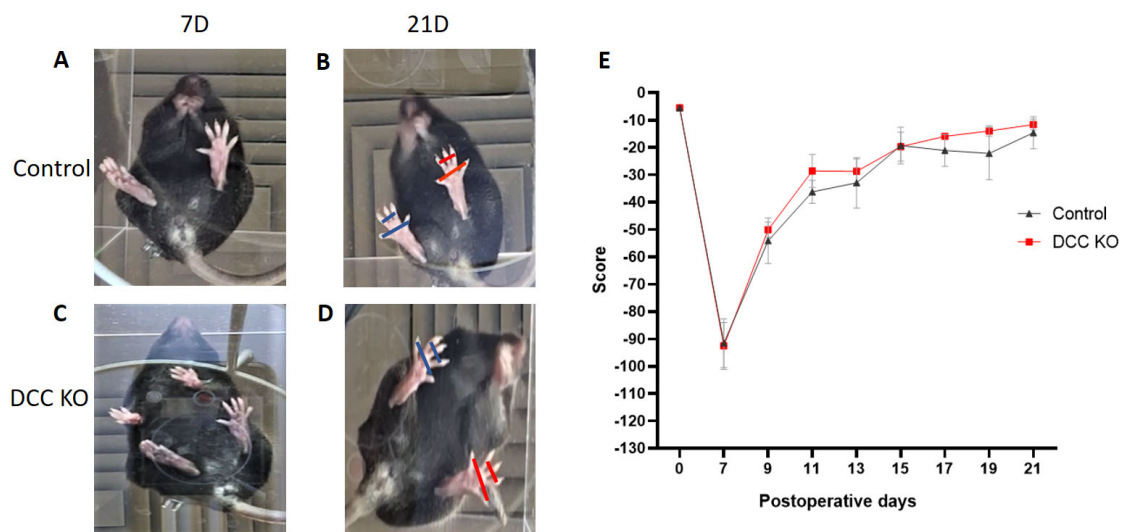


**Figure 48: Normal functional recovery in DCC knockout mice post-crush injury**

(A-D) The experimental setup for recording static sciatic index (SSI) for control and DCC knockout (DCC KO) mice following right sciatic nerve crush injury. A camera was positioned below a transparent box to record the toe spread of each mouse starting from day 0 (before injury), followed by day 7 (after injury) and every other day until day 21. (A, B) Control mouse at day 7 (7D) and day 21 (21D) after injury. (C, D) DCC KO mouse at day 7 and day 21 after injury. The blue lines show toe spread in the injured right paw whereas the red lines depict toe spread in the uninjured left paw. (E) Plotted graph for measured SSI, values approaching zero imply a trend to recovery of function (n=3 for control, n=5 for DCC KO). There was no statistically significant difference ($p > 0.05$; not significant) for SSI between the two groups at any time point. Error bars represent ($\pm$) SEM.

**4.5 Discussion and Conclusions**

As described previously, during development, Netrin-1 has been shown to have bi-functionality showing both chemoattraction and chemorepulsion during axon guidance, angiogenesis and vasculogenesis (Keino-Masu *et al*., 1996; Larrivée *et al*., 2007; Finci *et al*., 2014; Lu *et al*., 2014; Dun and Parkinson, 2017). Deleted in colorectal carcinoma (DCC) is a transmembrane receptor for Netrin-1. Netrin-1 can mediate axonal attraction on interaction with DCC, while repulsion is observed when Netrin-1 binds to uncoordinated-5 receptors (UNC5A-D). Moreover, it has been shown that DCC is required to switch the attractive cues to that of repulsion (Hong *et al*., 1999).

With Netrin-1/DCC interaction shown to be important for mediating both repulsion and attraction of axons in developmental axon pathfinding, DCC was primed as an important molecule for studying its role in peripheral nerve repair (PNR), in tandem with Netrin-1. Therefore, in the course of the present investigation, I studied the expression of DCC in the PNS of adult mice as well as its role in PNR by generating global knockout of DCC in mice.

Previously, Webber *et al*. (2011) showed a significant increase in expression of DCC mRNA by day 7 in the DRGs following sciatic nerve transection injury in rats. However, the previous results of my research group showed no change in DCC mRNA expression up until day 14 post-sciatic nerve injury in the mouse, both in the spinal cord and the

DRGs (Dun *et al*., 2018, unpublished). Webber *et al.* (2011) also reported DCC expression in the sensory neuronal cell bodies of adult rat DRGs, in unmyelinated axons of the sciatic nerve and in the paranodes and Schmidt-Lantermann incisures of myelinated axons before injury. However, after injury the authors reported that along with expression in a few axons, robust DCC expression was primarily observed in migrating SCs proximal and distal nerve segments, 7 days following transection injury. Lee *et al*. (2007) reported that DCC mRNA was not expressed in RT4 schwannoma cells (rat schwannoma cell line) and primary SCs cultured from adult rat sciatic nerves. Also immunoblotting did not detect DCC in RT4 and iSC schwannoma cells (an immortal Schwann cell line) (Lee *et al*., 2007). This was in agreement with the results of Lv *et al.* (2015), wherein the authors did not detect any DCC mRNA in RSC96 cells (an immortalised rat SC line).

My immunostaining results showed DCC expression only localised to axons (both motor and sensory) in intact sciatic nerves and no expression observed in SCs. Also, unlike Webber *et al.* (2011), DCC expression was localised to only regenerating axons with low expression in the nerve bridge and only in the axonal debris/degenerating axons of the distal nerve, 7-days post sciatic nerve transection in mice. Moreover, DCC was not detected in the single-cell RNA-seq analysis of the sciatic nerve before and after injury. This further suggested that DCC expression is confined only to axons.

Previously in DCC mutant zebrafish, the motor axons elongated along aberrant trajectories at the injury site, 48hrs after transection injury (Rosenberg *et al*., 2014). To validate this result in the DCC global knockout mouse model, I performed sciatic nerve transection injury and observed similar aberrant trajectory of axons in the bridge segment of the nerve, 14 days post-injury. However, I did not observe any significant difference in the number of axons that had innervated the tibial nerve at the same time point, indicating that although aberrant trajectories are evident after loss of DCC in mice, it is not enough to severely affect axonal regeneration. Possibly the misdirection of axons is more pronounced earlier than the 14-day time point, however this was not investigated in this study as there was no pronounced defect in innervation of the axons in the distal nerve segment at 14 days following PNI. My studies for functional recovery following a crush injury up until day 21 in the DCC knockout mice also did not show any difference compared to control, with almost full functional recovery as that of an uninjured nerve attained by day 21 post-injury. This indicated that following a less traumatic crush injury, axon regeneration and target innervation is not affected by the loss of DCC. Thus, data for DCC taken together with Netrin-1 suggests that Netrin-1/DCC might not be important for axonal regrowth and functional recovery following PNI.

# CHAPTER 5: EXPRESSION AND ROLE OF RUNT RELATED TRANSCRIPTION FACTOR 2 (RUNX2) IN PERIPHERAL NERVE REGENERATION

## 5.1 Runx2 mRNA upregulation post peripheral nerve injury

My lab is particularly interested in studying the role of SCs in peripheral nerve repair in terms of phenotypic changes, upregulation and downregulation of molecules, including the role of transcription factors regulated by SCs post PNI. One of the dramatically upregulated transcription factors following PNI is the transcription factor Runx2 and was shown to be expressed mainly by SCs (Hung *et al.*, 2015; Arthur-Farraj *et al.*, 2017; Ding *et al* 2018). My research group's work on identifying transcription factors upregulated post PNI also showed Runx2 upregulation in SCs of the distal nerve stump after mouse sciatic nerve transection injury on day 3 and day 9 (Li *et al.,* 2021).

Based on this data, Runx2 mRNA expression was also studied using the same datasets as described above for Netrin-1 and DCC projects. For crush injury I analysed microarray datasets GSE22291 and GSE74087 with data available for the distal nerve segment of the mouse sciatic nerve (Barrette *et al.*, 2010; Pan *et al.*, 2017), and I confirmed that Runx2 mRNA is significantly upregulated for all the analysed time points (day 3, 7 and 14) (Figure 49 A, B). Similar results with dramatic upregulation of Runx2 mRNA was also observed for the data analysed from microarray dataset GSE38693 for transection injury in mice 7 days post-sciatic nerve injury (Arthur-Farraj *et al.*, 2012).
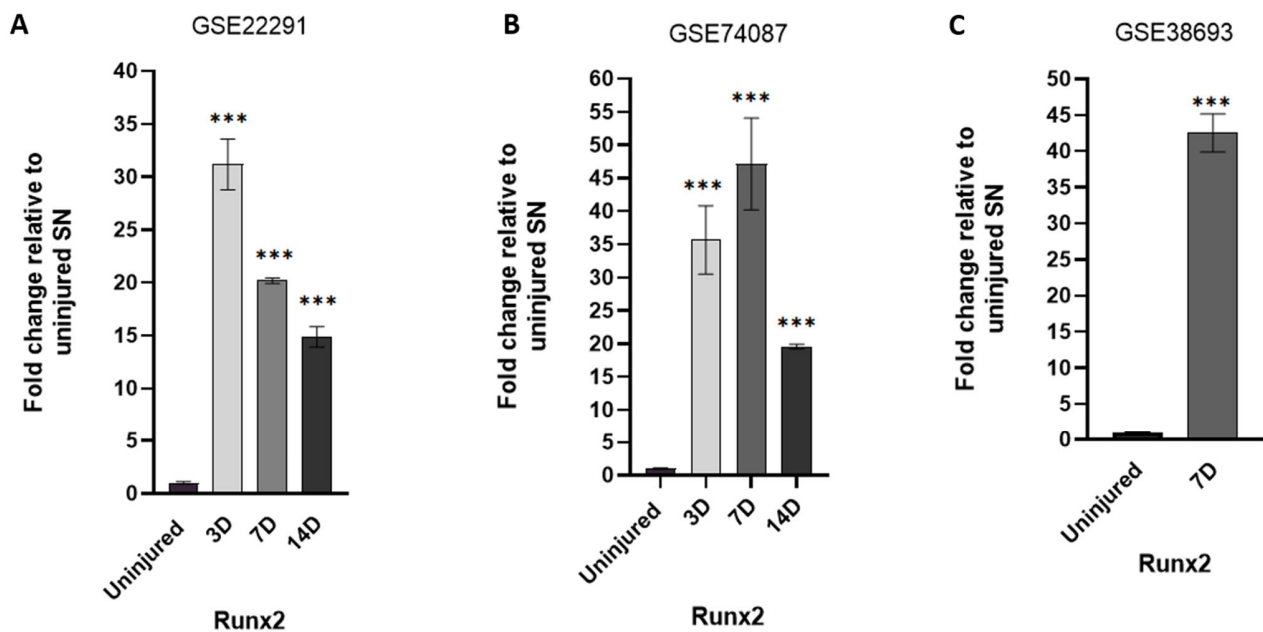
**Figure 49: Runx2 mRNA expression in the distal sciatic nerve following sciatic nerve injury.**

(A, B) Fold change upregulation of Runx2 in the distal sciatic nerve (SN) stump at day 3, 7 and 14 (3D, 7D, 14D, respectively) following SN crush injury in mouse, relative to uninjured SN. The data was analysed from publicly available microarray datasets GSE22291 (n=2 for each time point) and GSE74087 (n=3 for each time point). (C) Runx2 mRNA upregulation 7 days after SN transection injury in mice, relative to uninjured SN, from microarray dataset GSE38693 (n=2). *p<0.05, **p<0.01, ***p<0.001. Error bars represent (±) SEM.

I next compared the expression of Runx2 to c-Jun and Sox2, two well-characterised transcription factors, both of which have been widely studied for their role in PNR and their expression by SCs (Parkinson *et al.*, 2008; Parrinello *et al.*, 2010; Arthur-Farraj *et al.*, 2012; Fontana *et al.*, 2012; Roberts *et al.*, 2017). The same three microarray datasets as above were used to compare expression of Runx2, c-Jun and Sox2 in the distal sciatic nerve segment, after either a crush or transection injury.

In contrast to c-Jun and Sox2, the fold change expression of Runx2, relative to the uninjured nerve, was significantly higher for the three analysed datasets (Figure 50 A). I also looked at Runx2 mRNA expression in SCs isolated from the bridge and distal segments of the sciatic nerve 6 days after transection injury in mice from published RNA-seq dataset GSE103039 (Clements *et al.*, 2017). Our analysis confirmed that Runx2 was upregulated significantly in the SCs from both the bridge and the distal segment of the sciatic nerve post-transection injury (Figure 50 B).
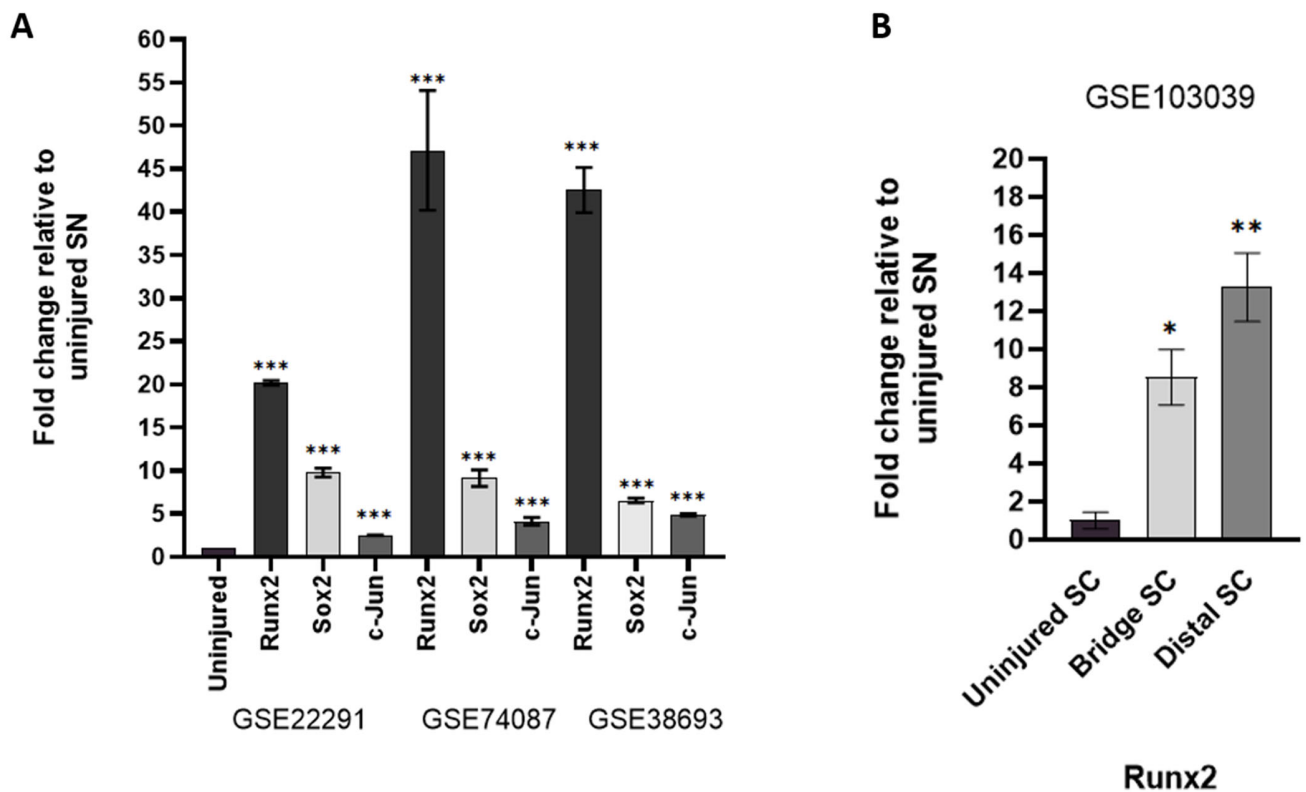
**Figure 50: Runx2 mRNA expression in comparison to c-Jun and Sox2 and its expression in Schwann cells post-crush injury.**

(A) A fold change comparison of expression of Runx2, Sox2 and c-Jun mRNA in the distal segment of mouse sciatic nerve (SN) 7-days after injury, relative to the uninjured SN from publicly available microarray datasets GSE22291 (crush injury; n=2), GSE74087 (crush injury; n=3) and GSE38693 (transection injury; n=2). (B) Runx2 mRNA fold change upregulation in the Schwann cells (SC) in the bridge and the distal nerve segment, relative to SCs from uninjured SN, 6 days post-mouse sciatic nerve transection injury, analysed from dataset GSE103039 (n=4). *p<0.05, **p<0.01, ***p<0.001.

## 5.2 Transcriptomic profiling of Runx2 post peripheral injury with single cell sequencing

With an interesting change in expression observed for the RNA-seq data in SCs for Runx2, as well as based on existing literature showing Runx2 upregulation in SCs (Hung *et al.*,

2015; Arthur-Farraj *et al*., 2017; Ding *et al* 2018), I wanted to confirm this evidence by single cell RNA-seq analysis of the sciatic nerve before and after injury. I accessed the publicly available Sciatic Nerve ATlas and ran a search query for Runx2 mRNA expression in cells of the sciatic nerve before injury (Gerber *et al*., 2021). My search for Runx2 showed that similar to microarray data, Runx2 mRNA expression is very weak prior to injury in adult mice (P60), with the expression observed in only very few epineurial and endoneurial cells and its expression in SCs is almost non-detectable  (Figure 51)

**A**

Runx2

0: Epineurial cells
1: Perineurial cells
2: Immune cells
3: Pericytes and vascular smooth muscle cells (Per/VSMC)
4: Schwann cells-nm(R)SC – non-melinating (Remak) Schwann cells and mSC – myelinating Schwann cells
5: Endoneurial cells
6,7: Endothelial cells
8: Pericytes/Endothelial cells

**B**
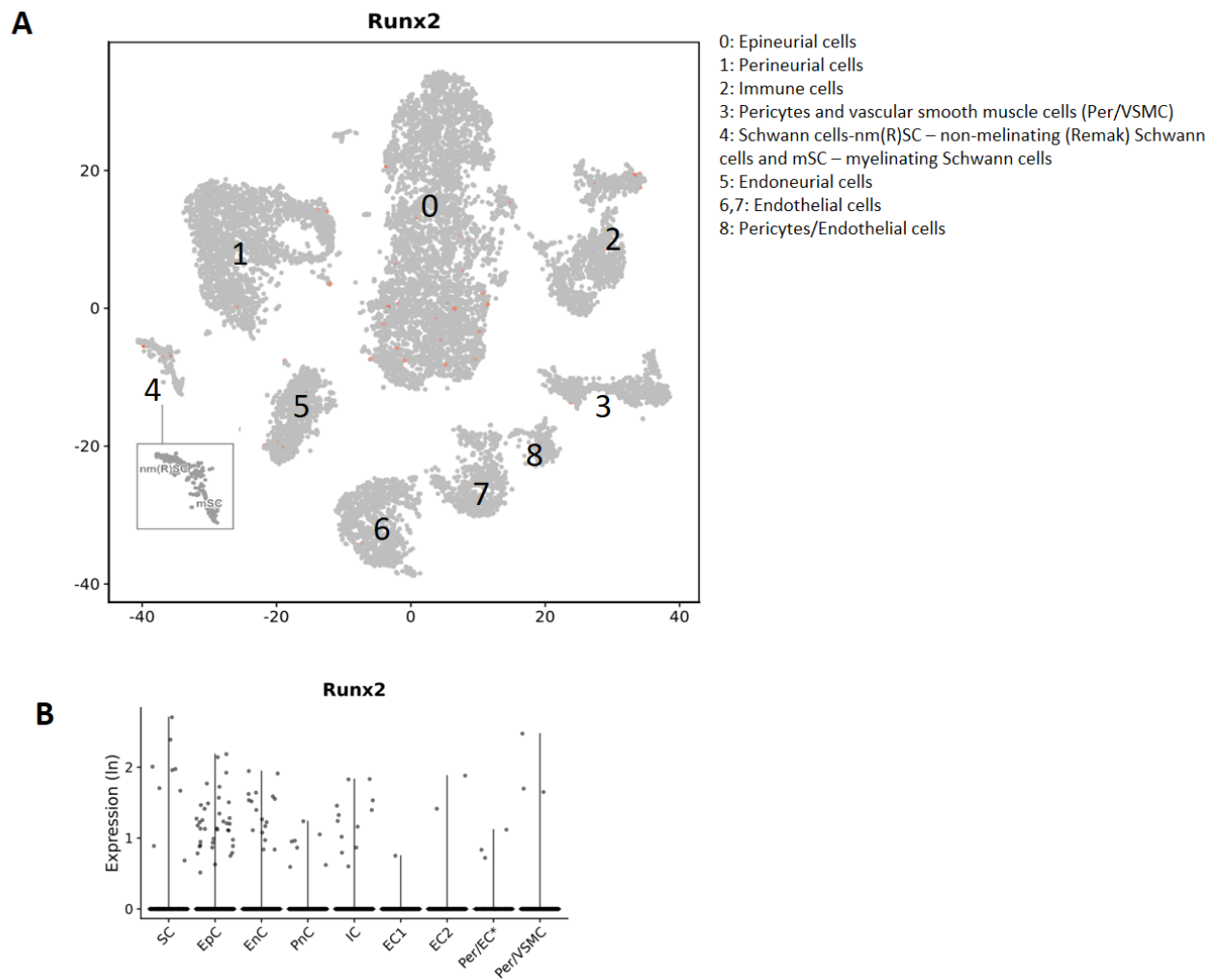
Runx2

**Figure 51: Runx2 single cell transcriptome profiling in mouse sciatic nerve cells at P60 from Sciatic Nerve ATlas**

(A) A t-SNE plot depicting clusters for single cell transcriptomic analysis (GSE137870) of uninjured P60 mouse sciatic nerve with Runx2 expression (orange) superimposed on non-Netrin-1 expressing cells (grey) after running a search query on the resource Sciatic nerve ATlas (https://snat.ethz.ch/). (B) Violin plot from the Sciatic nerve ATlas depicting Runx2 expression levels in uninjured sciatic nerve of adult mouse. (A, B) The figure key 1-8 describes the identity of the clusters as grouped by the authors.

250

Additionally, as mentioned previously, Dr. Dun and Dr. Banton compiled and re-analysed single cell RNA-seq data for the distal nerve segment, 3 days and 9 days post-transection injury (Toma *et al.,* 2020; Carr *et al*., 2019; Chen *et al*., 2021a). This combined data was used in this study to investigate Runx2 mRNA expression after injury. Again, in the uninjured sciatic nerve, Runx2 expression was almost negligible, both, in terms of the percentage of cells expressing Runx2 mRNA as well as the average expression and mainly observed in very few epineurial and endoneurial fibroblasts (Figure 52; Table 12).
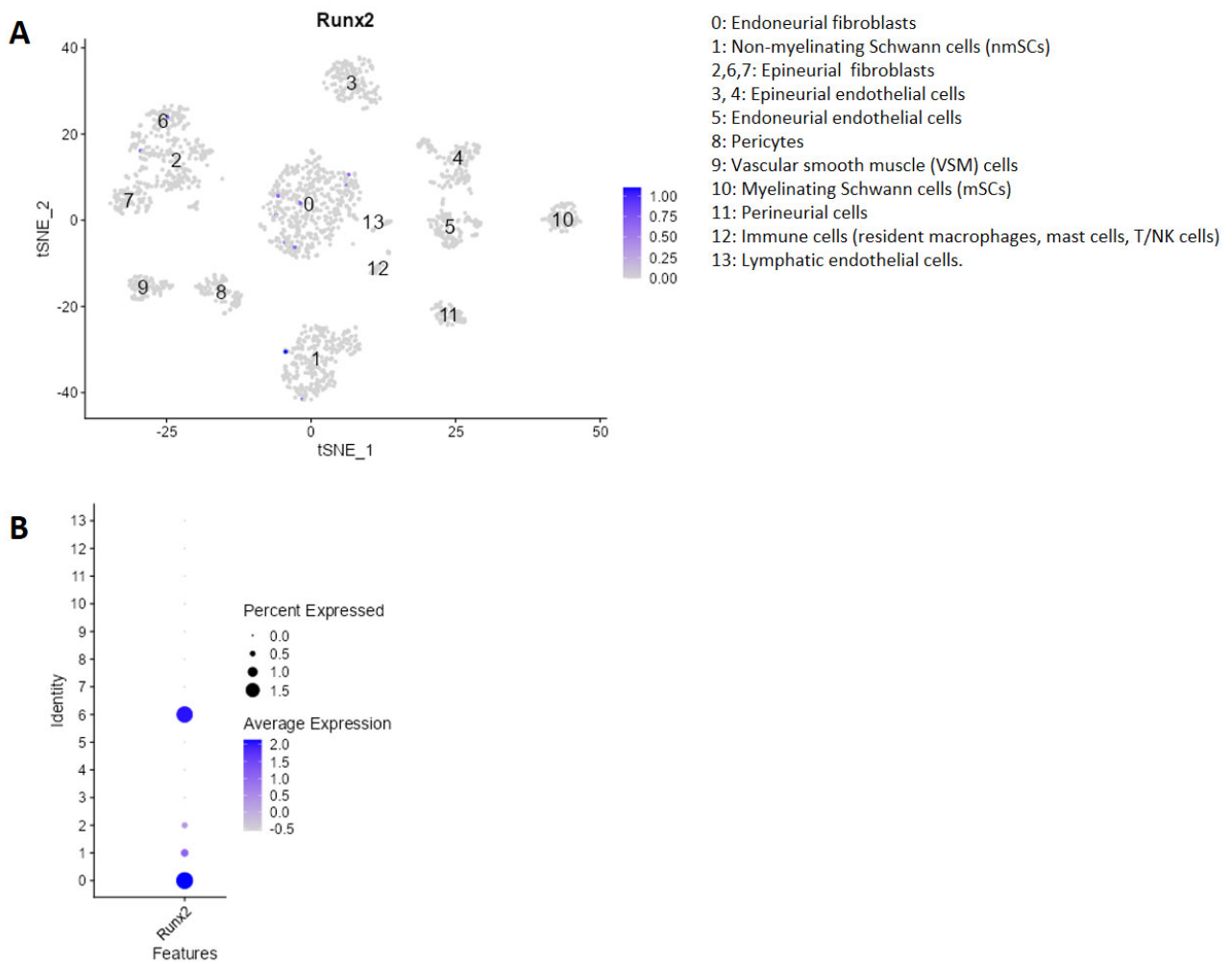
**Figure 52: Single cell transcriptomic profiling of Runx2 in uninjured sciatic nerves.**

Data published for single cell transcriptomic (GSE147285) of intact mouse sciatic nerve was re-analysed and a t-SNE cluster generated, annotated for cell types as identified by marker gene expression. (A) Runx2 expression (in blue) superimposed on the segregated cell clusters of the dataset. (B) Dot plot showing Runx2 expression in the clustered cell types in the intact sciatic nerve. (A, B) The figure key describes the identity of the 14 clusters.

**Table 12: Mouse Runx2 mRNA expression in uninjured, 3 days and 9 days post-transection injury in the distal sciatic nerve stump, re-analysed from published transcriptomic data GSE147285 and GSE120678 (Carr *et al.,* 2019; Toma *et al.,* 2020; Chen *et al.,* 2021a).**

| Runx2 in intact nerve cell types | Percentage of cells | | Average expression | |
|---|---|---|---|---|
| Endoneurial fibroblasts | 1.83 | | 0.02 | |
| Perineurial cells | 0 | | 0 | |
| Epineurial fibroblasts (cluster 2,6,7) | 2 | 0.56 | 2 | 0.01 |
| | 6 | 1.77 | 6 | 0.02 |
| | 7 | 0 | 7 | 0 |
| Non-myelinating Schwann cells (nmSC) | 0.73 | | 0.01 | |
| Myelinating Schwann cells (mSCs) | 0 | | 0 | |
| Arterial endothelial cells | 0 | | 0 | |
| Capillary endothelial cells | 0 | | 0 | |
| Venous endothelial cells | 0 | | 0 | |
| Lymphatic endothelial cells | 0 | | 0 | |
| Pericytes | 0 | | 0 | |
| Vascular smooth muscle (VSM) cells | 0 | | 0 | |
| Immune cells (resident macrophages, mast cells, T/NK cells) | 0 | | 0 | |

| Runx2 in day 3 nerve cell types | Percentage of cells | | Average expression | |
|---|---|---|---|---|
| Differentiating fibroblasts and perineurial cells | 13.66 | | 0.15 | |
| Endoneurial fibroblasts | 1.55 | | 0.02 | |
| Epineurial fibroblasts (cluster 3,5) | 3 | 2.88 | 3 | 0.04 |
| | 5 | 2.50 | 5 | 0.03 |
| Schwann cells | **29.41** | | **0.45** | |
| Endothelial cells | 0.81 | | 0.01 | |
| VSM/pericytes | 1.18 | | 0.01 | |
| Macrophages | 2.54 | | 0.03 | |
| T, NK and mast cells | 3.37 | | 0.07 | |
| Neutrophils | 2.33 | | 0.02 | |
| B cells | 2.44 | | 0.07 | |

| Runx2 in day 9 nerve cell types | Percentage of cells | Average expression |
|---|---|---|
| Differentiating fibroblasts | 10.92 | 0.13 |
| Endoneurial fibroblasts | 1.83 | 0.02 |
| Perineurial cells | 3.37 | 0.03 |
| Epineurial fibroblasts | 2.86 | 0.03 |
| Schwann cells | **22.90** | **0.30** |
| Endothelial cells | 0.57 | 0.01 |
| VSM/pericytes | 1.47 | 0.01 |
| Macrophages | 1.22 | 0.02 |
| Mast cells | 0 | 0 |
| Neutrophils | 0 | 0 |
| B cells | 0.52 | 0.01 |
| NK cells | 7.89 | 0.19 |
| T cells | 1.83 | 0.02 |

Analysis of the single cell RNA-seq data for day 3 post-sciatic nerve transection injury in the distal nerve showed Runx2 upregulation in SCs as compared to the intact nerves with 29.41% of SCs now expressing Runx2 with an average expression of 0.45 (Figure 53; Table 12). Runx2 was also expressed by differentiating fibroblasts and perineurial cells however the average expression was not as high as the SCs.
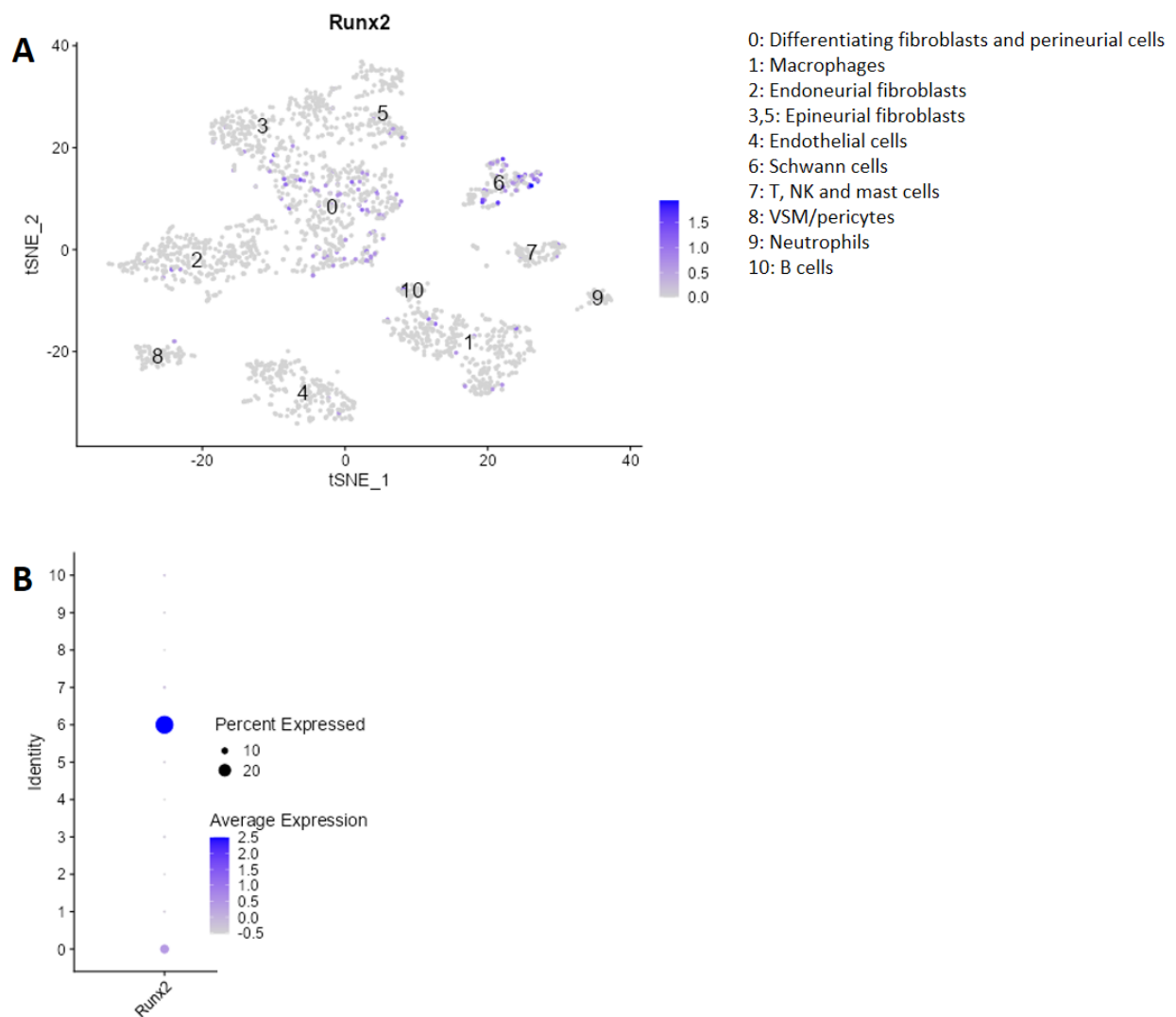
**Figure 53: Single cell transcriptomic profiling of Runx2 in distal mouse sciatic nerve on day 3 post-transection injury**

Single cell RNA sequencing data (GSE147285) from the mouse for day 3 post-sciatic nerve transection injury from the distal stump of the nerve re-analysed and a t-SNE cluster generated, annotated for cell types as identified by marker gene expression. (A) Runx2 expression (in blue) is the highest in the Schwann cell cluster and also expressed in differentiating fibroblasts and perineurial cells. (B) Dot plot showing Runx2 expression in the clustered cell types in the distal stump of the injured nerve. (A, B) The figure key describes the identity of the 11 clusters.

254

Finally, for day 9 days post-transection injury in distal sciatic nerve, Runx2 mRNA expression is still high in SCs with average expression of 0.30, albeit, slightly reduced in comparison to day 3 (Figure 54; Table 12). Differentiating fibroblasts and perineurial cells were segregated into separate clusters on day 9 and for differentiating fibroblasts 10.92% of cells showed an average expression of 0.13. The natural killer cells (NK cells) also expressed Runx2 mRNA on day 9, with 7.89% of cells showing an average expression of 0.19 (Figure 54; Table 12). The single cell transcriptomic profiling of Runx2 showed that Runx2 mRNA is highly upregulated by SCs post-injury.

**A**

Runx2

0: Differentiating fibroblasts
1: Endothelial cells
2: Macrophages
3: Schwann cells
4: Endoneurial fibroblasts
5: B cells
6: VSM/pericytes
7: Epineurial fibroblasts
8: T cells
9: Neutrophils
10: Perineurial cells
11: NK cells
12: Mast cells

**B**
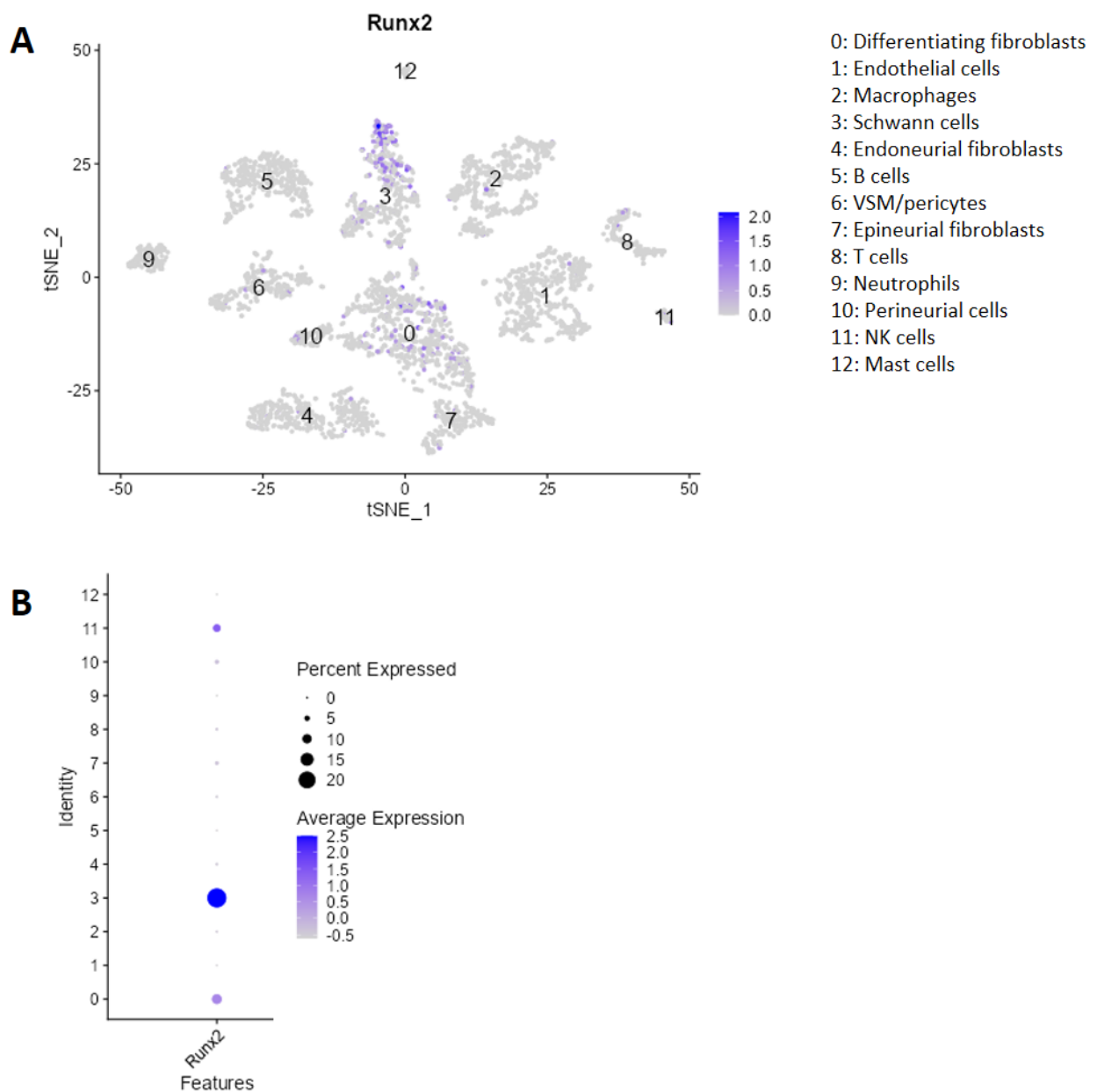
**Figure 54: Single cell transcriptomic profiling of Runx2 expression in the mouse distal sciatic nerve 9 days post-transection injury**

Published single cell transcriptomics (GSE120678) mouse data for 9 days post-sciatic nerve transection injury from the distal stump of the nerve was re-analysed and a t-SNE cluster generated, annotated for cell types as identified by marker gene expression. (A) Runx2 mRNA expression depicted in the cell clusters with the highest expression in the Schwann cell cluster. (B) Dot plot showing Runx2 expression

256

in the clustered cell types in the distal stump of the injured nerve. (A, B) The figure key 1-12 describes the identity of the clusters.


## 5.3 Generating a Schwann cell-specific knockout of Runx2

With SCs being the target cell of interest in my research group and the dramatic increase of Runx2 transcription factor by the SCs post-injury, this suggested a possible role for Runx2 in PNR. To validate the observed transcriptomic analysis of Runx2, my research group performed sciatic nerve transection injury on wild type adult C57BL/6 mice over the course of 4, 7, 10 and 14 days.  By RT-qPCR they showed strong upregulation of Runx2 until day 14, however peaking around day 7 (Rong *et al.*, 2021, unpublished).

Therefore, to understand the role of Runx2 in PNR we generated a SC-knockout of Runx2. Several experiments in this work were carried out in part by my colleagues Rong Hu and Dr. Xin-peng Dun (referred from here on as my research group), whereas animal breeding, genotyping, assistance with surgery, processing of several samples and few experiments, deemed necessary for the completion of the project, were performed by me and have been presented in this thesis.

To study Runx2 function in SCs, we generated a SC-specific knockout of Runx2 following the same methodology as that of the SC-specific Netrin-1 knockout mouse. Briefly, Runx2$^{loxP/loxP}$ mice (Ferrari *et al.*, 2015), were bred with P0-Cre$^{+}$ mice (mP0-TOTACRE) (Feltri *et al.*, 1999) to generate a SC-specific Runx2 knockout mouse line, homozygously

floxed for Runx2 with the P0-Cre transgene (P0-Cre$^+$ Runx2$^{loxP/loxP}$). Mice that did not

have the P0-Cre transgene were used as a control for all experiments (Runx2$^{loxP/loxP}$)

(Figure 55 A).
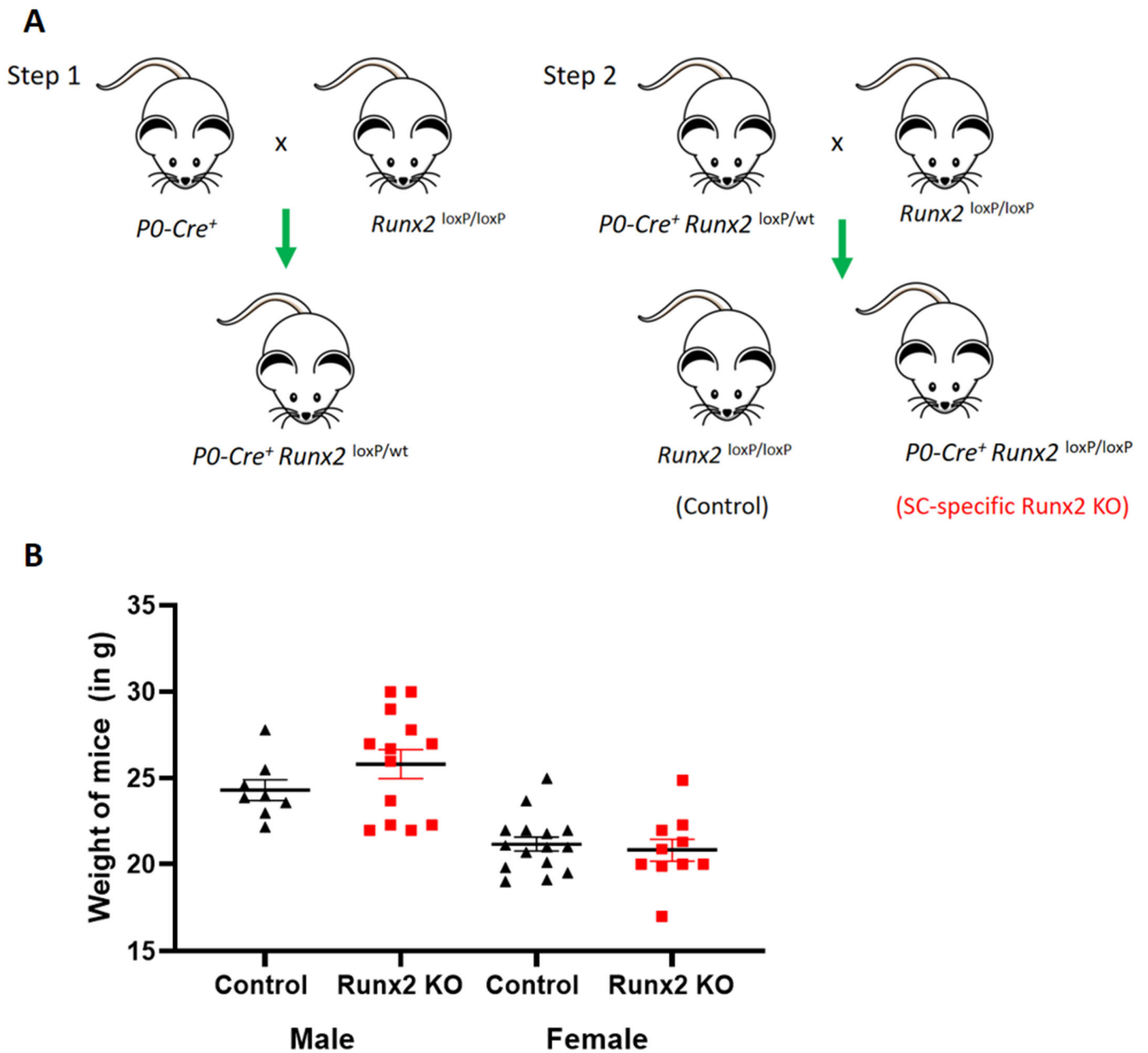


**Figure 55: Generating Schwann-cell specific knockout of Runx2 in mice**

(A) Breeding steps to generate a knockout of Runx2 in Schwann cells (Runx2 KO) in mice. Homozygous

mouse with loxP sites flanking exon 3 of Runx2 (Runx2 $^{loxP/loxP}$) was bred with P0-Cre$^+$ mouse wherein the Cre transgene is regulated by the myelin protein zero promoter in Schwann cells (P0-Cre). The resulting offspring was heterozygous for loxP sites and was back crossed with Runx2 $^{loxP/loxP}$ mouse. The resulting progeny that were homozygous for Runx2 loxP sites and had the P0-Cre transgene (P0-Cre$^+$ Runx2 $^{loxP/loxP}$) were used as the Schwann cell-specific knockout mice in my experiments and mice without P0-Cre but homozogyously floxed for Runx2 were used as controls. (B) Weight of mice approximately at day 60 post-birth (P60) plotted for control and Runx2 KO male and female mice (n=8 for control males; n=13 for Runx2 KO males; n=15 for control females; n=10 for Runx2 KO females). No significant difference (p > 0.05) was observed.

Global embryonic ablation of Runx2 results in death of the pups due to respiratory failure caused by a failure of ossification (Komori et al., 1997; Otto et al., 1997), however the SC-specific Runx2 KO mice in our lab were viable with no difference observed in body weight between the target and control mouse groups (Figure 55 B). We had also bred the Runx2 mouse line with the PLP-GFP line to get mice expressing endogenous GFP in SCs of the peripheral nerve (Mallon *et al*., 2002). I carried out immunohistochemical analysis of the sciatic nerve post-injury to confirm Runx2 knockout. Briefly, control and SC-specific Runx2 knockout mice underwent right sciatic nerve transection injury. 7 days post-injury the distal sciatic nerve was dissected, fixed in 4% PFA and 10 µm longitudinal cryosections were used for immunohistochemistry to stain for Runx2. Runx2 expression was observed in GFP-expressing SCs of distal sciatic nerve in control mice while a few non-GFP cells in the SC-specific Runx2 knockout mice expressed Runx2 (Figure 56 A-H).

A western blot for Runx2 with the uninjured and 7-day injured sciatic nerves also saw a marked decrease of Runx2 in the Runx2 KO mice 7 days post-injury (Figure 56 I, J). The western blot results also confirmed that Runx2 was not expressed in intact nerves (Figure 56 I, J).
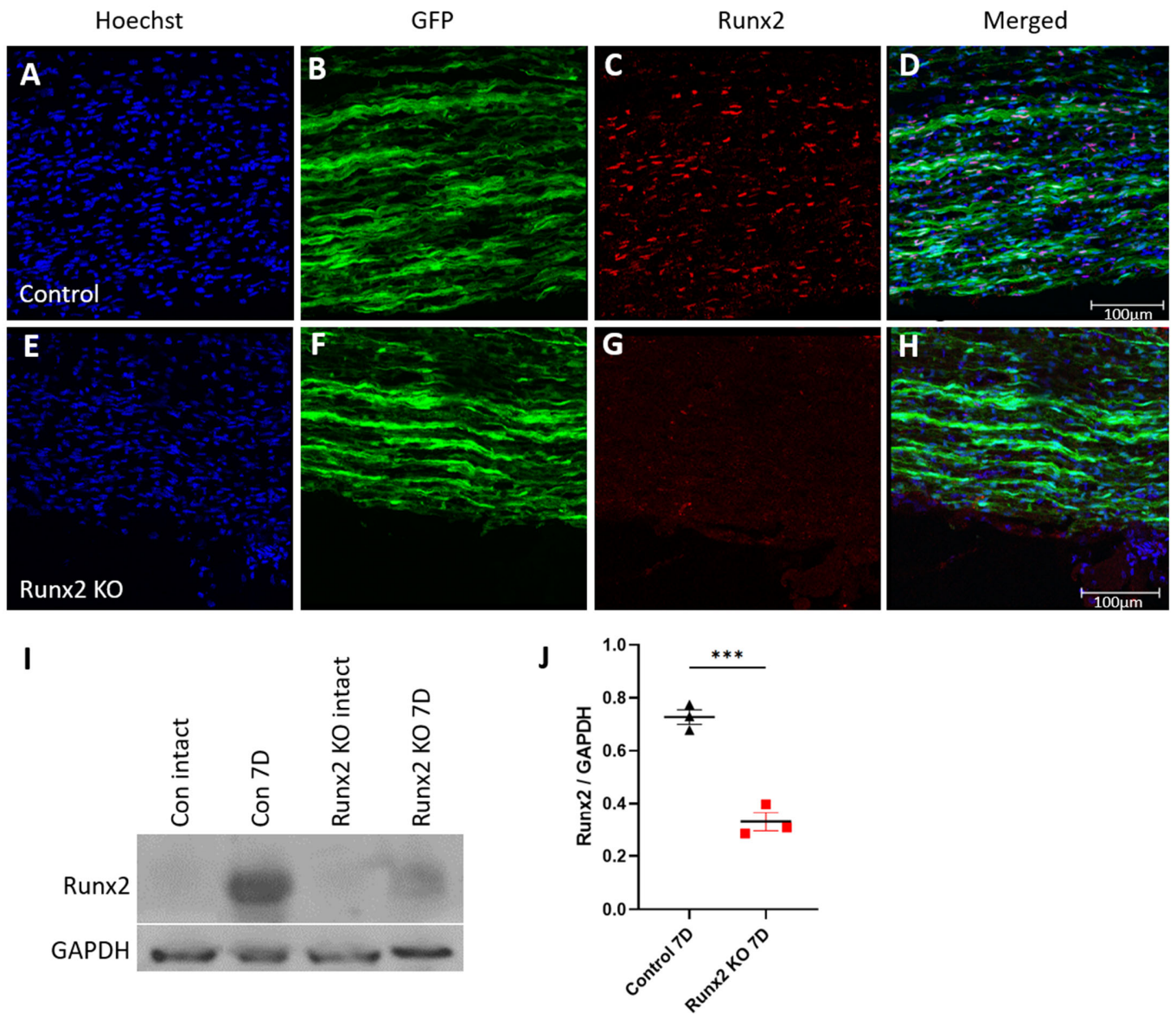
**Figure 56: Confirming Runx2 knockout in Schwann cells.**

(A-H) Immunohistochemistry on longitudinal sections of distal sciatic nerve from Schwann cell-specific Runx2 knockout mice (Runx2 KO) and control mice at 7 days post-sciatic nerve transection injury. Both mouse groups express endogenous GFP in SCs (green) and are labelled for Runx2 (red). (A-D) Runx2 expression in GFP positive cells in control mice after injury. (E-H) Runx2 KO mice do not express Runx2 in GFP positive SCs, confirming deletion. Hoechst labels nuclei of cells. (I, J) Western blot of intact and 7-day (7D) post-transection injury distal sciatic nerves of control (con) and SC-specific Runx2 KO mice.

Runx2 is not present in intact nerves and is upregulated 7 days after injury in control mice. Runx2 deletion is shown in Runx2 KO mice (n= 3 for each group). Error bars represent (±) SEM. ***p<0.001.

## 5.4 Runx2 regulates remyelination post-injury but not during development

My research group studied the levels of myelin proteins Mpz and myelin basic protein (Mbp) by western blot in the tibial nerve 28 days post-crush injury. Their results showed that both the myelin proteins were significantly downregulated in the SC-specific Runx2 knockout mice compared to control (Rong *et al.*, 2021, unpublished). They further examined remyelination using transmission electron microscopy (TEM) on tibial nerves, 28 days after crush injury and reported significant decrease in myelin thickness and an increase in g-ratio in the SC-specific Runx2 knockout mice as compared to control (Rong *et al.*, 2021, unpublished).

To look at this myelination defect at an earlier time point, I used tibial nerves for immunohistochemistry, 21 days post-crush injury. The tibial nerves were double stained for neurofilament heavy chain, to label axons, and Mbp. Staining revealed that many axons in the SC-specific Runx2 KO mice were unmyelinated in comparison to the control (Figure 57 ). On quantifying the number of myelinated axons relative to the total number of axons in the nerves, I observed that at 21 days post-crush injury the SC-specific Runx2 knockout mice had a severe demyelination defect thus confirming the results observed by my research group at 28 days post-injury (Figure 57 K). This led me to examine the

number of axons in the tibial nerve at day 21 post-crush injury, and my quantification

showed no significant difference in the number of axons that had innervated the tibial

nerve (Figure 57 L). Therefore, the remyelination defect observed in our mouse model

was seemingly attributed to Runx2-null SCs being unable to adequately myelinate axons

rather than a factor of reduced number of axons.
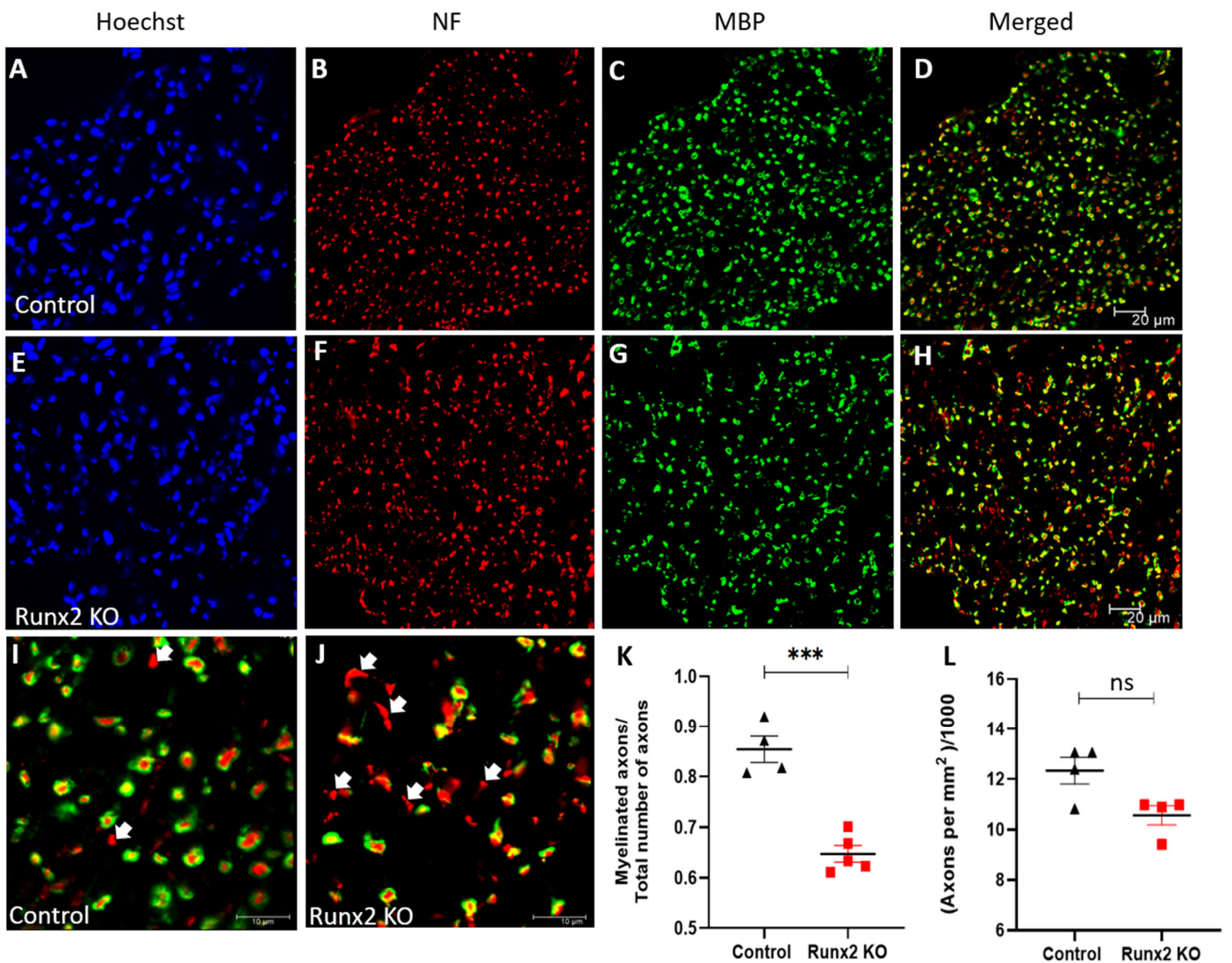
**Figure 57: Remyelination defect 21 days post-crush injury in Schwann cell-specific Runx2 knockout mice.**

(A-J) Tibial nerve of control and Schwann-cell specific Runx2 knockout (Runx2 KO) mice was stained with neurofilament heavy chain (NF, red) to label axons and myelin basic protein (MBP, green) to label myelin, 21 days after a crush injury to the right sciatic nerve. (D, H) The merged channels show axons surrounded by myelin with higher density of axons without myelin in the Runx2 KO tibial nerve. (I, J) Higher magnification of control and Runx2 KO tibial nerve with white arrows showing unmyelinated axons. Hoechst (blue) staining labels the nuclei of cells. (K) Graph depicting the number of myelinated axons to the ratio of total number axons counted in the tibial nerve (n=4 for each group). (L) Quantification of total number of axons per total area of cross section of the tibial nerve for control and

Runx2 KO mice (n=4 for each group) showed no significant difference (ns). Error bars represent (±) SEM. ***p<0.001. Scale bar is 20 µm for (A-H) and 10 µm for (I,J).

Although I have shown that Runx2 is not expressed in intact sciatic nerves, I wanted to confirm that the remyelination defect observed post-injury was not observed during development after loss of Runx2 in SCs. For this purpose, I dissected the sciatic nerves of SC-specific Runx2 knockout and control pups at postnatal day 7 (P7) and these were fixed in 2.5% glutaraldehyde in 0.1M sodium cacodylate buffer. Semithin sections of the sciatic nerves were cut and stained with toluidine blue and imaged on the confocal microscope. Total number of myelinated axons were counted across the whole cross section of the nerve and were represented as total number of myelinated axons per area of the cross section of the sciatic nerve imaged. No difference was observed on analysing the nerves from the control and SC-specific Runx2 knockout mouse groups (Figure 58). In agreement with this, transmission electron microscopy carried out by my research group showed normal myelination and unaltered axon diameter and g-ratio in two-month-old SC-specific Runx2 knockout mice compared to controls (Rong *et al.*, 2021, unpublished). Taken together, the data exhibited that SC-deletion of Runx2 does not affect myelination during development and in adult mice but remyelination was severely impaired after injury.
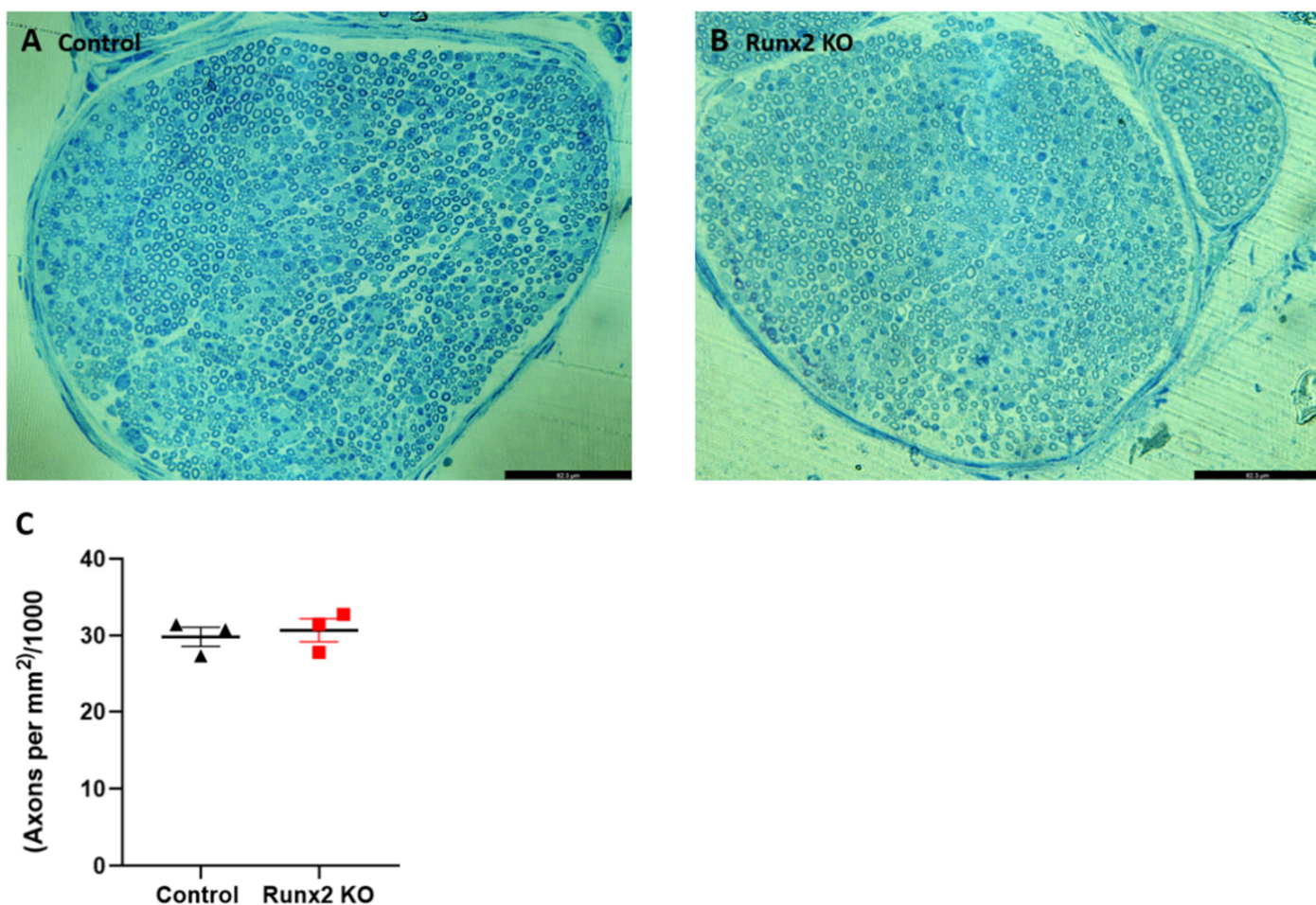
**Figure 58: Normal myelination of the sciatic nerve during development in Schwann cell specific Runx2 knockout mice.**

(A-B) Toluidine blue staining on sciatic nerve semithin sections from postnatal day 7 (P7) control and Schwann cell-specific Runx2 knockout mice (Runx2 KO) mouse pups. (C) Quantification of the number of myelinated fibres in sciatic nerve of P7 control and Runx2 KO mice (n= 3 for each group). All myelinated axons were counted for each cross section of the sciatic nerve and plotted as total number of myelinated axons per total area of a cross section of the sciatic nerve. Error bars represent (±) SEM. There was no statistically significant difference ($p > 0.05$; not significant) between the two studied groups.

## 5.5 Potential Runx2 targets after a peripheral nerve injury.

My research group had looked to identify potential genes that are activated by Runx2 in SCs after injury. Using SCENIC (Single-Cell Regulatory Network Inference and Clustering) (Aibar *et al.,* 2017) , they analysed the scRNA-seq data from dataset GSE147285 for post-injury day 3 distal nerve (Toma *et al.*, 2020), and data set GSE120678 for post-injury day 9 distal nerve (Carr *et al.*, 2019). Briefly, genes that are expressed in SCs at day 3 and day 9 post-injury were analysed for the Runx2 cis-regulatory binding motifs and genes with significant motif enrichment of the correct upstream regulator were retained. The SCs in the distal nerve were then resolved into two sub-clusters - SC1 and SC2. SC1 expressed high level of Runx2 while SC2 express low level of Runx2. They then analysed the identified genes with significant motif enrichment, i.e., Runx2 binding, to identify the genes that like Runx2 were highly expressed by SC1 cluster and saw low expression in SC2 cluster.

Thus, their in-silico analysis of potential genes with significant Runx2 cis-regulatory binding motif enrichment, identified nerve growth factor receptor (Ngfr) also known as neurotrophin receptor p75 (p75[NTR]) among several other targets. Additionally, Ngfr showed the highest expression in SCs and similar fold changes upregulation as that of Runx2 in the distal nerve stump following injury (Rong *et al.,* 2021, unpublished).

To initially study Ngfr as a potential injury-associated target of Runx2, distal and intact sciatic nerve of control and SC-specific Runx2 knockout mice was dissected out, 7 days post-transection injury for immunoblotting. My results showed that Ngfr was barely expressed in intact sciatic nerve of both control and SC-specific Runx2 knockout mice (Figure 59 A, B). Ngfr was upregulated after injury in the distal nerve stump of both control and SC-specific Runx2 knockout mice, however no significant difference was observed comparing the two groups (Figure 59 A, B). Immunohistochemistry of the distal sciatic nerve for Ngfr, 7 days after a crush injury also did not show any apparent difference when comparing the SC-specific Runx2 knockout mice to the control, suggesting that Ngfr was not a potential target of Runx2 (Figure 59 C, D).
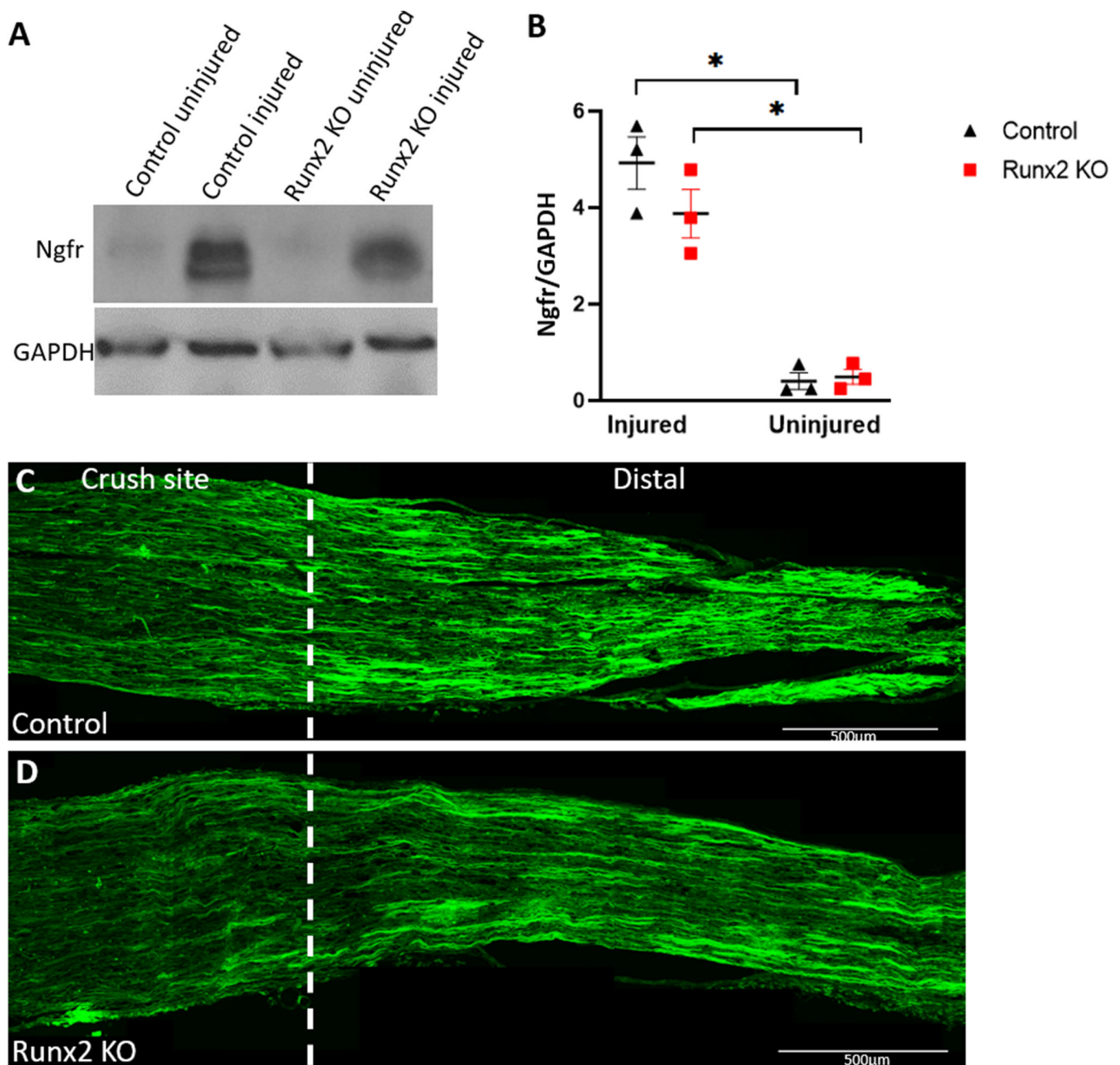
**Figure 59: Nerve growth factor receptor is not an injury-induced target of Runx2.**

(A) Immunoblotting for nerve growth factor receptor (Ngfr) on intact and 7-day transection injury sciatic nerves from control and Schwann cell specific Runx2 knockout mice (Runx2 KO). (B) Ngfr expression was low in intact sciatic nerve for both control and Runx2 KO mice and was upregulated significantly after injury in both groups. No significant difference was shown comparing the injured sciatic nerves of control and Runx2 KO mice (n=3 for each group). GAPDH was used as a loading control. (C, D)

Longitudinal sections of sciatic nerves from crush site, 7 days following injury, labelled for Ngfr (green) in control (C) and Runx2 KO mice (D). (B) *p<0.05 and error bars represent (±) SEM. (C, D) Scale is 500µm.

Hung *et al* (2015) previously showed that Runx2 siRNA transfection in primary rat SCs also resulted in downregulation of sonic hedgehog (Shh) and oligodendrocyte transcription factor 1 (Olig1). To study this in our mouse model, I first performed a 7-day crush injury in control and SC-specific Runx2 knockout mouse on the right sciatic nerve. Total RNA was extracted from the dissected injured sciatic nerve (from the nerve bridge to the distal nerve segment) of both mouse groups and reverse transcribed to cDNA. Quantitative PCR was performed for Olig1, Shh, Ngfr and Gapdh as a reference control (Figure 60). However, my results showed no difference in the gene expression for both Olig1 and Shh in the injured sciatic nerve from SC-specific Runx2 knockout mice relative to injured control sciatic nerve (Figure 60 B, C). Moreover, in agreement with my findings from the western blot and immunohistochemistry results for Ngfr (Figure 59), I did not see any difference for its gene expression in the injured distal nerve segment of SC-specific Runx2 knockout mice, relative to injured control by qPCR (Figure 60 A). Therefore, in the case of a crush injury, Runx2 does not appear to be an injury-induced activator of Ngfr, Olig1 and Shh.
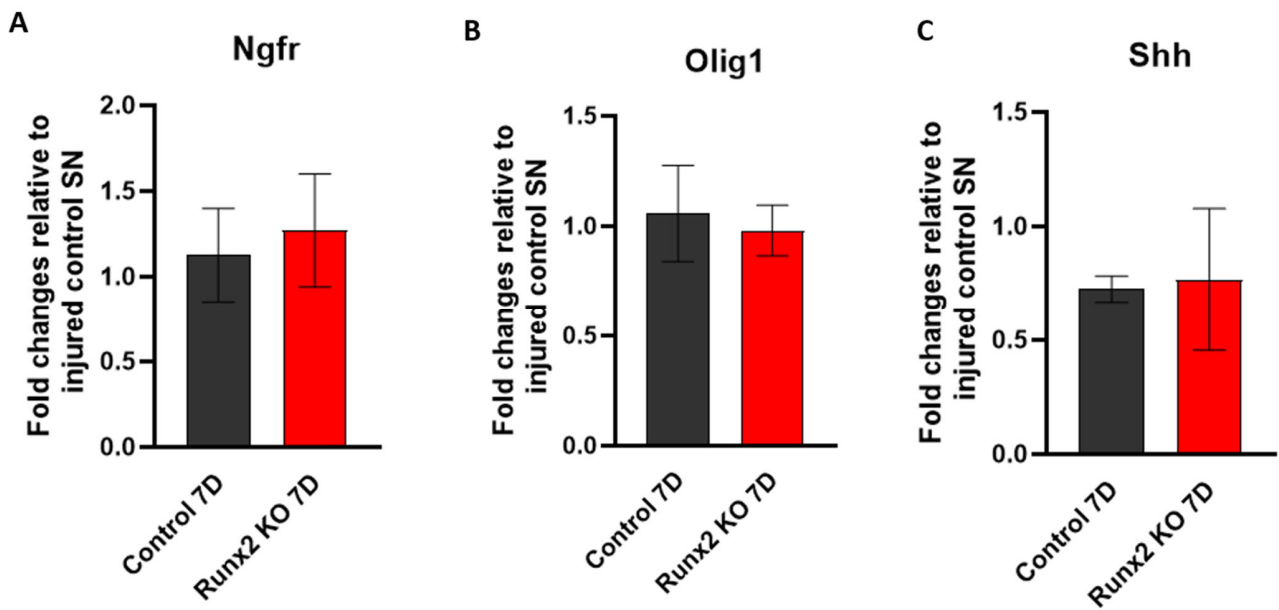
**Figure 60: Nerve growth factor receptor, oligodendrocyte transcription factor 1 and sonic hedgehog are not regulated by Runx2 after a crush injury.**

(A-C) Graphs plotted for gene expression by quantitative PCR, 7 days (7D) following a sciatic nerve (SN) crush injury in control and Schwann cell specific Runx2 knockout mice (Runx2 KO). No significant difference for gene expression of (A) nerve growth factor receptor (Ngfr), (B) oligodendrocyte transcription factor 1 (Olig1) and (C) sonic hedgehog (Shh), in the distal SN of injured Runx2 KO mice relative to injured control SN (n=3 for each group). GAPDH was used as a reference control. (A-C) There was no statistically significant difference ($p > 0.05$; not significant) between the two studied groups. Error bars represent (±) SEM.

## 5.6 Discussion and conclusions

After an injury to the peripheral nerve, several transcription factors are upregulated distal to the injury site and have been shown to be important for conversion of SCs into the repair phenotype, potential role in regulating macrophage recruitment as well as regulating the microenvironment of the distal nerve among other functions (Parkinson *et a*l., 2008; Arthur-Farraj *et al*., 2012; Doddrell *et al*., 2012; Roberts *et al*., 2017). In this context, although the role of few transcription factors has been studied (e.g Sox2, Pax3, c-Jun), recent in-silico analysis of the peripheral nerve post injury, suggests that there are several more transcription factors that are regulated after injury with no previously described role (Barrette *et al.,* 2010; Arthur-Farraj *et al.,* 2012; Hung *et al.,* 2015; Clements *et al.,* 2017; Li *et al.,* 2021). Runx2 is one such transcription factor that was shown to be upregulated post PNI however there is not much known about Runx2's involvement in peripheral nerve repair.

Hung *et al.* (2015) carried out analysis of injury-induced enhancers by Chromatin Immunoprecipitation sequencing (ChiP-seq) and identified a c-Jun binding enhancer motif proximal to Runx2 gene. siRNA mediated knockdown of c-Jun in primary rat SCs downregulated the expression of Runx2 showing that cJun is required for the activation of Runx2 however, Runx2 siRNA did not show the same effect on c-Jun (Hung *et al*., 2015). The authors also showed upregulation of Runx2 in Sox10 positive SCs, distal to

transection site, 3 days after mouse sciatic nerve injury (Hung *et al*., 2015). This data was in agreement to that of Arthur-Farraj *et al.* (2017), wherein the authors by qPCR showed Runx2 upregulation in the first 24 h in the distal nerve stump following sciatic nerve transection injury in wild-type mice. Moreover, Runx2 showed approximately 80-times fold change upregulation, 7 days after injury relative to an intact nerve in the same model. Their quantification for relative expression of Runx2 in cultured mouse SCs, nerve-derived fibroblasts and LPS-treated macrophages showed the highest expression in SCs and low expression in fibroblasts (Arthur-Farraj *et al.*, 2017). Ding *et al.* (2018) also reported an upregulation of Runx2, 3 days post-crush injury in rats with highest expression at 7 days post-injury and by immunohistochemistry showed Runx2 expression in SCs.

In this study, analysis of previously published RNA data for the expression of Runx2 in the distal nerve stump after sciatic nerve injury confirmed the dramatic fold change upregulation of Runx2. This upregulation was observed to be significantly higher in comparison to two other well-documented transcription factors – c-Jun and Sox2, that are known to be upregulated following injury (Parkinson *et a*l., 2008; Arthur-Farraj *et al.,* 2012; Fontana *et al*., 2012; Roberts *et al*., 2017; Li *et al*., 2021). Moreover, microarray and single cell RNA-seq data of the sciatic nerve following injury showed that SCs are the main source of this upregulation. The results of Dr. Xinpeng Dun and Rong Hu of our research group, who were the main lead on this project, along with my work (presented

in this thesis), confirmed Runx2 expression and upregulation by SCs distal to the injury site following mouse sciatic nerve injury.

Embryonic deletion of global Runx2 is not viable due to absence of bone ossification and respiratory failure (Otto *et al*., 1997; Komori *et al*., 1997). Therefore, to study the role of Runx2 in PNR, we generated SC-specific knockout of Runx2 using the previously described P0-Cre mouse line. Our research group's work on this mouse line showed an inhibitory role of Runx2 in SC proliferation after injury. Specifically, they reported increased SC proliferation in SC-specific Runx2 knockout mice, 7 days following sciatic nerve transection injury (Rong *et al*., 2021, unpublished). Their experiments on SC migration showed impaired SC migration in the nerve bridge of the SC-specific Runx2 knockout mice, 6 days after a sciatic nerve transection injury (Rong *et al*., 2021, unpublished ), suggesting that Runx2 is a promoter of SC migration following PNI. Their work on axon regeneration showed reduced axonal growth 7 days post-sciatic nerve crush injury and a transient delay in functional recovery on day 11 and day 13 following crush injury in the SC-specific Runx2 knockout mice (Rong *et al*., 2021, unpublished ). However, my data on axon innervation of the tibial nerve, 21 days following nerve crush injury showed no difference in the axon numbers. This data along with the functional recovery studies by my research group suggested that in the absence of Runx2 in SCs, any axonal outgrowth defect is corrected by day 21 following a crush injury.

The work of my research group also showed normal macrophage recruitment, however immunohistochemistry and electron microscopy studies exhibited an impaired macrophage clearance in SC-specific Runx2 knockout mice by day 28 following a crush injury (Rong *et al.,* 2021, unpublished). Finally, my research group observed low levels of myelin proteins (Mbp and Mpz) in the tibial nerve of SC-specific Runx2 knockout mice, 28 days following a crush injury (Rong *et al.,* 2021, unpublished). Transmission electron microscopy (TEM) on tibial nerves, 28 days after crush injury also showed a remyelination defect in the SC-specific Runx2 knockout mice (Rong et al., 2021, unpublished). My work on studying the remyelination defect in the tibial nerve of SC-specific Runx2 knockout mice at an earlier time point of 21 days following crush injury also saw a significant defect in the number of myelinated axons compared to the control. Moreover, as mentioned, there was no difference in the axon numbers in the tibial nerve 21 days following crush injury implying that the myelination defect is due to impaired ability of SCs to remyelinate axons (in this thesis). My examination of the sciatic nerve of postnatal day 7 (P7) SC-specific Runx2 knockout mouse pups and as studied in two-month-old animals by my research group (Rong *et al.,* 2021, unpublished) showed that the myelination defect appears to not be developmental or in intact adult nerves but instead, it is injury mediated.

Fry *et al*. (2007) showed that post-PNI, invading macrophages express Nogo receptors - NgR1 and NgR2 and show reduced binding to myelin and their ligands such as myelin

associated glycoprotein (MAG). This binding activates Rho-associated (RhoA) kinase in macrophages and induce a repulsive signaling in macrophages for clearance (Fry *et al.*, 2007). The authors also observed that in rat sciatic nerves, 14 days after a crush injury, regenerated axons with new myelin have fewer macrophages than transected nerves that lack axons and myelin at the same timepoint. Almost all macrophages in the transected nerves still lie within the SC basal lamina while in the crushed and regenerated nerves the majority macrophages have migrated out the SC basal lamina (Fry *et al.,* 2007). Our data showed a remyelination defect by SCs in SC-specific Runx2 knockout mice whereas the work of my research group showed a macrophage clearance defect in the same mouse model. Taken together, it can be suggested that impaired SC remyelination in SC-specific Runx2 knockout mice prevents the binding of myelin to Nogo receptors on macrophages and subsequent activation of RhoA-induced repulsive signalling in macrophages. This in turn results in an impaired macrophage efflux in the SC-specific Runx2 knockout mice.

Building on Hung *et al.* (2015)'s work that saw a downregulation of sonic hedgehog (Shh) and oligodendrocyte transcription factor 1 (Olig1), after siRNA mediated knockdown of Runx2 in primary rat SCs, in this study, I looked to confirm whether these two genes were injury-associated targets of Runx2 in our mouse model. Additionally, my research group's in silico work had shown nerve growth factor receptor (Ngfr) as a potential injury-induced SC target of Runx2 (Rong *et al*., 2021, unpublished). However, my qPCR

results showed no significant difference in gene expression for all three candidates in the distal sciatic nerve of SC-specific Runx2 knockout mouse 7 days after a crush injury. Additionally, even at protein level, SC-specific Runx2 knockout in mice did not affect Ngfr expression level 7 days after sciatic nerve injury (both transection and crush). Therefore, our data showed that Runx2 appears not to drive the activation of injury-associated genes - Ngfr, Olig1 and Shh, following peripheral nerve injury.

# CHAPTER 6: GENERAL DISCUSSION AND FUTURE WORK

Despite the enhancement in surgical methods, peripheral nerve injuries and specially transection injuries still pose a huge challenge to surgeons. Presently, several microsurgical repair techniques such as direct repair, autograft or allograft transplantation, fibrin glue and the use of biological and synthetic nerve guidance conduits have been employed in the clinical setting (Kornfeld *et al.*, 2019; Hussain *et al*., 2020). Nevertheless, complete functional recovery is very rarely achieved. Therefore, current research is centred on using suitable therapeutic cells (e.g. SCs or stem cell-derived alternatives) or novel adjuvant therapeutic strategies to enhance functional recovery. Thus, understanding the key molecular mechanisms of how cells guide regenerating axons across the injury site to finally innervate the distal end of the nerve, has great potential to underpin the future development of novel therapeutic strategies for repairing damaged peripheral nerves.

Repair SCs are integral to axon regeneration after a peripheral nerve injury. Besides being important for Wallerian degeneration, SCs regulate and express several neurotrophic factors, axon guidance molecules, cytokines, transcription factors, extracellular matrix proteins and signalling pathways to create a permissive environment for axonal growth. However, there is still a knowledge gap in the mechanism of PNR as well as all the roles fulfilled by SCs. In the current study I had therefore attempted to

elucidate the role of Netrin-1 and its receptor DCC as well as Runx2 transcription factor in peripheral nerve repair (PNR) after injury. Netrin-1 is one of the best characterised molecule for its role in axon guidance during development (Kennedy *et al.*, 1994; Serafini *et al.*, 1994). However, even though Netrin-1 and DCC have attracted attention regarding its potential in PNR in mainly in vitro studies, the underlying molecular mechanism of the molecule-receptor duo in regulating adult PNR in vivo has not been determined. This is mainly due to the embryonic lethality of Netrin-1 and DCC knockout mice and owing to contradictory results observed in literature largely due to the dose dependent functionality of Netrin-1 (Serafini *et al.*, 1996; Fazeli *et al.*, 1997). Therefore, initially Netrin-1 and DCC were primed as exciting new targets to study in SCs and PNR, following injury. This study also appeared to be feasible in vivo with the availability of Netrin-1 (Dominici *et al.*, 2017) and DCC (Krimpenfort *et al.*, 2012) floxed mouse lines as well as the P0-Cre (Feltri *et al.*, 1999), and R26-CreERT2 mice (Hameyer *et al.*, 2007). Thus, I originally thought I could circumvent embryonic lethality in Netrin-1 and DCC mice that would provide good animal models to study PNR.

In my experiments, I showed novel downregulation and expression of Netrin-1 in the PNS and most importantly showed that SC-derived Netrin-1 is not important for PNR. Although I observed several aberrant trajectories of axons in the nerve bridge of SC-specific Netrin-1 knockout mice following transection injury, end-target innervation by the axons was not affected. Potential future work could involve looking at axon

branching/sprouting in my mouse model. It is possible that the aberrant trajectories in the nerve bridge could mainly be caused by axon branches in the nerve bridge. However use of axonal markers in immunohistochemistry makes it difficult to look at the trajectory and branching of single axons. Therefore, it would be useful to sparsely label and quantify a subset of axons that are misdirected in the nerve bridge. For instance, using tamoxifen-induced, Cre-mediated recombination in fluorescently labelled single neurons to label distinct neuronal populations (Young *et al.,* 2008). Or by using mice that fluorescently label all axons under the control of a tamoxifen-inducible Cre but administer low doses of Tamoxifen in order to activate fluorescence in a few axons, as has been done previously for SCs (Gomez-Sanchez *et al*., 2017). However, in my mouse model, SC-specific Netrin-1 knockout is mediated by the P0-Cre transgene which would mean that along with neurons, the SCs will also display fluorescence making it difficult to distinguish between the SCs and the axons. Therefore, using other transgenic mice not reliant on a Cre system such as the thy1-YFP-H mice that express YFP in a subset of axons could be crossed with my mouse model and be used to study single axon branching and for quantification of axons following injury (Feng *et al*., 2000; Barrette *et al*., 2008). This model of sparsely labelling axons would also be useful to study the similar aberrant trajectories of axons observed in the nerve bridge of the DCC global knockout mice.

Seven days following a sciatic nerve crush injury in my SC-specific Netrin-1 knockout mouse model, axon outgrowth was comparable to that of the control. There is a

possibility that at earlier time-points, for instance on day 4 post-crush injury, there could be a delay in axon outgrowth which is corrected by day 7 (as shown in this thesis). Therefore, future experiments could be done to look at crush injury in my mouse model at earlier time-points to confirm this. Additionally, using alternative axon markers besides the neurofilament antibody (demonstrated in this thesis) to study axon regeneration such as growth-associated protein-43 (GAP-43), the neurotransmitter calcitonin gene-related peptide (CGRP) and galanin to label regenerating sensory and motor axons following injury (Arthur-Farraj et al., 2012; Carriel *et al.*, 2017). Another potential set of experiments would be to perform functional tests such as Hargreaves test (thermal pain sensation) and Von Frey hair test (mechanical sensitivity) to specifically assess sensory neuron regeneration following a crush injury in both SC-specific Netrin-1 knockout and DCC global knockout mouse models.

By immunohistochemistry I showed that Netrin-1 is localised to several other cell types other than SCs such as the axons, epineurial, perineurial, endoneurial and endothelial cells. Although the single-cell RNA sequencing data presented in this thesis provided the basis of the immunohistochemical analysis, in future, it would be also useful to confirm cell-specific mRNA expression of Netrin-1 by other techniques such as RNAscope or hybridisation chain reaction (Wang *et al.*, 2012). Moreover, using PLP-GFP mice I showed Netrin-1 expression mainly in non-myelinating SCs. However PLP-GFP mice show GFP expression in both myelinating and non-myelinating Remak SCs of the intact sciatic

nerve. Although the two cell types are disceriable by the intensity of GFP expression and their structure in an intact peripheral nerve, it would be useful in the future to use a Remak SC-specific marker such as glial fibrillary acidic protein (GFAP) and L1 neural cell adhesion molecule (L1CAM) to confirm Netrin-1 expression in the Remak SCs (Jessen and Mirsky, 2019).

Global knockout of DCC in adult mice also showed that DCC might not be important for axonal regrowth and functional recovery after PNI. This contrasts with previous work on the CNS that showed that both Netrin-1 and DCC deficient mouse embryos had significant defects in the development of commissural axonal projections (Serafini *et al.*, 1996; Fazeli *et al.*, 1997). However, I could not study the effect of Netrin-1 global knockout in adult mice on PNR, due to a failure in Cre-mediated deletion of Netrin-1.

Therefore, generating a complete knockout of Netrin-1 would be a potential future aim to determine how complete deletion of Netrin-1 affects PNR. In another project in my lab, we used Tamoxifen in P0-CreER[+] Ai9 Rosa tdTomato [loxP/loxP] mice. The Ai9 Rosa tdTomato mouse model has a loxP-flanked STOP cassette that prevents the transcription of a CAG promoter- mediated red fluorescent protein variant (tdTomato) which is inserted into the Gt(ROSA)26Sor locus (Madisen *et al.*, 2010). In the P0-CreER[+] Ai9 Rosa tdTomato [loxP/loxP] mice, administration of Tamoxifen would induce expression of red fluorescent protein (RFP) in SCs after removal of the floxed stop cassette through Cre-

mediated recombination. However, similar to the Netrin-1 mice, we did not see expression of RFP in SCs thus suggesting that Tamoxifen-inducible Cre systems are not always reliable and can often require intensive optimisation to determine the optimal dose and time required to achieve Cre-mediated recombination. Thus, in future experiments, further optimisation of the dose, method of Tamoxifen delivery and waiting time after dosage could be useful in knocking out Netrin-1 globally in the mouse model presented in this thesis.

Another option would be to potentially breed in a Cre reporter with expression of fluorescent proteins (as mentioned in the above example) such as the Ai9 Rosa tdTomato mice that express tdTomato fluorescence after Cre-mediated recombination (Madisen *et al*., 2010). This could be useful to study Cre-mediated recombination in my mouse model at a cellular level. Alternative route would be to breed Ntn1$^{loxP/loxP}$ mice with other Tamoxifen inducible Cre mice such as CAGGCre-ER$^{TM}$ transgenic mice (Hayashi and McMahon, 2002) or UBC-Cre-ERT2 mice (Ruzankina *et al*., 2007) to get a complete knockout of Netrin-1. If this is achieved, it would also be interesting to study angiogenesis and blood-nerve-barrier function of Netrin-1, if any, after PNI as my data showed downregulation of Netrin-1 largely in perineurial and endothelial cells following injury.

Netrin-1 has been shown to have a dual role in angiogenesis and morphogenesis of the vasculature during vertebrate development, with inhibition shown to be mediated by

UNC5B receptor and its pro-angiogenic role mediated by binding to its other receptor CD146, also known as melanoma cell adhesion molecule (MCAM) (Park *et al*., 2004; Wilson *et al.,* 2006; Larrivée *et al.,* 2007; Castets and Mehlen., 2010; Tu *et al*., 2015). Netrin-1 was also shown to be an inhibitor of UNC5B-expressing primary human umbilical artery endothelial cells (Lu *et al.,* 2004). In this context, CD146 and UNC5B are primed as important receptors, in conjunction with Netrin-1, to study angiogenesis and blood-nerve-barrier function in mice after PNI. Possibly the repulsive UNC5 receptors, in comparison to DCC, might be better candidates for Netrin-1-mediated axon guidance after a PNI. Therefore, future work on mice lacking UNC5 receptors such as UNC5B might be of interest to fully investigate this.

Another brief project presented in this thesis demonstrated the role of Runx2 transcription factor in PNR. The effect of transcription factors is often multiplied as one transcription factor can bind to several sites (promoter or enhancer) of one gene; one transcription factor can bind to several genes; and more than one transcription factor can regulate one gene. Not much was previously known about Runx2 in the peripheral nerve and its role in PNR. However, in this thesis, in collaboration with members of my lab group, we showed an important phenotype in mice lacking Runx2 in SCs. This included a defect in SC migration and axon regrowth, increase in SC proliferation, reduced remyelination of axons by SCs and impaired efflux of macrophages, after PNI.

These results suggest a novel role of Runx2 as a key regulator of SC plasticity and PNR following injury.

Future work on this project could involve looking at immune cells other than macrophages such as neutrophils in the SC-specific Runx2 knockout mice following injury. This would be of interest to see if there is any defect in their entry and clearance after PNI. Moreover, I can look to study Nogo receptor expression by macrophages as well as the expression of their ligands such as myelin associated glycoprotein (MAG) following injury in the SC-specific Runx2 knockout mice (Fry *et al*., 2007). This would be useful to test our hypothesis that impaired myelination in SC-specific Runx2 knockout mice reduces the repulsion of macrophages via the Nogo receptor-MAG binding and thus prevents the efflux of macrophages from the injured nerve following regeneration.

Runx2 is known to be upregulated by c-Jun after peripheral nerve injury however, Runx2 injury-associated targets are not well-known (Hung *et al*., 2015). In-silico analysis by my research group and previous in vitro work by Hung *et al*. (2015) identified several potential genes that are regulated by Runx2 following injury. However, my data on SC-specific Runx2 knockout mice could not validate three of those genes (Olig1, Shh and Ngfr) as Runx2 targets. Future work on Runx2 would thus, be poised to identify the injury-based genes upregulated by Runx2 following injury.

# 7. REFERENCES

1.  Ackerman, S.L., Kozak, L.P., Przyborski, S.A., Rund, L.A., Boyer, B.B. and Knowles, B.B., 1997. The mouse rostral cerebellar malformation gene encodes an UNC-5-like protein. Nature, 386(6627), pp.838-842.

2.  Adam, M., Potter, A.S. and Potter, S.S., 2017. Psychrophilic proteases dramatically reduce single-cell RNA-seq artifacts: a molecular atlas of kidney development. Development, 144(19), pp.3625-3632.

3.  Adya, N., Castilla, L.H. and Liu, P.P., 2000. Function of CBFβ/Bro proteins. In Seminars in cell & developmental biology (Vol. 11, No. 5, pp. 361-368). Academic Press.

4.  Aibar, S., González-Blas, C.B., Moerman, T., Huynh-Thu, V.A., Imrichova, H., Hulselmans, G., Rambow, F., Marine, J.C., Geurts, P., Aerts, J. and van den Oord, J., 2017. SCENIC: single-cell regulatory network inference and clustering. Nature methods, 14(11), pp.1083-1086.

5.  Aitken, J.T., Sharman, M. and Young, J.Z., 1947. Maturation of regenerating nerve fibres with various peripheral connexions. Journal of Anatomy, 81(Pt 1), p.1.

6.  Almad, A., Sahinkaya, F.R. and McTigue, D.M., 2011. Oligodendrocyte fate after spinal cord injury. Neurotherapeutics, 8, pp.262-273.

7.  Al-Majed, A.A., Neumann, C.M., Brushart, T.M. and Gordon, T., 2000. Brief electrical stimulation promotes the speed and accuracy of motor axonal regeneration. Journal of Neuroscience, 20(7), pp.2602-2608.

8.  Amado, S., Simoes, M.J., da Silva, P.A., Luís, A.L., Shirosaki, Y., Lopes, M.A., Santos, J.D., Fregnan, F., Gambarotta, G., Raimondo, S. and Fornaro, M., 2008. Use of hybrid chitosan membranes and N1E-115 cells for promoting nerve regeneration in an axonotmesis rat model. Biomaterials, 29(33), pp.4409-4419.

9.    Andrews, G.L., Tanglao, S., Farmer, W.T., Morin, S., Brotman, S., Berberoglu, M.A., Price, H., Fernandez, G.C., Mastick, G.S., Charron, F. and Kidd, T., 2008. Dscam guides embryonic axons by Netrin-dependent and-independent functions. Development, 135(23), pp.3839-3848.

10.   Arthur-Farraj, P., Wanek, K., Hantke, J., Davis, C.M., Jayakar, A., Parkinson, D.B., Mirsky, R. and Jessen, K.R., 2011. Mouse schwann cells need both NRG1 and cyclic AMP to myelinate. Glia, 59(5), pp.720-733.

11.   Arthur-Farraj, P.J., Latouche, M., Wilton, D.K., Quintes, S., Chabrol, E., Banerjee, A., Woodhoo, A., Jenkins, B., Rahman, M., Turmaine, M. and Wicher, G.K., 2012. c-Jun reprograms Schwann cells of injured nerves to generate a repair cell essential for regeneration. Neuron, 75(4), pp.633-647.

12.   Arthur-Farraj, P.J., Morgan, C.C., Adamowicz, M., Gomez-Sanchez, J.A., Fazal, S.V., Beucher, A., Razzaghi, B., Mirsky, R., Jessen, K.R. and Aitman, T.J., 2017. Changes in the coding and non-coding transcriptome and DNA methylome that define the Schwann cell repair phenotype after nerve injury. Cell reports, 20(11), pp.2719-2734.

13.   Atanasoski, S., Boentert, M., De Ventura, L., Pohl, H., Baranek, C., Beier, K., Young, P., Barbacid, M. and Suter, U., 2008. Postnatal Schwann cell proliferation but not myelination is strictly and uniquely dependent on cyclin-dependent kinase 4 (cdk4). Molecular and cellular neuroscience, 37(3), pp.519-527.

14.   Atanasoski, S., Scherer, S.S., Sirkowski, E., Leone, D., Garratt, A.N., Birchmeier, C. and Suter, U., 2006. ErbB2 signaling in Schwann cells is mostly dispensable for maintenance of myelinated peripheral nerves and proliferation of adult Schwann cells after injury. Journal of Neuroscience, 26(7), pp.2124-2131.

15.   Babetto, E., Beirowski, B., Janeckova, L., Brown, R., Gilley, J., Thomson, D., Ribchester, R.R. and Coleman, M.P., 2010. Targeting NMNAT1 to axons and

synapses transforms its neuroprotective potency in vivo. Journal of Neuroscience, 30(40), pp.13291-13304.

16. Bai, L., Mei, X., Shen, Z., Bi, Y., Yuan, Y., Guo, Z., Wang, H., Zhao, H., Zhou, Z., Wang, C. and Zhu, K., 2017. Netrin-1 improves functional recovery through autophagy regulation by activating the AMPK/mTOR signaling pathway in rats with spinal cord injury. Scientific reports, 7(1), pp.1-10.

17. Baichwal, R.R., Bigbee, J.W. and DeVries, G.H., 1988. Macrophage-mediated myelin-related mitogenic factor for cultured Schwann cells. Proceedings of the National Academy of Sciences, 85(5), pp.1701-1705.

18. Balakrishnan, A., Belfiore, L., Chu, T.H., Fleming, T., Midha, R., Biernaskie, J. and Schuurmans, C., 2021. Insights into the role and potential of schwann cells for peripheral nerve repair from studies of development and injury. Frontiers in Molecular Neuroscience, 13, p.608442.

19. Balakrishnan, A., Stykel, M.G., Touahri, Y., Stratton, J.A., Biernaskie, J. and Schuurmans, C., 2016. Temporal analysis of gene expression in the murine Schwann cell lineage and the acutely injured postnatal nerve. PLoS One, 11(4), p.e0153256.

20. Bannerman, P., Ara, J., Hahn, A., Hong, L., McCauley, E., Friesen, K. and Pleasure, D., 2008. Peripheral nerve regeneration is delayed in neuropilin 2–deficient mice. Journal of neuroscience research, 86(14), pp.3163-3169.

21. Bannerman, P.G., Mirsky, R., Jessen, K.R., Timpl, R. and Duance, V.C., 1986. Light microscopic immunolocalization of laminin, type IV collagen, nidogen, heparan sulphate proteoglycan and fibronectin in the enteric nervous system of rat and guinea pig. Journal of neurocytology, 15, pp.733-743.

22. Barnes, P.J. and Adcock, I.M., 1995. Transcription factors. Clinical & Experimental Allergy, 25, pp.46-49.

23. Baron-Van Evercooren, A., Gansmüller, A., Gumpel, M., Baumann, N. and Kleinman, H.K., 1986. Schwann cell differentiation in vitro: extracellular matrix deposition and interaction. Developmental neuroscience, 8(3), pp.182-196.

24. Barrette, B., Calvo, E., Vallières, N. and Lacroix, S., 2010. Transcriptional profiling of the injured sciatic nerve of mice carrying the Wld (S) mutant gene: identification of genes involved in neuroprotection, neuroinflammation, and nerve regeneration. Brain, behavior, and immunity, 24(8), pp.1254-1267.

25. Barrette, B., Hébert, M.A., Filali, M., Lafortune, K., Vallieres, N., Gowing, G., Julien, J.P. and Lacroix, S., 2008. Requirement of myeloid cells for axon regeneration. Journal of Neuroscience, 28(38), pp.9363-9376.

26. Battista, A. and Cravioto, H., 1981. Neuroma formation and prevention by fascicle ligation in the rat. Neurosurgery, 8(2), pp.191-204.

27. Bayat, M., Baluchnejadmojarad, T., Roghani, M., Goshadrou, F., Ronaghi, A. and Mehdizadeh, M., 2012. Netrin-1 improves spatial memory and synaptic plasticity impairment following global ischemia in the rat. Brain research, 1452, pp.185-194.

28. Beirowski, B., Adalbert, R., Wagner, D., Grumme, D.S., Addicks, K., Ribchester, R.R. and Coleman, M.P., 2005. The progressive nature of Wallerian degeneration in wild-type and slow Wallerian degeneration (WldS) nerves. BMC neuroscience, 6(1), pp.1-27.

29. Benninger, Y., Thurnherr, T., Pereira, J.A., Krause, S., Wu, X., Chrostek-Grashoff, A., Herzog, D., Nave, K.A., Franklin, R.J., Meijer, D. and Brakebusch, C., 2007. Essential and distinct roles for cdc42 and rac1 in the regulation of Schwann cell biology during peripheral nervous system development. The Journal of cell biology, 177(6), pp.1051-1061.

30. Bermingham, J.R., Scherer, S.S., O'Connell, S., Arroyo, E., Kalla, K.A., Powell, F.L. and Rosenfeld, M.G., 1996. Tst-1/Oct-6/SCIP regulates a unique step in peripheral myelination and is required for normal respiration. Genes & development, 10(14), pp.1751-1762.

31. Birchmeier, C. and Nave, K.A., 2008. Neuregulin-1, a key axonal signal that drives Schwann cell growth and differentiation. Glia, 56(14), pp.1491-1497.

32. Birchmeier, C., 2009. ErbB receptors and the development of the nervous system. Experimental cell research, 315(4), pp.611-618.

33. Blakemore, W.F. and Keirstead, H.S., 1999. The origin of remyelinating cells in the central nervous system. Journal of neuroimmunology, 98(1), pp.69-76.

34. Boissaud-Cooke, M., Pidgeon, T.E. and Tunstall, R., 2015. The microcirculation of peripheral nerves: the vasa nervorum. In Nerves and nerve injuries (pp. 507-523). Academic Press.

35. Bombeiro, A.L., de Melo Lima, B.H., Bonfanti, A.P. and de Oliveira, A.L.R., 2020. Improved mouse sciatic nerve regeneration following lymphocyte cell therapy. Molecular immunology, 121, pp.81-91.

36. Bouquet, C. and Nothias, F., 2007. Molecular mechanisms of axonal growth. Axon Growth and Guidance, pp.1-16.

37. Bourgin, C., Murai, K.K., Richter, M. and Pasquale, E.B., 2007. The EphA4 receptor regulates dendritic spine remodeling by affecting β1-integrin signaling pathways. The Journal of cell biology, 178(7), pp.1295-1307.

38. Boyd, J.G. and Gordon, T., 2001. The neurotrophin receptors, trkB and p75, differentially regulate motor axonal regeneration. Journal of neurobiology, 49(4), pp.314-325.

39. Boyer, N.P. and Gupton, S.L., 2018. Revisiting netrin-1: one who guides (axons). Frontiers in cellular neuroscience, 12, p.221.

40. Boyles, J.K., Zoellner, C.D., Anderson, L.J., Kosik, L.M., Pitas, R.E., Weisgraber, K., Hui, D.Y., Mahley, R.W., Gebicke-Haerter, P.J. and Ignatius, M.J., 1989. A role for apolipoprotein E, apolipoprotein AI, and low density lipoprotein receptors in cholesterol transport during regeneration and remyelination of the rat sciatic nerve. The Journal of clinical investigation, 83(3), pp.1015-1031.

41. Bozkurt, A., Tholl, S., Wehner, S., Tank, J., Cortese, M., mon O'Dey, D., Deumens, R., Lassner, F., Schügner, F., Gröger, A. and Smeets, R., 2008. Evaluation of functional nerve recovery with Visual-SSI—A novel computerized approach for the assessment of the static sciatic index (SSI). Journal of neuroscience methods, 170(1), pp.117-122.

42. Bradke, F., Fawcett, J.W. and Spira, M.E., 2012. Assembly of a new growth cone after axotomy: the precursor to axon regeneration. Nature Reviews Neuroscience, 13(3), pp.183-193.

43. Brecknell, J.E. and Fawcett, J.W., 1996. Axonal regeneration. Biological Reviews of the Cambridge Philosophical Society, 71(2), pp.227-255.

44. Bremer, M., Fröb, F., Kichko, T., Reeh, P., Tamm, E.R., Suter, U. and Wegner, M., 2011. Sox10 is required for Schwann-cell homeostasis and myelin maintenance in the adult peripheral nerve. Glia, 59(7), pp.1022-1032.

45. Britsch, S., Goerich, D.E., Riethmacher, D., Peirano, R.I., Rossner, M., Nave, K.A., Birchmeier, C. and Wegner, M., 2001. The transcription factor Sox10 is a key regulator of peripheral glial development. Genes & development, 15(1), pp.66-78.

46. Brose, K. and Tessier-Lavigne, M., 2000. Slit proteins: key regulators of axon guidance, axonal branching, and cell migration. Current opinion in neurobiology, 10(1), pp.95-102.

47. Brosius Lutz, A., Chung, W.S., Sloan, S.A., Carson, G.A., Zhou, L., Lovelett, E., Posada, S., Zuchero, J.B. and Barres, B.A., 2017. Schwann cells use TAM receptor-

mediated phagocytosis in addition to autophagy to clear myelin in a mouse model of nerve injury. Proceedings of the National Academy of Sciences, 114(38), pp.E8072-E8080.

48. Bruce, F.M., Brown, S., Smith, J.N., Fuerst, P.G. and Erskine, L., 2017. DSCAM promotes axon fasciculation and growth in the developing optic pathway. Proceedings of the National Academy of Sciences, 114(7), pp.1702-1707.

49. Brügger, V., Duman, M., Bochud, M., Münger, E., Heller, M., Ruff, S. and Jacob, C., 2017. Delaying histone deacetylase response to injury accelerates conversion into repair Schwann cells and nerve regeneration. Nature Communications, 8(1), p.14272.

50. Bull, S.J., Bin, J.M., Beaumont, E., Boutet, A., Krimpenfort, P., Sadikot, A.F. and Kennedy, T.E., 2014. Progressive disorganization of paranodal junctions and compact myelin due to loss of DCC expression by oligodendrocytes. Journal of Neuroscience, 34(29), pp.9768-9778.

51. Bunge, M.B., Wood, P.M., Tynan, L.B., Bates, M.L. and Sanes, J.R., 1989. Perineurium originates from fibroblasts: demonstration in vitro with a retroviral marker. Science, 243(4888), pp.229-231.

52. Bunge, R.P., 1987. Tissue culture observations relevant to the study of axon-Schwann cell interactions during peripheral nerve development and repair. Journal of experimental biology, 132(1), pp.21-34.

53. Carmeliet, P. and Tessier-Lavigne, M., 2005. Common mechanisms of nerve and blood vessel wiring. Nature, 436(7048), pp.193-200.

54. Carr M. J., Toma J. S., Johnston A. P. W., Steadman P. E., Yuzwa S. A., Mahmud N., et al. (2019). Mesenchymal precursor cells in adult nerves contribute to mammalian tissue repair and regeneration. Cell Stem Cell 24 240-256.e9. 10.1016/j.stem.2018.10.024

55. Carr, L., Parkinson, D.B. and Dun, X.P., 2017. Expression patterns of Slit and Robo family members in adult mouse spinal cord and peripheral nervous system. PloS one, 12(2).

56. Carriel, V., Garzón, I., Campos, A., Cornelissen, M. and Alaminos, M., 2017. Differential expression of GAP-43 and neurofilament during peripheral nerve regeneration through bio-artificial conduits. Journal of tissue engineering and regenerative medicine, 11(2), pp.553-563.

57. Carroll, S.L., Miller, M.L., Frohnert, P.W., Kim, S.S. and Corbett, J.A., 1997. Expression of neuregulins and their putative receptors, ErbB2 and ErbB3, is induced during Wallerian degeneration. Journal of Neuroscience, 17(5), pp.1642-1659.

58. Castets, M. and Mehlen, P., 2010. Netrin-1 role in angiogenesis: to be or not to be a pro-angiogenic factor?. Cell Cycle, 9(8), pp.1466-1471.

59. Cattin, A.L., Burden, J.J., Van Emmenis, L., Mackenzie, F.E., Hoving, J.J., Calavia, N.G., Guo, Y., McLaughlin, M., Rosenberg, L.H., Quereda, V. and Jamecna, D., 2015. Macrophage-induced blood vessels guide Schwann cell-mediated regeneration of peripheral nerves. Cell, 162(5), pp.1127-1139.

60. Chambers, I. and Tomlinson, S.R., 2009. The transcriptional foundation of pluripotency.

61. Chan, J.R., Cosgaya, J.M., Wu, Y.J. and Shooter, E.M., 2001. Neurotrophins are key mediators of the myelination program in the peripheral nervous system. Proceedings of the National Academy of Sciences, 98(25), pp.14661-14668.

62. Chan, S.Y., Zheng, H., Su, M.W., Wilk, R., Killeen, M.T., Hedgecock, E.M. and Culotti, J.G., 1996. UNC-40, a C. elegans homolog of DCC (Deleted in Colorectal Cancer), is required in motile cells responding to UNC-6 netrin cues. Cell, 87(2), pp.187-195.

63. Chao, T., Pham, K., Steward, O. and Gupta, R., 2008. Chronic nerve compression injury induces a phenotypic switch of neurons within the dorsal root ganglia. Journal of Comparative Neurology, 506(2), pp.180-193.

64. Chen, B., Banton, M.C., Singh, L., Parkinson, D.B. and Dun, X.P., 2021a. Single cell transcriptome data analysis defines the heterogeneity of peripheral nerve cells in homeostasis and regeneration. Frontiers in Cellular Neuroscience, 15, p.624826.

65. Chen, B., Chen, Q., Parkinson, D.B. and Dun, X.P., 2019a. Analysis of Schwann cell migration and axon regeneration following nerve injury in the sciatic nerve bridge. Frontiers in molecular neuroscience, 12, p.308.

66. Chen, J.T.C., Schmidt, L., Schürger, C., Hankir, M.K., Krug, S.M. and Rittner, H.L., 2021b. Netrin-1 as a multitarget barrier stabilizer in the peripheral nerve after injury. International Journal of Molecular Sciences, 22(18), p.10090.

67. Chen, P., Cescon, M., Zuccolotto, G., Nobbio, L., Colombelli, C., Filaferro, M., Vitale, G., Feltri, M.L. and Bonaldo, P., 2015. Collagen VI regulates peripheral nerve regeneration by modulating macrophage recruitment and polarization. Acta neuropathologica, 129, pp.97-113.

68. Chen, R., Yang, X., Zhang, B., Wang, S., Bao, S., Gu, Y. and Li, S., 2019b. EphA4 negatively regulates myelination by inhibiting Schwann cell differentiation in the peripheral nervous system. Frontiers in neuroscience, 13, p.1191.

69. Chen, Z.L., Yu, W.M. and Strickland, S., 2007. Peripheral regeneration. Annu. Rev. Neurosci., 30, pp.209-233.

70. Chen, Z.Y., Chai, Y.F., Cao, L., Lu, C.L. and He, C., 2001. Glial cell line-derived neurotrophic factor enhances axonal regeneration following sciatic nerve transection in adult rats. Brain research, 902(2), pp.272-276.

71. Chertov, O., Ueda, H., Xu, L.L., Tani, K., Murphy, W.J., Wang, J.M., Howard, O.Z., Sayers, T.J. and Oppenheim, J.J., 1997. Identification of human neutrophil-derived

cathepsin G and azurocidin/CAP37 as chemoattractants for mononuclear cells and neutrophils. The Journal of experimental medicine, 186(5), pp.739-747.

72. Cirulli, V. and Yebra, M., 2007. Netrins: beyond the brain. Nature reviews Molecular cell biology, 8(4), p.296.

73. Clements, M.P., Byrne, E., Guerrero, L.F.C., Cattin, A.L., Zakka, L., Ashraf, A., Burden, J.J., Khadayate, S., Lloyd, A.C., Marguerat, S. and Parrinello, S., 2017. The wound microenvironment reprograms Schwann cells to invasive mesenchymal-like cells to drive peripheral nerve regeneration. Neuron, 96(1), pp.98-114.

74. Coffman, J.A., 2003. Runx transcription factors and the developmental balance between cell proliferation and differentiation. Cell biology international, 27(4), pp.315-324.

75. Colamarino, S.A. and Tessier-Lavigne, M., 1995. The axonal chemoattractant netrin-1 is also a chemorepellent for trochlear motor axons. Cell, 81(4), pp.621-629.

76. Coleman, M.P. and Höke, A., 2020. Programmed axon degeneration: from mouse to mechanism to medicine. Nature Reviews Neuroscience, 21(4), pp.183-196.

77. Colognato, H. and Tzvetanova, I.D., 2011. Glia unglued: how signals from the extracellular matrix regulate the development of myelinating glia. Developmental neurobiology, 71(11), pp.924-955.

78. Conforti, L., Fang, G., Beirowski, B., Wang, M.S., Sorci, L., Asress, S., Adalbert, R., Silva, A., Bridge, K., Huang, X.P. and Magni, G., 2007. NAD+ and axon degeneration revisited: Nmnat1 cannot substitute for WldS to delay Wallerian degeneration. Cell Death & Differentiation, 14(1), pp.116-127.

79. D'Alonzo, R.C., Selvamurugan, N., Karsenty, G. and Partridge, N.C., 2002. Physical interaction of the activator protein-1 factors c-Fos and c-Jun with Cbfa1 for

collagenase-3 promoter activation. Journal of Biological Chemistry, 277(1), pp.816-822.

80. David, S. and Aguayo, A.J., 1981. Axonal elongation into peripheral nervous system" bridges" after central nervous system injury in adult rats. Science, 214(4523), pp.931-933.

81. Davis, J.B. and Stroobant, P., 1990. Platelet-derived growth factors and fibroblast growth factors are mitogens for rat Schwann cells. The Journal of cell biology, 110(4), pp.1353-1360.

82. de Castro, F., 2003. Chemotropic molecules: guides for axonal pathfinding and cell migration during CNS development. Physiology, 18(3), pp.130-136.

83. Decker, L., Desmarquet-Trin-Dinh, C., Taillebourg, E., Ghislain, J., Vallat, J.M. and Charnay, P., 2006. Peripheral myelin maintenance is a dynamic process requiring constant Krox20 expression. Journal of Neuroscience, 26(38), pp.9771-9779.

84. Dent, E.W. and Gertler, F.B., 2003. Cytoskeletal dynamics and transport in growth cone motility and axon guidance. Neuron, 40(2), pp.209-227.

85. Derby, A., Engleman, V.W., Frierdich, G.E., Neises, G., Rapp, S.R. and Roufa, D.G., 1993. Nerve growth factor facilitates regeneration across nerve gaps: morphological and behavioral studies in rat sciatic nerve. Experimental neurology, 119(2), pp.176-191.

86. Di Giovanni, S., Knights, C.D., Rao, M., Yakovlev, A., Beers, J., Catania, J., Avantaggiati, M.L. and Faden, A.I., 2006. The tumor suppressor protein p53 is required for neurite outgrowth and axon regeneration. The EMBO journal, 25(17), pp.4084-4096.

87. Ding, D., Zhang, P., Liu, Y., Wang, Y., Sun, W., Yu, Z., Cheng, Z. and Wang, Y., 2018. Runx2 was correlated with neurite outgrowth and schwann cell differentiation,

migration after sciatic nerve crush. Neurochemical Research, 43(12), pp.2423-2434.

88. Doddrell, R.D., Dun, X.P., Moate, R.M., Jessen, K.R., Mirsky, R. and Parkinson, D.B., 2012. Regulation of Schwann cell differentiation and proliferation by the Pax-3 transcription factor. Glia, 60(9), pp.1269-1278.

89. Dominici, C., Moreno-Bravo, J.A., Puiggros, S.R., Rappeneau, Q., Rama, N., Vieugue, P., Bernet, A., Mehlen, P. and Chédotal, A., 2017. Floor-plate-derived netrin-1 is dispensable for commissural axon guidance. Nature, 545(7654), pp.350-354.

90. Dong, Z., Brennan, A., Liu, N., Yarden, Y., Lefkowitz, G., Mirsky, R. and Jessen, K.R., 1995. Neu differentiation factor is a neuron-glia signal and regulates survival, proliferation, and maturation of rat Schwann cell precursors. Neuron, 15(3), pp.585-596.

91. Doron-Mandel, E., Fainzilber, M. and Terenzio, M., 2015. Growth control mechanisms in neuronal regeneration. FEBS letters, 589(14), pp.1669-1677.

92. Droz, B. and Leblond, C.P., 1963. Axonal migration of proteins in the central nervous system and peripheral nerves as shown by radioautography. Journal of Comparative Neurology, 121(3), pp.325-346.

93. Dun, X.P. and Parkinson, D.B., 2017. Role of netrin-1 signaling in nerve regeneration. International journal of molecular sciences, 18(3), p.491.

94. Dun, X.P. and Parkinson, D.B., 2018. Whole mount immunostaining on mouse sciatic nerves to visualize events of peripheral nerve regeneration. Schwann Cells: Methods and Protocols, pp.339-348.

95. Dun, X.P., Carr, L., Woodley, P.K., Barry, R.W., Drake, L.K., Mindos, T., Roberts, S.L., Lloyd, A.C. and Parkinson, D.B., 2019. Macrophage-derived Slit3 controls cell

migration and axon pathfinding in the peripheral nerve bridge. Cell reports, 26(6), pp.1458-1472.

96. Edström, A., Ekström, P.A.R. and Tonge, D., 1996. Axonal outgrowth and neuronal apoptosis in cultured adult mouse dorsal root ganglion preparations: effects of neurotrophins, of inhibition of neurotrophin actions and of prior axotomy. Neuroscience, 75(4), pp.1165-1174.

97. Egea, J. and Klein, R., 2007. Bidirectional Eph–ephrin signaling during axon guidance. Trends in cell biology, 17(5), pp.230-238.

98. Ellezam, B., Selles-Navarro, I., Manitt, C., Kennedy, T.E. and McKerracher, L., 2001. Expression of netrin-1 and its receptors DCC and UNC-5H2 after axotomy and during regeneration of adult rat retinal ganglion cells. Experimental neurology, 168(1), pp.105-115.

99. Essuman, K., Summers, D.W., Sasaki, Y., Mao, X., DiAntonio, A. and Milbrandt, J., 2017. The SARM1 toll/interleukin-1 receptor domain possesses intrinsic NAD+ cleavage activity that promotes pathological axonal degeneration. Neuron, 93(6), pp.1334-1343.

100. Faul, F., Erdfelder, E., Buchner, A. and Lang, A.G., 2009. Statistical power analyses using G* Power 3.1: Tests for correlation and regression analyses. Behavior research methods, 41(4), pp.1149-1160.

101. Fazal, S.V., Gomez-Sanchez, J.A., Wagstaff, L.J., Musner, N., Otto, G., Janz, M., Mirsky, R. and Jessen, K.R., 2017. Graded elevation of c-Jun in Schwann cells in vivo: gene dosage determines effects on development, remyelination, tumorigenesis, and hypomyelination. Journal of Neuroscience, 37(50), pp.12297-12313.

102. Fazeli, A., Dickinson, S.L., Hermiston, M.L., Tighe, R.V., Steen, R.G., Small, C.G., Stoeckli, E.T., Keino-Masu, K., Masu, M., Rayburn, H. and Simons, J., 1997.

Phenotype of mice lacking functional Deleted in colorectal cancer (Dec) gene. Nature, 386(6627), pp.796-804.

103. Fearon, E.R., Cho, K.R., Nigro, J.M., Kern, S.E., Simons, J.W., Ruppert, J.M., Hamilton, S.R., Preisinger, A.C., Thomas, G., Kinzler, K.W. and Vogelstein, B., 1990. Identification of a chromosome 18q gene that is altered in colorectal cancers. Science, 247(4938), pp.49-56.

104. Feltri, M.L., D'antonio, M., Previtali, S., Fasolini, M., Messing, A. and Wrabetz, L., 1999. P0-Cre transgenic mice for inactivation of adhesion molecules in SCs. Annals of the New York Academy of Sciences, 883(1), pp.116-123.

105. Feltri, M.L., Poitelon, Y. and Previtali, S.C., 2016. How Schwann cells sort axons: new concepts. The Neuroscientist, 22(3), pp.252-265.

106. Feltri, M.L., Porta, D.G., Previtali, S.C., Nodari, A., Migliavacca, B., Cassetti, A., Littlewood-Evans, A., Reichardt, L.F., Messing, A., Quattrini, A. and Mueller, U., 2002. Conditional disruption of β1 integrin in Schwann cells impedes interactions with axons. The Journal of cell biology, 156(1), pp.199-210.

107. Feng, G., Mellor, R.H., Bernstein, M., Keller-Peck, C., Nguyen, Q.T., Wallace, M., Nerbonne, J.M., Lichtman, J.W. and Sanes, J.R., 2000. Imaging neuronal subsets in transgenic mice expressing multiple spectral variants of GFP. Neuron, 28(1), pp.41-51.

108. Ferrari, N., Riggio, A.I., Mason, S., McDonald, L., King, A., Higgins, T., Rosewell, I., Neil, J.C., Smalley, M.J., Sansom, O.J. and Morris, J., 2015. Runx2 contributes to the regenerative potential of the mammary epithelium. Scientific reports, 5(1), pp.1-16.

109. Finci, L.I., Krüger, N., Sun, X., Zhang, J., Chegkazi, M., Wu, Y., Schenk, G., Mertens, H.D., Svergun, D.I., Zhang, Y. and Wang, J.H., 2014. The crystal structure of netrin-

1 in complex with DCC reveals the bifunctionality of netrin-1 as a guidance cue. Neuron, 83(4), pp.839-849.

110. Fontana, X., Hristova, M., Da Costa, C., Patodia, S., Thei, L., Makwana, M., Spencer-Dene, B., Latouche, M., Mirsky, R., Jessen, K.R. and Klein, R., 2012. c-Jun in Schwann cells promotes axonal regeneration and motoneuron survival via paracrine signaling. Journal of Cell Biology, 198(1), pp.127-141.

111. Fregnan, F., Muratori, L., Simões, A.R., Giacobini-Robecchi, M.G. and Raimondo, S., 2012. Role of inflammatory cytokines in peripheral nerve injury. Neural Regeneration Research, 7(29), p.2259.

112. Fricker, F.R., Antunes-Martins, A., Galino, J., Paramsothy, R., La Russa, F., Perkins, J., Goldberg, R., Brelstaff, J., Zhu, N., McMahon, S.B. and Orengo, C., 2013. Axonal neuregulin 1 is a rate limiting but not essential factor for nerve remyelination. Brain, 136(7), pp.2279-2297

113. Fry, E.J., Ho, C. and David, S., 2007. A role for Nogo receptor in macrophage clearance from injured peripheral nerve. Neuron, 53(5), pp.649-662.

114. Fu, S.Y. and Gordon, T., 1997. The cellular and molecular basis of peripheral nerve regeneration. Molecular neurobiology, 14, pp.67-116.

115. Fugleholm, K., 2013. The surgery of peripheral nerves (including tumors). In Handbook of clinical neurology (Vol. 115, pp. 781-802). Elsevier.

116. Fujiwara, T., Kubo, T., Koyama, Y., Tomita, K., Yano, K., Tohyama, M. and Hosokawa, K., 2008. mRNA expression changes of slit proteins following peripheral nerve injury in the rat model. Journal of chemical neuroanatomy, 36(3-4), pp.170-176.

117. Fukamachi, H. and Ito, K., 2004. Growth regulation of gastric epithelial cells by Runx3. Oncogene, 23(24), pp.4330-4335.

118. Funakoshi, H., Frisén, J., Barbany, G., Timmusk, T., Zachrisson, O., Verge, V.M. and Persson, H., 1993. Differential expression of mRNAs for neurotrophins and their receptors after axotomy of the sciatic nerve. The Journal of cell biology, 123(2), pp.455-465.

119. Fundin, B.T., Mikaels, A., Westphal, H. and Ernfors, P., 1999. A rapid and dynamic regulation of GDNF-family ligands and receptors correlate with the developmental dependency of cutaneous sensory innervation. Development, 126(12), pp.2597-2610.

120. Furlan, A. and Adameyko, I., 2018. Schwann cell precursor: a neural crest cell in disguise?. Developmental biology, 444, pp.S25-S35.

121. Gale, N.W., Holland, S.J., Valenzuela, D.M., Flenniken, A., Pan, L., Ryan, T.E., Henkemeyer, M., Strebhardt, K., Hirai, H., Wilkinson, D.G. and Pawson, T., 1996. Eph receptors and ligands comprise two major specificity subclasses and are reciprocally compartmentalized during embryogenesis. Neuron, 17(1), pp.9-19.

122. Gantus, M.A.V., Nasciutti, L.E., Cruz, C.M., Persechini, P.M. and Martinez, A.M.B., 2006. Modulation of extracellular matrix components by metalloproteinases and their tissue inhibitors during degeneration and regeneration of rat sural nerve. Brain research, 1122(1), pp.36-46.

123. Gardiner, N.J., Fernyhough, P., Tomlinson, D.R., Mayer, U., Von Der Mark, H. and Streuli, C.H., 2005. α7 integrin mediates neurite outgrowth of distinct populations of adult sensory neurons. Molecular and Cellular Neuroscience, 28(2), pp.229-240

124. Gaudet, A.D., Popovich, P.G. and Ramer, M.S., 2011. Wallerian degeneration: gaining perspective on inflammatory events after peripheral nerve injury. Journal of neuroinflammation, 8(1), p.110.

125. Geoffroy, V., Corral, D.A., Zhou, L., Lee, B. and Karsenty, G., 1998. Genomic organization, expression of the human CBFA1 gene, and evidence for an

alternative splicing event affecting protein function. Mammalian genome, 9, pp.54-57.

126. George, E.B., Glass, J.D. and Griffin, J.W., 1995. Axotomy-induced axonal degeneration is mediated by calcium influx through ion-specific channels. Journal of Neuroscience, 15(10), pp.6445-6452.

127. George, R. and Griffin, J.W., 1994. Delayed macrophage responses and myelin clearance during Wallerian degeneration in the central nervous system: the dorsal radiculotomy model. Experimental neurology, 129(2), pp.225-236.

128. Gerber, D., Pereira, J.A., Gerber, J., Tan, G., Dimitrieva, S., Yángüez, E. and Suter, U., 2021. Transcriptional profiling of mouse peripheral nerves to the single-cell level to build a sciatic nerve ATlas (SNAT). Elife, 10, p.e58591.

129. Gerdts, J., Brace, E.J., Sasaki, Y., DiAntonio, A. and Milbrandt, J., 2015. SARM1 activation triggers axon degeneration locally via NAD+ destruction. Science, 348(6233), pp.453-457.

130. Ghidinelli, M., Poitelon, Y., Shin, Y.K., Ameroso, D., Williamson, C., Ferri, C., Pellegatta, M., Espino, K., Mogha, A., Monk, K. and Podini, P., 2017. Laminin 211 inhibits protein kinase A in Schwann cells to modulate neuregulin 1 type III-driven myelination. PLoS biology, 15(6), p.e2001408.

131. Ghislain, J. and Charnay, P., 2006. Control of myelination in Schwann cells: a Krox20 cis-regulatory element integrates Oct6, Brn2 and Sox10 activities. EMBO reports, 7(1), pp.52-58.

132. Giger, R.J., Pasterkamp, R.J., Heijnen, S., Holtmaat, A.J. and Verhaagen, J., 1998. Anatomical distribution of the chemorepellent semaphorin III/collapsin-1 in the adult rat and human brain: predominant expression in structures of the olfactory-hippocampal pathway and the motor system. Journal of neuroscience research, 52(1), pp.27-42.

133. Giger, R.J., Wolfer, D.P., De Wit, G.M. and Verhaagen, J., 1996. Anatomy of rat semaphorin III collapsin-1 mRNA expression and relationship to developing nerve tracts during neuroembryogenesis. Journal of Comparative Neurology, 375(3), pp.378-392.

134. Gilley, J. and Coleman, M.P., 2010. Endogenous Nmnat2 is an essential survival factor for maintenance of healthy axons. PLoS biology, 8(1), p.e1000300.

135. Gilley, J., Adalbert, R., Yu, G. and Coleman, M.P., 2013. Rescue of peripheral and CNS axon defects in mice lacking NMNAT2. Journal of Neuroscience, 33(33), pp.13410-13424.

136. Gilley, J., Orsomando, G., Nascimento-Ferreira, I. and Coleman, M.P., 2015. Absence of SARM1 rescues development and survival of NMNAT2-deficient axons. Cell reports, 10(12), pp.1974-1981.

137. Goldberg, D.J. and Burmeister, D.W., 1986. Stages in axon formation: observations of growth of Aplysia axons in culture using video-enhanced contrast-differential interference contrast microscopy. The Journal of cell biology, 103(5), pp.1921-1931.

138. Gomez-Sanchez, J.A., Carty, L., Iruarrizaga-Lejarreta, M., Palomo-Irigoyen, M., Varela-Rey, M., Griffith, M., Hantke, J., Macias-Camara, N., Azkargorta, M., Aurrekoetxea, I. and De Juan, V.G., 2015. Schwann cell autophagy, myelinophagy, initiates myelin clearance from injured nerves. Journal of Cell Biology, 210(1), pp.153-168.

139. Gomez-Sanchez, J.A., Pilch, K.S., van der Lans, M., Fazal, S.V., Benito, C., Wagstaff, L.J., Mirsky, R. and Jessen, K.R., 2017. After nerve injury, lineage tracing shows that myelin and Remak Schwann cells elongate extensively and branch to form repair Schwann cells, which shorten radically on remyelination. Journal of Neuroscience, 37(37), pp.9086-9099.

140. Gonzalez-Perez, F., Udina, E. and Navarro, X., 2013. Extracellular matrix components in peripheral nerve regeneration. International review of neurobiology, 108, pp.257-275.

141. Goodman, C.S., 1996. Mechanisms and molecules that control growth cone guidance. Annual review of neuroscience, 19(1), pp.341-377.

142. Gray, M., Palispis, W., Popovich, P.G., van Rooijen, N. and Gupta, R., 2007. Macrophage depletion alters the blood–nerve barrier without affecting Schwann cell function after neural injury. Journal of neuroscience research, 85(4), pp.766-777.

143. Griffin, J.W. and Thompson, W.J., 2008. Biology and pathology of nonmyelinating Schwann cells. Glia, 56(14), pp.1518-1531.

144. Griffin, J.W., George, E.B., Hsieh, S.T. and Glass, J.D., 1995. 20 Axonal degeneration and disorders of the axonal cytoskeleton. The Axon: Structure, Function, and Pathophysiology, p.375.

145. Guertin, A.D., Zhang, D.P., Mak, K.S., Alberta, J.A. and Kim, H.A., 2005. Microanatomy of axon/glial signaling during Wallerian degeneration. Journal of neuroscience, 25(13), pp.3478-3487.

146. Guillaud, L., El-Agamy, S.E., Otsuki, M. and Terenzio, M., 2020. Anterograde axonal transport in neuronal homeostasis and disease. Frontiers in Molecular Neuroscience, 13, p.556175.

147. Gutmann, E., Guttmann, L., Medawar, P.B. and Young, J.Z., 1942. The rate of regeneration of nerve. Journal of Experimental Biology, 19(1), pp.14-44.

148. Haggerty, A.E., Bening, M.R., Pherribo, G., Dauer, E.A. and Oudega, M., 2019. Laminin polymer treatment accelerates repair of the crushed peripheral nerve in adult rats. Acta biomaterialia, 86, pp.185-193.

149. Hall, S., 2005. The response to injury in the peripheral nervous system. The Journal of bone and joint surgery. British volume, 87(10), pp.1309-1319.

150. Halloran, M.C. and Wolman, M.A., 2006. Repulsion or adhesion: receptors make the call. Current opinion in cell biology, 18(5), pp.533-540.

151. Hameyer, D., Loonstra, A., Eshkind, L., Schmitt, S., Antunes, C., Groen, A., Bindels, E., Jonkers, J., Krimpenfort, P., Meuwissen, R. and Rijswijk, L., 2007. Toxicity of ligand-dependent Cre recombinases and generation of a conditional Cre deleter mouse allowing mosaic recombination in peripheral tissues. Physiological genomics, 31(1), pp.32-41.

152. Hammarberg, H., Wallquist, W., Piehl, F., Risling, M. and Cullheim, S., 2000. Regulation of laminin-associated integrin subunit mRNAs in rat spinal motoneurons during postnatal development and after axonal injury. Journal of Comparative Neurology, 428(2), pp.294-304.

153. Hammond, R., Vivancos, V., Naeem, A., Chilton, J., Mambitisaeva, E., Andrews, W., Sundaresan, V. and Guthrie, S., 2005. Slit-mediated repulsion is a key regulator of motor axon pathfinding in the hindbrain.

154. Harty, B.L. and Monk, K.R., 2017. Unwrapping the unappreciated: recent progress in Remak Schwann cell biology. Current Opinion in Neurobiology, 47, pp.131-137.

155. Hayashi, S. and McMahon, A.P., 2002. Efficient recombination in diverse tissues by a tamoxifen-inducible form of Cre: a tool for temporally regulated gene activation/inactivation in the mouse. Developmental biology, 244(2), pp.305-318.

156. He, C., Chen, Z. and Chen, Z., 1992. Enhancement of motor nerve regeneration by nerve growth factor. Microsurgery, 13(3), pp.151-154.

157. He, Q., Dent, E.W. and Meiri, K.F., 1997. Modulation of actin filament behavior by GAP-43 (neuromodulin) is dependent on the phosphorylation status of serine 41, the protein kinase C site. Journal of Neuroscience, 17(10), pp.3515-3524.

158. Hedgecock, E.M., Culotti, J.G. and Hall, D.H., 1990. The unc-5, unc-6, and unc-40 genes guide circumferential migrations of pioneer axons and mesodermal cells on the epidermis in C. elegans. Neuron, 4(1), pp.61-85.

159. Heumann, R., Korsching, S., Bandtlow, C. and Thoenen, H., 1987a. Changes of nerve growth factor synthesis in nonneuronal cells in response to sciatic nerve transection. The Journal of cell biology, 104(6), pp.1623-1631.

160. Heumann, R., Lindholm, D., Bandtlow, C., Meyer, M., Radeke, M.J., Misko, T.P., Shooter, E. and Thoenen, H., 1987b. Differential regulation of mRNA encoding nerve growth factor and its receptor in rat sciatic nerve during development, degeneration, and regeneration: role of macrophages. Proceedings of the National Academy of Sciences, 84(23), pp.8735-8739.

161. Himanen, J.P., Chumley, M.J., Lackmann, M., Li, C., Barton, W.A., Jeffrey, P.D., Vearing, C., Geleick, D., Feldheim, D.A., Boyd, A.W. and Henkemeyer, M., 2004. Repelling class discrimination: ephrin-A5 binds to and activates EphB2 receptor signaling. Nature neuroscience, 7(5), pp.501-509.

162. Hirata, K. and Kawabuchi, M., 2002. Myelin phagocytosis by macrophages and nonmacrophages during Wallerian degeneration. Microscopy research and technique, 57(6), pp.541-547.

163. Hirose, T., Tani, T., Shimada, T., Ishizawa, K., Shimada, S. and Sano, T., 2003. Immunohistochemical demonstration of EMA/Glut1-positive perineurial cells and CD34-positive fibroblastic cells in peripheral nerve sheath tumors. Modern pathology, 16(4), pp.293-298.

164. Höke, A., Gordon, T., Zochodne, D.W. and Sulaiman, O.A.R., 2002. A decline in glial cell-line-derived neurotrophic factor expression is associated with impaired regeneration after long-term Schwann cell denervation. Experimental neurology, 173(1), pp.77-85.

165. Höke, A., Ho, T., Crawford, T.O., LeBel, C., Hilt, D. and Griffin, J.W., 2003. Glial cell line-derived neurotrophic factor alters axon schwann cell units and promotes myelination in unmyelinated nerve fibers. Journal of Neuroscience, 23(2), pp.561-567.

166. Holmberg, J. and Frisén, J., 2002. Ephrins are not only unattractive. Trends in neurosciences, 25(5), pp.239-243.

167. Holmes, G.P., Negus, K., Burridge, L., Raman, S., Algar, E., Yamada, T. and Little, M.H., 1998. Distinct but overlapping expression patterns of two vertebrate slit homologs implies functional roles in CNS development and organogenesis. Mechanisms of development, 79(1-2), pp.57-72.

168. Hong, K., Hinck, L., Nishiyama, M., Poo, M.M., Tessier-Lavigne, M. and Stein, E., 1999. A ligand-gated association between cytoplasmic domains of UNC5 and DCC family receptors converts netrin-induced growth cone attraction to repulsion. Cell, 97(7), pp.927-941.

169. Hoyng, S.A., De Winter, F., Gnavi, S., de Boer, R., Boon, L.I., Korvers, L.M., Tannemaat, M.R., Malessy, M.J. and Verhaagen, J., 2014. A comparative morphological, electrophysiological and functional analysis of axon regeneration through peripheral nerve autografts genetically modified to overexpress BDNF, CNTF, GDNF, NGF, NT3 or VEGF. Experimental neurology, 261, pp.578-593.

170. Huber, A.B., Kania, A., Tran, T.S., Gu, C., Garcia, N.D.M., Lieberam, I., Johnson, D., Jessell, T.M., Ginty, D.D. and Kolodkin, A.L., 2005. Distinct roles for secreted semaphorin signaling in spinal motor axon guidance. Neuron, 48(6), pp.949-964.

171. Huminiecki, L., Gorn, M., Suchting, S., Poulsom, R. and Bicknell, R., 2002. Magic roundabout is a new member of the roundabout receptor family that is endothelial specific and expressed at sites of active angiogenesis. Genomics, 79(4), pp.547-552.

172. Hung, H.A., Sun, G., Keles, S. and Svaren, J., 2015. Dynamic regulation of Schwann cell enhancers after peripheral nerve injury. Journal of Biological Chemistry, 290(11), pp.6937-6950.

173. Huot, J., 2004. Ephrin signaling in axon guidance. Progress in Neuro-Psychopharmacology and Biological Psychiatry, 28(5), pp.813-818.

174. Hussain, G., Wang, J., Rasul, A., Anwar, H., Qasim, M., Zafar, S., Aziz, N., Razzaq, A., Hussain, R., de Aguilar, J.L.G. and Sun, T., 2020. Current status of therapeutic approaches against peripheral nerve injuries: a detailed story from injury to recovery. International journal of biological sciences, 16(1), p.116.

175. Ignatius, M.J., Gebicke-Haerter, P.J., Pitas, R.E. and Shooter, E.M., 1987. Apolipoprotein E in nerve injury and repair. Progress in brain research, 71, pp.177-184.

176. Ilicic, T., Kim, J.K., Kolodziejczyk, A.A., Bagger, F.O., McCarthy, D.J., Marioni, J.C. and Teichmann, S.A., 2016. Classification of low quality cells from single-cell RNA-seq data. Genome biology, 17(1), pp.1-15.

177. Inoue, K.I., Ozaki, S., Shiga, T., Ito, K., Masuda, T., Okado, N., Iseda, T., Kawaguchi, S., Ogawa, M., Bae, S.C. and Yamashita, N., 2002. Runx3 controls the axonal projection of proprioceptive dorsal root ganglion neurons. Nature neuroscience, 5(10), pp.946-954.

178. Inoue, K.I., Shiga, T. and Ito, Y., 2008. Runx transcription factors in neuronal development. Neural development, 3(1), pp.1-7.

179. Ishii, N., Wadsworth, W.G., Stern, B.D., Culotti, J.G. and Hedgecock, E.M., 1992. UNC-6, a laminin-related protein, guides cell and pioneer axon migrations in C. elegans. Neuron, 9(5), pp.873-881.

180. Ito, K., Liu, Q., Salto-Tellez, M., Yano, T., Tada, K., Ida, H., Huang, C., Shah, N., Inoue, M., Rajnakova, A. and Hiong, K.C., 2005. RUNX3, a novel tumor suppressor, is

frequently inactivated in gastric cancer by protein mislocalization. Cancer research, 65(17), pp.7743-7750.

181. Jaakkola, S., Peltonen, J. and Uitto, J.J., 1989. Perineurial cells coexpress genes encoding interstitial collagens and basement membrane zone components. The Journal of cell biology, 108(3), pp.1157-1163..

182. Jaegle, M., Mandemakers, W., Broos, L., Zwart, R., Karis, A., Visser, P., Grosveld, F. and Meijer, D., 1996. The POU factor Oct-6 and Schwann cell differentiation. Science, 273(5274), pp.507-510.

183. Jaminet, P., Köhler, D., Schäufele, M., Rahmanian-Schwarz, A., Lotter, O., Fornaro, M., Ronchi, G., Geuna, S., Rosenberger, P. and Schaller, H.E., 2013. Evaluating the role of Netrin-1 during the early phase of peripheral nerve regeneration using the mouse median nerve model. Restorative neurology and neuroscience, 31(3), pp.337-345.

184. Jang, S.Y., Shin, Y.K., Park, S.Y., Park, J.Y., Lee, H.J., Yoo, Y.H., Kim, J.K. and Park, H.T., 2016. Autophagic myelin destruction by Schwann cells during Wallerian degeneration and segmental demyelination. Glia, 64(5), pp.730-742.

185. Jankowski, M.P., McIlwrath, S.L., Jing, X., Cornuet, P.K., Salerno, K.M., Koerber, H.R. and Albers, K.M., 2009. Sox11 transcription factor modulates peripheral nerve regeneration in adult mice. Brain research, 1256, pp.43-54.

186. Jenkins, R. and Hunt, S.P., 1991. Long-term increase in the levels of c-jun mRNA and jun protein-like immunoreactivity in motor and sensory neurons following axon damage. Neuroscience letters, 129(1), pp.107-110.

187. Jessen, K.R. and Mirsky, R., 2005. The origin and development of glial cells in peripheral nerves. Nature Reviews Neuroscience, 6(9), pp.671-682.

188. Jessen, K.R. and Mirsky, R., 2008. Negative regulation of myelination: relevance for development, injury, and demyelinating disease. Glia, 56(14), pp.1552-1565.

189. Jessen, K.R. and Mirsky, R., 2019. The success and failure of the Schwann cell response to nerve injury. Frontiers in cellular neuroscience, 13, p.33.

190. Jessen, K.R., Mirsky, R. and Morgan, L., 1987. Axonal signals regulate the differentiation of non-myelin-forming Schwann cells: an immunohistochemical study of galactocerebroside in transected and regenerating nerves. Journal of Neuroscience, 7(10), pp.3362-3369.

191. Joseph, N.M., Mukouyama, Y.S., Mosher, J.T., Jaegle, M., Crone, S.A., Dormand, E.L., Lee, K.F., Meijer, D., Anderson, D.J. and Morrison, S.J., 2004. Neural crest stem cells undergo multilineage differentiation in developing peripheral nerves to generate endoneurial fibroblasts in addition to Schwann cells.

192. Kanda, T., 2013. Biology of the blood–nerve barrier and its alteration in immune mediated neuropathies. Journal of Neurology, Neurosurgery & Psychiatry, 84(2), pp.208-212.

193. Kawasaki, T., Oka, N., Tachibana, H., Akiguchi, I. and Shibasaki, H., 2003. Oct6, a transcription factor controlling myelination, is a marker for active nerve regeneration in peripheral neuropathies. Acta neuropathologica, 105(3), pp.203-208.

194. Keast, J.R., Forrest, S.L. and Osborne, P.B., 2010. Sciatic nerve injury in adult rats causes distinct changes in the central projections of sensory neurons expressing different glial cell line-derived neurotrophic factor family receptors. Journal of Comparative Neurology, 518(15), pp.3024-3045

195. Keino-Masu, K., Masu, M., Hinck, L., Leonardo, E.D., Chan, S.S.Y., Culotti, J.G. and Tessier-Lavigne, M., 1996. Deleted in Colorectal Cancer (DCC) encodes a netrin receptor. Cell, 87(2), pp.175-185.

196. Keleman, K. and Dickson, B.J., 2001. Short-and long-range repulsion by the Drosophila Unc5 netrin receptor. Neuron, 32(4), pp.605-617.

197. Kennedy, T.E., Serafini, T., de la Torre, J. and Tessier-Lavigne, M., 1994. Netrins are diffusible chemotropic factors for commissural axons in the embryonic spinal cord. Cell, 78(3), pp.425-435.

198. Kidd, T., Bland, K.S. and Goodman, C.S., 1999. Slit is the midline repellent for the robo receptor in Drosophila. Cell, 96(6), pp.785-794.

199. Kidd, T., Brose, K., Mitchell, K.J., Fetter, R.D., Tessier-Lavigne, M., Goodman, C.S. and Tear, G., 1998. Roundabout controls axon crossing of the CNS midline and defines a novel subfamily of evolutionarily conserved guidance receptors. Cell, 92(2), pp.205-215.

200. Kim, H.A., Pomeroy, S.L., Whoriskey, W., Pawlitzky, I., Benowitz, L.I., Sicinski, P., Stiles, C.D. and Roberts, T.M., 2000. A developmentally regulated switch directs regenerative growth of Schwann cells through cyclin D1. Neuron, 26(2), pp.405-416.

201. Klagsbrun, M. and Eichmann, A., 2005. A role for axon guidance receptors and ligands in blood vessel development and tumor angiogenesis. Cytokine & growth factor reviews, 16(4-5), pp.535-548.

202. Knott, E.P., Assi, M. and Pearse, D.D., 2014. Cyclic AMP signaling: a molecular determinant of peripheral nerve regeneration. BioMed research international, 2014.

203. Kobayashi, N.R., Bedard, A.M., Hincke, M.T. and Tetzlaff, W., 1996. Increased expression of BDNF and trkB mRNA in rat facial motoneurons after axotomy. European Journal of Neuroscience, 8(5), pp.1018-1029.

204. Koch, M., Murrell, J.R., Hunter, D.D., Olson, P.F., Jin, W., Keene, D.R., Brunken, W.J. and Burgeson, R.E., 2000. A novel member of the netrin family, β-netrin, shares homology with the β chain of laminin: identification, expression, and functional characterization. The Journal of cell biology, 151(2), pp.221-234.

205. Koeppen, A., 2004. Wallerian degeneration: history and clinical significance. Journal of the Neurological Sciences, 220(1-2), pp.115-117.

206. Kolodkin, A.L., 1996. Semaphorins: mediators of repulsive growth cone guidance. Trends in cell biology, 6(1), pp.15-22.

207. Kolodziej, P.A., Timpe, L.C., Mitchell, K.J., Fried, S.R., Goodman, C.S., Jan, L.Y. and Jan, Y.N., 1996. frazzled encodes a Drosophila member of the DCC immunoglobulin subfamily and is required for CNS and motor axon guidance. Cell, 87(2), pp.197-204.

208. Komori, T., 2018. Runx2, an inducer of osteoblast and chondrocyte differentiation. Histochemistry and cell biology, 149(4), pp.313-323.

209. Komori, T., Yagi, H., Nomura, S., Yamaguchi, A., Sasaki, K., Deguchi, K., Shimizu, Y., Bronson, R.T., Gao, Y.H., Inada, M. and Sato, M., 1997. Targeted disruption of Cbfa1 results in a complete lack of bone formation owing to maturational arrest of osteoblasts. cell, 89(5), pp.755-764.

210. Kornfeld, T., Vogt, P.M. and Radtke, C., 2019. Nerve grafting for peripheral nerve injuries with extended defect sizes. Wiener Medizinische Wochenschrift, 169(9-10), pp.240-251.

211. Krimpenfort, P., Song, J.Y., Proost, N., Zevenhoven, J., Jonkers, J. and Berns, A., 2012. Deleted in colorectal carcinoma suppresses metastasis in p53-deficient mammary tumours. Nature, 482(7386), pp.538-541.

212. Krull, C.E., Lansford, R., Gale, N.W., Collazo, A., Marcelle, C., Yancopoulos, G.D., Fraser, S.E. and Bronner-Fraser, M., 1997. Interactions of Eph-related receptors and ligands confer rostrocaudal pattern to trunk neural crest migration. Current Biology, 7(8), pp.571-580.

213. Kuhlbrodt, K., Herbarth, B., Sock, E., Hermans-Borgmeyer, I. and Wegner, M., 1998. Sox10, a novel transcriptional modulator in glial cells. Journal of Neuroscience, 18(1), pp.237-250.

214. Kuhlmann, T., Bitsch, A., Stadelmann, C., Siebert, H. and Brück, W., 2001. Macrophages are eliminated from the injured peripheral nerve via local apoptosis and circulation to regional lymph nodes and the spleen. Journal of Neuroscience, 21(10), pp.3401-3408.

215. Kuliasha, C.A., Spearman, B.S., Atkinson, E.W., Rustogi, P., Furniturewalla, A.S., Nunamaker, E.A., Otto, K.J., Schmidt, C.E. and Judy, J.W., 2018. Robust and scalable tissue-engineerined electronic nerve interfaces (Teeni). In Presented at the Solid-State Sensors, Actuators and Microsystems Workshop (p. 4).

216. Lackmann, M. and Boyd, A.W., 2008. Eph, a protein family coming of age: more confusion, insight, or complexity?. Science signaling, 1(15), pp.re2-re2.

217. Laraba, L., Hillson, L., De Guibert, J.G., Hewitt, A., Jaques, M.R., Tang, T.T., Post, L., Ercolano, E., Rai, G., Yang, S.M. and Jagger, D.J., 2022. Inhibition of YAP/TAZ-driven TEAD activity prevents growth of NF2-null schwannoma and meningioma. Brain.

218. Larrivée, B., Freitas, C., Trombe, M., Lv, X., DeLafarge, B., Yuan, L., Bouvrée, K., Bréant, C., Del Toro, R., Bréchot, N. and Germain, S., 2007. Activation of the UNC5B receptor by Netrin-1 inhibits sprouting angiogenesis. Genes & development, 21(19), pp.2433-2447.

219. Lasek RJ, Dabrowski C, Nordlander R. Analysis of axoplasmic RNA from invertebrate giant axons. Nat. New Biol. 1973;244:162–65.

220. Le, N., Nagarajan, R., Wang, J.Y., Araki, T., Schmidt, R.E. and Milbrandt, J., 2005. Analysis of congenital hypomyelinating Egr2Lo/Lo nerves identifies Sox2 as an inhibitor of Schwann cell differentiation and myelination. Proceedings of the National Academy of Sciences, 102(7), pp.2596-2601.

221. LeBlanc, A.C. and Poduslo, J.F., 1990. Axonal modulation of myelin gene expression in the peripheral nerve. Journal of neuroscience research, 26(3), pp.317-326.

222. LeBlanc, S.E., Jang, S.W., Ward, R.M., Wrabetz, L. and Svaren, J., 2006. Direct regulation of myelin protein zero expression by the Egr2 transactivator. Journal of Biological Chemistry, 281(9), pp.5453-5460.

223. Lee, H.K., Shin, Y.K., Jung, J., Seo, S.Y., Baek, S.Y. and Park, H.T., 2009. Proteasome inhibition suppresses Schwann cell dedifferentiation in vitro and in vivo. Glia, 57(16), pp.1825-1834.

224. Lee, H.K., Seo, I.A., Seo, E., Seo, S.Y., Lee, H.J. and Park, H.T., 2007. Netrin-1 induces proliferation of SCs through UNC5b receptor. Biochemical and biophysical research communications, 362(4), pp.1057-1062.

225. Leonardo, E.D., Hinck, L., Masu, M., Keino-Masu, K., Ackerman, S.L. and Tessier-Lavigne, M., 1997. Vertebrate homologues of C. elegans UNC-5 are candidate netrin receptors. Nature, 386(6627), pp.833-838.

226. Letourneau, P., 2009. Axonal pathfinding: Extracellular matrix role. Encyclopedia of neuroscience, 1, pp.1139-1145.

227. Levanon, D., Bettoun, D., Harris-Cerruti, C., Woolf, E., Negreanu, V., Eilam, R., Bernstein, Y., Goldenberg, D., Xiao, C., Fliegauf, M. and Kremer, E., 2002. The Runx3 transcription factor regulates development and survival of TrkC dorsal root ganglia neurons. The EMBO journal, 21(13), pp.3454-3463.

228. Levi-Montalcini, R. and Hamburger, V., 1951. Selective growth stimulating effects of mouse sarcoma on the sensory and sympathetic nervous system of the chick embryo. Journal of experimental zoology, 116(2), pp.321-361.

229. Li, G.L., Farooque, M., Holtz, A. and Olsson, Y., 1999. Apoptosis of oligodendrocytes occurs for long distances away from the primary injury after compression trauma to rat spinal cord. Acta neuropathologica, 98, pp.473-480.

230. Li, M., Banton, M.C., Min, Q., Parkinson, D.B. and Dun, X., 2021. Meta-analysis reveals transcription factor upregulation in cells of injured mouse sciatic nerve. Frontiers in Cellular Neuroscience, p.431.

231. Li, S., Liu, Q., Wang, Y., Gu, Y., Liu, D., Wang, C., Ding, G., Chen, J., Liu, J. and Gu, X., 2013. Differential gene expression profiling and biological process analysis in proximal nerve segments after sciatic nerve transection. PloS one, 8(2), p.e57000.

232. Liao, S.J., Gong, Q., Chen, X.R., Ye, L.X., Ding, Q., Zeng, J.S. and Yu, J., 2013. Netrin-1 rescues neuron loss by attenuating secondary apoptosis in ipsilateral thalamic nucleus following focal cerebral infarction in hypertensive rats. Neuroscience, 231, pp.225-232.

233. Lin, C.H. and Forscher, P., 1995. Growth cone advance is inversely proportional to retrograde F-actin flow. Neuron, 14(4), pp.763-771.

234. Lindborg, J.A., Mack, M. and Zigmond, R.E., 2017. Neutrophils are critical for myelin removal in a peripheral nerve injury model of Wallerian degeneration. Journal of Neuroscience, 37(43), pp.10258-10277.

235. Lindholm, D., Heumann, R., Meyer, M. and Thoenen, H., 1987. Interleukin-1 regulates synthesis of nerve growth factor in non-neuronal cells of rat sciatic nerve. Nature, 330, pp.658-659.

236. Lisabeth, E.M., Falivelli, G. and Pasquale, E.B., 2013. Eph receptor signaling and ephrins. Cold Spring Harbor perspectives in biology, 5(9), p.a009159.

237. Liu, G., Beggs, H., Jürgensen, C., Park, H.T., Tang, H., Gorski, J., Jones, K.R., Reichardt, L.F., Wu, J. and Rao, Y., 2004. Netrin requires focal adhesion kinase and

Src family kinases for axon outgrowth and attraction. Nature neuroscience, 7(11), pp.1222-1232.

238. Liu, G., Li, W., Wang, L., Kar, A., Guan, K.L., Rao, Y. and Wu, J.Y., 2009. DSCAM functions as a netrin receptor in commissural axon pathfinding. Proceedings of the National Academy of Sciences, 106(8), pp.2951-2956.

239. Liu, H.M., Yang, L.H. and Yang, Y.J., 1995. Schwann cell properties: 3. C-fos expression, bFGF production, phagocytosis and proliferation during Wallerian degeneration. Journal of Neuropathology & Experimental Neurology, 54(4), pp.487-496.

240. Lonze, B.E., Riccio, A., Cohen, S. and Ginty, D.D., 2002. Apoptosis, axonal growth defects, and degeneration of peripheral neurons in mice lacking CREB. Neuron, 34(3), pp.371-385.

241. Lowery, L.A. and Vactor, D.V., 2009. The trip of the tip: understanding the growth cone machinery. Nature reviews Molecular cell biology, 10(5), pp.332-343.

242. Lu, X., Le Noble, F., Yuan, L., Jiang, Q., De Lafarge, B., Sugiyama, D., Bréant, C., Claes, F., De Smet, F., Thomas, J.L. and Autiero, M., 2004. The netrin receptor UNC5B mediates guidance events controlling morphogenesis of the vascular system. Nature, 432(7014), pp.179-186.

243. Luís, A.L., Rodrigues, J.M., Geuna, S., Amado, S., Simões, M.J., Fregnan, F., Ferreira, A.J., Veloso, A.P., Armada-Da-Silva, P.A.S., Varejão, A.S.P. and Maurício, A.C., 2008. Neural cell transplantation effects on sciatic nerve regeneration after a standardized crush injury in the rat. Microsurgery: Official Journal of the International Microsurgical Society and the European Federation of Societies for Microsurgery, 28(6), pp.458-470.

244. Lunn, E.R., Perry, V.H., Brown, M.C., Rosen, H. and Gordon, S., 1989. Absence of Wallerian degeneration does not hinder regeneration in peripheral nerve. European Journal of Neuroscience, 1(1), pp.27-33.

245. Luttges, M., Kelly, P. and Gerren, R., 1976. Degenerative changes in mouse sciatic nerves: Electrophoretic and electrophysiologic characterizations. Experimental Neurology, 50(3), pp.706-733.

246. Lutz, A.B. and Barres, B.A., 2014. Contrasting the glial response to axon injury in the central and peripheral nervous systems. Developmental cell, 28(1), pp.7-17.

247. Lv, J., Sun, X., Ma, J., Ma, X., Zhang, Y., Li, F., Li, Y. and Zhao, Z., 2015. Netrin-1 induces the migration of SCs via p38 MAPK and PI3K-Akt signaling pathway mediated by the UNC5B receptor. Biochemical and biophysical research communications, 464(1), pp.263-268.

248. Ly, A., Nikolaev, A., Suresh, G., Zheng, Y., Tessier-Lavigne, M. and Stein, E., 2008. DSCAM is a netrin receptor that collaborates with DCC in mediating turning responses to netrin-1. Cell, 133(7), pp.1241-1254.

249. Lykissas, M.G., Batistatou, A.K., Charalabopoulos, K.A. and Beris, A.E., 2007. The role of neurotrophins in axonal growth, guidance, and regeneration. Current neurovascular research, 4(2), pp.143-151.

250. Lytle, J.M. and Wrathall, J.R., 2007. Glial cell loss, proliferation and replacement in the contused murine spinal cord. European Journal of Neuroscience, 25(6), pp.1711-1724.

251. Ma, Y.H., Zeng, X., Qiu, X.C., Wei, Q.S., Che, M.T., Ding, Y., Liu, Z., Wu, G.H., Sun, J.H., Pang, M. and Rong, L.M., 2018. Perineurium-like sheath derived from long-term surviving mesenchymal stem cells confers nerve protection to the injured spinal cord. Biomaterials, 160, pp.37-55.

252. Mack, T.G., Reiner, M., Beirowski, B., Mi, W., Emanuelli, M., Wagner, D., Thomson, D., Gillingwater, T., Court, F., Conforti, L. and Fernando, F.S., 2001. Wallerian degeneration of injured axons and synapses is delayed by a Ube4b/Nmnat chimeric gene. Nature neuroscience, 4(12), pp.1199-1206.

253. MacKinnon, S.E., Dellon, A.L. and O'brien, J.P., 1991. Changes in nerve fiber numbers distal to a nerve repair in the rat sciatic nerve model. Muscle & Nerve: Official Journal of the American Association of Electrodiagnostic Medicine, 14(11), pp.1116-1122.

254. Madisen, L., Zwingman, T.A., Sunkin, S.M., Oh, S.W., Zariwala, H.A., Gu, H., Ng, L.L., Palmiter, R.D., Hawrylycz, M.J., Jones, A.R. and Lein, E.S., 2010. A robust and high-throughput Cre reporting and characterization system for the whole mouse brain. Nature neuroscience, 13(1), pp.133-140.

255. Madison, R.D., Zomorodi, A. and Robinson, G.A., 2000. Netrin-1 and peripheral nerve regeneration in the adult rat. Experimental neurology, 161(2), pp.563-570.

256. Magill, C.K., Tuffaha, S.H., Yee, A., Luciano, J.P., Hunter, D.A., Mackinnon, S.E. and Borschel, G.H., 2009. The short-and long-term effects of Seprafilm® on peripheral nerves: a histological and functional study. Journal of reconstructive microsurgery, 25(06), pp.345-354.

257. Mahar, M. and Cavalli, V., 2018. Intrinsic mechanisms of neuronal axon regeneration. Nature Reviews Neuroscience, 19(6), pp.323-337.

258. Mallon, B.S., Shick, H.E., Kidd, G.J. and Macklin, W.B., 2002. Proteolipid promoter activity distinguishes two populations of NG2-positive cells throughout neonatal cortical development. Journal of Neuroscience, 22(3), pp.876-885.

259. Malong, L., Napoli, I., Casal, G., White, I.J., Stierli, S., Vaughan, A., Cattin, A.L., Burden, J.J., Hng, K.I., Bossio, A., Flanagan, A., Zhao,T.H, Lloyd, A.C, 2023.

Characterization of the structure and control of the blood-nerve barrier identifies avenues for therapeutic delivery. Developmental Cell, 58(3), pp.174-191.

260. Mandolesi, G., Madeddu, F., Bozzi, Y., Maffei, L. and Ratto, G.M., 2004. Acute physiological response of mammalian central neurons to axotomy: ionic regulation and electrical activity. The FASEB journal, 18(15), pp.1934-1936.

261. Mao, X., Fujiwara, Y., Chapdelaine, A., Yang, H. and Orkin, S.H., 2001. Activation of EGFP expression by Cre-mediated excision in a new ROSA26 reporter mouse strain. Blood, The Journal of the American Society of Hematology, 97(1), pp.324-326.

262. Marsh, S.E., Walker, A.J., Kamath, T., Dissing-Olesen, L., Hammond, T.R., de Soysa, T.Y., Young, A.M., Murphy, S., Abdulraouf, A., Nadaf, N. and Dufort, C., 2022. Dissection of artifactual and confounding glial signatures by single-cell sequencing of mouse and human brain. Nature Neuroscience, 25(3), pp.306-316.

263. Martini, R., Fisher, S., López-Vales, R. and David, S., 2008. Interactions between SCs and macrophages in injury and inherited demyelinating disease. Glia, 56(14), pp.1566-1577.

264. McKerracher, L. and Hirscheimer, A., 1992. Slow transport of the cytoskeleton after axonal injury. Journal of neurobiology, 23(5), pp.568-578.

265. Meier, C., Parmantier, E., Brennan, A., Mirsky, R. and Jessen, K.R., 1999. Developing Schwann cells acquire the ability to survive without axons by establishing an autocrine circuit involving insulin-like growth factor, neurotrophin-3, and platelet-derived growth factor-BB. Journal of Neuroscience, 19(10), pp.3847-3859.

266. Messersmith, E.K., Leonardo, E.D., Shatz, C.J., Tessier-Lavigne, M., Goodman, C.S. and Kolodkin, A.L., 1995. Sernaphorin III can function as a selective

chemorepellent to pattern sensory projections in the spinal cord. Neuron, 14(5), pp.949-959.

267. Meyer, D. and Birchmeier, C., 1995. Multiple essential functions of neuregulin in development. Nature, 378(6555), pp.386-390.

268. Meyer, M., Matsuoka, I., Wetmore, C., Olson, L. and Thoenen, H., 1992. Enhanced synthesis of brain-derived neurotrophic factor in the lesioned peripheral nerve: different mechanisms are responsible for the regulation of BDNF and NGF mRNA. The Journal of cell biology, 119(1), pp.45-54.

269. Michaelevski, I., Segal-Ruder, Y., Rozenbaum, M., Medzihradszky, K.F., Shalem, O., Coppola, G., Horn-Saban, S., Ben-Yaakov, K., Dagan, S.Y., Rishal, I. and Geschwind, D.H., 2010. Signaling to transcription networks in the neuronal retrograde injury response. Science signaling, 3(130), pp.ra53-ra53.

270. Michailov, G.V., Sereda, M.W., Brinkmann, B.G., Fischer, T.M., Haug, B., Birchmeier, C., Role, L., Lai, C., Schwab, M.H. and Nave, K.A., 2004. Axonal neuregulin-1 regulates myelin sheath thickness. Science, 304(5671), pp.700-703.

271. Miledi, R. and Slater, C.R., 1970. On the degeneration of rat neuromuscular junctions after nerve section. The Journal of Physiology, 207(2), p.507.

272. Miller, R.H., Lasek, R.J. and Katz, M.J., 1987. Preferred microtubules for vesicle transport in lobster axons. Science, 235(4785), pp.220-222.

273. Mindos, T., Dun, X.P., North, K., Doddrell, R.D., Schulz, A., Edwards, P., Russell, J., Gray, B., Roberts, S.L., Shivane, A. and Mortimer, G., 2017. Merlin controls the repair capacity of Schwann cells after injury by regulating Hippo/YAP activity. Journal of Cell Biology, 216(2), pp.495-510.

274. Ming, G.L., Wong, S.T., Henley, J., Yuan, X.B., Song, H.J., Spitzer, N.C. and Poo, M.M., 2002. Adaptation in the chemotactic guidance of nerve growth cones. Nature, 417(6887), pp.411-418.

275. Mirakaj, V. and Rosenberger, P., 2017. Immunomodulatory functions of neuronal guidance proteins. Trends in immunology, 38(6), pp.444-456.

276. Moalem, G., Xu, K. and Yu, L., 2004. T lymphocytes play a role in neuropathic pain following peripheral nerve injury in rats. Neuroscience, 129(3), pp.767-777.

277. Mogha, A., Benesh, A.E., Patra, C., Engel, F.B., Schöneberg, T., Liebscher, I. and Monk, K.R., 2013. Gpr126 functions in Schwann cells to control differentiation and myelination via G-protein activation. Journal of Neuroscience, 33(46), pp.17976-17985.

278. Monaco, S., Gehrmann, J., Raivich, G. and Kreutzberg, G.W., 1992. MHC-positive, ramified macrophages in the normal and injured rat peripheral nervous system. Journal of neurocytology, 21(9), pp.623-634.

279. Monk, K.R., Feltri, M.L. and Taveggia, C., 2015. New insights on Schwann cell development. Glia, 63(8), pp.1376-1393.

280. Monk, K.R., Naylor, S.G., Glenn, T.D., Mercurio, S., Perlin, J.R., Dominguez, C., Moens, C.B. and Talbot, W.S., 2009. AG protein–coupled receptor is essential for Schwann cells to initiate myelination. Science, 325(5946), pp.1402-1405.

281. Monk, K.R., Oshima, K., Jörs, S., Heller, S. and Talbot, W.S., 2011. Gpr126 is essential for peripheral nerve development and myelination in mammals. Development, 138(13), pp.2673-2680.

282. Morris, J.H., Hudson, A.R. and Weddell, G., 1972. A study of degeneration and regeneration in the divided rat sciatic nerve based on electron microscopy. Zeitschrift für Zellforschung und mikroskopische Anatomie, 124(2), pp.131-164.

283. Mueller, M., Wacker, K., Ringelstein, E.B., Hickey, W.F., Imai, Y. and Kiefer, R., 2001. Rapid response of identified resident endoneurial macrophages to nerve injury. The American journal of pathology, 159(6), pp.2187-2197.

284. Murphy, P.L., Isaacman-Beck, J. and Granato, M., 2022. Robo2 drives target-selective peripheral nerve regeneration in response to glia-derived signals. Journal of Neuroscience, 42(5), pp.762-776.

285. Nadeau, S., Hein, P., Fernandes, K.J., Peterson, A.C. and Miller, F.D., 2005. A transcriptional role for C/EBP β in the neuronal response to axonal injury. Molecular and cellular neuroscience, 29(4), pp.525-535.

286. Nakashiba, T., Ikeda, T., Nishimura, S., Tashiro, K., Honjo, T., Culotti, J.G. and Itohara, S., 2000. Netrin-G1: a novel glycosyl phosphatidylinositol-linked mammalian netrin that is functionally divergent from classical netrins. Journal of Neuroscience, 20(17), pp.6540-6550.

287. Nakashiba, T., Nishimura, S., Ikeda, T. and Itohara, S., 2002. Complementary expression and neurite outgrowth activity of netrin-G subfamily members. Mechanisms of development, 111(1-2), pp.47-60.

288. Nathaniel, E.J. and Pease, D.C., 1963. Regenerative changes in rat dorsal roots following Wallerian degeneration. Journal of ultrastructure research, 9(5-6), pp.533-549.

289. Naveilhan, P., ElShamy, W.M. and Ernfors, P., 1997. Differential regulation of mRNAs for GDNF and its receptors Ret and GDNFRα after sciatic nerve lesion in the mouse. European Journal of Neuroscience, 9(7), pp.1450-1460.

290. Nguyen, A. and Cai, H., 2006. Netrin-1 induces angiogenesis via a DCC-dependent ERK1/2-eNOS feed-forward mechanism. Proceedings of the National Academy of Sciences, 103(17), pp.6530-6535.

291. Nichol, R.H., Hagen, K.M., Lumbard, D.C., Dent, E.W. and Gómez, T.M., 2016. Guidance of axons by local coupling of retrograde flow to point contact adhesions. Journal of Neuroscience, 36(7), pp.2267-2282.

292. Niemi, J.P., DeFrancesco-Lisowitz, A., Roldán-Hernández, L., Lindborg, J.A., Mandell, D. and Zigmond, R.E., 2013. A critical role for macrophages near axotomized neuronal cell bodies in stimulating nerve regeneration. Journal of Neuroscience, 33(41), pp.16236-16248.

293. Nocera, G. and Jacob, C., 2020. Mechanisms of Schwann cell plasticity involved in peripheral nerve repair after injury. Cellular and Molecular Life Sciences, pp.1-13.

294. Nodari, A., Zambroni, D., Quattrini, A., Court, F.A., D'Urso, A., Recchia, A., Tybulewicz, V.L., Wrabetz, L. and Feltri, M.L., 2007. β1 integrin activates Rac1 in Schwann cells to generate radial lamellae during axonal sorting and myelination. The Journal of cell biology, 177(6), pp.1063-1075.

295. Ochoa, J. and Mair, W.G.P., 1969. The normal sural nerve in man: I. Ultrastructure and numbers of fibres and cells. Acta neuropathologica, 13, pp.197-216

296. Ogawa, Y., Eto, A., Miyake, C., Tsuchida, N., Miyake, H., Takaku, Y., Hagiwara, H. and Oishi, K., 2015. Induced pluripotent stem cells generated from P0-Cre; Z/EG transgenic mice. PloS one, 10(9), p.e0138620.

297. Olsson, Y., Kristensson, K. and Klatzo, I., 1971. Permeability of blood vessels and connective tissue sheaths in the peripheral nervous system to exogenous proteins. In Symposium on Pathology of Axons and Axonal Flow: Organized by the Österreichische Arbeitsgemeinschaft für Neuropathologie and the Research Group of Neuropathology of the World Federation of Neurology Wein, September 10 and 11, 1970 (pp. 61-69). Springer Berlin Heidelberg.

298. Oñate, M., Catenaccio, A., Martínez, G., Armentano, D., Parsons, G., Kerr, B., Hetz, C. and Court, F.A., 2016. Activation of the unfolded protein response promotes axonal regeneration after peripheral nerve injury. Scientific reports, 6(1), p.21709.

299. Onesto, M.M., Short, C.A., Rempel, S.K., Catlett, T.S. and Gomez, T.M., 2021. Growth factors as axon guidance molecules: Lessons from in vitro studies. Frontiers in Neuroscience, 15, p.678454.

300. Otto, F., Thornell, A.P., Crompton, T., Denzel, A., Gilmour, K.C., Rosewell, I.R., Stamp, G.W., Beddington, R.S., Mundlos, S., Olsen, B.R. and Selby, P.B., 1997. Cbfa1, a candidate gene for cleidocranial dysplasia syndrome, is essential for osteoblast differentiation and bone development. Cell, 89(5), pp.765-771.

301. Oya, T., Zhao, Y.L., Takagawa, K., Kawaguchi, M., Shirakawa, K., Yamauchi, T. and Sasahara, M., 2002. Platelet-derived growth factor-b expression induced after rat peripheral nerve injuries. Glia, 38(4), pp.303-312.

302. Palmesino, E., Haddick, P.C., Tessier-Lavigne, M. and Kania, A., 2012. Genetic analysis of DSCAM's role as a Netrin-1 receptor in vertebrates. Journal of Neuroscience, 32(2), pp.411-416.

303. Pan, B., Zhou, H.X., Liu, Y., Yan, J.Y., Wang, Y., Yao, X., Deng, Y.Q., Chen, S.Y., Lu, L., Wei, Z.J. and Kong, X.H., 2017. Time-dependent differential expression of long non-coding RNAs following peripheral nerve injury. International journal of molecular medicine, 39(6), pp.1381-1392.

304. Park, J.I., Seo, I.A., Lee, H.K., Park, H.T., Shin, S.W., Park, Y.M. and Ahn, K.J., 2007. Netrin inhibits regenerative axon growth of adult dorsal root ganglion neurons in vitro. Journal of Korean medical science, 22(4), pp.641-645.

305. Park, K.W., Crouse, D., Lee, M., Karnik, S.K., Sorensen, L.K., Murphy, K.J., Kuo, C.J. and Li, D.Y., 2004. The axonal attractant Netrin-1 is an angiogenic factor. Proceedings of the National Academy of Sciences, 101(46), pp.16210-16215.

306. Parkinson, D.B., Bhaskaran, A., Droggiti, A., Dickinson, S., D'Antonio, M., Mirsky, R. and Jessen, K.R., 2004. Krox-20 inhibits Jun-NH2-terminal kinase/c-Jun to control

Schwann cell proliferation and death. The Journal of cell biology, 164(3), pp.385-394.

307. Parkinson, D.B., Bhaskaran, A., Arthur-Farraj, P., Noon, L.A., Woodhoo, A., Lloyd, A.C., Feltri, M.L., Wrabetz, L., Behrens, A., Mirsky, R. and Jessen, K.R., 2008. c-Jun is a negative regulator of myelination. The Journal of cell biology, 181(4), pp.625-637.

308. Parrinello, S., Napoli, I., Ribeiro, S., Digby, P.W., Fedorova, M., Parkinson, D.B., Doddrell, R.D., Nakayama, M., Adams, R.H. and Lloyd, A.C., 2010. EphB signaling directs peripheral nerve regeneration through Sox2-dependent Schwann cell sorting. Cell, 143(1), pp.145-155.

309. Pasterkamp, R.J., Giger, R.J. and Verhaagen, J., 1998. Regulation of semaphorin III/collapsin-1 gene expression during peripheral nerve regeneration. Experimental neurology, 153(2), pp.313-327.

310. Patodia, S. and Raivich, G., 2012. Role of transcription factors in peripheral nerve regeneration. Frontiers in molecular neuroscience, 5, p.8.

311. Paves, H. and Saarma, M., 1997. Neurotrophins as in vitro growth cone guidance molecules for embryonic sensory neurons. Cell and tissue research, 290, pp.285-297.

312. Pellegrino, R.G. and Spencer, P.S., 1985. Schwann cell mitosis in response to regenerating peripheral axons in vivo. Brain research, 341(1), pp.16-25.

313. Peltonen, S., Alanne, M. and Peltonen, J., 2013. Barriers of the peripheral nerve. Tissue barriers, 1(3), p.e24956.

314. Perkins, N.M. and Tracey, D.J., 2000. Hyperalgesia due to nerve injury: role of neutrophils. Neuroscience, 101(3), pp.745-757.

315. Perry, V.H., Tsao, J.W., Feam, S. and Brown, M.C., 1995. Radiation-induced reductions in macrophage recruitment have only slight effects on myelin

degeneration in sectioned peripheral nerves of mice. European Journal of Neuroscience, 7(2), pp.271-280.

316. Petersen, S.C., Luo, R., Liebscher, I., Giera, S., Jeong, S.J., Mogha, A., Ghidinelli, M., Feltri, M.L., Schöneberg, T., Piao, X. and Monk, K.R., 2015. The adhesion GPCR GPR126 has distinct, domain-dependent functions in Schwann cell development mediated by interaction with laminin-211. Neuron, 85(4), pp.755-769.

317. Pleasure, D., Bora Jr, F.W., Lane, J. and Prockop, D., 1974. Regeneration after nerve transection: effect of inhibition of collagen synthesis. Experimental Neurology, 45(1), pp.72-78.

318. Purohit, A.A., Li, W., Qu, C., Dwyer, T., Shao, Q., Guan, K.L. and Liu, G., 2012. Down syndrome cell adhesion molecule (DSCAM) associates with uncoordinated-5C (UNC5C) in netrin-1-mediated growth cone collapse. Journal of Biological Chemistry, 287(32), pp.27126-27138.

319. Püschel, A.W., Adams, R.H. and Betz, H., 1996. The sensory innervation of the mouse spinal cord may be patterned by differential expression of and differential responsiveness to semaphorins. Molecular and Cellular Neuroscience, 7(5), pp.419-431.

320. Qin, J., Wu, J.C., Wang, Q.H., Zhou, S.L., Mao, S.S. and Yao, C., 2018. Transcription factor networks involved in cell death in the dorsal root ganglia following peripheral nerve injury. Neural regeneration research, 13(9), p.1622.

321. Raabe, T., Nguyen, T., Archer, C. and Bittner, G., 1996. Mechanisms for the maintenance and eventual degradation of neurofilament proteins in the distal segments of severed goldfish mauthner axons. The Journal of Neuroscience, 16(5), pp.1605-1613.

322. Raivich, G., Bohatschek, M., Da Costa, C., Iwata, O., Galiano, M., Hristova, M., Nateri, A.S., Makwana, M., Riera-Sans, L., Wolfer, D.P. and Lipp, H.P., 2004. The

AP-1 transcription factor c-Jun is required for efficient axonal regeneration. Neuron, 43(1), pp.57-67.

323. Rajasekharan, S., Baker, K.A., Horn, K.E., Jarjour, A.A., Antel, J.P. and Kennedy, T.E., 2009. Netrin-1 and DCC regulate oligodendrocyte process branching and membrane extension via Fyn and RhoA. Development, 136(3), pp.415-426.

324. Raper, J. and Mason, C., 2010. Cellular strategies of axonal pathfinding. Cold Spring Harbor perspectives in biology, 2(9), p.a001933.

325. Raper, J.A., 2000. Semaphorins and their receptors in vertebrates and invertebrates. Current opinion in neurobiology, 10(1), pp.88-94.

326. Rechthand, E, Smith, Q.R. and Rapoport, S.I., 1987. Transfer of nonelectrolytes from blood into peripheral nerve endoneurium. American Journal of Physiology-Heart and Circulatory Physiology, 252(6), pp.H1175-H1182.

327. Richard, L., Topilko, P., Magy, L., Decouvelaere, A.V., Charnay, P., Funalot, B. and Vallat, J.M., 2012. Endoneurial fibroblast-like cells. Journal of neuropathology and experimental neurology, 71(11), pp.938-947.

328. Richard, L., Védrenne, N., Vallat, J.M. and Funalot, B., 2014. Characterization of endoneurial fibroblast-like cells from human and rat peripheral nerves. Journal of Histochemistry & Cytochemistry, 62(6), pp.424-435.

329. Roberts, S.L., Dun, X.P., Doddrell, R.D., Mindos, T., Drake, L.K., Onaitis, M.W., Florio, F., Quattrini, A., Lloyd, A.C., D'Antonio, M. and Parkinson, D.B., 2017. Sox2 expression in Schwann cells inhibits myelination in vivo and induces influx of macrophages to the nerve. Development, 144(17), pp.3114-3125.

330. Rosenberg, A.F., Isaacman-Beck, J., Franzini-Armstrong, C. and Granato, M., 2014. Schwann cells and deleted in colorectal carcinoma direct regenerating motor axons towards their original path. Journal of Neuroscience, 34(44), pp.14668-14681.

331. Rotshenker, S., 2011. Wallerian degeneration: the innate-immune response to traumatic nerve injury. Journal of Neuroinflammation, 8(1), p.109.

332. Rushton, W.A.H., 1934. A physical analysis of the relation between threshold and interpolar length in the electric excitation of medullated nerve. The Journal of physiology, 82(3), p.332.

333. Ruzankina, Y., Pinzon-Guzman, C., Asare, A., Ong, T., Pontano, L., Cotsarelis, G., Zediak, V.P., Velez, M., Bhandoola, A. and Brown, E.J., 2007. Deletion of the developmentally essential gene ATR in adult mice leads to age-related phenotypes and stem cell loss. Cell stem cell, 1(1), pp.113-126.

334. Sahenk, Z., Nagaraja, H.N., McCracken, B.S., King, W.M., Freimer, M.L., Cedarbaum, J.M. and Mendell, J.R., 2005. NT-3 promotes nerve regeneration and sensory improvement in CMT1A mouse models and in patients. Neurology, 65(5), pp.681-689.

335. Saijilafu, Hur, E.M., Liu, C.M., Jiao, Z., Xu, W.L. and Zhou, F.Q., 2013. PI3K–GSK3 signalling regulates mammalian axon regeneration by inducing the expression of Smad1. Nature communications, 4(1), pp.1-14.

336. Sandlesh, P., Juang, T., Safina, A., Higgins, M.J. and Gurova, K.V., 2018. Uncovering the fine print of the CreERT2-LoxP system while generating a conditional knockout mouse model of Ssrp1 gene. PLoS One, 13(6), p.e0199785.

337. Sarlak, G. and Vincent, B., 2016. The roles of the stem cell-controlling Sox2 transcription factor: from neuroectoderm development to Alzheimer's disease?. Molecular neurobiology, 53(3), pp.1679-1698.

338. Scarlato, M., Ara, J., Bannerman, P., Scherer, S. and Pleasure, D., 2003. Induction of neuropilins-1 and-2 and their ligands, Sema3A, Sema3F, and VEGF, during Wallerian degeneration in the peripheral nervous system. Experimental neurology, 183(2), pp.489-498.

339. Schaefer, A.W., Schoonderwoert, V.T.G., Ji, L., Mederios, N., Danuser, G. and Forscher, P., 2008. Coordination of actin filament and microtubule dynamics during neurite outgrowth. Developmental cell, 15(1), pp.146-162.

340. Scheib, J. and Höke, A., 2013. Advances in peripheral nerve regeneration. Nature Reviews Neurology, 9(12), p.668.

341. Scherer, S.S., Wang, D.Y., Kuhn, R., Lemke, G., Wrabetz, L. and Kamholz, J., 1994. Axons regulate Schwann cell expression of the POU transcription factor SCIP. Journal of Neuroscience, 14(4), pp.1930-1942.

342. Schlaepfer, W.W. and Bunge, R.P., 1973. Effects of calcium ion concentration on the degeneration of amputated axons in tissue culture. The Journal of cell biology, 59(2), pp.456-470.

343. Schlomann, U., Schwamborn, J.C., Müller, M., Fässler, R. and Püschel, A.W., 2009. The stimulation of dendrite growth by Sema3A requires integrin engagement and focal adhesion kinase. Journal of cell science, 122(12), pp.2034-2042.

344. Schröder, J.M., 1972. Altered ratio between axon diameter and myelin sheath thickness in regenerated nerve fibers. Brain research, 45(1), pp.49-65.

345. Schröder, J.M., May, R. and Weis, J., 1993. Perineurial cells are the first to traverse gaps of peripheral nerves in silicone tubes. Clinical neurology and neurosurgery, 95, pp.78-83.

346. Schubert, D., 1992. Synergistic interactions between transforming growth factor beta and fibroblast growth factor regulate Schwann cell mitosis. Journal of neurobiology, 23(2), pp.143-148.

347. Schwaiger, F.W., Schmitt, G.H.A.B., Horvat, A., Hager, G., Streif, R., Spitzer, C., Gamal, S., Breuer, S., Brook, G.A., Nacimiento, W. and Kreutzberg, G.W., 2000. Peripheral but not central axotomy induces changes in Janus kinases (JAK) and

signal transducers and activators of transcription (STAT). European Journal of Neuroscience, 12(4), pp.1165-1176.

348. Seddon, H.J., 1943. Three types of nerve injury. Brain, 66(4), pp.237-288.

349. Seddon, H.J., Medawar, P.B. and Smith, H., 1943. Rate of regeneration of peripheral nerves in man. The Journal of physiology, 102(2), p.191.

350. Seijffers, R., Mills, C.D. and Woolf, C.J., 2007. ATF3 increases the intrinsic growth state of DRG neurons to enhance peripheral nerve regeneration. Journal of Neuroscience, 27(30), pp.7911-7920.

351. Sendtner, M., 1992. Holtmann B, Kolbeck R, Thoenen H, and Barde YA. Brain-derived neurotrophic factor prevents the death of motoneurons in newborn rats after nerve section. Nature, 360, pp.757-759.

352. Serafini, T., Colamarino, S.A., Leonardo, E.D., Wang, H., Beddington, R., Skarnes, W.C. and Tessier-Lavigne, M., 1996. Netrin-1 is required for commissural axon guidance in the developing vertebrate nervous system. Cell, 87(6), pp.1001-1014.

353. Serafini, T., Kennedy, T.E., Gaiko, M.J., Mirzayan, C., Jessell, T.M. and Tessier-Lavigne, M., 1994. The netrins define a family of axon outgrowth-promoting proteins homologous to C. elegans UNC-6. Cell, 78(3), pp.409-424.

354. Shah, N.M., Marchionni, M.A., Isaacs, I., Stroobant, P. and Anderson, D.J., 1994. Glial growth factor restricts mammalian neural crest stem cells to a glial fate. Cell, 77(3), pp.349-360.

355. Shamash, S., Reichert, F. and Rotshenker, S., 2002. The cytokine network of Wallerian degeneration: tumor necrosis factor-α, interleukin-1α, and interleukin-1β. Journal of Neuroscience, 22(8), pp.3052-3060.

356. Shanthaveerappa, T.R. and Bourne, G.H., 1962. Theperineural epithelium', a metabolically active, continuous, protoplasmic cell barrier surrounding peripheral nerve fasciculi. Journal of anatomy, 96(Pt 4), p.527.

357.  Shen, Z.L., Lassner, F., Bader, A., Becker, M., Walter, G.F. and Berger, A., 2000. Cellular activity of resident macrophages during Wallerian degeneration. Microsurgery, 20(5), pp.255-261.

358.  Sherman, D.L. and Brophy, P.J., 2005. Mechanisms of axon ensheathment and myelin growth. Nature Reviews Neuroscience, 6(9), pp.683-690.

359.  Shy, M.E., Shi, Y.J., Wrabetz, L., Kamholz, J. and Scherer, S.S., 1996. Axon-Schwann cell interactions regulate the expression of c-jun in Schwann cells. Journal of neuroscience research, 43(5), pp.511-525.

360.  Siconolfi, L.B. and Seeds, N.W., 2001. Induction of the plasminogen activator system accompanies peripheral nerve regeneration after sciatic nerve crush. Journal of Neuroscience, 21(12), pp.4336-4347.

361.  Sidney, L.E., Branch, M.J., Dunphy, S.E., Dua, H.S. and Hopkinson, A., 2014. Concise review: evidence for CD34 as a common marker for diverse progenitors. Stem cells, 32(6), pp.1380-1389.

362.  Siebert, H., Sachse, A., Kuziel, W.A., Maeda, N. and Brück, W., 2000. The chemokine receptor CCR2 is involved in macrophage recruitment to the injured peripheral nervous system. Journal of neuroimmunology, 110(1-2), pp.177-185.

363.  Siemionow, M. and Brzezicki, G., 2009. Current techniques and concepts in peripheral nerve repair. International review of neurobiology, 87, pp.141-172.

364.  Simon, M., Porter, R., Brown, R., Coulton, G.R. and Terenghi, G., 2003. Effect of NT-4 and BDNF delivery to damaged sciatic nerves on phenotypic recovery of fast and slow muscles fibres. European Journal of Neuroscience, 18(9), pp.2460-

365.  Snow, D.M., Smith, J.D. and Gurwell, J.A., 2002. Binding characteristics of chondroitin sulfate proteoglycans and laminin-1, and correlative neurite outgrowth behaviors in a standard tissue culture choice assay. Journal of neurobiology, 51(4), pp.285-301.

366. Song, H.J., Ming, G.L. and Poo, M.M., 1997. cAMP-induced switching in turning direction of nerve growth cones. Nature, 388(6639), pp.275-279.

367. Squarzoni, P., Thion, M.S. and Garel, S., 2015. Neuronal and microglial regulators of cortical wiring: usual and novel guideposts. Frontiers in neuroscience, 9, p.248.

368. Stewart, H.J.S., Eccleston, P.A., Jessen, K.R. and Mirsky, R., 1991. Interaction between cAMP elevation, identified growth factors, and serum components in regulating Schwann cell growth. Journal of neuroscience research, 30(2), pp.346-352.

369. Stierli, S., Napoli, I., White, I.J., Cattin, A.L., Monteza Cabrejos, A., Garcia Calavia, N., Malong, L., Ribeiro, S., Nihouarn, J., Williams, R. and Young, K.M., 2018. The regulation of the homeostasis and regeneration of peripheral nerve is distinct from the CNS and independent of a stem cell population. Development, 145(24), p.dev170316.

370. Stoeckli, E.T., 2018. Understanding axon guidance: are we nearly there yet?. Development, 145(10), p.dev151415.

371. Stoll, G., Griffin, J.W., Li, C.Y. and Trapp, B.D., 1989. Wallerian degeneration in the peripheral nervous system: participation of both Schwann cells and macrophages in myelin degradation. Journal of neurocytology, 18(5), pp.671-683.

372. Stoll, G., Jander, S. and Myers, R.R., 2002. Degeneration and regeneration of the peripheral nervous system: from Augustus Waller's observations to neuroinflammation. Journal of the Peripheral Nervous System, 7(1), pp.13-27.

373. Stuhlmiller, T.J. and García-Castro, M.I., 2012. Current perspectives of the signaling pathways directing neural crest induction. Cellular and Molecular Life Sciences, 69, pp.3715-3737.

374. Sulaiman, W. and Gordon, T., 2013. Neurobiology of peripheral nerve injury, regeneration, and functional recovery: from bench top research to bedside application. Ochsner Journal, 13(1), pp.100-108.

375. Sun, K.L.W., Correia, J.P. and Kennedy, T.E., 2011. Netrins: versatile extracellular cues with diverse functions. Development, 138(11), pp.2153-2169.

376. Sunderland, S., 1947. Rate of regeneration of motor fibers in the ulnar and sciatic nerves. Archives of Neurology & Psychiatry, 58(1), pp.7-13.

377. Taïb, S., Lamandé, N., Martin, S., Coulpier, F., Topilko, P. and Brunet, I., 2022. Myelinating Schwann cells and Netrin-1 control intra-nervous vascularization of the developing mouse sciatic nerve. Elife, 11, p.e64773.

378. Takahashi, K. and Yamanaka, S., 2006. Induction of pluripotent stem cells from mouse embryonic and adult fibroblast cultures by defined factors. cell, 126(4), pp.663-676.

379. Tannemaat, M.R., Eggers, R., Hendriks, W.T., De Ruiter, G.C., Van Heerikhuize, J.J., Pool, C.W., Malessy, M.J., Boer, G.J. and Verhaagen, J., 2008. Differential effects of lentiviral vector-mediated overexpression of nerve growth factor and glial cell line-derived neurotrophic factor on regenerating sensory and motor axons in the transected peripheral nerve. European Journal of Neuroscience, 28(8), pp.1467-1479.

380. Tepavčević, V., Kerninon, C., Aigrot, M.S., Meppiel, E., Mozafari, S., Arnould-Laurent, R., Ravassard, P., Kennedy, T.E., Nait-Oumesmar, B. and Lubetzki, C., 2014. Early netrin-1 expression impairs central nervous system remyelination. Annals of Neurology, 76(2), pp.252-268.

381. Terenghi, G., 1999. Peripheral nerve regeneration and neurotrophic factors. The Journal of Anatomy, 194(1), pp.1-14.

382. Tessier-Lavigne, M. and Goodman, C.S., 1996. The molecular biology of axon guidance. Science, 274(5290), pp.1123-1133.

383. Tetzlaff, W., Bisby, M.A. and Kreutzberg, G.W., 1988. Changes in cytoskeletal proteins in the rat facial nucleus following axotomy. Journal of Neuroscience, 8(9), pp.3181-3189.

384. Theriault, F.M., Roy, P. and Stifani, S., 2004. AML1/Runx1 is important for the development of hindbrain cholinergic branchiovisceral motor neurons and selected cranial sensory neurons. Proceedings of the National Academy of Sciences, 101(28), pp.10343-10348.

385. Tofaris, G.K., Patterson, P.H., Jessen, K.R. and Mirsky, R., 2002. Denervated Schwann cells attract macrophages by secretion of leukemia inhibitory factor (LIF) and monocyte chemoattractant protein-1 in a process regulated by interleukin-6 and LIF. Journal of Neuroscience, 22(15), pp.6696-6703.

386. Toma, J.S., Karamboulas, K., Carr, M.J., Kolaj, A., Yuzwa, S.A., Mahmud, N., Storer, M.A., Kaplan, D.R. and Miller, F.D., 2020. Peripheral nerve single-cell analysis identifies mesenchymal ligands that promote axonal growth. Eneuro, 7(3).

387. Tomita, K., Kubo, T., Matsuda, K., Fujiwara, T., Yano, K., Winograd, J.M., Tohyama, M. and Hosokawa, K., 2007. The neurotrophin receptor p75NTR in Schwann cells is implicated in remyelination and motor recovery after peripheral nerve injury. Glia, 55(11), pp.1199-1208.

388. Topilko, P., Levi, G., Merlo, G., Mantero, S., Desmarquet, C., Mancardi, G. and Charnay, P., 1997. Differential regulation of the zinc finger genes Krox-20 and Krox-24 (Egr-1) suggests antagonistic roles in Schwann cells. Journal of neuroscience research, 50(5), pp.702-712.

389. Topilko, P., Schneider-Maunoury, S., Levi, G., Evercooren, B.V., Chennoufi, A.B.Y., Seitanidou, T., Babinet, C. and Charnay, P., 1994. Krox-20 controls myelination in the peripheral nervous system. Nature, 371(6500), pp.796-799.

390. Torigoe, K., Tanaka, H.F., Takahashi, A., Awaya, A. and Hashimoto, K., 1996. Basic behavior of migratory Schwann cells in peripheral nerve regeneration. Experimental neurology, 137(2), pp.301-308.

391. Touma, E., Kato, S., Fukui, K. and Koike, T., 2007. Calpain-mediated cleavage of collapsin response mediator protein (CRMP)-2 during neurite degeneration in mice. European Journal of Neuroscience, 26(12), pp.3368-3381.

392. Truett, G.E., Heeger, P., Mynatt, R.L., Truett, A.A., Walker, J.A. and Warman, M.L., 2000. Preparation of PCR-quality mouse genomic DNA with hot sodium hydroxide and tris (HotSHOT). Biotechniques, 29(1), pp.52-54.

393. Tserentsoodol, N., Shin, B.C., Koyama, H., Suzuki, T. and Takata, K., 1999. Immunolocalization of tight junction proteins, occludin and ZO-1, and glucose transporter GLUT1 in the cells of the blood-nerve barrier. Archives of histology and cytology, 62(5), pp.459-469.

394. Tu, T., Zhang, C., Yan, H., Luo, Y., Kong, R., Wen, P., Ye, Z., Chen, J., Feng, J., Liu, F. and Wu, J.Y., 2015. CD146 acts as a novel receptor for netrin-1 in promoting angiogenesis and vascular development. Cell research, 25(3), pp.275-287.

395. van Kesteren, R.E., Mason, M.R., MacGillavry, H.D., Smit, A.B. and Verhaagen, J., 2011. A gene network perspective on axonal regeneration. Frontiers in molecular neuroscience, 4, p.46.

396. Van Raay, T.J., Foskett, S.M., Connors, T.D., Klinger, K.W., Landes, G.M. and Burn, T.C., 1997. TheNTN2LGene Encoding a Novel Human Netrin Maps to the Autosomal Dominant Polycystic Kidney Disease Region on Chromosome 16p13. 3. Genomics, 41(2), pp.279-282.

397. Vejsada, R., Tseng, J.L., Lindsay, R.M., Acheson, A., Aebischer, P. and Kato, A.C., 1998. Synergistic but transient rescue effects of BDNF and GDNF on axotomized neonatal motoneurons. Neuroscience, 84(1), pp.129-139.

398. Wagner, A., 1999. Genes regulated cooperatively by one or more transcription factors and their identification in whole eukaryotic genomes. Bioinformatics (Oxford, England), 15(10), pp.776-784.

399. Waller, A.V., 1850. XX. Experiments on the section of the glossopharyngeal and hypoglossal nerves of the frog, and observations of the alterations produced thereby in the structure of their primitive fibres. Philosophical transactions of the Royal society of London, (140), pp.423-429.

400. Wallquist, W., Zelano, J., Plantman, S., Kaufman, S.J., Cullheim, S. and Hammarberg, H., 2004. Dorsal root ganglion neurons up-regulate the expression of laminin-associated integrins after peripheral but not central axotomy. Journal of Comparative Neurology, 480(2), pp.162-169.

401. Wang, F., Flanagan, J., Su, N., Wang, L.C., Bui, S., Nielson, A., Wu, X., Vo, H.T., Ma, X.J. and Luo, Y., 2012. RNAscope: a novel in situ RNA analysis platform for formalin-fixed, paraffin-embedded tissues. The Journal of molecular diagnostics, 14(1), pp.22-29.

402. Wang, G. and Scott, S.A., 2000. The "waiting period" of sensory and motor axons in early chick hindlimb: its role in axon pathfinding and neuronal maturation. Journal of Neuroscience, 20(14), pp.5358-5366.

403. Wang, H.U. and Anderson, D.J., 1997. Eph family transmembrane ligands can mediate repulsive guidance of trunk neural crest migration and motor axon outgrowth. Neuron, 18(3), pp.383-396.

404. Wang, Y., Zheng, Z. and Hu, D., 2013. Inhibition of EphA4 expression promotes Schwann cell migration and peripheral nerve regeneration. Neuroscience letters, 548, pp.201-205.

405. Wanner, I.B., Guerra, N.K., Mahoney, J., Kumar, A., Wood, P.M., Mirsky, R. and Jessen, K.R., 2006. Role of N-cadherin in Schwann cell precursors of growing nerves. Glia, 54(5), pp.439-459.

406. Watanabe, M., Toyama, Y. and Nishiyama, A., 2002. Differentiation of proliferated NG2-positive glial progenitor cells in a remyelinating lesion. Journal of neuroscience research, 69(6), pp.826-836.

407. Waxman, F., 1995. The axon: structure, function, and pathophysiology. Oxford University Press, USA.

408. Webber, C.A., Christie, K.J., Cheng, C.H.U., Martinez, J.A., Singh, B., Singh, V., Thomas, D. and Zochodne, D.W., 2011. Schwann cells direct peripheral nerve regeneration through the Netrin-1 receptors, DCC and UNC5H2. Glia, 59(10), pp.1503-1517.

409. Webster, H.D., Martin, J.R. and O'Connell, M.F., 1973. The relationships between interphase Schwann cells and axons before myelination: a quantitative electron microscopic study. Developmental biology, 32(2), pp.401-416.

410. Weerasuriya, A. and Hockman, C.H., 1992. Perineurial permeability to sodium during Wallerian degeneration in rat sciatic nerve. Brain research, 581(2), pp.327-333.

411. Weerasuriya, A. and Mizisin, A.P., 2011. The blood-nerve barrier: structure and functional significance. The Blood-Brain and Other Neural Barriers: Reviews and Protocols, pp.149-173.

412. Weiner, J.A. and Chun, J., 1999. Schwann cell survival mediated by the signaling phospholipid lysophosphatidic acid. Proceedings of the National Academy of Sciences, 96(9), pp.5233-5238.

413. Werner, A., Willem, M., Jones, L.L., Kreutzberg, G.W., Mayer, U. and Raivich, G., 2000. Impaired axonal regeneration in α7 integrin-deficient mice. Journal of Neuroscience, 20(5), pp.1822-1830.

414. Wilkinson, D.G., 2001. Multiple roles of EPH receptors and ephrins in neural development. Nature Reviews Neuroscience, 2(3), pp.155-164.

415. Wilson, B.D., Ii, M., Park, K.W., Suli, A., Sorensen, L.K., Larrieu-Lahargue, F., Urness, L.D., Suh, W., Asai, J., Kock, G.A. and Thorne, T., 2006. Netrins promote developmental and therapeutic angiogenesis. science, 313(5787), pp.640-644.

416. Woodhoo, A. and Sommer, L., 2008. Development of the Schwann cell lineage: from the neural crest to the myelinated nerve. Glia, 56(14), pp.1481-1490.

417. Woodhoo, A., Alonso, M.B.D., Droggiti, A., Turmaine, M., D'antonio, M., Parkinson, D.B., Wilton, D.K., Al-Shawi, R., Simons, P., Shen, J. and Guillemot, F., 2009. Notch controls embryonic Schwann cell differentiation, postnatal myelination and adult plasticity. Nature neuroscience, 12(7), pp.839-847.

418. Wright, D.E., White, F.A., Gerfen, R.W., Silos-Santiago, I. and Snider, W., 1995. The guidance molecule semaphorin III is expressed in regions of spinal cord and periphery avoided by growing sensory axons. Journal of Comparative Neurology, 361(2), pp.321-333.

419. Yamagishi, S., Yamada, K., Sawada, M., Nakano, S., Mori, N., Sawamoto, K. and Sato, K., 2015. Netrin-5 is highly expressed in neurogenic regions of the adult brain. Frontiers in cellular neuroscience, 9, p.146.

420. Yan, Q., Elliott, J. and Snider, W.D., 1992. Brain-derived neurotrophic factor rescues spinal motor neurons from axotomy-induced cell death. Nature, 360(6406), pp.753-755.

421. Ye, X., Qiu, Y., Gao, Y., Wan, D. and Zhu, H., 2019. A subtle network mediating axon guidance: intrinsic dynamic structure of growth cone, attractive and repulsive molecular cues, and the intermediate role of signaling pathways. Neural Plasticity, 2019.

422. Yin, Q., Kemp, G.J., Yu, L.G., Wagstaff, S.C. and Frostick, S.P., 2001. Neurotrophin-4 delivered by fibrin glue promotes peripheral nerve regeneration. Muscle & Nerve: Official Journal of the American Association of Electrodiagnostic Medicine, 24(3), pp.345-351.

423. Yoon, B.C., Zivraj, K.H. and Holt, C.E., 2009. Local translation and mRNA trafficking in axon pathfinding. Cell biology of the axon, pp.108-138.

424. You, S., Petrov, T., Chung, P.H. and Gordon, T., 1997. The expression of the low affinity nerve growth factor receptor in long-term denervated Schwann cells. Glia, 20(2), pp.87-100.

425. Young, P., Qiu, L., Wang, D., Zhao, S., Gross, J. and Feng, G., 2008. Single-neuron labeling with inducible Cre-mediated knockout in transgenic mice. Nature neuroscience, 11(6), pp.721-728.

426. Yu, H., Liu, J., Ma, J. and Xiang, L., 2014. Local delivery of controlled released nerve growth factor promotes sciatic nerve regeneration after crush injury. Neuroscience letters, 566, pp.177-181.

427. Yu, W.M., Feltri, M.L., Wrabetz, L., Strickland, S. and Chen, Z.L., 2005. Schwann cell-specific ablation of laminin γ1 causes apoptosis and prevents proliferation. Journal of Neuroscience, 25(18), pp.4463-4472.

428. Yuan, S.S.F., Cox, L.A., Dasika, G.K. and Eva, Y.H.L., 1999. Cloning and functional studies of a novel gene aberrantly expressed in RB-deficient embryos. Developmental biology, 207(1), pp.62-75.

429. Yuan, W., Zhou, L., Chen, J.H., Wu, J.Y., Rao, Y. and Ornitz, D.M., 1999. The mouse SLIT family: secreted ligands for ROBO expressed in patterns that suggest a role in morphogenesis and axon guidance. Developmental biology, 212(2), pp.290-306.

430. Yzaguirre, A.D., de Bruijn, M.F. and Speck, N.A., 2017. The role of Runx1 in embryonic blood cell formation. RUNX proteins in development and cancer, pp.47-64.

431. Zang, Y., Chaudhari, K. and Bashaw, G.J., 2021. New insights into the molecular mechanisms of axon guidance receptor regulation and signaling. Current topics in developmental biology, 142, pp.147-196.

432. Zelená, J., Lubińska, L. and Gutmann, E., 1968. Accumulation of organelles at the ends of interrupted axons. Zeitschrift für Zellforschung und mikroskopische Anatomie, 91(2), pp.200-219.

433. Zhao, Z.Y., Xie, X.J., Li, W.H., Liu, J., Chen, Z., Zhang, B., Li, T., Li, S.L., Lu, J.G., Zhang, L. and Zhang, L.H., 2019. A cell-permeant mimetic of NMN activates SARM1 to produce cyclic ADP-ribose and induce non-apoptotic cell death. IScience, 15, pp.452-466.

434. Zochodne, D.W., 2012. The challenges and beauty of peripheral nerve regrowth. Journal of the Peripheral Nervous System, 17(1), pp.1-18.